CARDIFF UNIVERSITY
PRIFYSGOL CAERDYDD

Sir Herbert Duthie Library

Llyfrgell Syr Herbert Duthie

University Hospital
of Wales
Heath Park
Cardiff
CF14 4XN

Ysbyty Athrofaol Cymru
Parc y Mynydd Bychan
Caerdydd
CF14 4XN

029 2074 2875
duthieliby@cardiff.ac.uk

Studies to determine the molecular mechanism of global genome nucleotide excision repair in *S. cerevisiae*

Zheng Zhou

Department of Pathology

School of Medicine

Cardiff University

A thesis submitted to School of Medicine, Cardiff University

for the degree of Doctor of Philosophy

November 2007

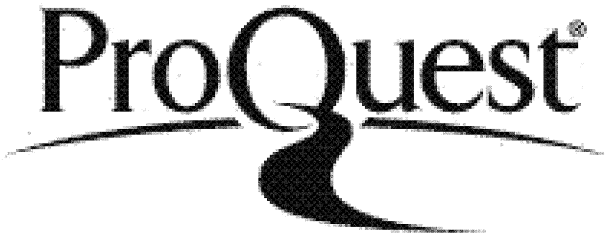

ProQuest LLC
789 East Eisenhower Parkway
P.O. Box 1346
Ann Arbor, MI 48106-1346

Declaration

This work has not previously been accepted in substance for any degree and is not being concurrently submitted in candidature for any degree.

Signed.....Zheng Zhou.....(candidate)

Date.....6/12/07.....

Statement 1

This is the result of my own investigation, except where otherwise stated. Other sources are acknowledged by footnotes giving explicit references. A bibliography is appended.

Signed.....Zheng Zhou.....(candidate)

Date.....6/12/07.....

Statement 2

I hereby give consent for my thesis, if accepted, to be available for photocopying and for inter-library loan, and for the title and summary to be available to outside organisations.

Signed.....Zheng Zhou.....(candidate)

Date.....6/12/07.....

Acknowledgement

Firstly, I thank Dr. Simon H Reed for the many insightful conversations that have guided me through my research, and for his helpful comments on the text. He possibly does not realize how much I have learned from him. Without his common sense, knowledge and perceptiveness, I would never have completed my PhD. I would like to thank both, Dr. Simon H Reed and Prof. Raymond Waters, for their wisdom, understanding, patience, and for teaching me how to become a (hopefully successful) researcher in this interesting area, DNA repair.

I would also like to thank the many people who have helped me: Dr. Shirong Yu, who taught me many techniques that were used in my research and provided me a clear outline of research in our group; Dr. Yumin Teng and Dr. Yachuan Yu, who helped me understand DNA repair in detail and resolved problems in my experiments. Dr. Rhiannon Jones, who helped me correct spelling mistakes in my thesis. Thanks also to the support of Mrs. Mary Alam and Dr. Huayun Zhuang-Jackson.

Many thanks to my wife, Hairong, for her love, warm support and full understanding. I would also give special thanks to my lovely son, Zichi (Leo), who was a source for fun and reassurance when I needed a break from writing my thesis.

Thanks to my parents, who have encouraged me to do what I like to do. And thanks to my parents-in-law, without whose help in caring for my son, I would not have finished my PhD.

Finally, I would like to acknowledge the ORS award committee and the Medical School, Cardiff for providing funds for my PhD studentship.

Zheng Zhou

November, 2007

SUMMARY

My thesis focuses on functions of Rad7/Rad16/ABF1 complex (GG-NER complex) that is required for global genome repair (GG-NER), a subpathway of the nucleotide excision repair (NER) pathway, both *in vivo* and *in vitro*. Firstly, a putative DNA translocase activity of the GG-NER complex was investigated by using a triple helix strand displacement assay. Previous work in the lab showed that the complex could generate supercoiling in DNA. One way that DNA supercoiling can be induced is via DNA translocase activity. The GGR complex exhibits a similar level of DNA translocase activity to the SV-40 large T-antigen (a well characterised DNA translocase), indicating that the generation of superhelical torsion results from a translocase activity of the GG-NER complex. The activity is required during GGR to facilitate oligonucleotide excision.

Secondly, I investigated a putative E3 ubiquitin ligase activity of a complex containing Rad7 and Rad16, and the stability of one of its substrates, Rad4. In response to UV irradiation, the native Rad4 protein which has a half-life of over three hours, is rapidly degraded by the ubiquitin-proteasome pathway. A novel Elongin-Cullin-Socs-box (ECS) type ubiquitin ligase complex, consisting of Rad7, Rad16, Cul3 and Elc1, was identified and was shown to be required for the UV-dependent ubiquitination and degradation of Rad4 *in vivo*. Furthermore, my data show that the SOCS box domain of Rad7 protein, which is required for the novel E3 ligase activity, was required for the UV-dependent ubiquitination and degradation of Rad4 protein and that Rad4 is a physiological target of this ligase. I showed that this Rad7 containing ubiquitin ligase ubiquitinates Rad4 protein *in vitro* and that a specific anti-Rad7 antibody inhibited this reaction, suggesting that the SOCS box protein Rad7 is an essential component of this novel ECS type ubiquitin ligase activity. When this ubiquitin ligase is inactive as is the case in the SOCS box mutated *rad7* strain (psocs), no significant change in UV survival is observed compared to WT strain. However, when a *Δrad23* mutation is combined with the psocs mutation a significant increase in UV sensitivity is observed in Δ*rad23*/psocs strain compared with Δ*rad23* strain. This shows that the effect of the Rad7 containing ECS ligase on UV survival is predominantly observed in the absence of Rad23. I showed that the steady level of Rad4 after UV in psocs/Δ*rad23* strain remains higher than in pRAD7/Δ*rad23* strain, but this does not rescue the UV sensitivity of psocs/Δ*rad23*, indicating that the degradation of Rad4 protein does not correlate with UV survival. My results demonstrate that inducible NER is influenced by the Rad7 ECS ligase complex. Based on my data and other work from our group, it was revealed that ubiquitination of Rad4 in response to UV specifically regulates NER via a pathway that requires *de novo* protein synthesis, a pathway that is referred to as pathway II.

Finally, preliminary experiments were designed and carried out to understand how the ubiquitination of Rad4 by the Rad7 ECS ligase functions in pathway II. In the absence of Rad23, the mRNA level of *DDR2* is elevated. Furthermore, Rad23 binds to

the promoter region of *DDR2* in the absence of DNA damage. This suggests that Rad23 might regulate the transcription of *DDR2* by directly binding to the regulatory elements of *DDR2*. Furthermore, the occupancy of Rad23 at the *DDR2* promoter significantly decreased in *Δelc1* mutant cells, in psocs cells (an E3 ligase mutant), and after cells are exposed to UV, suggesting the possibility that Rad7 ECS ligase regulates a component of the transcriptional response to DNA damage.

Abbreviations

19S RC	19S regulatory complex
AP	Apurinic/Apyrimidinic
ACF	ATP-utilizing chromatin assembly and remodelling factor
BER	Base excision repair
ChIP	Chromatin Immunoprecipitation
CPD(s)	Cyclobutane pyrimidine dimmer(s)
CS	Cockayne syndrome
E. coli	*Escherichia coli*
DNA	Deoxyribonucleic Acid
dsDNA	Double-stranded DNA
ECS	Elongin-Cullin-Socs-box
ERCC	Excision repair cross complementing protein
GG-NER	Global genome NER
HAT	Histone acetyltransferase
HDAC	Histone deacetylase
HR	Homologous recombination
ML endo	*Micrococcus luteus* CPD endonuclease
MMR	Mismatch repair
MPC	Magnetic particle concentrator
mRNA	Messenger RNA
NER	Nucleotide excision repair
NHEJ	Nonhomologous End-joining pathways
NTS	Non-transcribed strand
PCR	Polymerase chain reaction
PCNA	Proliferating cell nuclear antigen
Pol I (II)	Polymerase I (II)
6-4PPs	Pyrimidine-pyrimidone (6-4) lesions
qPCR	Quantitative PCR
RFC	Replication factor C
RNA	Ribonucleic acid
RNA pol II	RNA Polymerase II
RPA	Replication protein A
RSC	Remodel the structure of chromatin
SAGA	Spt-Ada-Gcn5-Acetyltransferase
S. cerevisiae	*Saccharomyces cerevisiae*
SUG	SUppressor of Gal
ssDNA	Single-stranded DNA
SWI/SNF	Switch/Sucrose nonfermenting
TAF	TBP associated factor
TC-NER	Transcription coupled NER
TFIIH	Transcription factor II H
TLS	Translesion synthesis
TS	Transcribed strand
TTD	Trichothiodystrophy
Ubl	Ubiquitin like
Uba	Ubiquitin associated
UPP	Ubiquitin proteasome pathway
UV	Ultraviolet (light)

WCE	Whole cell extract
XP	Xeroderma pigmentosum
YC	Yeast complete medium

CONTENTS

Chapter 1
General Introduction

1.1 DNA damages

It is well known that deoxyribonucleic acid (DNA) is a macromolecule that stores the genetic information to encode proteins that are required to build the cells and tissues of an organism. Its unique chemical structure has resulted in the evolution of an information rich, non-equilibrium system that we refer to as life. Our genetic material is not inherently stable - it is constantly exposed to the damaging effects of normal metabolic processes and it is frequently at risk from the damaging effects of genotoxic agents found in the environment. Even in the absence of any environmental source of DNA damage, everyday a human cell must repair 10,000 to 25,000 DNA lesions caused by the effects of both normal cellular metabolism and spontaneous base changes in the DNA (Peterson and Côté, 2004; Friedberg, 2001). Spontaneous or induced alterations of the chemical structure of DNA include the deamination of cytosine, adenine, guanine or 5-methylcytosine, and converting these bases to the miscoding uracil, hypoxanthine, xanthine and thymine, respectively (Lindahl, 1993; Friedberg *et al.*, 1995, 2006; Hoeijmakers, 2001). Moreover, there is a measurable half-life of certain DNA bases that results in spontaneous depurination that can generate abasic sites in DNA strands at an estimated rate of 2,000-10,000 lesions per human cell per day (Lindahl, 1993; Peterson and Côté, 2004). Besides this, a variety of DNA lesions, like 8-oxoguanine and O^6-methyldeoxyguanosine, are caused by the

byproducts of normal cellular metabolism such as reactive oxygen species (ROS), and endogenous alkylating agents (Hasty *et al.*, 2003). Meanwhile some DNA damages like single- and double-strand breaks result from collapsed DNA replication forks or from oxidative destruction of deoxyribose residues. (Friedberg *et al.*, 2006, Lindahl and Wood, 1999; Peterson and Côté, 2004)

Exogenous and endogenous damaging agents can induce lesions in DNA. Environmental agents such as abundant genotoxic chemicals, UV radiation, and ionizing radiations are sources of DNA damage which can threaten the viability of a cell or an organism. In the case of some higher eukaryotes, failure to remove DNA damage can lead to mutations that result in enhanced cancer risk (Friedberg *et al.*, 1995). DNA bases can be altered by UV light directly and these lesions are discussed later. Ionizing radiations, such as X-rays, or γ -rays etc., can directly induce single- and double- strand breaks (SSBs and DSBs), or indirectly damage DNA through oxidative stress. Many genotoxic chemicals possess carcinogenic properties which react directly with DNA. But only a few reactive electrophiles, e.g. ethylmethane sulfonate (EMS), methyl nitrosourea (MNU), are direct-acting carcinogens. These chemicals modify the DNA structure by chemically reacting with nitrogen and oxygen atoms in the bases. Meanwhile, indirect-acting carcinogens are unreactive, water-insoluble compounds that need to be activated by enzymes in metabolic processes or other oxidative pathways prior to reacting with DNA (Friedberg *et al.*, 2006; Hoeijmakers, 2001).

From all of the above, it is clear that genetic stability must be maintained over

many generations of cells and organisms, and this is a fundamental requirement for life. Without the capacity for robust DNA repair the accumulation of DNA damage, would fuel genetic instability in cells, and it is evident that this is one of the factors postulated to drive the processes of ageing and cancer in organisms ranging from simple eukaryotes to humans. Therefore, DNA repair — biochemical pathways by which damaged, inappropriate, and mispaired bases as well as defects in the DNA backbone are restored to their native state — is an essential process for the survival of all kinds of cells and organisms. So, it can be concluded that DNA repair plays a crucial role in life maintenance, ageing, cancer, evolution and heredity.

The research presented here focuses on how UV induced DNA damage is removed from the genome.

1.1.1 DNA base damage

Apart from DNA damage from spontaneous alteration of DNA bases, other base damages include 8-oxoguanine, O^6-methylguanine, thymine glycols, and other reduced, oxidized, or fragmented bases in DNA that are produced by reactive oxygen species or by ionizing radiation. UV radiation also generates reactive oxygen species, as well as producing specific DNA adducts such as cyclobutane pyrimidine dimers (CPDs) and pyrimidine-pyrimidone (6-4) photoproducts. DNA bases are also damaged by genotoxic chemicals generating base adducts, either bulky adducts caused by large polycyclic hydrocarbons or simple alkyl adducts caused by alkylating agents. Some of the chemotherapeutic drugs, including cisplatin, mitomycin C, psoralen, nitrogen mustard, and adriamycin, create base adducts, and a major

challenge in chemotherapy is to discover or develop drugs that damage DNA without invoking DNA repair or checkpoint responses in cancer cells. (Friedberg *et al.*, 1995; Sancar *et al.*, 2004)

The ability of living cells to survive high doses of damaging UV irradiation had been observed as early as the mid-1930s (Friedberg, 2003). But it wasn't until the end of the 1940s that the concept of DNA repair was proposed following observations made by two groups independently (Kelner, 1949; Dulbecco, 1949). They found enhanced survival rates when cells or bacteriophage were inadvertently exposed to long-wavelength light after UV irradiation. Now the phenomenon is known as photoreactivation, and it is the means by which UV-induced DNA lesions are repaired by a light-dependent enzyme reaction. Solar UV radiation is a potent environmental agent that can induce lesions in the DNA of exposed organisms/tissues. In humans UV penetrates the skin, and can induce both acute and chronic reactions. The UV radiation spectrum has been subdivided into three wavelengths designated UV-A (400 to 320nm), UV-B (320-290nm), and UV-C (290-100nm). It is inferred from the maximum absorption spectrum of DNA bases (~260nm) that UV wavelengths closer to 260nm are more damaging to DNA. However, the majority of solar UV radiation comprises UV-A and UV-B, because UV rays with wavelengths below 320nm are absorbed by atmospheric ozone (Friedberg *et al.*, 1995). It is believed, however, that the existence of holes in the ozone layer means such radiation is playing an increasing role as an environmental mutagen (Diffey, 2004). UV-B is highly mutagenic and carcinogenic in animals, due to a variety of DNA damages, including CPDs and (6-4)

photoproducts, as well as a smaller number of other types of DNA damage. Defective repair of these lesions can lead to the development of skin cancer. The phototoxic effect of UV-A is much lower compared to UV-B, since DNA is not a chromophore of UV-A. Cyclobutane pyrimidine dimers (CPDs) and (6-4) photoproducts account for the majority (~95%) of UV induced lesions after exposure to UV-C, with CPDs predominating at levels of up to about 75% of the total damage. (6-4) photoproducts account for about 20% of the total damage, whereas other damages occurring at low frequency include purine or pyrimidine hydrates, thymine glycols, DNA cross-links and strand breaks (Friedberg, *et al.*, 1995; Ichihashi, 2003).

Cyclobutane Pyrimidine Dimers (CPDs)

CPD's form between adjacent pyrimidines. After the DNA base receives energy from UV light at a wavelength of about 260nm, adjacent pyrimidines in the same strand can form two covalent bonds at C5-C5 and C6-C6 (Fig. 1.1), resulting in a four-membered ring formed by the saturation of the C5= C6 double bonds in both pyrimidines. The structure of this cyclobutyl ring is referred to as a Cyclobutane Pyrimidine Dimer (CPD). Theoretically, there are 12 isomeric forms of CPDs. However, only four of them, with the configuration of *cis-syn*, *cis-anti*, *trans-syn*, and *trans-anti* can have significant yields naturally. In the double stranded B-form of DNA, the cis-syn isomer is thought to be the major form of CPD induced by UV irradiation. The *trans-syn* form can exist to some extent *in vivo* at single stranded regions and in duplex DNA in certain conformations (Friedberg *et al.*, 1995).

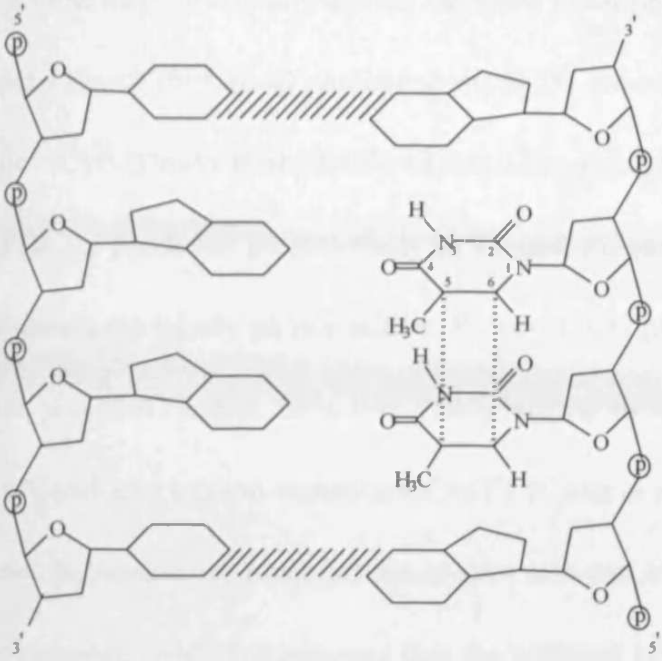

Figure 1.1 Structure of a CPD. In the same polynucleotide chain two covalent bonds of two adjacent pyrimidines forms a four-membered cyclobutyl ring linking the two pyrimidines. (Adapted from Friedberg *et al.*, 1995)

Table 1.1 Distribution of bipyrimidine photoproducts within DNA of Chinese hamster ovary cells upon exposure to UVB[a], UVA[b] radiation and solar simulated light as inferred from HPLC–MS/MS measurements and expressed as number of lesions per 10^9 bases. (DewarTT means Dewar valence isomer of (6-4) photoproduct TT.)

	UVB (per Jm^{-2})	UVA (per kJm^{-2})	SSL (per kJm^{-2})
Thy<>Thy	17.51±1.24	19.15±3.71	15.86±1.81
6-4TT	1.66±0.13	n.d.[d]	0.09±0.05
DewarTT	n.d.[d]	n.d.[d]	0.87±0.23
Thy<>Cyt	13.90±2.16	1.19±0.11	6.19±1.05
6-4TC	14.33±1.60	n.d.[d]	2.05±0.53
DewarTC	n.d.[d]	n.d.[d]	3.72±0.36
Cyt<>Cyt	1.19±0.29	0.09±0.06	0.62±0.07

[a] 15W fluorescent lamps ($\lambda > 290$ nm) equipped with UVC radiation cutoff filters.

[b] SUPERSUN 500 lamp ($340 < \lambda < 440$ nm).

[c] XBO xenon arc lamp equipped with cutoff filters to remove short UVB wavelengths.

[d] Not detectable.

A detailed study of UV-induced dimeric photoproducts under UVA, UVB, and

solar simulated light respectively shows that the three main photoproducts are CPDs at TT sequences (Thy<>Thy), (6-4) photoproducts at TC sequences, and CPDs at TC sequences (Thy<>Cyt) (Douki *et al.*, 2003). (Table 1.1) From the data of table 1.1, it is seen that CPDs are produced preferentially at TT and TC site whereas CC and CT bipyrimidine clusters are poorly photoreactive. However, CC photoproducts exhibit a high mutagenic potential despite their low yield, leading to the observation of the characteristic UV-induced tandem mutation CC→TT (Cadet *et al.*, 2005).

The flanking sequences for potential dimer sites also can influence the formation of CPDs at a detectable level. It is reported that the different sites of potential T=T at 5'ATTG3', 5'CTTC3' and 5'CTTTA3' reached different saturated levels that varied from 4% to 16 %. Generally, the saturated level of dimers for TT sites at 5'ATTA3' is greater than that at 5'ATTG3' (Gordon and Haseltine, 1982). Moreover, CPD formation is also affected by the upstream and downstream sequences of the potential dimer sites, and is different in single- or double-stranded DNA (Friedberg *et al.*, 1995).

Additionally, proteins that interact with DNA affect the formation of CPDs, as reported for the *lac* repressor bound to the *lac* operator in *Escherichia coli* (Becker and Wang, 1984) and for several promoter elements that interact with sequence-specific proteins in yeast and mammalian cells. Similarly, transcription factors have direct influences on the induction and repair of CPDs (Selleck and Majors, 1987; Pfeifer *et al.*, 1992; Axelrod *et al.*, 1993; Tornaletti and Pfeifer, 1995; Teng *et al.*, 1997). Chromatin structure can also modulate damage formation induced

by UV light. For example, the bending of DNA around the histone octamer may facilitate the induction of CPDs at sites where the DNA minor groove faces outside. However, CPDs can be detected throughout the nucleosome core. So, it appears that nucleosomes have an important influence on both the induction of DNA damage and DNA repair (Thoma, 1999).

CPDs are often considered as bulky, helix-distorting DNA damages, which are strictly noncoding and can induce arrest of DNA replication and transcription, but this arrest can be overcome in the case of replication via damage tolerance pathways also known as translesion synthesis (TLS) (Lehmann, 2005; Lehmann *et al.*, 2007). A group of specialized DNA polymerases are involved in TLS, many of which belong to Y family of DNA polymerases (Lehmann, 2005). In human cells, the special TLS polymerases include pol η, ι, κ and Rev1 in Y family and polζ in B-family (Lehmann *et al.*, 2007). There are homologues of Rev1, pol η and polζ in yeast (Friedberg *et al.*, 2005). The difference between the Y family and other DNA polymerases is their much more open and flexible structure (Friedberg, 2005; Lehmann, 2005). During the DNA replication process, the blocked normal DNA polymerase is firstly displaced from the lesion sites and the appropriate TLS polymerase is loaded in order (Lehmann *et al.*, 2007). This replacement by a TLS polymerase is referred to as polymerase switching (Friedberg *et al.*, 2005). The mono-ubiquitination of PCNA mediates the switch to translesion synthesis, and PCNA is mono-ubiquitinated on lysine-164 by Rad6 and Rad18 (Hoege *et al.*, 2002; Lehmann *et al.*, 2007). Moreover, the ubiquitin-biding domain in Y family polymerases is required for the direct interaction

with mono-ubiquitinated PCNA and regulates translesion synthesis (Bienko *et al.*, 2005; Gao *et al.*, 2006). Interestingly, polκ plays a role in both TLS and NER, since both repair synthesis and photoproduct removal are reduced in the Pol κ-deficient cells (Ogi and Lehmann, 2006; Lehmann, 2006).

Pyrmidine-Pyrimdone (6-4) photoproducts

After DNA bases are directly excited by UV photons, the Pyrmidine-Pyrimdone (6-4) photoproduct is another prevalent type of UV- induced lesion by UV (Mitchell *et al.*, 1989). This type of lesion forms predominantly at cytosine but occasionally also forms at positions of thymine while the adjacent C or T is located 3' to a pyrimidine nucleotide. After reaction (6-4) photoproducts introduce a major distortion (a bend or kink of about 44°) in the double helical structure of DNA by forming a stable bond between the two pyrimidines (5'C^6-$C^4$3') (Fig. 1.2) (Friedberg *et al.*, 1995; Kim *et al.* 1995). Moreover, (6-4) photoproducts that absorb light at around 320nm can photoisomerize into the related Dewar valence isomer upon exposure to the latter wavelengths (Ravanat *et al.*, 2001; Cadet *et al.*, 2005).

In cells (6-4) photoproducts are mostly found at TC sites, whereas they are relatively less abundant at TT and CC (Lippke *et al.*, 1981; Franklin *et al.*, 1985). In contrast to CPDs, (6-4) photoproduct distribution does not extend into nucleosomal regions (Gale and Smerdon, 1990). Apparently, there is no natural distortion in

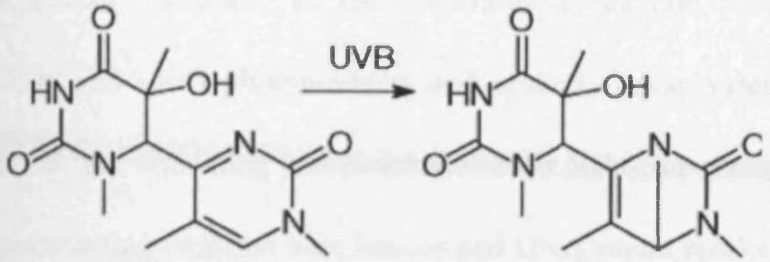

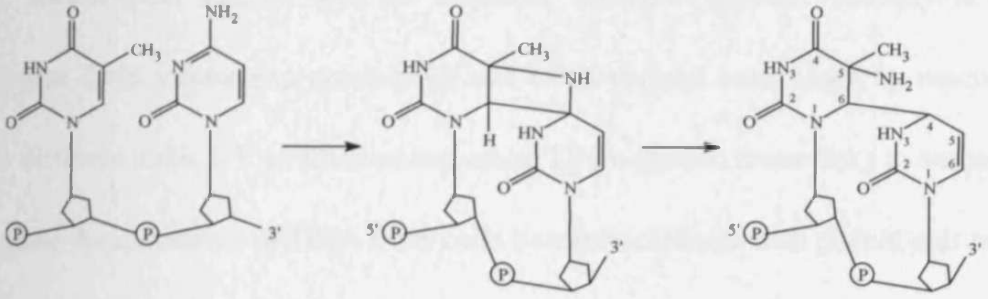

Figure 1.2 Formation of the UV induced T-C (6-4) crosslink. The covalent linkage between the C^6 position of one thymine and the C^4 position of the 3' adjacent cytosine forms due to UV radiation. It can be assumed that (6-4) photoproduct is a major distortion of the double helix. (Friedberg *et al.*, 1995; Cadet *et al.*, 2005)

nucleosomal DNA which enables formation of the (6-4) photoproduct at any specific site. Hence, (6-4) photoproducts occur predominantly in linker DNA, where there is a higher flexibility compared to DNA folded in nucleosomes (Niggli and Cerutti, 1982). It should also be noted that, proteins and protein complexes that disturb the B-form structure of DNA influence both the yields and the types of DNA damage including CPDs and (6-4) photoproducts (Becker and Wang, 1984).

In conclusion, direct excitation of DNA bases by UVB gives rise, mostly through oxygen independent reactions, to the formation of dimeric pyrimidine lesions including CPDs and (6-4) photoproducts and related Dewar valence isomers. In contrast to UVB, the remaining components of solar light can generate a variety of DNA damage including oxidized base lesions and DNA strand breaks at relativly low rates, mainly through oxygen dependent reactions.

1.1.2 Interstrand Cross links

Bifunctional agents such as cisplatin, nitrogen mustard, mitomycin D, and psoralen form interstrand cross-links and DNA-protein cross-links by reacting with two different sites. UV irradiation can cause DNA-protein cross-links to some degree, because the extraction of DNA from cells becomes difficult with phenol-salt treatment after exposure of living cells to UV radiation. Theoretically, a reversible DNA-protein binding like transcription factors bind to DNA, is not regarded as cross-link damage. However, when such DNA-protein binding become irreversible after UV radiation, these are lesions requiring repair (Friedberg *et al.*, 1995; Minko, 2001; Sancar *et al.*, 2004).

1.1.3 DNA backbone damage

Both ionizing radiation, such as X-rays, γ -rays etc., and UV radiation can give rise to DNA backbone damages. There are three principal types of backbone damage. These are abasic sites and single- and double-strand DNA breaks. Abasic sites are generated spontaneously, by the formation of unstable base adducts or by base

excision repair. Single-strand breaks and double-strand breaks can be produced directly by UV light through reactions that require participation of endogenous photosensitizers together with oxygen. Whilst single-strand breaks with a gap in the range of 1–30 nucleotides, can be produced as intermediates of base and nucleotide excision repair. Besides UV radiation, single-strand breaks and double-strand breaks are formed by ionizing radiation and other DNA damaging agents. In addition, double-strand breaks can be formed as intermediates during recombination.

1.2 DNA repair pathways and their molecular mechanisms

It is clearly the case that genomes of RNA and DNA evolved as specialized complementary molecules adapted for information storage and transmission. During genome evolution an 'error threshold' is reached that relates the rate and fidelity of replication of individual bases in a population to the maximum genome size that can be maintained over many generations. Clearly, as genomes evolved with increasing size and complexity, the storage and output of this evolving genetic information needed to include increasingly more sophisticated ways of metabolising the genome. A range of other cellular processes, including the evolution of DNA repair systems occurred in order to maintain the integrity of the genome. Here, DNA repair systems are classified into 6 pathways, which are direct repair, nucleotide excision repair (NER), base excision repair (BER), mismatch repair (MMR), homologous recombination (HR), and non-homologous end-joining repair (NHEJ). (Hoeijmakers, 2001, Sancar *et al.*, 2004; Reed, 2005)

1.2.1 Direct repair

The discovery of DNA damage reversal mechanisms occurred in the 1940s, whereas DNA repair mechanisms were discovered much later. Two independent groups observed anomalous survival rates when cells were exposed to UV light then long-wavelength light separately. (Kelner, 1949; Dulbecco, 1949). Their observations were explained following the discovery of mechanism directly reversing of DNA damage. One is the photoreversal of UV-induced pyrimidine dimers by DNA photolyase. The second direct damage reversal mechanism deals with alkylation damage in DNA with specialized proteins, which are commonly found in many organisms (Friedberg, 2003; Cline and Hanawalt, 2003; Sancar *et al.*, 2004).

Photolayse

In yeast, plants, some bacteria and in organisms as evolved as marsupials, photolyase repairs UV-induced cyclobutane pyrimidine dimers and (6-4) photoproducts using blue-light photons as an energy source. It appears that placental mammals including humans have lost the proteins that catalyse photoreversal during their evolution. Photolyase, a monomeric protein of 55–65 kDa with two chromophore cofactors, a pterin in the form of methenyltetrahydrofolate and a flavin in the form of $FADH^-$, can be subdivided into two types. One repairs CPDs (photolyase) and the other repairs (6-4) photoproducts (6-4 photolyase) (Todo *et al.*, 1993; Sancar *et al.*, 1984; Sancar, 1994). Since the structures and reaction mechanisms of the two types from many species are similar, the reaction mechanism is illustrated here using *E. coli* photolyase as a model (Figure 1.3). Firstly, the reaction

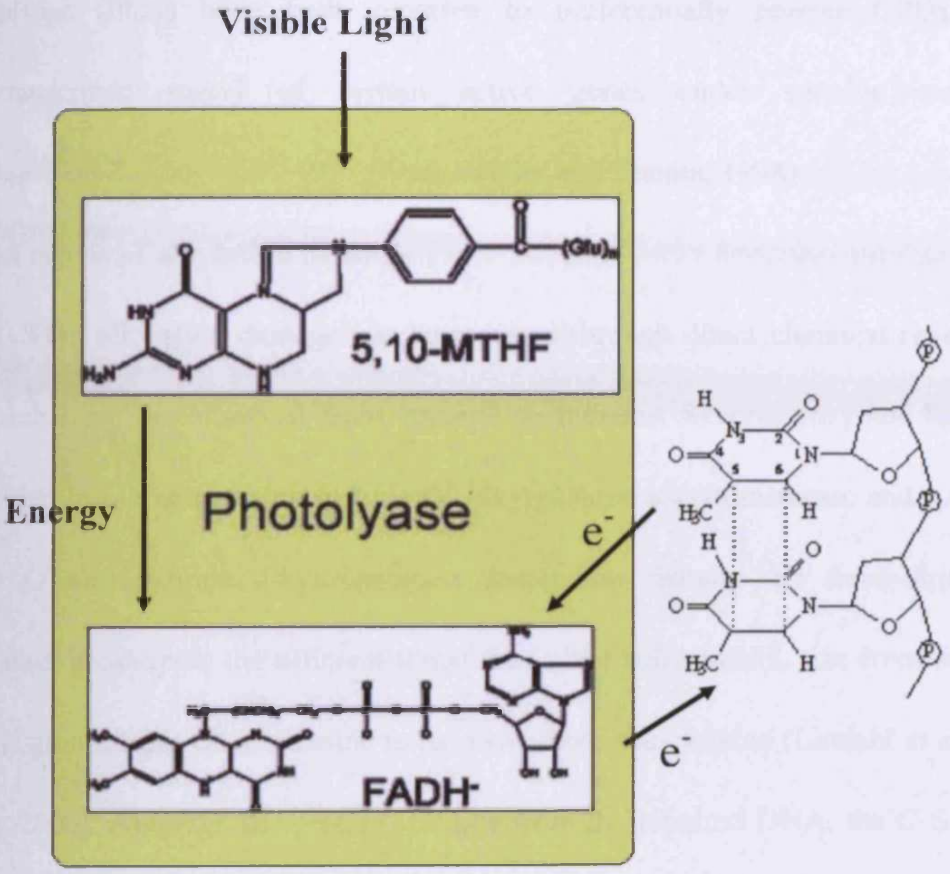

Figure 1.3. Direct repair by photoreactivation.

starts with the folate, which is located at the surface of the enzyme and functions as a photo-antenna. It absorbs a violet/blue-light photon (350–450 nm) and transfers the excitation energy to the flavin cofactor. The excited $FADH^-$ donates an electron to the CPD to produce a dimer radical anion that splits into two canonical pyrimidines concomitantly. Meanwhile an electron returns to the flavin to restore its catalytically competent form. Moreover, photolyase not only reverses DNA damage directly, but it also can assist the NER of CPDs in the absence of photoreactivating wavelengths in some cases (Sancar *et al.*, 1984; Sancar and Smith, 1989). Both bacterial and yeast

photolyase (Phr1) have been reported to preferentially reverse CPDs in the non-transcribed strand of certain active genes under suitable conditions. (Livingstone-Zatchej *et al.*, 1997; Aboussekhra and Thoma, 1998).

Direct repair of alkylation damage

Like CPDs, alkylation damage can be repaired through direct chemical reversal and its mechanism is conserved from bacteria to humans. Several enzymes have been identified in humans, which include O^6-alkylguanine alkyltransferase and hABH1-3. After O^6-alkylguanine alkyltransferase recognizes damage by three-dimensional diffusion, it catalyses the efficient transfer of alkyl substituents, size from methyl to benzyl group, from O^6 of guanine to its own active site cysteine (Lindahl *et al.*, 1988; Pegg, 2000). Although the protein releases from the repaired DNA, the C-S bond of methylcysteine is stable, and therefore, after one catalytic event the enzyme becomes inactivated. Mice lacking O^6MethylGuanine methyltransferase are highly susceptible to tumorigenesis by alkylating agents. In addition to these ubiquitous enzymes, there are oxidative methyl transferases in bacteria (AlkB) and humans (hABH1–3), which catalyse the oxidation of and repair 1-methyladenine and 3-methylcytosine. The AlkB and hABH3 repair both DNA and RNA, require molecular oxygen, Fe^{2-} and 2-oxoglutarate, and release the hydroxylated methyl group as formaldehyde (Duncan *et al.*, 2002; Falnes *et al.*, 2002; Trewick *et al.*, 2002; Aas *et al.*, 2003).

1.2.2 Nucleotide excision repair (NER) and its molecular mechanism

Nucleotide excision repair (NER), is a complex excision repair pathway and it is highly conserved in many organisms. It is the major repair system for removing a

wide range of DNA damages including bulky DNA lesions of the exposure to radiation or chemicals, and operate to repair CPDs and (6-4) photoproducts (Hoeijmakers, 2001; Reed and Waters, 2003). The discovery of the human hereditary cancer-prone disease xeroderma pigmentosum (XP), which is due to a defect in NER, had an important impact on our drive to understand NER in mammals (Cleaver, 1968; Friedberg, 2004). Since then, other hereditary diseases concerned with deficiency of NER have been revealed. These include Cockayne's Syndrome (CS), combined XP/CS, trichothiodystrophy (TTD) and a fifth disease known as cerebro-oculo-facial-skeletal syndrome (COFS) (Lehmann, 2001; 2003; de Boer and Hoeijmakers, 2000; Reed, 2005). In addition to NER-related hereditary diseases, mutation(s) of a DNA polymerase (polη) gives rise to the variant form of xeroderma pigmentosum (XP-V) (Masutani *et al.*, 1999; Johnson *et al.*, 1999; Lehmann *et al.*, 2007).

There are more than 30 polypeptides that are involved in NER to remove damages from naked DNA *in vitro.* Some of these factors also take part in other aspects of DNA metabolism such as replication and transcription (Petit and Sancar, 1999). NER can be divided into two sub-pathways: repair of lesions over the entire genome, referred to as global genome NER (GG-NER), and repair of transcription-blocking lesions present in transcribed strands, hence called transcription coupled NER (TC-NER). The details of GG-NER and TC-NER will be discussed in the context of yeast and human cells.

1.2.2.1 Transcription coupled NER (TC-NER)

Theoretically, the termination of transcription in an essential gene by a single irreversibly stalled RNA polymerase II complex has the potential to result in the eventual death of the affected cell. It is perhaps not surprising then that one of the most common causes of prolonged RNA polymerase II stalling, DNA damage, should be repaired very rapidly to ensure this event rarely occurs. Hanawalt and co-workers first investigated whether the rate of repair in active genes is significantly different from that in non-transcribed regions. Our basic understanding of TC-NER is founded on their observation that only the transcribed strand of active genes is preferentially repaired (Bohr *et al.*, 1985; Mellon *et al.*, 1986; 1987). From the analysis of the rate of TC-NER and GG-NER at nucleotide level in and around active genes, TC-NER only occurs in the transcribed region while beyond this region the repair rate becomes similar in the two complementary strands (Teng *et al.*, 2000; Tijsterman *et al.*, 1996; 1997; Tijsterman and Brouwer, 1999; Tu *et al.*, 1996; 1997). However, in the promoter region of Gal1-10 genes a faster repair rate of the transcribed strand has been reported in the absence of elongation but with RNA pol II loaded compared with the non-transcribed strand (Li and Smerdon, 2004). How NER operates in the promoter region of transcriptionally active genes where the transcription machinery starts to load but without elongation is poorly understood. The fundamental importance of TC-NER is evident since individuals suffering from Cockayne's Syndrome have a severe hereditary disorder due to mutations in TC-NER genes. Moreover, TC-NER is conserved not only in eukaryotes, but also in prokaryotes.

The molecular mechanism of TC-NER

The stalled RNA polymerase triggers the TC-NER pathway

During transcription elongation, a phosphorylated RNA polymerase II (RNA pol IIo) stalled at a lesion, such as CPDs or (6-4) photoproducts, as well as other bulky lesions, has been proposed to constitute the signal triggering the TC-NER pathway. However, the arrest of any single RNA pol IIo by a particular form of damage depends on the stereochemistry and DNA-sequence context of the lesion (Bohr, *et al.*, 1985; Tornaletti *et al.*, 1997; Tornaletti and Hanawalt, 1999; Hanawalt, 2003, Perlow and Broyde, 2002). In addition to RNA pol II, RNA polymerase I of *S. cerevisiae* has also been reported to mediate TC-NER of UV-induced DNA damage in ribosomal genes while RNA polymerase I and III do not elicit TC-NER in mammalian cells (Conconi *et al.*, 2002, Christains and Hanawalt, 1993; Dammann and Pfeifer, 1997). Several lines of evidence support the suggestion that a stalled RNA polymerase is required to elicit TC-NER both in mammalian and yeast cells. In Chinese hamster ovary (CHO) cells, TC-NER ceases immediately after the addition of α-amanitin, a RNA pol II inhibitor (Christians and Hanawalt, 1992). A similar dependence of TC-NER on active RNA pol II transcription was shown in yeast using a strain expressing a temperature-sensitive allele of *RPB1*(encoding the catalytic RNA pol II subunit), which immediately ceases RNA pol II transcription on changing to the non-permissive temperature (Sweder and Hanawalt, 1992).

The removal/remodeling of stalled RNA polymerase II and proteins related to it

In yeast, Rad26 (the yeast homolog of mammalian CSB), a DNA-dependent

ATPase in the SNF2 family (Table 1.2), is needed to overcome the obstacle to TC-NER posed by the stalled polymerase (Tijsterman and Brouwer, 1999; Teng and Waters, 2000). In the absence of the TC-NER factor Rad26, certain lesions in the inter-nucleosomal regions are repaired more slowly in the transcribed strand than in the non-transcribed strand by inhibition of stalled RNA pol IIo. Moreover, Rad26 was observed to promote efficient transcription through a damaged DNA strand (Lee *et al.*, 2001, 2002; Woudstra *et al.*, 2002; Svejstrup, 2002). It is interesting that mutants of the RAD26 gene do not exhibit sensitivity to UV radiation, but still have diminished preferential repair of the transcribed strand (Tijsterman *et al.*, 1997; Teng and Waters, 2000). However, cells lacking RAD28, the presumed human CSA homolog, are not defective in TC-NER (Bhatia *et al.*, 1996).

CSA and CSB, the TC-NER factors in mammals, appear to play a more prevalent role in DNA repair than their homologues do in yeast. Cell lines expressing defective forms of CSA and CSB proteins are almost completely unable to repair lesions in the transcribed strand of active genes (Henning *et al.*, 1995; Troelstra *et al.*, 1992; van Hoffen *et al.*, 1993; Venema *et al.*, 1990; Andrews *et al.*, 1978). During TC-NER, CSB can bind to a stalled polymerase and recruit TFIIH to this complex (Tantin *et al.*, 1997; Tantin, 1998) Moreover, CSA and CSB are necessary for the recovery of RNA synthesis following UV-irradiation. CSB can affect transcription in both the presence and absence of exogenous induction of DNA damage (Dianov *et al.*, 1997; Balajee *et al.*, 1997). XPA-binding protein, XAB2 is also involved in TC-NER via interaction with CSA, CSB, and RNA pol II (Nakatsu *et al.*, 2000).

In prokaryotes it is clear that the transcription-coupling repair factor (TCRF), now known as Mutation Frequency Decline (MFD), dissociates the stalled polymerase from DNA using its DNA-dependent ATPase activity (Selby and Sancar, 1993). MFD recognizes RNA pol II stalled at a non-coding template site of DNA damage, and disrupts the transcription complex releasing the transcript and enzyme. The DNA repair machinery also can be recruited to the damage site by MFD. It was shown that the mechanism of RNA release by MFD was driven by the forward translation of RNA pol II by the RecG-like ATP-dependent motor of MFD (Roberts and Park, 2004). Despite the similar DNA-dependent ATPase with TCRF, CSB/Rad26 cannot dissociate a damage-stalled RNA pol II elongation complex *in vitro* but can enable RNA pol IIo to add an extra nucleotide when stalled at a transcription-blocking DNA lesion (Selby and Sancar, 1997a; 1997b). This means that CSB mediates the modification of RNA pol II-DNA interface and recruits TFIIH to promote rapid lesion removal following the subsequent recruitment of the remaining repair factors.

Most recently, in order to answer the question that how the arrested polymerase allows repair to proceed, three independent groups reported their findings *in vitro* or *in vivo* to describe this process (Sarasin and Stary, 2007). The work published by Sarker *et al.* showed XPG and CSB can bind in a cooperative manner with RNA pol IIo stalled at a Cis–Pt adduct *in vitro* (Sarker *et al.*, 2005). Moreover, XPG enhanced CSB binding to bubble DNA and stimulated CSB ATPase activity. Interestingly, in this *in vitro* system the XPG incision does not lead to RNA pol IIo release. This work is based on an artificial transcription bubble-like substrate and purified proteins and

more evidences are still required to reveal the true process *in vivo*. Lainé and Egly set up a totally different *in vitro* system in which the elongating RNA pol IIo stalled at Cis-Pt lesion of a true transcription template (Lainé and Egly, 2006). With this system, NER factors like TFIIH, XPA, RPA, XPG and XPF/ERCC1 were successfully recruited to the damaged site of the transcription template following incubation with a whole cell extracts from an XPC mutant. Moreover, CSB does not affect the recruitment of these NER factors, but enhances the dual incision. Based on this research, TFIIH and XPA are recruited first onto the stalled RNA pol IIo while RPA appears as soon as single strand-stranded DNA is created by elongating RNA pol IIo. However, the release of RNA pol IIo does not dependent on the ATPase activity of CSB but relates to the ATPase activity of TFIIH and the integrity of five NER factors, which are XPA, RPA, TFIIH, XPG and XPF. The *in vivo* results provided by Fousteri et al. confirmed some *in vitro* findings by an *in vivo* crosslinking approach in concert with chromatin immunoprecipitation (ChIP) with specific antibodies (Fousteri *et al.*, 2006). A milestone finding in this report is the crucial role of CSB, which is indispensable for the recruitment of the CSA/DDB E3-ubiquitin ligase/CSN complex, the NER machinery and chromatin remodeling factors like p300 to the stalled RNA pol IIo. Furthermore, it was suggested that CSB was one of the first factors to be recruited to the lesion-stalled RNA pol IIo, directing the orchestration of subsequent TC-NER-related events. In this paper the authors suggest that functional TC-NER complex assembly does not require the dissociation of UV-stalled RNA pol IIo from DNA.

Table 1.2 Nucleotide excision repair (NER) genes in yeast and humans

S. cerevisiae	*Human*	*Activities*
RAD14	*XPA*	*binding DNA damage*
RAD4	*XPC*	*binding damaged DNA with Rad23*
RAD23	*HHR23A/B*	*associated with Rad4*
RAD1	*XPF*	*DNA endonuclease with Rad10 for 5' of damage*
RAD10	*ERCC1*	
RAD2	*XPG*	*DNA endonuclease for 3' of damage*
TFIIH		
RAD25/SSL2	*XPB*	*3' to 5' DNA helicase*
Rad3	*XPD*	*5' to 3' DNA helicase*
SSL1	*GTF2H2*	*core TFIIH subunit p44*
TFB1	*GTF2H1*	*core TFIIH subunit p62*
TFB2	*GTF2H4*	*core TFIIH subunit p52*
TFB4	*GTF2H3*	*core TFIIH subunit p34*
TFB3	*MAT1*	*CDK assembly factor (MAT1)*
TFB5	*TTD-A/(p8)*	*core TFIIH subunit p8*
	CDK7	*Kinase subunit*
	Cyclin H	*Kinase Subunit*
RFA1-3	*RPA70/32/14*	*binding to ssDNA*
RAD28	*CSA*	*WD40 repeat*
RAD26	*CSB*	*Swi/Snf-like ATPase*
MMS19	*MMS19*	
ABF1	*?*	*Binding with Rad7/16*
RAD7	*?*	*SOCS box protein/E3 ligase*
RAD16	*?*	*Snf2-like ATPase/Ring finger*
?	*DDB1/2*	*Damage binding/E3 ligase*
?	*XAB2*	*Binding with RNA pol II, CSA, CSB*

Other evidence for the displacement of stalled RNA pol IIo, comes from the subsequent ubiquitination of RNA pol II following UV-irradiation, suggesting that the rapid degradation of RNA pol II lets the repair machinery replace it quickly (Bregman *et al.*, 1996; Beaudenon *et al.*, 1999; Huibregtse *et al.*, 1997; Ratner *et al.*, 1998). Recent work shows that CSA is integrated into a complex, which displays ubiquitin

ligase activity and is regulated by the COP9 signalosome, together with DDB1, cullin 4A, and Roc1 (Groisman *et al.*, 2003). Moreover, in CSA and CSB cells, ubiquitination and degradation of RNA pol II are defective and are therefore CSA/CSB-dependent after exposure to UV light (Bregman *et al.*, 1996; Mckay *et al.*, 2001). However, in yeast, ubiquitination of RNA pol II does not seem to be required for TC-NER (Lommel *et al.*, 2000a). It was suggested that ubiquitination and Pol II degradation in response to DNA damage constitutes an alternative to DNA repair – a last resort (Woudstra *et al.*, 2002). The Rad26-Def1 complex coordinates repair and RNA pol II proteolysis in response to DNA damage (Woudstra *et al.*, 2002). Moreover, it was suggested that the RNA pol II ternary complex rather than the specific structure of stalled RNA pol II is recognized by the ubiquitination machinery (Somesh *et al.*, 2005). Def1 promotes ubiquitination of RNA pol II only in an elongation complex (Somesh *et al.*, 2005). In addition to Def1, the C-terminal repeat domain (CTD) of RNA pol II is also required for ubiquitination of RNA pol II. CTD phosphorylation at serine 5 residue but not at serine 2 residue blocks ubiquitination reaction *in vitro* (Somesh *et al.*, 2005). In my view, the fate of a DNA damage stalled RNA pol IIo is very unclear.

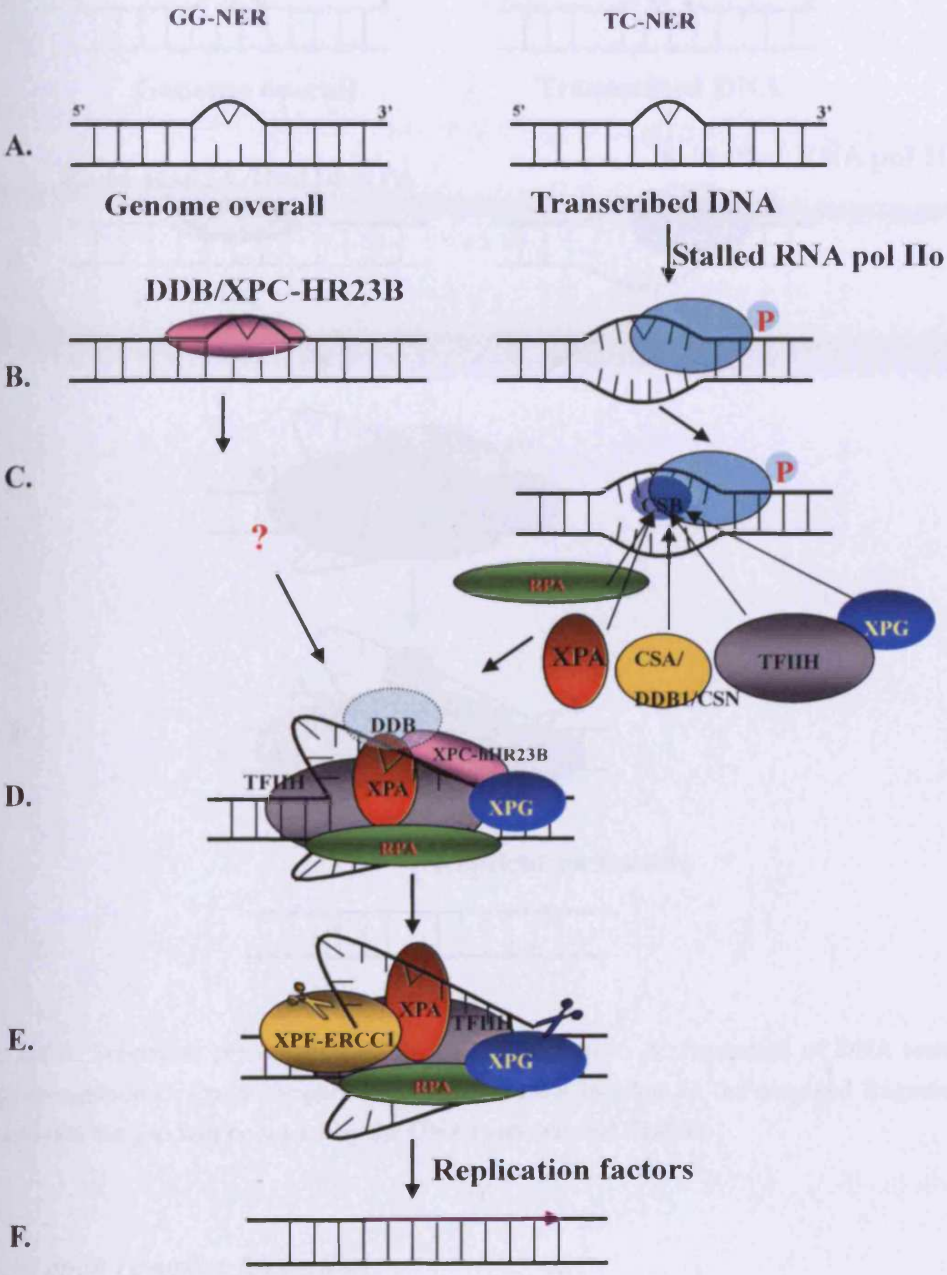

Figure 1.4 A. Schematic presentation of NER in *Humans*. A: Formation of DNA lesion. B: Damage recognition C: The recruitment of NER machinery D: Open complex formation. E: Dual incision. F: the damaged fragment will be excised and the gap will be sealed by the DNA synthesis and ligation.

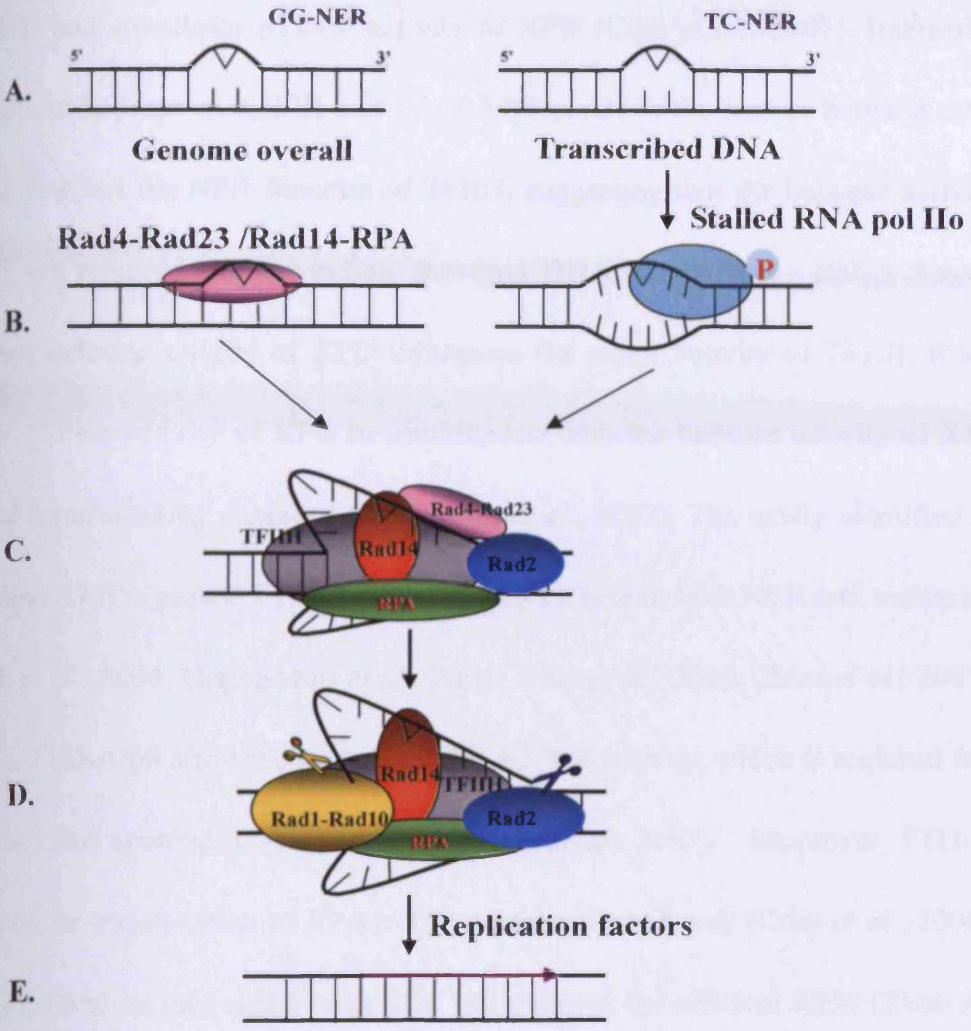

Figure 1.4 B. Schematic presentation of NER in *S. cerevisiae*. A: Formation of DNA lesion. B: Damage recognition C: Open complex formation. D: Dual incision. E: the damaged fragment will be excised and the gap will be sealed by the DNA synthesis and ligation.

Transient open complex formation

When TFIIH is recruited to the stalled RNA pol II, its components XPB/Rad25 and XPD/Rad3 asymmetrically open the DNA helix around the lesion using their DNA helicase functions. XPB/Rad25 can unwind DNA in a 3' to 5' direction whilst XPD/Rad3 unwinds in the opposite direction (Schaeffer *et al.*, 1993; 1994; Roy *et al.*, 1994). Recently, it has been reported that p52, the core component of TFIIH, interacts

with XPB and stimulates ATPase activity of XPB (Coin *et al.*, 2007). Interestingly, mutations in helicase motifs III and IV of XPB result in the loss of helicase activity but do not affect the NER function of TFIIH, suggesting that the helicase activity of XPB is not required for unwinding damaged DNA (Coin *et al.*, 2007). Since the decreased helicase activity of XPD influences the repair activity of TFIIH, it seems that the ATPase activity of XPB in combination with the helicase activity of XPD is required for unwinding damaged DNA (Coin *et al.*, 2007). The newly identified tenth component TFB5 (yeast)/ TTD-A (Human) plays a role in both NER and transcription (Ranish *et al.*, 2004; Giglia-Mari *et al.*, 2004; Coin *et al.*, 2006; Zhou *et al.*, 2007). In humans, TTD-A/p8 also stimulates the XPB ATPase activity, which is required for the damaged DNA opening (Coin *et al.*, 2006; Coin *et al.*, 2007). Moreover, TTD-A/p8 facilitates the translocation of XPA to UV damage sites as well (Coin *et al.*, 2006). In yeast, Tfb5 and its interaction with Tfb2 are required for efficient NER (Zhou *et al.*, 2007).TFIIH, a ten protein complex, not only plays an essential role NER, but also acts as a crucial component in transcription initiation and possibly in cell cycle regulation (Drapkin *et al.*, 1994b; van Vuuren *et al.*, 1994; Wang *et al.*, 1994; 1995; Conaway and Conaway, 1989; Serizawa *et al.*, 1995; Shiekhattar *et al.*, 1995; Sung et al., 1996). Detailed analysis suggests that XPC-hHR23B and TFIIH together are required for an initial opening of ~10 nucleotides, and that addition of XPG, RPA and XPA is needed to obtain full opening of ~25 nucleotides (Evans *et al.*, 1997a; 1997b). During the procedure of DNA strand opening, the transient open complex forms and includes the two separated strands around the DNA damage and all repair factors,

including TFIIH, XPA/Rad14, RPA, XPC-hHR23B/Rad4-Rad23, and XPG/Rad2 (Shown in Figure 1.4). However, one study revealed that XPC-hHR23B was effectively displaced from the damaged DNA by the combined action of XPA and RPA, suggesting that damage recognition occurs as a multistep process (You *et al.*, 2003). In addition to unwinding, TFIIH may have a structural role in the preincision complex, as premelted lesions still require TFIIH for repair (Mu and Sancar 1997; Mu *et al.*, 1997).

XPA/Rad14, a Zn^{2+} finger protein with a DNA damage binding property, has an important role at early stage of both TC-NER and GG-NER (Tanaka *et al.*, 1990; Bankmann *et al.*, 1992). As a core NER factor XPA recognises various NER specific types of damage including CPDs and (6-4) photoproducts and, in general, the affinity of XPA for a lesion correlates with the extent of helical distortion (Robins *et al.*, 1991; Jones and Wood 1993; Asahina *et al.*, 1994). It is reasoned that XPA may determine correct positioning of the opened DNA–protein preincision complex, because it can bind the DNA adduct in an open conformation and interacts with both TFIIH and RPA (Park *et al.*, 1995a; Nocentini *et al.*, 1997; He *et al.*, 1995; Li *et al.*, 1995b; Saijo *et al.*, 1996; Stigger *et al.*, 1998).

RPA, a heterotrimeric protein, may stabilize the unwound DNA intermediate by binding the undamaged strand in repair, and it is tempting to implicate the ssDNA-binding characteristics of RPA in the creation of a full open repair complex (Evans *et al.*, 1997b; Mu *et al.*, 1997; de Laat *et al.*, 1998). RPA was originally identified for its requirement in *in vitro* SV40 replication (Wobbe *et al.*, 1987; Wold

and Kelly, 1988; Wold *et al.*, 1989; Kenny *et al.*, 1990). On the basis of its dual involvement in replication and repair, so perhaps RPA not only acts at preincision stages but also during DNA repair synthesis. Although human RPA contains three subunits, which are 70, 32, and 14 KD polypeptide, binding of an RPA molecule to ssDNA involves the 70-KD subunit (Wold *et al.*, 1989; Gomes and Wold, 1996; Kim *et al.*, 1996). Within two identified binding modes, RPA interacts with a minimal region of 8–10 nucleotides (Blackwell and Borowiec, 1994) that is prior to the 30-nucleotide binding mode, which is 100-fold more stable than the former (Kim *et al.*, 1992; 1994; Blackwell *et al.*, 1996). Moreover, it is reported that the 5'-oriented side of RPA contains a strong DNA binding domain and this domain associates with 8-to 10-nucleotide DNA regions (Blackwell and Borowiec 1994; Blackwell *et al.*, 1996; de Laat *et al.*, 1998). The initial region of strand separation around the lesion created by TFIIH exposes ~10–20 nucleotides of the undamaged strand and this is an ideal docking site for the 5'-oriented side of RPA. After the 5'-oriented side of RPA binds to the ~10 nucleotides of unwound ssDNA, subsequent RPA stretching in the 3' direction contributes to the formation of a fully opened complex, which matches the observed ~30-nucleotide open intermediate. RPA may not only participate in forming a fully open repair complex, but also it is crucial for coordinating the positioning of the NER nucleases. Bound to the undamaged strand, the 3'-oriented side of RPA binds ERCC1–XPF, whereas the 5'-oriented side binds XPG (He *et al.*, 1995; Matsunaga *et al.*, 1996; Bessho *et al.*, 1997; de Laat *et al.*, 1998).

Although XPG/Rad2 is an endonuclease, it also plays a structural role in the

core NER reaction and in open complex formation. Evidence to support this comes from the experiments involving the D812A active-site mutant of XPG, which had to be present to detect ERCC1–XPF-mediated 5' incisions in an *in vitro*-reconstituted repair assay with purified factors (Mu *et al.*, 1997; Wakasugi *et al.*, 1997). Furthermore, this same XPG mutant was found to stabilize a preincision complex containing XPC–hHR23B, TFIIH, XPA, and RPA *in vitro*. Without XPG present, the preincision complex formed first is unstable and XPF-ERCC1 cannot bind to this DNA-protein complex. Moreover, XPG forms a stable protein complex with TFIIH and plays a role in maintaining the integrity of TFIIH in cooperation with XPD (Ito *et al.*, 2007). In cells from an XPG/CS patient, the mutations in the C-terminal of XPG gives rise to the dissociation of the cdk-activating kinase (CDK) subcomplex and XPD from the TFIIH core complex (Ito *et al.*, 2007).

Rad4-Rad23 is an essential factor for both RNA pol II-dependant TC-NER and GG-NER in yeast, but its homolog in human cells, XPC is dispensable for TC-NER (Gietz and Prakash, 1988, Mu and Sancar, 1997). The details of this complex are discussed later.

Dual incision

Endonucleolytic incisions are made asymmetrically around the lesion, with the 3' incision 2–8 nucleotides and the 5' incision 15–24 nucleotides away from the lesion, by the structure-specific endonucleases XPG (3' incision) and XPF– ERCC1 (5' incision) in human cells (O'Donovan *et al.*, 1994; Matsunaga *et al.*, 1995; Sijbers *et al.*, 1996, Huang *et al.*, 1992; Moggs *et al.*, 1996; Evans *et al.*, 1997a). In *S.*

cerevisiae, Rad1 and Rad10 form a complex, and the complex formation is essential for the biological function of these proteins. Rad1-Rad10 is a single-strand DNA endonuclease and acts in a structure specific manner to cleave 5'-ended single stranded DNA at its junction with duplex DNA (Bailly *et al.*, 1992; Tomkinson, *et al.*, 1993; Sung, *et al.*, 1993; Bardwell, *et al.*, 1994; Prakash and Prakash, 2000). In addition to their requirement in NER, the Rad1-Rad10 complex is required for a specific mitotic recombination pathway called single-strand annealing (Fishman-Lobel and Haber 1992).

Studies indicate that Rad2 shares strong sequence similarity with mammalian FEN-1, while XPG is also a member of the FEN-1 family. The members of the FEN-1 family were known as structure-specific endonucleases, which all cut with similar polarity at junctions of duplex and unpaired DNA. Rad2/XPG also possesses this single-strand DNA and structure-specific endonuclease activity (Habraken *et al.*, 1993; Harrington and Lieber, 1994). Like XPG, during NER in yeast Rad2 makes the 3' incision of the damaged strand around the lesion. Moreover, it is reported that incision of the damaged strand on the 3' side of a lesion usually occurs before 5' incision by ERCC1-XPF (O'Donovan *et al.*, 1994; Mu *et al.*, 1996).

Gap-filling DNA synthesis and ligation

RPA, is a NER factor that is required for both the incision and DNA synthesis stages of NER. It may remain bound to the unwound strand to facilitate repair synthesis. Repair synthesis needs both DNA Pol δ and Pol ε in yeast and human cells (Dresler and Frattini 1986; Nishida *et al.*, 1988; Hunting *et al.*, 1991; Coverley *et al.*,

1992; Budd and Campbell, 1995). Since PCNA serves as a processivity factor for these DNA polymerases with cooperation of replication factor C (RF-C), the combination of RPA, PCNA, RF-C (five subunits) and either Pol δ and Pol ε was sufficient for repair synthesis *in vitro* (Shivji *et al.*, 1992; 1995).

The final step in NER is ligation of the 5' end of the newly synthesized patch to the original sequence by DNA ligase I (Barnes *et al.*, 1992, Friedberg *et al*, 2006). There are three mammalian genes, LIG1, LIG3 and LIG4, which encode DNA ligase. DNA Ligase I is required for the joining of Okazaki fragments during lagging strand synthesis and is implicated in long-patch or replicative base-excision repair and nucleotide excision repair (Friedberg *et al.*, 2006; Mortusewicz *et al.*, 2006). Human DNA ligase I is a 102-KDa nuclear enzyme. The orthologous enzyme in *S. cerevisiae* is encoded by *CDC9*. The LIG1 cDNA can phenotypically correct temperature-sensitive mutants of *cdc9* (Barnes *et al.*, 1990). The DNA ligase I can be recruited to a proper site, which may be a DNA repair site or a DNA replication site, by interacting with PCNA (Montecucco *et al.*, 1995; Mortusewicz *et al.*, 2006)

1.2.2.2 Global genome NER (GG-NER)

GG-NER is responsible for repairing DNA lesions within non-transcribed DNA throughout the genome, and which in humans comprises the majority of the genome. Interestingly, the proteins that participate in GG-NER in yeast and human cells are apparently not conserved, unlike the majority of NER proteins. The specific factors that participate in GG-NER are Rad7-Rad16 in yeast, and DDB1/DDB2 in humans

(Bang *et al.*, 1992; Verhage *et al.*, 1994; Wang *et al.*, 1997; Reed *et al.*, 1998; Chu *et al.*, 1988). The rate of lesion removal alters for different types of lesions repaired via the GG-NER pathway, but TC-NER appears to repair different lesions at a similar rate (Mitchell *et al.*, 1989). It is thought that the reason for differences in the rates of lesion removal between GG-NER and TC-NER efficiency may be related to how these respective subpathways recognize DNA damage while the downstream stages of NER are similar.

Damage recognition

The DNA damage recognition process is perhaps the least well understood stage of the NER process. In budding yeast, Rad4-Rad23, Rad14, and RPA are all required for damage recognition in both TC-NER and GG-NER, while in human cells, XPC-hHR23B, XPA, RPA, XPE group (DDB1/DDB2) are involved in damage recognition during GG-NER (Prakash and Prakash, 2000; Batty and Wood, 2000).

In humans, XPC cells are less sensitive than other XP group cells to the lethal effects of UV, even though functional XPC protein is completely absent (Tyrell and Amaudruz, 1987). However, in yeast absence of Rad4 causes severe UV sensitivity as do mutations in genes for other core NER factors like Rad2 (Gietz *et al.*, 1988). From band-shift experiments, XPC (106KDa)-hHR23B (43KDa) only shows a modest preference for damaged DNA, but in the presence of non-damaged competitor DNA it can give a considerable preference for binding to damaged DNA (Reardon *et al.*, 1996; Wakasugi and Sancar, 1998; 1999). The yeast homologue Rad4 copurifies with Rad23 and shows a strong preference for damaged DNA binding in the presence of

non-damaged competitors (Guzder *et al.*, 1998; Jansen *et al.*, 1998). The XPC-hHR23B complex is thought to perform the crucial damage-sensing step within the GG-NER pathway and triggers subsequent association of TFIIH, XPG, XPA and RPA (Evans *et al.*, 1997b; Sugasawa *et al.*, 1998; Yokoi *et al.*, 2000; Volker *et al.*, 2001). The XPC complex has been found to copurify with TFIIH through several chromatographic steps and a similar co-purification of Rad4 has also been observed in yeast (Drapkin *et al.*, 1994a; Bardwell *et al.*, 1994). This implies that Rad4 may act in yeast in a similar way to XPC in human cells. A recent paper reported that ubiquitination of XPC after UV radiation by the UV-DDB-ubiquitin ligase complex may play a role in the transfer of the UV-induced lesion from UV-DDB to XPC (Sugasawa *et al.*, 2005). In yeast the steady state level of Rad4 is mediated by both Rad23 and Rad7/Rad16 after cells are exposed to UV light. It was suggested, that Rad7/Rad16 might act as an E3 ubiquitin ligase that regulated Rad4 levels after UV (Ramsey *et al.*, 2004).

The XPA protein was the first human NER protein supposed to be a damage recognition factor during NER (Robins *et al.*, 1991). Both XPA and its yeast homologue Rad14 have a preference for binding to damaged DNA (Jones and Wood, 1993; Asahina *et al.*, 1994; Bankmann *et al.*, 1992; Guzder *et al.*, 1993). As shown by analysis of the NMR spectra of the XPA-DNA complex, XPA binds DNA in a cleft lined with basic residues, and which is large enough to accommodate either single- or double-stranded DNA (Ikegami *et al.*, 1998). Furthermore, XPA can bind to various lesions caused by UV light and cisplatin with different affinities that correlate with the

extent of helical distortion associated with it (Robins *et al.*, 1991; Jones and Wood, 1993; Asahina *et al.*, 1994; Wakasugi and Sancar, 1999) and XPA prefers to bind with partially duplex DNA instead of single-strand substrates of the same length (Buschta-Hedayat *et al.*, 1999).

Two subunits of RPA, 70kDa and 34 kDa, have been shown to interact with XPA, and this may increase their affinity for damaged DNA (Li *et al.*, 1995a; Saijo *et al.*, 1996; He *et al.*, 1995; Wakasugi and Sancar, 1999). RPA itself also has a damage binding ability and it has been proposed to be involved in DNA damage recognition (Clugston *et al.*, 1992; He *et al.*, 1995, Saijo *et al.*, 1996). However, on the basis that RPA is anticipated to bind the undamaged strand during TC-NER and GG-NER, RPA may not directly recognize the lesion itself but, rather it has an affinity for single-stranded regions exposed by lesion-induced helical distortion (de Laat *et al.*, 1998).

UV-DDB is a heterodimeric protein complex composed of a 127 kDa subunit (DDB1) with variable amounts of a 48 kDa subunit (DDB2) (Hwang and Chu, 1993; Keeney *et al.*, 1993), and it has a relativly high specific binding to UV-induced DNA damage (Feldberg and Grossman, 1976). Moreover, it also can recognize DNA damage by cisplatin, nitrogen mustard, denaturation and depurination (Chu and Chang, 1988; Payne and Chu, 1994). The DDB1/DDB2 complex was first identified as having an accessory role in repair of UV-damaged DNA. In a reconstituted *in vitro* NER system without DDB, addition of DDB1 to the reconstituted reactions stimulated repair synthesis only two fold and in another dual incision system had no effect

(Aboussekhra *et al.*, 1995; Kazantsev *et al.*, 1996). However, *in vivo* microinjection of purified DDB protein to XPE cells restored the NER activity (Keeney *et al.*, 1994) and DDB2 also enhances GG-NER *in vivo* (Tang *et al.*, 2000). The evidence above has led to the suggestion that UV-DDB may play a role in damage recognition during GG-NER in a chromatin context. Studies have revealed that UV-DDB is subject to a complex regulatory mechanism (Otrin *et al.*, 1997; Liu *et al.*, 2000; Shiyanov *et al.*, 1999; Groisman *et al.*, 2003; Sugasawa *et al.*, 2005; Matsuda *et al.*, 2005). After cell exposure to UV radiation, the DDB complex binds tightly to damaged chromatin. Then, DDB2 is directly ubiquitylated by the Cullin 4A based ubiquitin ligase complex and degraded rapidly. However, well after repair is completed, the DDB2 mRNA level spikes to around 3-fold higher than in untreated cells. Furthermore, two complexes, which differ only in that one complex contains DDB2 while the other contains CSA, are found to display ubiquitin E3 ligase activity in response to UV damage, and both contain DDB1 (Groisman *et al.*, 2003). Since this report, one substrate of the DDB2 ubiquitin E3 ligase complex has been identified as XPC, which is ubiquitylated by the DDB2 complex following UV irradiation (Sugasawa *et al.*, 2005).

In the *S. cerevisiae*, Rad7 and Rad16 physically interact and both are specifically GG-NER proteins (Bang *et al.*, 1992; Verhage *et al.*, 1994; Wang *et al.*, 1997). The repair of nontranscribed DNA strands and of transcriptionally inactive regions is severely reduced in *ΔRad7* and *ΔRad16* mutants, whereas the repair of transcribed strands is not affected (Verhage *et al.*, 1994; Mueller and Smerdon, 1995). Rad7 does not appear to have a DNA binding activity while Rad16 contains two

potential zinc finger DNA binding motifs, a C_4 motif and a C_3HC_4 ring finger motif (Prakash and Prakash, 2000). It has been suggested that a complex of Rad7 and Rad16 plays a role in DNA damage recognition (Guzder *et al.*, 1997). However, the same authors also show that the Rad7/Rad16 complex is not essential for incision in their reconstituted NER assay. Furthermore, Reed *et al* show that the Rad7/Rad16 genes are not crucial for the early stages of GG-NER including bi-modal incision, but are involved in the stages after incision during GG-NER (Reed *et al.*, 1998; Guzder *et al.*, 1997; 1998). Yeast autonomously replicating sequence binding factor 1 (ABF1) copurifies with the Rad7/Rad16 complex through multiple chromatographic steps and participates in NER (Reed *et al.*, 1999). Sequence analysis of Rad16 reveals that it is a member of SWI/SNF superfamily, the Rad7/Rad16/ABF1 generates super helical torsion using the Rad16's ATPase function, and this facilitates the removal of lesions during the excision stage of the NER process (Peterson and Workman, 2000; Yu *et al.*, 2004). Apart from this core GG-NER function, the work described later in this thesis identifies a novel function of the Rad7/Rad16/ABF1 complex (see later).

Clearly, the process of damage recognition during GG-NER is complex and multiple proteins participate, both in yeast and in human cells. Since there is a wide substrate range, it has been suggested that the relatively small number of potential recognition factors involved in NER does not account for the recognition of the lesion directly, since there appears to be no common features in the chemistry of the broad spectrum of lesions that are recognised by NER. It has also been proposed that damage recognition during NER involves detection of changes in the DNA backbone

caused by damage. However, the precise mechanism of DNA damage recognition during NER remains unclear.

A common repair mechanism occurs in TC-NER and GG-NER following damage recognition

In yeast, after a lesion is recognized by damage binding proteins, Rad14, Rad4-Rad23, RPA, and other NER factors are recruited to the damage site, the remaining steps of the process continue as described for the TC-NER pathway.

In human cells the first protein binding to CPDs, appears to be UV-DDB since the efficiency of CPD removal is dramatically increased by this factor during GG-NER (Tang *et al.*, 2000; Sugasawa *et al.*, 2005). The other proteins that are also likely to promote DNA damage recognition are XPA-RPA, XPC-hHR23B and the DDB complex, the remaining step of the reaction being common to both pathways.

1.2.3 Base-Excision repair (BER)

BER is a major guardian against DNA lesions caused by cellular metabolism, which may arise from cellular hydrolytic events such as deamination or base loss, oxygen free radical attack or the methylation of ring nitrogens by endogenous agents (Lindahl, 1993; Hoeijmakers, 2001). A battery of DNA glycosylases, each dealing with a relatively narrow, partially overlapping spectrum of lesions, play a role as the initiator of BER. During the first stage of BER, a glycosylase catalyses the hydrolysis of the N-glycosyl bond linking a modified base to the deoxyribose-phosphate chain to excises the base residue in the free form (Wood, 1996). Some glycosylases not only

remove the damaged base, but also cleave off the base by a lyase mechanism and catalyze a subsequent AP lyase reaction. Generally, lyase reactions are associated only with glycosylases that deal with oxidized bases (Friedberg *et al*, 1995; Sancar *et al.*, 2004).

Following the lyase reaction, the 3' cleaved deoxyribose residue is replaced by an AP endonuclease incising 5' to the abasic sugar to form a gap that is filled by DNA polymerase, and the resulting nick is ligated. When the glycosylase lacks lyase activity, an enzyme known as APE1 in mammals (XthA in *E. coli*) can make a 5' incision to the abasic sugar, and then the abasic sugar can be removed by a dRP lyase activity associated with DNA Polβ, which concurrently fills in the 1-nucleotide gap (Matsumoto and Kim, 1995; Beard and Wilson, 2000, Friedberg *et al.*, 2006). The two mechanisms described above are referred to as short-patch BER.

During long-patch BER, an alterative mechanism also employing APE1, can make 5' incisions at the AP site, and subsequently a flap of 2-10 nucleotides is generated by the activity of DNA Polδ/ε, PCNA, and FEN1. After the flap is cut at the junction of the single to double-strand transition by FEN1, a patch of the same size is filled following DNA synthesis by DNA Polδ/ε with the aid of PCNA, and the strand is ligated by DNA ligase I (Frosina *et al.*, 1996; Klungland *et al.*, 1997).

1.2.4 Other DNA repair pathways

Double-strand breaks (DSBs) are not only generated by ionizing radiation, reactive oxygen species, and some chemicals that can produce reactive oxygen

species, but also occur abnormally during replication as a consequence of replication fork arrest and collapse. They are also normally generated by V(D)J recombination and immunoglobulin class-switching processes. If DSBs are unrepaired or misrepaired they can initiate events leading to mutagenesis, tumorigenesis and cell death. They are repaired either by homologous recombination (HR) or nonhomologous end-joining pathways. Some of the key proteins are conserved from yeast to humans e.g. Ku70, Ku80, XRCC4, ligase IV, *etc.* (Rouse and Jackson, 2002; Khanna and Jackson, 2001; Sancar *et al.*, 2004; Hoeijmakers, 2001; Lombard *et al.*, 2005). HR seems to dominate in cell cycle stages S and G2 when a second copy of the sequence (a sister chromatid) is present. In contrast, the less-accurate NHEJ is most relevant in the G1 phase of the cell cycle, when a second copy is not available (Hoeijmakers, 2001).

Among the six DNA repair pathways, the general DNA mismatch repair (MMR) pathway is responsible for correcting base substitution mismatches and insertion-deletion mismatches generated during DNA replication. It operates in organisms ranging from bacteria to mammals. In essence, MMR repairs nucleotides mismatched by DNA polymerases and insertion/deletion loops (ranging from one to ten or more bases), which result from slippage during replication of repetitive sequences or during recombination (Hoeijmakers, 2001; Kunkel and Erie, 2005). MMR proteins participate in a wide variety of DNA transactions, such that their inactivation can have a profound biological consequence to cells or organisms. One certain consequence is that the rate of point mutations dramatically increases

genome-wide to give rise to genetic variation in cells. Bacteria may benefit from this mechanism because the genetic variation provides a chance to adapt to environmental changes. In mammals, the loss of MMR activity has been clearly demonstrated to contribute to the initiation and promotion of multistage carcinogenesis (Loeb *et al.*, 2003; Kunkel and Erie, 2005).

1.3 The ubiquitin-proteasome pathway and NER

Eukaryotes contain a highly conserved multi-enzyme system that covalently links ubiquitin or polyubiquitin chains to a variety of intracellular proteins. The precise nature of the ubiquitin modification of protein substrates appears to act as a signal for the eventual fate of the protein (Ciechanover *et al.*, 1980; 1994; Varshavsky, 1997; Glickman and Ciechanover, 2002; Pickart, 2004). For example, proteins with a polyubiquitin chain normally are degraded by the 26S proteasome, a large ATP-dependent protease. However, monoubiquitin-modified proteins can result in a specific signal that does not necessarily result in the proteolytic degradation of the target protein. How this signal is recognized by cells remains poorly understood even now (Pickart, 2004).

Ubiquitin, a 76-amino acid residue protein, exists in the cell either free or covalently linked to other proteins. Its sequence is highly conserved from yeast to humans (Varshavsky, 1997). In yeast, ubiquitin is encoded by four genes, (*UBI1, UBI2, UBI3,* and *UBI4*) and has an unusual mode of synthesis (Hanna *et al.*, 2007). *UBI1, UBI2 and UBI3* encode fusions of ribosomal proteins to the C terminal of

ubiquitin, while the product of *UBI4* contains five head-to-tail repeats of ubiquitin (Ozkaynak *et al.*, 1984). The generation of free ubiquitin requires the translation of a fusion protein and a post-translational cleavage of ubiquitin at its C-terminus by deubiquitinating enzymes (Ozkaynak *et al.*, 1987; Finley *et al.*, 1987).

Conjugation of ubiquitin to proteins generally occurs through a hierarchical series of steps. Ubiquitin is activated by an ubiquitin-activating enzyme (Uba/E1), which couples ATP hydrolysis to the formation of a high-energy thiol ester intermediate with a covalent bond between Gly76 of ubiquitin and a specific Cys residue of E1 (Hershko *et al.*, 1983). Following activation, E2 (ubiquitin carrier protein or ubiquitin- conjugating enzyme (Ubc) transfers ubiquitin from E1 to the substrate with the participation of an ubiquitin ligase E3, which recognizes and binds to the substrate. Finally, between the activated C-terminal Gly of ubiquitin and a ε-NH_2 group of a Lys residue of the substrate forms an isopeptide to yield an ubiquitinated protein (Ciechanover, 1994). Then, additional ubiquitin molecules can be attached to the protein with the promotion of ubiquitin chain assembly factors (E4) to form a polyubiquitin chain, which targets the protein to the 26S proteasome (Koegl *et al.*, 1999; Hofmann and Pickart, 1999). Ubiquitin-dependent pathways have been shown to play a major role in a legion of biological processes, including the stress response, transcription, cell cycle, apoptosis, signal transduction, DNA repair, and cell differentiation (Salghetti *et al.*, 2001; Gillette *et al.*, 2004; Reed and Gillette, 2007; Kodadek et al., 2006; Mukhopadhyay and Reizman, 2007; DeMartino and Gillette, 2007).

Rad6, the key component of Rad6-dependent post-replication DNA repair, is an ubiquitin-conjugating enzyme (E2) (Jentsch *et al.*, 1987). This observation was the first evidence that the ubiquitin-proteasome pathway is linked to DNA repair.

The proteolysis-independent regulation of the proteasome during NER

Rad23 is considered to be one of the multiple proteins that make up the NER machinery in *Saccharomyces cerevisiae*. Deletion of the *RAD23* gene results in moderate UV sensitivity that is intermediate between that of wild-type strains and strains deleted for other core NER genes, such as *RAD1* or *RAD2* (Watkins *et al.*, 1993; Mueller and Smerdon, 1996). The rate of UV-induced lesion removal significantly decreases in *Δrad23* cells *in vivo* and extracts of these cells are defective for NER *in vitro* (Mueller and Smerdon, 1996; Wang *et al.*, 1997).

Rad23 has a specific N-terminal ubiquitin-like [Ubl] domain with significant amino acid identity and similarity to ubiquitin. Furthermore, the ubl domain can be functionally replaced by the actual ubiquitin sequence (Watkins *et al.*, 1993). The ubiquitin-like (Ubl) domain is required for optimal Rad23 function *in vivo*, because deletion of this domain of Rad23 results in a level of UV radiation sensitivity intermediate between that observed in wild type and *Δrad23* complete deletion strains. Moreover, GST-Rad23 fusion protein physically interacts with components of the 26S proteasome and the Ubl domain is needed for this interaction (Schauber *et al.*, 1998). Based on these observations, it was suggested that the Ubl domain of Rad23 mediates an interaction of the NER repair machinery with the proteasome which resulted in the degradation of Rad23 by the proteasome. This was thought to be a mechanism that

might regulate NER by dissociating or recycling NER complexes during NER (Schauber *et al.*, 1998).

Typically, the 26S proteasome contains a previously identified 20S core proteasome and two copies of a 19S regulatory complex comprised of multiple ATPases which can associate with both ends of the 20S proteasome (Orlowski and Wilk, 1981; Groll *et al.*, 1997; Gray *et al.*, 1994; Jentsch and Schlenker, 1995). However, the composition of subunits of the proteasome is altered in response to changing physiological demands (Glickman and Raveh, 2005; Hanna *et al.*, 2007; DeMartino and Gillette, 2007). Two sub-complexes of the 26S proteasome play different roles during the degradation of proteins. The 20S core particle, a barrel-shaped protein complex, is composed of two copies of 14 subunits (α1-7 and β1-7) and confers the proteolytic activities of the proteasome (Baumeister *et al.*, 1998; DeMartino and Gillette, 2007). In *S. cerevisiae*, the 19S regulatory complex contains at least 17 subunits, which can bind substrate-linked polyubiquitin chains, unwind the proteins and translocate the polypeptide chains into the 20S core cylinder (Glickman *et al.*, 1998). Among these subunits, there are six homologues (Rpt1-6) of AAA (ATPases associated with a variety of cellular activities) ATPases, which are believed to facilitate unfolding of substrates to permit their passage through the proteolytic chamber of the proteasome (Weissman *et al.*, 1995, Rubin and Finley, 1995). Moreover, Three non-ATPase subunits (Rpn1, 2, and 13) associate with 6 triple ATPase subunits to form a subcomplex termed the "base" while the remaining subunits of 19S regulatory complex constitute a separate subcomplex termed the "lid"

(DeMartino and Gillette, 2007).

Using NER-competent extracts, two ATPase components of the 19S regulator complex, Sug1/Rpt6 and Sug2/Rpt4, can coimmunoprecipitate with Rad23 but subunits of the 20S core particle do so much less efficiently (Russell *et al.*, 1999). Only the interaction of the 19S regulator complex and the Ubl domain of Rad23 is required for optimal NER activity *in vitro*, while the proteolytic functions of the proteasome are dispensable for NER *in vitro*. Inhibition of Sug1/Rpt6 and Sug2/Rpt4 or deletion of Ubl domain of Rad23 results in defective NER *in vitro* but when the Ubl domain of Rad23 is deleted, inhibition of Sug1/Rpt6 does not diminish NER *in vitro* any further, indicating that the effect of Sug inhibition on NER requires an interaction with the Ubl domain of Rad23 (Russell *et al.*, 1999). These observations revealed a novel non-proteolytic function of the 19S regulator complex required for the regulation of NER.

Further studies on the 19S regulator complex shows that it can affect NER *in vivo* in the absence of Rad23 protein (Lommel *et al.*, 2000b; Gillette *et al.*, 2001). This indicated that the Ubl domain of Rad23 didn't simply recruit the proteasome to the NER machinery, but rather mediated functional interactions between the two. In contrast, strains with mutations in 20S subunits that are severely defective in proteolysis, have no observable effect on NER *in vivo* irrespective of the presence of Rad23 (Gillette *et al.*, 2001). Observations that mutations in the 19S ATPases Sug1 and Sug2 can partially enhance UV survival and NER *in vivo* in the absence of Rad23 indicate that the 19S regulator complex negatively modulates the rate of NER *in vivo*

in the absence of Rad23 (Gillette *et al.*, 2001). Hence, the Ubl domain of Rad23 plays a role in modulating the negative regulation of NER by the 19S regulator complex.

Several groups have investigated whether Rad23 plays a proteolytic role in down-regulating NER. Rad23 and related proteins that contain Ubl domains can also bind to a component of the 26S proteasome, Rpn1 (Elsasser *et al.*, 2002). Rad23 can inhibit poly-ubiquitylation of H2B *in vitro* and the degradation and abundance of model substrates *in vivo* in an Ubl domain independent manner (Ortolan *et al.*, 2000). This is consistent with the observation that proteins (including Rad23) with Ubl domains often contain ubiquitin-associated (UBA) domains that bind poly-ubiquitinated proteins and inhibit 26S proteasome-catalyzed proteolysis (Hoffmann and Bucher, 1996; Bertolaet *et al.*, 2001a; 2001b; Chen *et al.*, 2001; Wilkinson *et al.*, 2001; Raasi and Pickart, 2003). In mHR23A/B double-mutant cells, stable expression of hXPC-GFP appear to rescue the UV sensitivity of these cells (Ng *et al.*, 2003). Collectively, these observations led to a model in which Rad23 was thought to enhance NER through inhibiting NER factors from proteolysis by the proteasome. Based on an observation that over-expression of Rad4 could result in enhanced NER and UV survival, it was suggested that Rad4 was a NER limiting factor whose levels were regulated by proteolysis. This model predicted an important proteolytic role of the proteasome in NER. Later this model was apparently supported by the observation that Rad4 steady state protein levels are influenced by Rad23 in *S. cerevisiae* (Ortolan *et al.*, 2004), and it was assumed that the Rad4 steady state level was regulated by changes in the half-life of Rad4 in the presence or absence of Rad23.

This led to the notion that the primary role of Rad23 in NER involved regulating the steady state levels of Rad4. However, it was subsequently shown that constant overexpression of Rad4 protein only slightly enhances UV resistance of *Δrad23* mutant cells (Xie *et al.*, 2004). Purified Rad4 cannot complement the deficient NER of *Δrad23* cell-free extracts *in vitro*, even at a high concentration of Rad4 (Wang *et al.*, 1993; Xie *et al.*, 2004). Taken together, the current data do not support a major role for proteolysis in regulating NER in *S. cerevisiae*.

Ubiquitination of Rad4/XPC

Rad4, one of the yeast NER core factors, binds to Rad23 as its human homologue XPC does with hHR23B (Gietz *et al.*, 1988; Wang *et al.*, 1997; Masutani *et al.*, 1994). The Rad4-Rad23 complex shows a preferential binding activity to damaged DNA in the presence of non-damaged competitor. (Guzder *et al.*, 1998; Jansen *et al.*, 1998). A physical interaction between the Rad4-Rad23 complex and the Rad7/Rad16 complex is observed in the yeast two-hybrid *in vivo* system, in which Rad7 interacts with Rad4 directly (Wang *et al.*, 1997). The Rad7/Rad16 complex not only possesses core NER functions [as described earlier] (Yu *et al.*, 2004), but is also shows a putative novel E3 ligase function on a Rad4 substrate (Ramsey *et al.*, 2004; Gillette *et al.*, 2006). Rad16 contains a zinc finger DNA binding domain, so it may act as a ring finger protein that interacts with ubiquitin-conjugating enzymes (Ubc/E2) during the ubiquitination pathway (Joazeiro and Weissman, 2000; Lorick *et al.*, 1999). It has been suggested that Rad7 bears similarity to substrate recognition subunits of SCF-type E3 ubiquitin ligases and 12 C-terminal leucine rich repeats (Ramsey *et al.*,

2004; Schneider and Schweiger, 1991). Elc1, the yeast homologue of a mammalian Elongin C, might participate in the ubiquitination of Rad4 with binding to the Rad7/Rad16 complex (Kamura *et al.*, 2001; Ho *et al.*, 2002; Ramsey *et al.*, 2004). Rad4 levels are regulated by a Rad7/Rad16/Elc1 complex through a proteolytic function of the ubiquitin-proteasome pathway following UV irradiation (Ramsey *et al.*, 2004). The precise details of this putative novel E3 ubiquitin ligase and its role in regulating NER is the primary subject of this thesis.

XPC forms a heterotrimeric complex with binding to hHR23B, one of two human homologues of yeast Rad23, and Centrin 2 (CEN2) *in vivo* (Araki *et al.*, 2001; Masutani *et al.*, 1994). In the GG-NER pathway XPC-hHR23B plays a crucial role at an early stage including damage recognition and recruitment of other NER factors such as TFIIH, RPA, *etc.* (Sugasawa *et al.*, 2001; 2002; Volker *et al.*, 2001).

DDB2 and CSA are respectively integrated into two protein complexes containing at least 11 polypeptides via interaction with DDB1 (Groisman *et al.*, 2003). The two complexes all contain Cullin 4A, Roc1, and the COP9 signalosome (CSN), and display ubiquitin ligase activity (Groisman *et al.*, 2003). The CSN negatively regulates the two complexes in a different way in response of DNA damage (Groisman *et al.*, 2003). One of the substrates of the complex containing DDB2 is the GG-NER factor XPC (Sugasawa *et al.*, 2005). The ubiquitination of XPC occurs after exposure to UV, and this is consistent with Groisman's observation that shows CSN disassociation from the complex containing DDB2 to activate their ubiquitin ligase function following UV irradiation (Groisman *et al.*, 2003; Sugasawa *et al.*, 2005).

Moreover, DDB2 itself is also ubiquitinated by the Cullin 4A complex and is degraded quickly after UV radiation (Rapic-Otrin *et al.*, 2002; Matsuda *et al.*, 2005). It has been suggested that ubiquitination of XPC might enhance the affinity of XPC for a specific DNA damage, (6-4) photoproducts. The degradation of DDB2 may give the site to ubiquitinated XPC following its recruitment, while the UV-DDB-ubiquitin ligase complex plays a role in transfer of a UV-induced lesion from the early sensor UV-DDB to ubiquitined XPC (Sugasawa *et al.*, 2005; Matsuda *et al.*, 2005).

Recently, it has been suggested that DDB1 and CUL4-associated factors (DCAFs) regulate a broad spectrum of cellular process by functioning as substrate receptor (Lee and Zhou, 2007), while different DCAFs, including DDB2 and CSA, and the Cul4-DDB1 core complex are assembled to target distinct cellular substrate for ubiquitination (Lee and Zhou, 2007).

1.4 Chromatin remodeling factors related to NER

It has been demonstrated that *in vitro* repair of some NER substrates, including CPDs, (6-4) photoproducts, and N-acetoxy-2-acety-aminoflurence (AAF) adducts, is dramatically reduced *in vitro* on DNA substrates assembled into nucleosomes (Wang *et al.*, 1991; Thoma, 1999; Hara and Sancar, 2000; Ura *et al.*, 2001; Wang *et al.*, 2003). This implies that efficient NER can be achieved *in vivo* via the activity of chromatin remodeling enzymes that facilitate the removal of lesions from chromatin (Reed, 2005). There are two classes of highly conserved proteins that regulate the accessibility of DNA in chromatin known as chromatin-remodeling/modification enzymes (Peterson and Côté, 2004; Fischle *et al.*, 2003; Kurdistani and Grustein,

2003; Lusser and Kadonaga, 2003).

One class of chromatin-remodeling/modification enzymes catalyzes the covalent attachment or removal of posttranslational histone modifications (e.g., lysine acetylation, serine phosphorylation, lysine and arginine methylation, lysine ubiquitylation, *etc.*). The nucleosome comprises an octamer of core histones, a tetramer of histones H3 and H4 and two dimers of histones H2A and H2B, with 147 base pairs of DNA wrapped around them in 1.75 left-handed superhelical turns (Kornberg and Lorch, 1999). A N-terminal "tail" domain of 20-35 amino acid residues in length of each histone stretches from the surface of the nucleosome and provides the majority of sites for histone posttranslational modification.

In addition to histone-modifying enzymes, a distinct class of chromatin-remodeling/modification enzymes comprises a family of related ATP-dependent complexes that use the free energy derived from ATP hydrolysis to enhance the accessibility of nucleosomal DNA (Vignali *et al.*, 2000). This class contains three subgroups that are SWI/SNF, ISWI and Mi-2/CHD families.

Histone acetylation and NER

Early work from Smerdon and Lieberman illustrated that chromatin structure is altered during UV induced DNA synthesis in mammalian cells and treatment of human cells with butyrate, a histone deacetylase inhibitor gives rise to increased levels of histone acetylation and rapid NER (Smerdon and Lieberman, 1978; Smerdon *et al.*, 1982). More recent work in yeast, showed chromatin is hyperacetylated after exposure to UV light without requirement of the NER damage recognition proteins

Rad4 and Rad14, suggesting that chromatin remodeling may occur prior to NER initiation, perhaps in response to DNA damage, although the precise mechanism is currently unknown (Yu *et al.*, 2005; Teng *et al.*, 2005). This observation is coincident with the *in vivo* repair of UV-damaged chromatin being associated with increased levels of histone acetylation in human cells (Brand *et al.*, 2001). Acetylation of lysines in the N-terminal domain of histones neutralizes their positive charge, decreasing interactions with DNA and histone-histone interactions between neighboring nucleosomes (Luger *et al.*, 1997; Deckert and Struhl, 2001).

In yeast, the histone acetyltransferase (HAT) Gcn5 is important for the expression of a subset of genes, so mutation of the Gcn5 catalytic domain results in eliminating or significantly reducing the transcription and the acetylation of histones (Georgakopoulos and Thireos, 1992; Brownell *et al.*, 1996; Kuo *et al.*, 1996). Two distinct multiprotein complexes, ADA and SAGA, have been found to both contain Gcn5 (Grant *et al.*, 1997). Deletion of *GCN5* causes diminished NER *in vivo*, possibly due to the partial loss of chromatin remodelling activity via reduced acetylation of histones (Teng *et al.*, 2002; Yu *et al.*, 2005).

Although the post-translational modification of histone tails can affect the state of chromatin compaction (Shogren-Knaak *et al.*, 2006), a notion suggested that these modifications indirectly alter chromatin structure by affecting the binding of non-histone effector proteins that have the capacity to change histone-DNA contact in chromatin (Downs *et al.*, 2007).

In human cells, TFTC, a complex highly similar to the yeast SAGA complex,

has been shown to contain a protein SAP130 which is 50.7% similar to DDB1, a component of the UV-DDB complex (Will *et al.*, 1999; Brand *et al.*, 2001; Green and Almouzni, 2003). Because TFTC subunits are recruited in parallel with a core NER factor XPA, it may participate in NER utilising its chromatin remodeling function (Brand *et al.*, 2001). The UV-DDB complex including DDB1 and DDB2, and the SAP130 are included in a Gcn5-containing HAT complex, STAGA (Martinez *et al.*, 2001). Moreover, UV-DDB also associates with the CBP/p300 family of histone acetyltransferases (Datta *et al.*, 2001). It was suggested that DDB2 together with STAGA is responsible for targeting histone acetyltransferase activity to specific damage DNA sites.

Chromatin remodeling: the link to NER

SWI/SNF, ISWI, and Mi-2/CHD are three groups of ATP-dependent chromatin remodeling family proteins based on their biochemical properties and the overall sequence similarity of their ATPase subunits (Boyer *et al.*, 2000).

It has been shown that AAF adducts present on a 200-bp mononucleosome substrate, are more readily removed by a human excision nuclease in an *in vitro* assay in the presence of yeast SWI/SNF complex, whereas no such stimulation is observed on naked DNA (Hara and Sancar, 2002). However, the repair of CPDs seems to be unaffected even in the presence of SWI/SNF complex *in vitro* (Hara and Sancar, 2003). Interestingly, SWI/SNF and ISW2 can stimulate the repair of CPDs through the photoreactivation pathway *in vitro* (Gaillard *et al.*, 2003).

Although the SWI/SNF family is thought to stimulate repair through the

GG-NER pathway, CSB, a member of the SWI2/SNF2 family, is believed to be the ATP-dependent chromatin-remodeling enzyme associated with TC-NER in human cells (Citterio *et al.*, 2000). The DNA accessibility of a chromatin substrate can be enhanced via stimulation of the CSB proteins *in vitro* (Citterio *et al.*, 2000). More recent work demonstrated that two subunits of the SWI/SNF chromatin-remodeling complex in yeast, Snf6 and Snf5, copurified with the Rad4/Rad23 complex. Moreover, the interaction between them was enhanced after UV treatment. Since the UV-induced nucleosome rearrangement at the silent *HML* locus is dependent on the activity of SWI/SNF, it was suggested that the SWI/SNF chromatin-remodeling complex is recruited to a DNA lesions by the damage-recognition complex to increase DNA accessibility for NER in chromatin (Gong *et al.*, 2006).

In yeast, the core function of Rad7/Rad16 may have an important role in repairing DNA damage in chromatin that is independent of their E3 ligase activity. Rad16 protein belongs to the SWI/SNF family of chromatin remodelling factors as revealed by sequence analysis (Bang *et al.*, 1992; Ramsey *et al.*, 2004; Reed *et al.*, 2005). Reed *et al.* demonstrated that NER competent extracts prepared from rad7/rad16 mutants were defective in NER *in vitro* by measuring DNA repair synthesis, a late stage of the NER reaction. They also noted a requirement for Rad7 and Rad16 even when naked DNA was used as the substrate (Reed *et al.*, 1998). This meant that one fundamental activity of Rad7/Rad16 was at the level of DNA rather than at the level of nucleosomes or chromatin, at least in the context of the *in vitro* cell free system they used. They also noted that when preassembled nucleosomal

substrates are used as *in vitro* NER substrates, NER is completely inhibited even in the presence of the Rad7/Rad16 complex (Reed *et al.*, 2005). It is clear that the chromatin remodeling process needs some other factor[s] working possibly in combination with the Rad7/Rad16 complex to facilitate NER in nucleosome assembled DNA. Work from our group shows that GG-NER complex, containing Rad7, Rad16, and ABF1, is capable of generating negative supercoiling in DNA through the ATPase activity of Rad16 (Yu *et al.*, 2004). The generation of supercoiling in the DNA by the GG-NER complex is crucial for the excision of the damage containing oligonucleotide during GG-NER (Yu *et al.*, 2004). However, our recent work (Teng *et al.*, in press) shows that Rad16 is needed *in vivo* for post-UV histone hyperacetylation. Hence, it is possible that Rad16 participates in more than one event during NER. It is indeed that our understanding of the precise mechanism of NER in chromatin is still at an early stage.

Chapter 2

Materials and Methods

In this chapter, general techniques related to cell culture, UV treatment, isolation of genome DNA and total RNA, detection of them, preparation of whole cell extraction, purification of protein complex, and protein analysis are described in detail. Moreover, several specific methods only employed for this research are also illustrated in this chapter.

2.1 Yeast strains and plasmid

The haploid *S. cerevisiae* strains used in this study are listed in Table 2.1.

Table 2.1 *S. cerevisiae* strains used in this thesis.

Strain	Genotype	Source
YPH/RAD7:6His		Reed *et al.*, 1998
WCG4a	MATa ura3 leu2-3, 112 his-11, 15 CanS Gal$^+$	Hilt *et al.*, 1993
YH129/14	WCG4a pre1-1 pre4-1	Hilt *et al.*, 1993
BY4741	MATa his3Δ1 leu2 Δ 0 met15 Δ 0 ura3 Δ 0	Dr. Thomas G Gillette
2782	BY4741 *Δelc1*	Dr. Thomas G Gillette
1982	BY4741 *Δela1*	Dr. Thomas G Gillette
4633	BY4741 *Δcul3*	Dr. Thomas G Gillette
WH201R23	W303-1A *sug2-1 rad23*::HIS3	Gillette *et al.*, 2001
Sc507	MATa T7-SUG1 ade2–1 trp1–1 leu2–3, 112 his3–11, 15 ura3–1 can1–100 [W303-1A S10-SUG1]	Russell *et al.*, 1999
Sc507R7	Sc507 Δ*rad7*	Dr. Simon H Reed
Sc507R23	Sc507 Δ*rad23*	Gillette *et al.*, 2001
Sc507R7pRAD7	Sc507 Δ*rad7* pRS314-Rad7	Dr. Simon H Reed
Sc507R7psocs	Sc507 Δ*rad7* pRS314-Rad7 (L168A and C172A)	Dr. Simon H Reed
Sc507R7R23 pRAD7	Sc507 Δ*rad23* Δ*rad7* pRS314-Rad7	This study
Sc507R7R23 psocs	Sc507 Δ*rad23* Δ*rad7* pRS314-Rad7 (L168A and C172A)	This study
WH201R23R7 pRAD7	W303-1A *sug2-1 rad23*::HIS3 Δ*rad7* pRS314-Rad7	This study

WH201R23R7 psocs	W303-1A *sug2-1 rad23*::HIS3 Δ*rad7* pRS314-Rad7 (L168A and C172A)	This study

Following the *RAD7* gene in WH201R23 were deleted, pRS314 contained *RAD7* gene or SOCS mutated *RAD7* (Gillette *et al.*, 2006) was transferred into this strain to create two stains, that were pRAD7/*Δrad23/sug2-1* and psocs/*Δrad23/sug2-1* strains.

2.2 Storage and growth conditions

The strains in use were stored and grown in their appropriate medium including the yeast complete medium (YC), minimal medium, and synthesis medium (see Appendix).

For long period storage, yeast cells in exponential phase were frozen in medium containing 30% glycerol and kept at -70° C. When strains were needed for experiments, a fresh preculture was made from the stock by inoculating 25 ml of medium. This culture was then incubated at 30°C with shaking, allowing it to reach stationary phase and subsequently stored at 4°C. The requirements for large scale cultures for repair experiments were met by inoculating fresh medium overnight with this stationary phase liquid culture, also at 30°C and under continued shaking. The amount of preculture used was empirically calibrated so as to achieve a cell density between 2 and 4×10^7 cells/ml by the next morning.

The growth media, all the glassware, cylinders and other containers for storage or growth of the yeast cells were autoclaved. Moreover, all manipulations were carried out under standard aseptic conditions.

2.3 The UV treatment of yeast cells

After yeast cells were resuspended in pre-chilled phosphate buffered saline (PBS, see Appendix) at a density of 2×10^7 cells/ml, 50ml aliquots of this mixture were exposed to 254 nm UV light. The UV lamp was switched on at least half an hour before irradiation to ensure a stable emission. Except for during UV treatment, all the cells were kept on ice and stored in the dark to avoid additional visible light during the experiment. Then, cells were collected by using a Beckman Avanti J-25 centrifuge at 4°C. After centrifugation, the cells were resuspended in fresh medium suitable for them, and allowed to repair for various times in the dark at 30° C on a shaker prior to the isolation of DNA. The details of the procedure were described as follows:

1) Yeast cells in exponential phase [density of $2\sim4\times10^7$ cells/ml] were collected by centrifugation at 4,000 rpm for 5 min using a Beckman Avanti J-25 centrifuge and a Beckman JA-10 rotor.
2) Cells were washed and then resuspended in 400ml prechilled 1xPBS. Brief sonication might be applied to disperse clumps of cells if necessary. Cell density was checked by using a haemocytometer to count cells and the suspension was adjusted to 2×10^7 cells/ml by the addition of chilled PBS.
3) Prior to UV irradiation, a 200ml sample was removed from the cell suspension and kept on ice, providing an untreated (U) control sample.
4) One by one, 50ml of cell suspension were placed in a Pyrex dish (Φ=14 cm) such that the depth of cell suspension was about 0.3 cm. The dish was gently shaken to

ensure a uniform dose to all cells while the cell suspension was irradiated under a VL-215G UV lamp (Vilber Lourmat, France) at a dose rate of 10 J/sec/m^2. This irradiation was repeated until all the cell suspension requiring UV had been treated.

5) 200ml of cell suspension after irradiation was collected by centrifugation at 4,000 rpm for 5 min and kept on ice to serve as a sample (**0**) with no repair time. The remainder of the UV-treated cells was collected as above, then resuspended in 300 ml/400ml of appropriate fresh medium and incubated at 30°C in the dark on a shaker for DNA repair. At each repair time (0.5, 1, 2 or 3 hours), the same volume of cells were taken from the medium. All samples were centrifuged as above after collection and then were resuspended in 40 ml of chilled PBS in the dark to prevent photoreactivition.

UV Survival

Cells were grown in appropriate medium to mid-log phase (around 2×10^7 cells/ml). Serial 10-fold dilutions of each culture were plated onto growth medium plates, then irradiated with the germicidal UV lamp at 1 J/sec/m^2. For the experiments involving UV sensitive strains like the Δ*rad4* mutant strains, the rate of irradiation was reduced to 0.1-0.2 J/sec/m^2 by increasing the distance between the plates and the UV lamp. Following irradiation, the plates were wrapped with aluminum foil and incubated at 30°C until colonies appeared. Colonies were then counted by eye.

2.4 Preparation of yeast genomic DNA

The protocol employed for isolation of genomic DNA from yeast cells, was described in Teng *et al.* (1997), which is suitable for extraction of genomic DNA from as many as 1×10^{10} cells per sample. The details of the procedure as follow;

1) Cells of each sample were collected by centrifugation at 4,000 rpm for 5 minutes using a Beckman JA-10 rotor. Following removal of the supernatant, the cells were resuspended in 5ml of sorbitol-TE solution (see Appendix I).
2) 0.5ml of zymolyase 20T (10 mg/ml in sorbitol solution, ICN Biochemicals, Inc.) and 0.5ml of 0.28M β-mercaptoethanol (Sigma) were added to each sample. After vortexing samples, they were incubated either at 37°C for 1 hour in a shaking incubator, or at 4°C overnight in the dark. The production of spheroplasts was monitored under a light microscope.
3) All samples were gently centrifuged at 3,000 rpm for 5 min with a Beckman JA20 rotor and resuspended in 5ml of 1:1(v/v) lysis buffer/1xPBS solution (see Appendix I). 0.2ml RNase A (pancreatic RNAse, Sigma. 10mg/ml in TE buffer) was added to each sample, then it had been incubated at 95°C for 10 minutes to eliminate DNase activity. All samples were incubated at 37°C for 1 hour with occasional shaking. Then, 0.5ml of proteinase K solution (Amresco, freshly made in 5mg/ml in TE buffer) was added. The samples were incubated at 65°C for 2 hours with shaking at regular intervals.

4) An equal volume (5.7ml) of phenol:chloroform:isoamyl alcohol (25:24:1 in volume, Sigma) was added to each sample. The tubes were shaken vigorously and then centrifuged at 10,000 rpm for 10 minutes using a JA-20 rotor. The upper aqueous phase containing genomic DNA was then carefully transferred to a fresh 50ml disposable polypropylene tube using a 3ml plastic Pasteur Pipette. Care was taken not to disturb the interface and the phenol/chloroform phase.

5) To ensure complete deproteinization, a second extraction same as above was performed, and then a third extraction with chloroform:isoamyl alcohol (24:1 in volume, Sigma). The aqueous phase was transferred to a fresh tube.

6) 2 volumes (12ml) of pre-chilled 100% ethanol (-20°C) were added to each sample. After being mixed gently by inversion, the samples were kept at -20°C overnight to precipitate the DNA.

7) DNA pellets were collected by centrifugation at 4,000 rpm for 15 minutes with a Beckman JS 4.2 rotor in a Beckman J6B centrifuge. The pellets were allowed to air dry, and then dissolved in 1 ml of TE. After being completely dissolved, the DNA was reprecipitated by addition of an equal volumn of pre-chilled (-20°C) isopropanol. The samples were left at room temperature for 20 minutes. The DNA pellets were carefully removed with pipette tips into new eppendorfs. Finally, the DNA was resuspended in 1ml of TE.

8) The quality of the DNA samples was checked by both non-denaturing agarose gel electrophoresis (see 2.5.1) and UV spectrophotometery (Beckman DU-530). Samples with clean DNA should give a sharp bright band on an ethidium bromide

(EtBr) stained agarose gel upon a UV transilluminator and a ratio of absorbance at 260nm to that at 280nm of around 1.8. The DNA samples were stored at -20° C until further research.

2.5 DNA electrophoresis

DNA electrophoresis on agarose or polyacrylamide gels was routinely used for checking DNA quality, monitoring DNA manipulation and sequencing DNA fragments. Typically, DNA is negatively charged, DNA fragments migrate from the cathode to the anode of the gel. The electrophoretic mobility of DNA fragments is dependent on their size as the shorter fragments migrate quickly through the gel. The agarose and polyacrylamide gels used in this study are described here.

2.5.1 Non-denaturing agarose gel electrophoresis

1 % non-denaturing agarose gels were used to check double-stranded DNA routinely for DNA quality, restriction efficiency, *etc.*

1. 1.5 g of agarose powder was rendered molten in 150 ml 1 × TAE/TBE buffer using a microwave oven. Then 1 μl of 10 mg/ml EtBr was added and mixed well.
2. The molten agarose was left to cool down to ~ 60 °C, and then poured into a gel tray (11 × 14 cm, in a horizontal electrophoretic tank). A comb was quickly put in the molten agarose to form the sample wells. The gel was set for about 1 hr at room temperature. Then 1 × TAE/TBE was added as running buffer.

3. After removing the comb, the DNA samples (2 μl of DNA preparation mixed with 8 μl of H_2O and 3 μl of non-denaturing loading buffer) were carefully loaded onto the gel wells. Electrophoresis was carried out at a constant voltage of 80V for 40 min using a Sigma powerpack. The gel was visualised by UV transillumination.

Genomic DNA ran as a discrete high molecular weight band visible with the UV transilluminator. To check the efficiency of yeast DNA digestion, 5 μl of restricted DNA dissolved in TE buffer was routinely examined by non-denaturing agarose gel as described above. Here, the efficiently digested genomic DNA migrated on the gel as a smear.

2.5.2 Denaturing polyacrylamide gel electrophoresis

In this study, a 0.4 mm denaturing polyacrylamide gel was used for DNA sequencing, analysis of nucleosome positions and for examining DNA repair at the level of the nucleotide.

1. Two glass plates (20 × 60 cm and 20 × 62 cm) were cleaned with detergent and washed thoroughly with water, then were wiped with ethanol carefully to remove grease, finger-prints *etc.* After the shorter plate was siliconised with dimethyldichlorosilane solution on its inner surface, the two plates and two 0.4mm side spacer strips between them were firmly sealed with vinyl insulation tape.

2. 80 ml of 6 % acrylamide EASI gel (acrylamide:bis-acrylamide = 19:1, 7 M urea,

1×TBE, ScottLab) was degassed under vacuum conditions in a flask for 10 min, and then 650 µl of 10 % APS and 35 µl of TEMED were added and mixed with gentle shaking. The gel mixture was poured slowly into the gel mould without any bubbles. A comb was inserted into the top part of the gel immediately to form the sample wells. The gel was set at room temperature for at least 1 hour.

3. A GIBCO electrophoresis system (Model SA) and a Pharmacia powerpack (EPS 3500) were used for running the sequencing gel. Pre-running of the gel in 1×TBE buffer was carried out at 70 W for 30 min, with loading buffer added to check sample wells.

4. DNA samples were loaded carefully into the gel wells. Electrophoresis was carried out under the same conditions as gel pre-running for the desired time that depended on the size of DNA fragment. When electrophoresis had finished, the plates were separated carefully. The gel was covered with a piece of Whatman filter paper (3 MM) carefully to make sure the whole gel contacted the paper. Finally, the gel was carefully taken off with the filter paper from the glass plate, and covered with cling film.

5. Then the gel was dried in a Bio-Rad gel dryer under vacuum at 80 °C for 2 hrs followed by exposure to a phosphorimager screen in a cassette for an appropriate time dependent on the labeling efficiency. The phosphorimager screen was scanned with a phosphorimager screen scanner (Molecular Dynamics) for further analysis.

2.6 Northern blotting

Northern blotting was used to examine the relative levels of certain RNA on different backgrounds. It is very similar to Southern blotting except that it targets RNA rather than DNA. Extra care was taken when dealing with RNA as all the glassware, tips and solutions *etc.* were pre-treated according to the standard requirement of working with RNA. The procedure is described here.

2.6.1 Isolation of total RNA

Yeast total RNA was extracted by using the hot phenol method (Schmitt *et al.*, 1990). 3×10^8 cells (at a density of $2\sim4\times10^7$ cells/ml) were collected by centrifugation. After washing with sterile H_2O, the cells were transferred to a 1.5 ml eppendorf tube. 0.5 ml of RNA lysis buffer (10 mM Tris, pH 7.5; 10mM EDTA, pH 8.0; 0.5% SDS) and an equal volume of phenol (pH 4.3±0.2, Sigma) were added, after which the tube was incubated at 65°C for at least 30 min with regular vigorous vortexing before cooling down rapidly on ice for 10 min. Following centrifugation at maximum speed in a microfuge for 5 min, the top aqueous layer was transferred to a fresh tube where a normal phenol/chloroform extraction (once with phenol/chloroform and once with chloroform, see section 2.4) was performed to complete the RNA extraction. The RNA was then precipitated by the addition of 2.5 volumes of absolute ethanol at -20°C for 1 hour. The RNA pellets were collected, washed and redissolved in 80μl of sterile H_2O (autoclaved twice) plus 20μl of 5x RNA loading buffer (see Appendix I)

and thereafter kept at -70°C until further use.

2.6.2 Separation of RNA under formaldehyde-agarose (FA) gel electrophoresis

Formaldehyde-agarose (FA) gel electrophoresis was routinely used with RNA fragments. 1.2~1.5% of agarose (depending on the size of the RNA fragments to be resolved) was melted in 200ml of 1x FA gel buffer. After the gel mixture had cooled down to 65°C in a water bath, 1μl of EtBr (10mg/ml) and 3.6ml of 37% formaldehyde were added, and then the gel mixture was poured into a gel mould with a comb plugged in, and left to completely set (more than 30min at room temperature). The gel was mounted in the electrophoresis tank filled with 1x FA gel running buffer. The gel was maintained at equilibrium with the running buffer for 30 to 45 min before RNA samples were loaded. About 10μl of each RNA sample (the amount of loading was adjusted among samples to give an equal signal of the internal control gene after hybridisation) was loaded into the well, and finally the gel was run at 10V/cm for 2-3 hours.

2.6.3 Northern hybridisation

Transferring RNA from the gel to the membrane and the subsequent hybridisation with radioactive probes was similar to Southern blotting except for the buffers for transfer and hybridization.

RNA was transferred to a nylon-based membrane (GeneScreen Plus, PerkinElmer Life Sciences, Inc., USA) under 20 times SSC buffer (see Appendix I)

by capillary elution. Capillary elution was carried out as following;

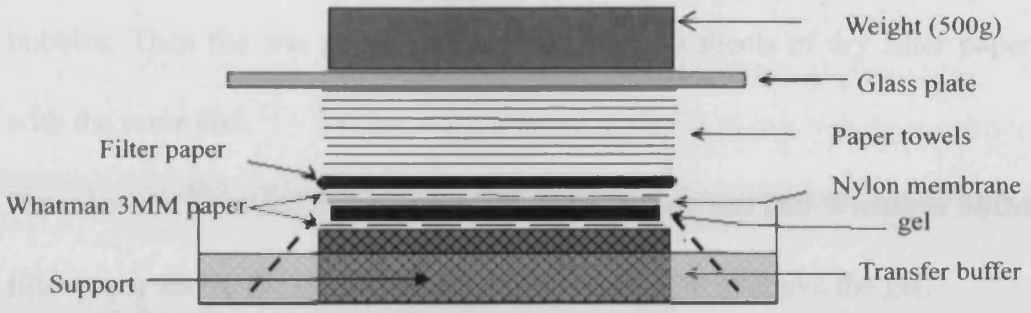

Figure 2.1 Schematic representation of the total RNA transfers from gel to nylon membrane by capillary elution. Buffer is drawn from a reservoir and passes through the gel into a stack of paper towels. The RNA is eluted from the gel by the moving stream of buffer and is deposited on a nylon membrane. A weight to the top of the paper towels helps to ensure a tight connection between the layers of material used in the transfer system.

1. The gel was soaked in transfer buffer (20× SSC buffer) for 2×15 minutes.
2. The transfer system was set up as follows:

   - In a pool of transfer buffer (20× SSC),a solid support with Whatman 3MM filter paper wicks were placed.
   - The Whatman 3MM filter paper was wetted with transfer buffer. All bubbles between solid support and filter paper were removed carefully.
   - The agarose gel was lowered onto Whatman 3MM filter paper. Then, all air bubbles between the gel and filter paper were removed.
   - An appropriate membrane to the size of the gel was cut. To wet the membrane, it was soak in water for 5 minutes. Then, the membrane was placed on the gel avoiding air bubbles.

- The membrane was flooded with transfer buffer and covered with 2 sheets of Whatman 3MM filter paper cut to the same size as the membrane without any bubbles. Then the wet paper was covered with 20 sheets of dry filter paper with the same size.
- Paper towels were cut to the same size as the membrane and Whatman 3MM filter paper above the gel and stacked to a height of 4cm above the gel.
- A glass plate was covered on the top of the towel stack. Then, a weight was added on this glass plate to hold everything in place (not too much weight as it could crush the gel).

3. Capillary elution was carried out overnight.
4. Paper towels and filter papers were removed. The membrane was carefully collected and washed once with 2× SSC buffer.
5. The position of the wells and orientation of the membrane were marked in pencil (an asymmetric cut at the corner is sufficient).
6. The RNA-side of the membrane was irradiated by using a UV transilluminator (254nm) for 2 minutes to allow RNA and membrane cross-linking.

The membrane carrying the transferred RNA was rinsed with distilled water and rolled inside a glass tube containing hybridisation solution (0.5M phosphate buffer, 7% SDS, 1% BSA, 1mM EDTA) at 65°C for 1 hour on the rotating spindle in a Hybaid Oven. 100µl of radioactive strand specific probe (see section 2.7) was added to the tube. The tube was placed back into a Hybaid Oven and kept at 65°C overnight under constant rotation. After hybridisation, the membrane was washed twice with

washing buffer (2× SSC, 1% SDS) on a shaking platform at 65°C for 15 to 30 minutes.

Following the washing step, the membrane was covered by cling film and placed in a cassette against a phosphorimager screen (Molecular Dynamics, Inc.). Exposure was overnight at room temperature. The image was generated by scanning the phosphorimager screen using a scanner (Storm 860, Molecular Dynamics, Inc.) and quantified using ImageQuant software (Molecular Dynamics, Inc.) The analysis of image data will be described in section 2.8.

In this study, all manipulations involving radioactive isotopes were performed according to the safety guidelines.

2.7 Preparation of specific probes

In this study all DNA or RNA probes synthesised for hybridisation were strand specific so they can detect the TS and NTS or transcripts separately. The essence of this approach is to employ a 5' biotinylated primer and Dynabeads so as single stranded DNA can be retrieved. The synthesis began from PCR amplification of the DNA sequence of interest by using genomic DNA as a template. PCR primers were designed using the Oligo software and were checked by BLAST on line. Normally PCR utilized one biotinylated and one non-biotinylated primer (Oswel, UK or MWG, UK). Once PCR had finished, the product was loaded onto a 1% non-denaturing agarose gel and visualized by UV transillumination to measure its concentration and

length roughly. Based on this measurement, PCR conditions were optimized in order to obtain unique PCR of the sequence desired. The required PCR product was isolated by using Dynabeads and a magnetic particle concentrator (MPC). Dynabeads are streptavidin coated superparamagnetic spheres which are able to bind tightly to 5' biotinylated residue on one strand of the PCR product and then be separated from the rest of PCR mixture in a magnetic field provided by a MPC. The bound double stranded PCR product was then denatured by incubation in a NaOH solution. Once again, by placing the mixture in the MPC the biotin labelled strand was separated from the non-biotinylated strand by collecting the beads and removing the supernatant with a pipette. The probe was synthesised upon this biotinylated single stranded DNA template by primer extension using Sequenase Version 2.0 T7 DNA Polymerase (Amersham Pharmacia Biotech) and α-[^{32}P] dATP (6000 Ci/mmol, Amersham) spiked dNTP mixture. The [^{32}P] incorporated probe was collected with a pipette as a supernatant when directly placing the mixture at a denaturing condition (0.1 M NaOH) in the MPC.

2.7.1 Preparation of PCR product for Northern blotting

A pair of one biotinylated primer and one non-biotinylated primer was designed for standard PCR amplifications as described below:

1μl of each primer (20μM), 1.75μl of dNTPs (10mM), 5μl of 10×Taq buffer (Promega), 4μl (may be altered for different primers) of $MgCl_2$ (25 mM), 10 μl of 100x diluted untreated (U) DNA template, and 1.25 units of Taq polymerase

(Promega) were mixed and supplemented with RNA-free water to a final volume of 50μl.

PCR was carried out in an OmniGene thermal cycler (Hybaid) and the program was run as: (1) denaturation at 95°C for 3 min; (2) 30-35 cycles of: 30 seconds of denaturation at 95°C; 30 seconds of annealing (Tm-5°C); 1.5 min of extension at 72°C, and (3) finally, at 72°C for 10 min to complete the DNA synthesis.

2.7.2 Synthesis of the radioactive probe by primer extension

1) 20μl of washed Dynabeads in 2×BW (binding and washing) buffer (see Appendix I) were added to 10μl of PCR product to bind to the biotin end of the PCR products. This was undertaken at room temperature for 15 minutes, with occasional mixture by pipette. The MPC was used to collect the beads associated with the PCR product and the supernatant discarded.
2) After two washes with H_2O, the beads were resuspended in 30μl of 0.1M NaOH at room temperature for 10 minutes to denature the dsDNA. MPC was used to keep the biotinylated strand associated with beads on the Eppendorf wall, while the supernatant containing the other strand was abandoned.
3) The beads were washed twice with H_2O and resuspended in 20μl of 1xBW. 1μl of the appropriate non-biotinylated primer (20 μM) was added. The solution was mixed thoroughly by pipetting. Afterwards the tube was incubated at 65°C for 2 min, then allowed to cool down slowly to room temperature over a period of about 30 minutes. Using a MPC, beads and bound fragments were separated from the

supernatant, and then washed twice with 60µl H_2O.

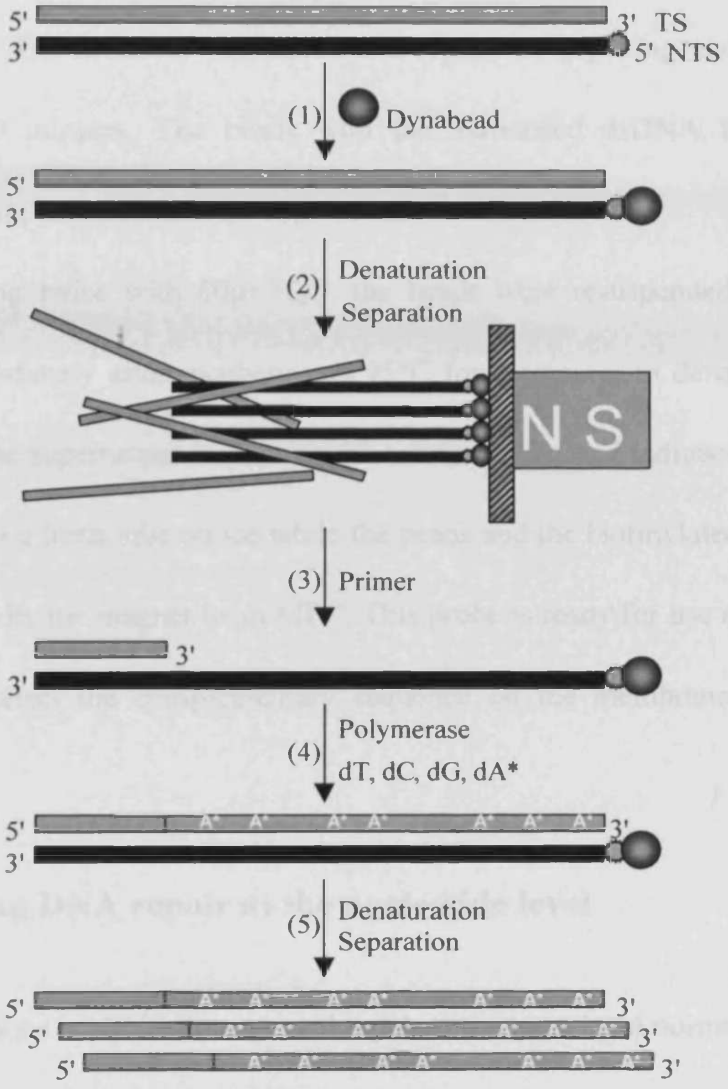

Figure 2.2 Schematic representation of the procedure for the Northern Blotting probe synthesis. (1) Dynabeads bind to the biotin (○) end to enrich appropriate PCR products (2) Double stranded DNA is denatured in 0.1 M NaOH. The beads with associated single stranded DNA are kept on the Eppendorf wall in a MPC. The supernatant is removed. (3) The second primer annealed to the 3' end of the single stranded DNA. (4) [α^{32}P]dATP (dA*) and the other three dNTPs are recruited for the primer extension reaction by DNA polymerase. (5) The newly synthesized probe is separated from the template in a MPC. (Figure adapted from Teng, PhD thesis, 2000)

4) The beads were resuspended in 17.2µl of water. 8 µl of 5 × Sequenase reaction buffer (Amersham), 4µl of dATP buffer (0.1 mM dTTP, dGTP and dCTP), 2µl of

α-[^{32}P] dATP (6000 Ci/mmol, Amersham), **6** μl of Sequenase mixture (1 μl Sequenase in 5μl sequenase dilution buffer, Amersham), 2.8μl of DTT (0.1M) were added. The solution was mixed thoroughly by pipetting and incubated at 37°C for 10 minutes. The beads with the associated dsDNA fragment were collected using the MPC and the supernatant was discarded.

5) After washing twice with 60μl H_2O, the beads were resuspended in 100μl TE buffer. Immediately after incubation at 95°C for 3 minutes to denature the DNA fragments, the supernatant containing the newly synthesised radioactive probe was transferred to a fresh tube on ice while the beads and the biotinylated ssDNA were immobilized by the magnet in an MPC. This probe is ready for use as in following section to detect the complementary sequence on the membrane for Northern blotting.

2.8 Examining DNA repair at the nucleotide level

Investigations on DNA damage and repair at the gene level normally are carried out by Southern blotting. However, it cannot give subtle information on repair at a specific nucleotide positions. An alternative end-labelling high resolution method was developed in this group to examine DNA damage and repair at nucleotide resolution by running the sequencing gel, and it has been used for detecting CPDs and oxidative damage in budding yeast and *E. coli* (Teng *et al.*, 1997, 1998; Li and Waters, 1996, 1997; Meniel and Waters, 1999; Teng and Waters, 2000; Yu *et al.*, 2001; Teng *et al.*, 2002; Ferreiro *et al.*, 2004; 2006).

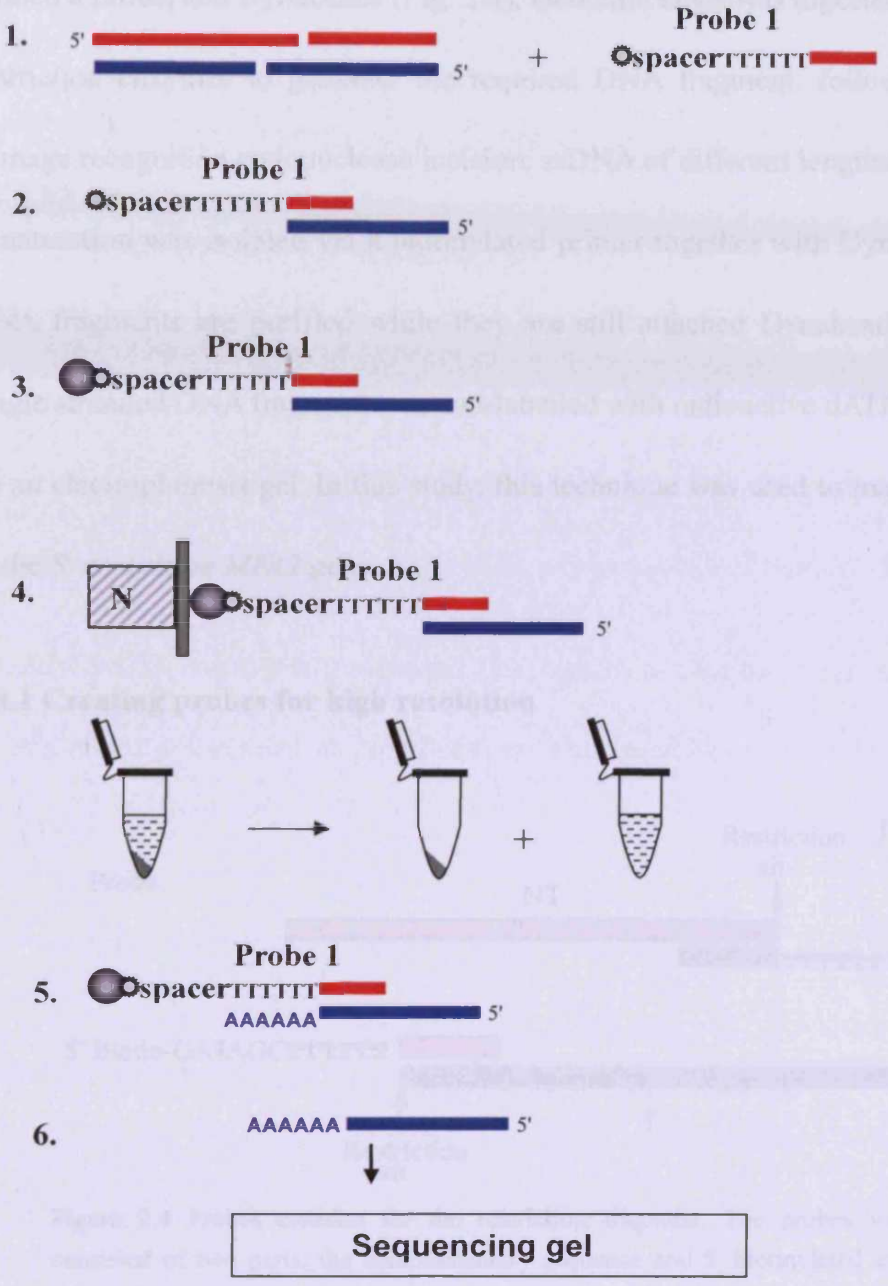

Figure 2.3 *Purification and end-labelling DNA fragment.* **1.** Probe 1 is added to the restricted and CPD cut DNA. **2.** Probes anneal to the complementary TS sequences at 3' end. **3.** Dynabeads are added to bind the biotin at the 5' end of the probe. **4.** Dynabeads and the associated DNA fragments are isolated, and the supernatant is saved for purification of the NTS strand. **5.** purified DNA is radioactively labelled at 3' end. **6.** After denatured, end-labelled DNA are loaded onto a sequencing gel.

The end-labelling method involves a biotin modification of the primer, which was termed a probe, and Dynabeads (Fig. 2.3). Genomic DNA was digested by appropriate restriction enzymes to generate the required DNA fragment, followed by specific damage recognition endonuclease incision. ssDNA of different lengths generated from denaturation was isolated via a biotinylated primer together with Dynabeads, and the DNA fragments are purified while they are still attached Dynabeads. Finally, each single stranded DNA fragment was end-labelled with radioactive dATPs and separated on an electrophoresis gel. In this study, this technique was used to map DNA damage in the *S. cerevisiae MFA2* gene.

2.8.1 Creating probes for high resolution

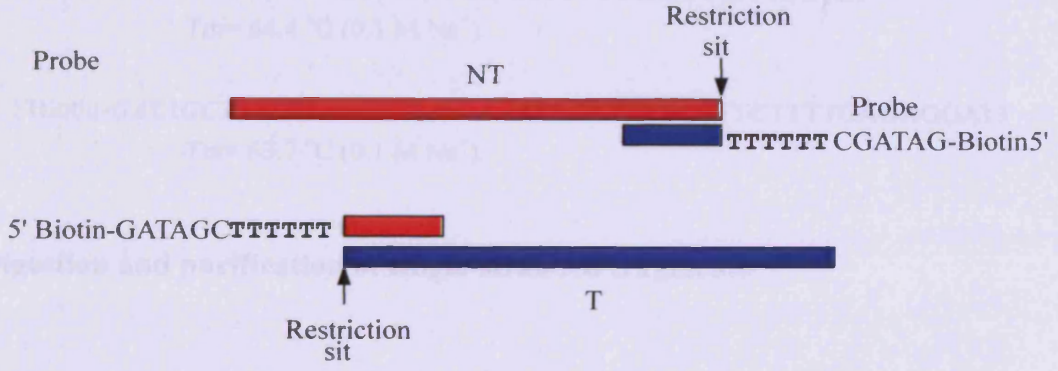

Figure 2.4 Probes creation for the restriction fragment. The probes were designed and consisted of two parts; the complementary sequence and 5' biotinylated extension sequence (GATAGCTTTTTT).

In this study, probes for high resolution sequencing gels were created complementary to the 3' ends of the restriction fragments containing the *MFA2* gene. Probe 1 is complementary to, and anneals to the TS, whereas Probe 2 is complementary to, and anneals to the NTS. These probes were designed so that they

had an overhang of six dTs followed by 5'-biotin-NNNNNN3' with no thymine residues at the N3' end (Fig. 2.4). The dTs overhang serve as a template for the polymerization of radioactive dATPs at the 3' end of the complementary DNA fragment. The 5'-biotin binds to Dynabeads, hence the beads and the associated DNA fragments can be separated from the solution with MPC simply by removing the supernatant. The overhanging sequence of six dNs (gatagc) was designed to prevent folding back of the probe itself, and was inserted between six dTs and biotin to keep the relatively large Dynabeads a distance from the dTs. This design ensured the complete polymerisation of six dAs without steric hindrance from the Dynabeads.

HaeIH-HaeIII restriction fragment The *HaeIII* restriction fragment is 599 bp in length; it contains the part of *MFA2* coding region and the upstream promoter region.

Probe 1: 5'Biotin-***GATAGCTTTTTT***CCCTCATCTATTTTCTCGGAAAACTTGGTG3'
Tm= 64.4 °C (0.1 M Na^+).

Probe 2: 5'Biotin-***GATAGCTTTTTT***CCCTTGATTATATAGATTGTCTTTCTTTTCAGAGGAT3'
Tm= 63.7 °C (0.1 M Na^+).

2.8.2 Digestion and purification of single-stranded fragments

1. 50 μg of genomic DNA (about 100μl volume) was digested by restriction endonucleases at 37 °C for 90 min at the recommended working condition in a reaction volume of 200 μl.
2. The restricted DNA fragments were extracted by 1 volume (200 μl) of phenol/chloroform/iso-amyl alcohol (24:24:1) and followed by 1 volume (200 μl) of chloroform/iso-amyl alcohol (24:1). The upper phase containing restricted

DNA fragments was carefully removed to a fresh tube without disturbing the interface.

3. 1/10 volume (20 μl) of 3 M NaOAc was added to each tube. The DNA was then precipitated by the addition of 1 volume (220 μl) of pre-chilled iso-proponol (-20°C) with gentle inverting. After precipitation at –70 °C for 10 min, the DNA pellets were collected by centrifugation at 10,000 rpm using a bench-top microfuge.
4. The DNA was dissolved completely in 110 μl of TE buffer, and then 10 μl of *ML* CPD endonuclease was added to cut the DNA at CPD sites. Incubation was carried out at 37 °C for 60 min.
5. 120 μl of phenol/chloroform/iso-amyl alcohol (24:24:1) followed by 120 μl of chloroform/iso-amyl alcohol (24:1) were used for protein extraction as described in step 2. The upper phase containing DNA fragments was transferred to a fresh 0.5 ml Eppendorf tube.
6. 30 μl of 5 M NaCl and 2 μl of Probe 1 (1 μM) were added to each sample and mixed by vortexing. After a brief centrifugation, samples were heated at 95 °C for 5 min to denature the dsDNA and then incubated at the annealing temperature for 15 min, allowing the probes to anneal to the complementary *MFA2* TS.
7. 10 μl of washed Dynabeads (10 mg/ml in 1 × BW buffer) was added to each tube to bind the 5' biotin at room temperature for 15 min with occasional inverting. The beads associated with DNA fragments were collected by a MPC. The supernatant was then transferred to a fresh tube for the NTS purification (step 8). The

Dynabeads associated with the restricted fragments were resuspended in 60 µl of 1 × BW buffer for step 9.

8. 2 µl of Probe 2 (1 µM) was added to the supernatant for the purification of the NTS as described in steps 6 and 7. The beads associated with the NTS were resuspended in 60 µl of 1 × BW buffer.
9. 60 µl of bead suspension in 1 × BW buffer was heated at annealing temperature for 5 min to eliminate non-specific annealing. The beads with associated DNA fragments were collected with an MPC and the supernatant was removed. Two washes were carried out with 60 µl of water at room temperature.

2.8.3 Labelling the fragments

1. Resuspended Dynabeads with associated restricted DNA fragments in 5 µl of H_2O, and then 2 µl of 5 × Sequenase Reaction Buffer (200 mM Tris.HCl, pH 7.5, 100 mM $MgCl_2$, 250 mM NaCl), 0.7 µl of 0.1 M DTT, 0.5 units of T7 DNA polymerase and 1 µl (5 µCi) of [α^{32}P] dATP (6000 Ci/mmol Amersham) were added. The solution was mixed by pipette and incubated at 37 °C for 10 min for the polymerization of radioactive dATP.
2. The Dynabeads associated with radioactive labelled DNA fragments were immobilized on the Eppendorf wall by an MPC, and washed twice with 40 µl of TE buffer at room temperature.
3. Following the removal of the 2nd TE wash, 3 µl of loading buffer (95 % Formamide, 20 mM EDTA, 0.05 % Bromophenol Blue) was added and mixed

thoroughly by pipette. The mixture was left at room temperature for 5 min. The labelled DNA fragments were eluted from the Dynabead-probe.

4. The MPC was used to immobilize the Dynabead-probe, and the loading buffer containing the labelled fragments was loaded onto a 6% denaturing polyacrylamide gel for electrophoresis as described in section 2.5.2.

2.8.4 Sequencing the *MFA2* containing fragments

To indicate the precise position of CPDs within the DNA sequence investigated, a sequencing ladder for *MFA2* containing fragment was run alongside the UV treated DNA samples during electrophoresis. The procedure for sequencing the *MFA2* fragment is described here.

The sequencing ladder was synthesised by using T7 Sequenase Version 2.0 DNA sequencing kit (Amersham Pharmacia Biotech) according to the manufacturer's instructions. Since the single stranded DNA fragments were purified with a probe complementary to their 3' ends (see Figure 2.2) and DNA synthesis can only proceeds from the 5' end to the 3' end, it is required to load the sequencing ladder reflecting the sequence of the opposite strand to indicate the actual position of a DNA lesion in a specific DNA strand. The probe used to generate sequencing ladders was modified as well, and was different from that served to isolate single stranded DNA after damage incision. Six random nucleotides were added to the primer at the 5' end before the complementary sequence to compensate in the length of the ladder in the same way as the single stranded DNA samples are labelled with six radioactive dATPs. This allows

a direct reference from the running positions of the sequencing ladder to that of the DNA damage ladder.

The fragments of interest were amplified via PCR using the primers indicated below. Primer 1 and Primer 2 are the same sequence as the biotinylated Probe 1 and Probe 2, respectively. Primers 3 and 4 are the modified versions of Primer 2 and Primer 1, respectively. The modification involves removal of the 12 bp overhang of Primers 1 and 2 and replacement with a random hexanucleotide. The purpose of the random hexanucleotide added to the 5' end of Primers 3 and 4 is to allow the sequencing ladder to run alongside the DNA damage ladder at the same position, since the DNA damage ladder is end-labelled with 6 dAs residues.

HaeIII-HaeIII fragment

Primer 1: 5'Biotin-gatagctttttt CCCTCATCTATTTTCTCGGAAAACTTGGTG3'

Primer2:5'Biotin-gatagctttttCCCTTGATTATATAGATTGTCTTTCTTTTCAGAGGAT3'

Primer 3: 5'gatagcAAGAGGCCCTTGATTATATAGATTGTCTTTCTTTT3'

Primer 4: 5'gatagcAACAGGCCCTCATCTATTTTCTCGGA3'

1. 1 μl (20 μM) of Primers 1 and 3 for TS (or Primer 2 and 4 for NTS), 8 μl of dNTP mixture (1.25 mM of each dATP, dCTP, dGTP, and dTTP), 5 μl of Thermophilic DNA polymerase 10 × Buffer, 1 unit of Taq DNA polymerase (Promega), 1 ng of DNA templates were mixed in a tube in a final volume of 50 μl.

2. The tube was incubated at 95°C for 2 min and then 30 PCR cycles were carried out: denaturation at 95°C for 30 s, primer annealing at 57°C for 30 s and primer

extension at 72°C for 30 s. Finally the tube was incubated at 72°C for 4 min to complete the primer extension.

3. 20 µl of Dynabeads (in 2 × BW) were added to 20 µl of the PCR product to bind to the biotin at the 5' end of the extended Primer 1 at r.t. for 10 min, mixing occasionally with a pipette. The beads associated with the PCR product were collected using an MPC and the supernatant was discarded.

4. The beads with associated DNA fragments were resuspended in 30 µl of 0.1 M NaOH at r.t. for 10 min to denature the DNA. The supernatant was removed, and the beads were washed twice with 30 µl of H_2O, and then the beads were resuspended in 20 µl of 1 × BW.

5. 1 µl of Primer 3 (20 µM) was added to the bead suspension and the tube was incubated at 65 °C for 2 min., then allowed to cool slowly to r.t.. After a brief spin in a microfuge, the beads were washed twice with 40 µl of H_2O, and resuspended in 8 µl of H_2O and 2 µl of 5 × sequenase reaction buffer.

6. 5.5 µl of reaction mixture containing 2 µl of 8 times diluted Labelling Mix (dGTP) (7.5 µM dGTP, 7.5 µM dCTP, 7.5 µM dTTP), 0.5 µl of [^{35}S] dATP (10 µCi/ml at >1000 Ci /mmol), 2 µl of Sequenase (8 times dilution, 1.6 U/µl) and 1 µl 0.1 M DTT were added and the tube was incubated at room temperature for 2 min.

7. 4 fresh tubes each contains 2.5 µl of one of the four termination mixtures (ddATP, ddGTP, ddCTP, ddTTP) were incubated at 37 °C. 3.5 µl of the reaction mixture

(step 6) was added to each termination tube and the tubes were incubated at 37 °C for 5 min.

8. The beads with associated DNA fragments were washed twice with 40 µl of TE buffer, and resuspended in 20 µl of stop solution (95 % formamide, 20 µM EDTA, 0.05 % bromophenol blue, 0.05 % xylene cyanol FF).

Because the analysis was of cyclobutane pyrimidine dimers, a mixture of ddCTP and ddTTP termination reactions was loaded to one lane and a mixture of ddGTP and ddATP termination reactions to another.

2.8.5 Damage quantification and repair analysis

The sequencing gel data was analysed by using ImageQuant software version 5.0. The intensity of each band, which reflects the frequency of DNA damage at a specific site, was measured as collective pixel values. To avoid a false judgement about repair resulting from a slightly varied loading of DNA samples in each lane, an adjustment was made as the total signal from individual lanes were multiplied by a factor to give equal values, and then the signal of each band was accordingly multiplied. The value from non-irradiated DNA was subtracted as a non-specific background. The damage remaining after particular repair times was presented as a percentile with respect to the initial damage (0 lane, 100% CPD damage).

$$\%\,(\text{CPD remaining}) = \frac{[\text{CPD}]_t}{[\text{CPD}]_0} \times 100$$

Here t represents a particular repair time and 0 represents when the repair starts (no repair time). % (repaired CPD) can be used for expressing the result alternatively as follows:

% (repaired CPD) = 100% - % (CPD remaining)

To generate repair curves, the data points representing % damage at defined sites at each repair time were fitted to an exponential curve. Finally the time, where 50% of the damage was removed ($T_{50\%}$ value), was calculated to compare repair rates of individual damages.

2.9 Purification of His-tagged Rad7 protein

Rad7/Rad16/ABF1 was purified using the following steps: cell culture, cell harvesting, disruption of cells with a French Press, Sepharose CL-6B conventional chromatography, Ni-NTA agarose conventional chromatography, P11 resin conventional chromatography, DEAE sephacel conventional chromatography, FPLC Mono_Q chromatography, glycerol gradient centrifugation purification. The presence of Rad7p/Rad16p/ABF1p in the fragments of each step is checked with western blotting.

1. Cell culture and cell harvesting

   Yeast cell culture was carried out as described at **2.2**, with the following exception. The density of cells can be up to 8×10^7 cells/ml. After 2 clean bottles are weighed, cells are collected in these bottles with centrifugation at 4000 rpm for 8 minutes. Before the bottles with cells are weighed again, cells are washed with

pre-chilled ddH_2O and cold Extraction buffer A (40 mM Hepes pH7.3, 350 mM NaCl, 0.1% tween 20, 10% Glycerol, and 1mM DTT) [The concentration of all components remains the same unless stated otherwise.] without protease inhibitors respectively.

2. French press disruption of cells

   Cells are resuspended with suitable Extraction buffer A containing 1× protease inhibitors with a ratio at 2ml buffer per 1g wet cells. The cell suspension is disrupted with a French press twice in the cold room and centrifugation is carried out at 20000 rpm for 30 mins. Then, the supernatant is transferred to high-speed tubes for centrifuging at 48,000 rpm for 2 hours. The supernatant is carefully transferred to a pre-chilled container on ice.

3. Sepharose CL-6B conventional chromatography

   The supernatant from the high-speed centrifugation is mixed with 10 ml Sepharose CL-6B, which is washed three times with pre-chilled ddH_2O and once with cold Extraction buffer A. The mixture is incubated for 60 mins on swing in the cold room. Centrifugation is carried out twice at 1000×g for 20 mins to remove the resins, and then the pH of supernatant is adjusted to 7.3-7.5 with 1M KOH (potassium hydroxide). After the concentration of proteins is measured by protein assay, it is adjusted to 5-7 mg/ml if beyond this range.

4. Ni-NTA agarose purification

   Binding of this tagged Rad7p to Ni-NTA is carried out at 4°C. After 3 hours binding, the suspension was transferred to a glass column. Then the column was

washed with 50 ml of Extraction Buffer A supplemented with 1mM 2-mercaptoethanol and 5 mM imidazole at a flow rate of 1ml/min. The Rad7 complex was eluted using 15 ml of Extraction Buffer A supplemented with 1mM 2-mercaptoethanol and 25 mM imidazole, 15 ml of Extraction Buffer A supplemented with 1mM 2-mercaptoethanol and 50 mM imidazole, and 30 ml of Extraction Buffer A supplemented with 1mM 2-mercaptoethanol and 100 mM imidazole. The eluate was collected in 5 ml fractions.

5. Purification of P11 resin

Previously prepared P11 resin (5g) was washed with 100 ml of Extraction Buffer A (100 mM NaCl) at a flow rate of 1ml/min. Peak fractions contained Rad7p from Ni-NTA were pooled and the salt concentration adjusted to 100 mM by dilution. The pooled material was loaded at the same flow rate. Then, the resin was washed with 30 ml of Extraction Buffer A (100 mM NaCl) at the same flow rate. The proteins were eluted by Extraction Buffer A with a gradient concentration of NaCl from 100 mM to 1000mM. 1 ml eluate fractions were collected.

6. Purification of DEAE sephacel

After DEAE sephacel was transferred to the glass column, it was equilibrated with Extraction Buffer A (100 mM NaCl) at the flow rate of 1 ml/min. The pooled P11 fractions (NaCl concentration is adjusted to 100 mM by dilution) were loaded with the same flow rate. Then, the column was washed with 30 ml of Extraction Buffer A (100 mM NaCl). The proteins were eluted by Extraction Buffer A with a NaCl gradient concentration from 100 mM to 1000mM. 1 ml of eluate was

collected in each fraction.

7. FPLC Mono_Q purification

   The FPLC column was equilibrated once with 30 ml of Extraction Buffer A (100 mM NaCl) and 30 ml of Extraction Buffer A (1000 mM NaCl) at a flow rate of 1 ml/minute. Then, it was equilibrated with 30 ml of Extraction Buffer A (100 mM NaCl) again. The mixture of all the selected fragments (the concentration of NaCl is adjusted to 100 mM) was injected at same flow rate. The complex was eluted with a linear gradient of NaCl in Extraction Buffer A (from 100 mM to 1000 mM).

8. Glycerol gradient purification

   Mono_Q fractions were pooled and concentrated in a cut-off column to 200µl. This was layered on a glycerol gradient (10-30% glycerol). The gradient is centrifuged at 39,000 rpm for 16 hours. Fractions were collected for further use.

2.10 Preparation whole cell extract (WCE)

1. When the density of yeast cells reached 2-4 × 10^7 cells/ml, the cells were collected and were irradiated by UV light following the instructions in **2.3**.
2. 1 × 10^9 cells (50ml of the cell suspension at a density of 2× 10^7 cells/ml) were collected for one sample by centrifugation at 4,000 rpm for 5 mins.
3. The cells were washed once with 1ml yeast dialysis buffer, then the pellet was resuspended in 300µm yeast dialysis buffer, the mixture was transferred to an autoclaved 1.5ml eppendorf tube that was pre-chilled in ice.
4. Afterwards 0.3-0.5g glass beads were added to the tube, it was sealed and was vortexed for 4 × 30 secs in the cold room (4°C). Between two vortexings the tube

was put into ice for 1 min to cool the heat from collision of glass beads.

5. The mixture was separated by centrifugation at 13,200 rpm for 15 minutes. The supernatant was transferred to a clean tube for further use.

2.11 Preparation WCE capable of supporting NER *in vitro*

1. When cell density reached 2-4 × 10^7 cells/ml, the cells were collected and washed with water once, then with hypotonic buffer.
2. Cells were weighed and were resuspended in hypotonic buffer with a ratio at 4ml buffer per 1g wet cells.
3. Cells were disrupted with a French press twice in cold room.
4. Followed the solution was transferred to a clean container on the ice, the same volume of sucrose solution was dropwisely added to the solution with gently stirring.
5. Appropriate amount of 4M $(NH_4)_2SO_4$ solution was dropwisely added to the solution to make a final concentration of 0.9M $(NH_4)_2SO_4$. Then, the stir was continued for 30 mins.
6. Followed the solution was transferred to 70Ti tube, centrifugation was carried out at 50,000 rpm for 1 hour at 4°C.
7. The supernatant was transferred to a new beaker on the ice, and then the volume of the supernatant was measured quickly.
8. Ground $(NH_4)_2SO_4$ powder was slowly (20 mins is the minimal time to do this step) added to the solution in the cold room. (0.35g $(NH_4)_2SO_4$/ml supernatant)
9. The solution was neutralized with 1M NaOH solution with a ratio at 10μl NaOH

solution for per 1g $(NH_4)_2SO_4$. Then the stir was continued for 30 mins in the cold room.

10. The solution was centrifuged at 13,000 rpm for 15 mins at 4°C. The supernatant was removed and measured.
11. The loose protein pellet was resuspended in yeast dialysis buffer with protease inhibitors ($1/30^{th}$ volume of the supernatant).
12. Followed the mixture was transferred to a dialysis tube, the dialysis was carried out for overnight in yeast dialysis buffer containing 1 × protease inhibitors.
13. The cell extract was centrifuged in the next morning at 13,200 rpm for 15 mins in the cold room. Then, the supernatant was ready for NER *in vitro* experiment.

2.12 Expression of Rad4 protein *in vitro*

1. The following two primers were used to produce the Rad4 protein coding sequence

Forward PCR primer:

5'AAGAGTACTTAATACGACTCACTATAGGAACAGCCACCATGAATGAA GACCTGCCCAA3'

Reverse PCR primer:

5'TTTTTTTTTTTTTTTTTTTTTTTTTTTTTTTTTAATCAGTCTGATTCCTCTGA CATCT3'

PCR was performed using genomic DNA as the template. For this case, especially the low efficiency for the two long primers, 10 tubes of raw PCR product were pooled and precipitated with the same volume of 99% alcohol (-20°C) overnight. The mixture was spun down at 13,000 rpm for 15 mins then the supernatant discarded.

The pellet was dried for 30 mins at room temperature. The pellet was resuspended with twice-autoclaved ddH_2O (pH7-8) or nuclease free water provide by Promega enclosed in the TNT kit at room temperature for at least 30 mins with an occasion gentle vortex. It was kept at -20°C for short-term storage.

2. Expression of Rad4 protein via coupled *in vitro* transcription/translation

a. The reagents were removed from storage at –70°C. The TNT® T7 PCR Quick Master Mix was rapidly thawed by hand-warming and placed on ice. The other components were thawed at room temperature and then stored on ice.

b. Following the table below, the reaction components were assembled in a 0.5ml thin-wall tube. After addition of all the components, it was gently mixed by pipetting. If necessary, it might be centrifuged briefly to return the reaction to the bottom of the tube.

c. A control reaction containing no added DNA should be always carried out with the DNA for expression in vitro. This reaction allows measurement of any background incorporation of labelled amino acids.

Components	Radio Label	Normal
TNT Master Mix	40μl	40μl
Methionine	----	1μl -2μl
[^{35}S]Methionine	2μl	----
Nuclease free water	3μl-0μl	3μl-0μl
PCR-generated DNA template	5μl-8μl	5μl-8μl

d. The reaction was incubated at 30°C for 60–90 minutes.

e. The results of translation were analyzed via the western blotting following a SDS-PAGE gel electrophoresis separation.

2.13 Immunoprecipitation (IP)

1. Afterwards the concentration of total proteins in whole cell extract (WCE) was measured, 400 μg of total proteins of each sample was added to a clean tube on ice.
2. Following this, 5μl of antibody were added to each tube, yeast dialysis buffer was added to make a total volume of 500μl. Then, all samples were incubated on ice for 1-2 hours.
3. Protein A beads slurry was washed 3 times with 1ml pre-chilled yeast dialysis buffer, then the beads were resuspended in pre-chilled yeast dialysis buffer to make a 10% (w/v) solution (slurry).
4. Following the antibody-antigen reaction, 100 μl of protein A beads slurry was added to each tube, then all samples were incubated with rocking in the cold room for 1 hour.
5. Centrifugation was carried out to separate the beads and supernatant at 13,200 rpm for 10 mins.
6. The pellets were washed three times with 1 ml pre-chilled yeast dialysis buffer, meanwhile unbound proteins in the supernatant were precipitated with adding 100% (w/v) tricholoroacetic acid (TCA) to final concentration of TCA at 10%.
7. The pellets of precipitated unbound proteins were washed once with 500μl

per-chilled acetone, and then all pellets were dried for 30 mins at room temperature. The dried pellet can be used for SDS-PAGE gel electrophoresis.

8. The pellets, including protein A beads pellets and precipitated pellets of unbound proteins, were separated by SDS-PAGE gel electrophoresis immediately.

2.14 Protein Assay

1. Dye reagent was prepared by diluting 1 part Dye Reagent Concentrate with 4 part ddH_2O. Filter through Whatman #1 filter (or equivalent) to remove particulates.
2. 6 standard protein concentration solutions, which were 1μg/ml, 2μg/ml, 4μg/ml, 6μg/ml, 8μg/ml, and 10μg/ml, were prepared by adding appropriate pure BSA to 5 ml of diluted dye reagent in its container.
3. 0.5μl or 1μl of unknown samples were added to 5 ml of diluted dye reagent and vortexed.
4. There were incubated at room temperature for at least 5 mins. Absorbance will increase over time *(Samples should not be incubated at room temperature for over 1 hour).*
5. Finally, the absorbance at 595 nm of all standard samples and unknown samples were measured, the concentration of unknown samples was provided by software.

2.15 Western Blotting

1. The 5× SDS-PAGE gel running buffer and 2× SDS-PAGE gel loading buffer were prepared first. Then the glass gel containers were cleaned with 70% ethanol.
2. The SDS-PAGE resolution gel was prepared as the following table:

8% SDS-Page Resolving Gel	1Gel (1.5mm)	2Gel	4Gel
40% Acrylamide/Bis 19:1	***1.5 ml***	***3 ml***	***6 ml***
1.5M Tris-base pH8.8	***1.8 ml***	***3.75 ml***	***7 ml***
Temed	***5 µl***	***10 µl***	***20 µl***
10% SDS	***75 µl***	***150 µl***	***300 µl***
10% APS	***38 µl***	***75 µl***	***150 µl***
ddH$_2$O	***4 ml***	***8 ml***	***16 ml***

3. Afterwards the solution was quickly added to the glass gel container, almost 500 µl 0.1% SDS solution was added above each SDS-Page resolution gel surface.
4. After the resolution gels had set, the solution above the gel surface was discarded and the surface of gels was washed gently with ddH_2O twice. Following the remained water was removed with Whatman filter paper, and the gels containers were dried at room temperature for 15 mins.
5. The Stacking gel for SDS-PAGE gel electrophoresis was produced as the following table:

Stacking Gel	1Gel (1.5mm)	2Gel	4Gel
40% Acrylamide/Bis 19:1	***0.5 ml***	***1.0 ml***	***2.0 ml***
1.0M Tris-HCl pH6.8	***0.65 ml***	***1.3 ml***	***2.6 ml***
Temed	***10 µl***	***20 µl***	***40 µl***
10% SDS	***50 µl***	***100 µl***	***200 µl***
10% APS	***50 µl***	***100 µl***	***200 µl***
ddH$_2$O	***3.2 ml***	***6.4 ml***	***12.8 ml***

6. The stacking gel solution was transferred into glass gel container, and then the comb was put into the solution quickly and left to set.
7. The samples were boiled together with loading buffer.
8. Under the running buffer (1× SDS-Page running Buffer), the comb was removed

after the stacking gel had set. Then, the wells were cleaned by a gentle buffer flow.

9. Electrophoresis was performed at 100V for 1.5 hours or 150V for 1.0 hour.
10. Meanwhile, the PVDF membrane for Western blotting was cut to a size larger than the gel. The membrane was wet in methanol and was submerge in water in sequence. Finally, the wet membrane was equilibrated in cold western transfer buffer for at least 10 mins.
11. The sponge, a piece of filter paper, the gel containing proteins, the PVDF membrane, another piece of filter paper, and the sponge were assembled in order on the black plastic plank.
12. After the Western transfer sandwich had completed the electrophoresis transfer was carried out with stirring in the cold room.
13. The membrane was removed away and dried on the filter paper. The membrane was wet again in methanol and water in order.
14. The membrane was blotted in 5% blocking reagent in tris-buffered saline Tween (1× TBST) overnight in the cold room or 1 hour at room temperature.
15. This was then incubated with primary antibody 2 hours at room temperature.
16. Then it was washed with TBST twice. Once for 5 mins, and another for 15 mins.
17. It was incubated with the second antibody for 1 hour at room temperature.
18. Then it was washed with TBST twice. Once for 5 mins, another for 15 mins.
19. The membrane was incubated with ECL reagent (Amersham, UK) mixture for 1-2 minutes. Any excess liquid was removed with clean filter paper before images were taken by UVP bioimaging system.

2.16 Ubiquitination reaction of Rad4 protein

1. The reaction solutions were added to each chilled tube that contains 1μg E1 (Yeast, Sigma), 1μg hUbc4a, 1μg hUbc4b, 1.3μg hUbc4c (Human, BostonBiochem), 0.1 μg GG-NER complex, 6μl 5× Reaction buffer (20mM $MgCl_2$, 200mM KCl 180mM Tris pH8.0), 6μl ATP (20mM), 1μl or 2μl raw TNT-expressed Rad4 protein.
2. The Ubiquitylation reaction was initiated by adding 5μl ubiquitin then ddH_2O to total volume of 30μl.
3. The reaction was performed at 28°C for 60 minutes. After the reaction had finished, 0.2-0.3 μl additional 100× protease inhibitors was added to the reaction products. Then, the products were run on SDS-PAGE gels immediately (The denaturing temperature of western blotting for this reaction product is 60-80 °C.).

2.17 Pulse-chase assay

1. Pulse chase experiments were performed by growing cells to a density of about 1-2× 10^7 cells/ml, then pelleted and washed twice with PBS.
2. Cells were resuspended in appropriate warmed media and a pulse of 25 μCi ^{35}S-methionine per ml was applied at 30°C for 1 hour.
3. Cells were then pelleted, washed with PBS twice and 1/4 of the total cells collected as a '0' sample. The remaining cells were divided into 3 parts and were resuspended in pre-warmed YPD. Then those 3 samples were incubated with non-radiolabel medium at 30°C for 1, 2, 4 hours respectively before them were collected.

4. Whole cell extracts were made by the method described in 2.10.

2.18 Production of Rad4 antibody

1. A synthesized peptide was chosen as the antigen. The amino acid sequence of this peptide is as follows:

   N-Cys-Gly-Glu-Asp-Tyr-Ser-Asp-Phe-Met-Lys-Glu-Leu-Glu-Met-Ser-Glu-Glu-Ser-Asp-C

2. The peptide contains an extra N-terminal cysteine with the amino acid sequence of Rad4 protein from 737 to 754. The peptide was synthesized by using solid-phase peptide synthesis methodology under optimized conditions.
3. The crude peptide product was purified by reverse phase high performance liquid chromatography (HPLC). Additionally, the purified peptide was subjected to mass spectrometry in order to confirm peptide integrity.
4. Following the purification and confirmation process, the peptide (5mg) was conjugated to keyhole limpet haemocyanin (KLH) (7mg) using a maleimido based coupling procedure via the N-terminal cysteine sulphydryl moieties to afford an N-terminally conjugated peptide.
5. The conjugated product was diluted in physiological saline and aliquot made ready for emulsion preparation.
6. New Zealand white specific pathogen free rabbits were used. The immunization was carried out by AFFINITI Research Product Ltd. The pre-immune serum and antisera from selected rabbits were collected by this company.
7. Sodium azide was added to all sera to a final concentration of 0.1%w/v. All sera were frozen and stored at -20°C.

Chapter 3
How does the Rad7/Rad16/ABF1 complex (GG-NER complex) generate superhelical torsion?

3.1 Introduction

NER is one of the most versatile DNA repair pathways capable of removing a broad spectrum of DNA damage caused by radiation and chemicals. In *S. cerevisiae*, Rad7 and Rad16 interact directly and both are specifically required for most of GG-NER function (Bang *et al.*, 1992; Verhage *et al.*, 1994; Wang *et al.*, 1997). The repair of the nontranscribed DNA strand (NTS) and transcriptionally inactive regions of the genome are severely reduced in *Δrad7* and *Δrad16* mutants, whereas the repair of the transcribed strand (TS) is not affected (Verhage *et al.*, 1994; Mueller and Smerdon, 1995). Rad16 contains one zinc binding motif, a C_3HC_4 ring finger motif (Prakash and Prakash, 2000; Ramsey *et al.*, 2004). Although a complex of Rad16 and Rad7 (referred to as NEF4) has been suggested to participate in DNA damage recognition, Reed *et al* showed using yeast whole cell extracts capable of supporting GG-NER, that Rad7/Rad16 is not crucial for the early stages of GG-NER *in vitro* including damage recognition and incision. Reed's study reveals that one primary role of Rad7 and Rad16 during GG-NER is to facilitate lesion removal, a stage after incision, and often referred to as the excision step of NER (Reed *et al.*, 1998; Guzder *et al.*, 1997; 1998). In this chapter, I describe experiments where I used a previously developed *in vitro* NER assay to examine the repair of UV-damaged plasmid DNA. The assay was employed to test whether a purified complex of Rad7/Rad16/ABF1 proteins restores the repair activity of yeast whole cell extracts prepared from Rad7 and Rad16 defective cells, and to examine the biochemical activity of the purified Rad7/Rad16/ABF1 complex.

The amino acid sequence of Rad16 protein shares homology with the Snf2 protein, the catalytic subunit of the SWI/SNF chromatin remodeling complex (Bang *et al.*, 1992). Rad16 and Snf2 are members of SNF2 superfamily of proteins. The SNF2 family proteins contain a conserved set of amino-acid motifs including archetypal motifs which are embraced by a large family of ATPases (Eisen *et al.*, 1995). Most of the ATPase family members are subunits of complexes that exhibit chromatin remodeling capacity, and all are endowed with ATPase activity that is stimulated in the presence of DNA or chromatin (Whitehouse *et al.*, 1999; Peterson *et al.*, 2000). A report has provided important insight into the mechanisms by which the ATPase motors of SNF2 family complex change chromatin structure (Havas *et al.*, 2000). Using linear DNA fragments instead of chromatin the authors have found that those complexes can generate superhelical torsion which may help to remodel DNA in the chromatin context. These studies revealed that the fundamental acitivity of the ATPase motors of SNF2 superfamily proteins involves the generation of superhelical torsion in DNA.

A third member of the GG-NER complex, ABF1, has been found to copurify with Rad7/Rad16 in a protein complex, after several chromatographic steps (Reed *et al.*, 1999). Using an *in vitro* assay, it has been confirmed that whole cell extracts prepared from strains carrying mutations in the genes encoding any of those three proteins are defective in NER *in vitro.* They are also NER defective *in vivo* (Reed *et al.*, 1999). Moreover, it has been demonstrated that the Rad7/Rad16/ABF1 complex generates superhelical torsion in a DNA molecule to facilitate the excision of the oligonucleotide containing sites of base damage during NER in yeast (Yu *et al.*, 2004). In that report it was shown that the generation of superhelicity in the damaged DNA substrate by Rad7/Rad16/ABF1 complex is obligatory to observe oligonucleotide

excision during NER, but is not necessary to detect the presence of NER-dependent incision (Yu *et al.*, 2004). From these studies it was concluded that the mechanism of excision in the GG-NER pathway of NER includes the generation of superhelical torsion in DNA.

It has been reported that an essential and abundant SWI/SNF family chromatin remodeler from *S. cerevisiae*, RSC, composed of 15 proteins, exhibits an ATP-dependent DNA translocation activity (Saha *et al.*, 2002). Sth1 is one of the DNA-dependent ATPase components of the RSC complex. Although the chromatin remodeling properties of this protein in isolation have not been reported, Sth1 also displays a similar ATP-dependent DNA translocase activity as the RSC complex (Saha *et al.*, 2002). Therefore, the generation of superhelical torsion in DNA is directly generated by the DNA translocase activity of the DNA-dependent ATPase motors, which are components of SWI/SNF family of chromatin remodelers. This combination of DNA translocation and generation of superhelicity provides the energy necessary to break the initial histone–DNA contact, which subsequently leads to chromatin remodeling.

I speculated that the Rad7/Rad16/ABF1 complex generates superhelical torsion in DNA to facilitate oligonucleotide excision by utilizing an ATP-dependent DNA translocase activity of the Rad16 component of the GG-NER complex in a similar fashion to the RSC complex. To detect whether the Rad7/Rad16/ABF1 complex has this property, I developed and adapted a triple-helix strand displacement assay.

3.2 Materials and Methods

Triple-helix strand displacement assay

All of the double-stranded DNAs for triple-helix construction contain a 40-bp d(GA) · d(TC) tract. Double-stranded DNA for centre-positioned triplexes (190 bp)

was prepared by PCR using a BSCR plasmid containing the centrally located 40-bp d(GA) · d(TC) tract. The third strand, consisting of a 40-nt single-stranded homopyrimidine repeat $(dTC)_{20}$, was end-labeled with [γ-^{32}P]dATP at the 5' end. Substrates were formed by incubating the labeled $(dTC)_{20}$ with a two fold molar excess of double-stranded DNA, in a buffer containing 33 mM Tris-acetate (pH 5.5), 66 mM potassium acetate, 100 mM NaCl, 10 mM $MgCl_2$, and 0.4 mM spermine (Kopel *et al.* 1996). Triple-helix displacement assays were carried out at 30°C in a reaction buffer containing 36 mM Tris-acetate (pH 7.3), 20 mM potassium acetate, 8mM $MgCl_2$, 5% (v/v) glycerol, 0.5 mM DTT, and (when indicated) 1 mM ATP. Reactions (25 µl) contained 30 ng of triple-helix DNA and 10 µl (1000 ng) of Rad7/Rad16/ABF1 complex (or SV-40 large T-antigen). After 30 min, reactions were quenched with 0.5 % SDS, 15 mM EDTA, 3% (v/v) glycerol, 2 mM Tris-HCl (pH 8.0), and 25 ng of unlabeled $(dTC)_{20}$. Products were resolved on a 15% native polyacrylamide gel and analyzed using ImageQuant (Molecular Dynamics Inc.).

Purification of the Rad7/Rad16/ABF1 complex

Since the three components form a stable complex, Rad16 and ABF1 can be co-purified with C-terminal 6-His tagged Rad7 protein. Approximately, 100g wet weight of cells were used to purify the endogenously expressed 6-His tagged Rad7 protein using a protocol described in 2.9 (also in Reed *et al.*, 1998). After the final glycerol gradient step of the purification we obtained ~30,000-fold enrichment of a Rad7/Rad16/ABF1 complex from the whole cell extract.

The *in vitro* NER assay

Plasmid pUC18 (100µg/ml) in TE buffer was treated with a 300J/m^2 of UV radiation. Then pUC18 containing CPDs was purified by a 5-20% sucrose gradient centrifugation following incubation with *E. coli* endonuclease III. Standard reaction

mixtures (50 μl) contained 300 ng of damaged plasmid pUC18, 300 ng of undamaged plasmid pGEM DNA, 45 mM Hepes-KOH (pH 7.8), 7.4mM MgCl2, 0.9mM dithiothreitol, 0.4mM EDTA, 2 mM ATP, 20 μM dATP, 20 μM dGTP, 20 μM dTTP, 8 μM dCTP, 1 μCi of [a-^{32}P]dCTP (3000 Ci/mmol; 1Ci = 37 GBq), 40 mM phosphocreatine (disodium salt), 2.5 μg of creatine kinase, 4% glycerol, 5 μg of bovine serum albumin, 5% polyethylene glycol 8000 (PEG), and 250 μg of yeast whole cell extract. After incubation for 2 hr at 28°C, plasmid DNA was purified via the phenol/chloroform method and linearized with HindIII enzyme. DNA was resolved by 1% agarose gel electrophoresis in the presence of ethidium bromide (0.5 μg/ml). After drying, the gels were autoradiographed and analyzed with Imagine Quant software.

Preparation of whole cell extract (WCE) for *in vitro* NER

Yeast cells were grown overnight at 30°C in 2 litres of YPD medium. Cells were harvested by centrifugation and washed twice with cold water (4°C) and hypotonic buffer respectively. The preparation of WCE supporting *in vitro* NER was described in 2.11.

Coomassie blue stain

Gels were stained by an appropriate volume of working coomassie blue solution at 50°C for 30 mins followed the gel electrophoresis. The stained gel was washed by destain solution twice at 50°C for 30 mins. Then the gel was destained overnight at room temperature.

3.3 Results

3.3.1 Purification of the Rad7/Rad16/ABF1 complex

Typically, the GG-NER complex was purified from 80g to 100g wet cells through

several steps which were described in 2.9. After Ni-NTA purification had been carried out, fractions of Ni-NTA were analyzed by Western blotting with anti-Rad7 antibody. As shown at Figure 3.1 fractions 1-10 were eluted with 15 ml of Extraction Buffer A/1mM 2-mercaptoethanol supplemented with 25 mM imidazole, 50 mM imidazole, 100 mM imidazole and 100 mM imidazole respectively.

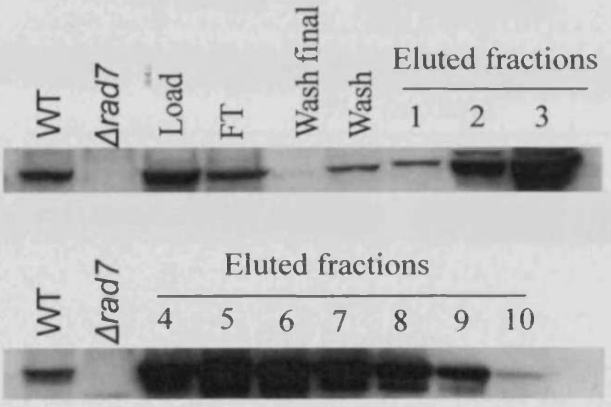

Figure 3.1. The Western blot analysis of Ni-NTA fractions. "FT" represents the flow through fraction from the Ni-NTA column during the loading step.

Fractions 3-8 of the Ni-NTA were pooled and the NaCl concentration adjusted to 100 mM by dilution. Further purification was carried out following chromatography using a P11 column. The proteins bound to the P11 column were eluted using Extraction Buffer A with a NaCl gradient concentration from 100 mM to 1000mM. Then, the resulting P11 fractions were analyzed by Western blot using Rad7 antibody to identify peak fractions for further purification (see Figure 3.2).

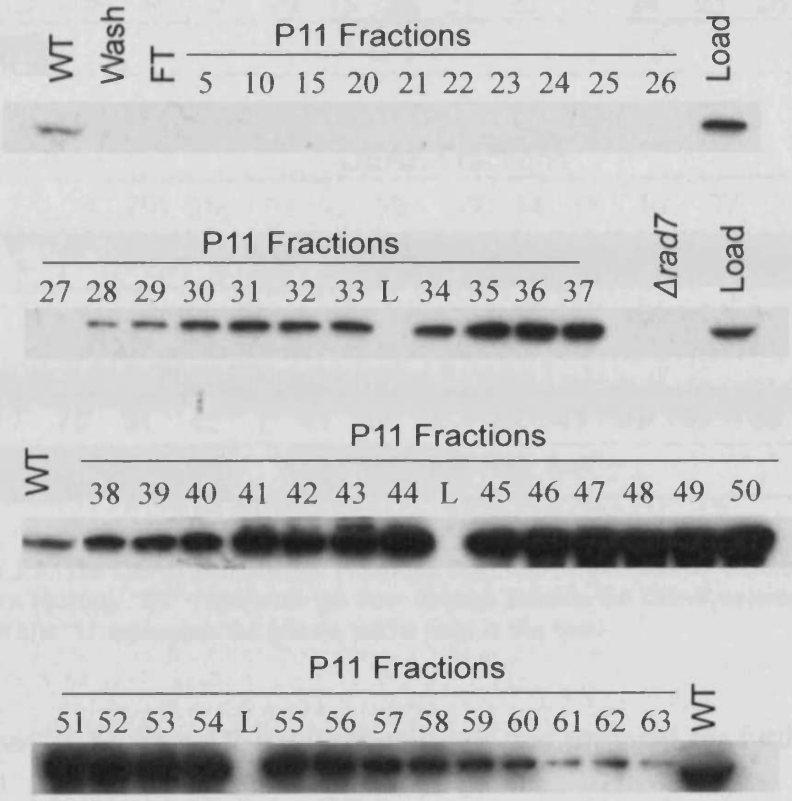

Figure 3.2. The Western blot analysis with anti-Rad7 antibody followed the P11 purification. "L" represents the protein ladder used in this blot. While "FT" represents the solution flow through the P11 column during the loading step.

As described in 2.9, peak fractions, from 40 to 56, were prepared and loaded to an equilibrated DEAE column. The eluted fractions from DEAE sephacel were checked by Rad7 western blot (results were shown at Figure 3.3).

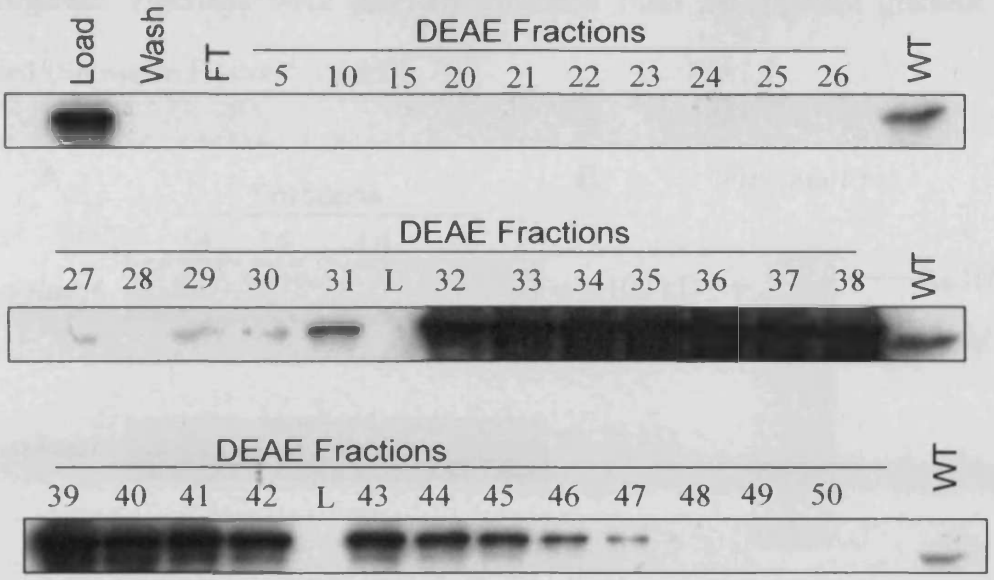

Figure 3.3. The DEAE purification. Fractions from DEAE purification were checked by the Rad7 Western blotting. "FT" represents the flow through fraction the DEAE column during the loading step. While "L" represents the protein ladder used in this blot.

Fractions 33-43 form DEAE were collected and prepared for further purification on a mono-Q column. After the FPLC system was cleaned and adjusted using the appropriate solutions, peak DEAE fractions were pooled and loaded onto a mono-Q column. Proteins were eluted with a linear gradient of NaCl (100mM – 1000mM) in Extraction buffer A. All fractions were checked by Rad7 Western blots (Figure 3.4).

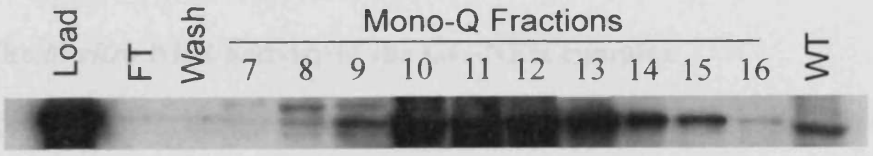

Figure 3.4. The FPLC mono-Q purification. Fractions from mono-Q purification were analyzed with anti-Rad7 Western blotting assay. "FT" represents the flow through fraction the DEAE column during the loading step. "Load" represents the solution was loaded onto mono-Q column.

The peak Rad7 containing mono-Q fractions were pooled and loaded to the surface of a glycerol gradient solution containing Extraction buffer A supplemented with glycerol at 10% - 30%. The final purification step was performed by

centrifugation. Fractions were carefully collected from the glycerol gradient and analyzed (Shown in Figure 3.5 A&B).

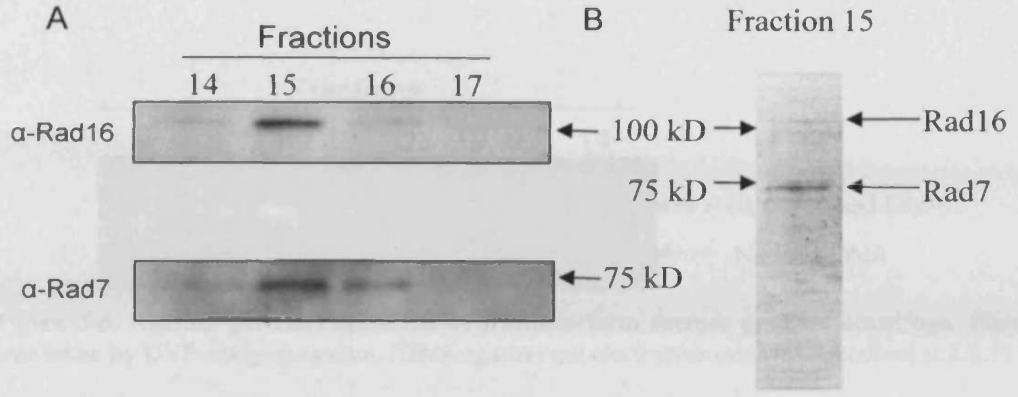

Figure 3.5. A. The Western blot analysis of glycerol gradient fractions. Top panel was probed with anti-Rad16 antibody, while the lower panel was the same blot but re-probed with anti-Rad7 antibody. B. SDS-PAGE gel stained with Coomassie blue shows the presence of Rad7 and Rad16 proteins.

Based on Figure 3.5 A, fraction 15 has the peak concentration of both Rad7 and Rad16 proteins. Moreover, the presence of Rad7 and Rad16 proteins were confirmed by Coomassie blue stain assay (Figure 3.5B). I did not test the presence of ABF1 protein in the peak fraction, but according to previous work this peak fraction contains ABF1 (Reed *et al.*, 1999).

3.3.2 The *in vitro* NER activity of the GG-NER complex

Before I examined the purified Rad7/Rad16/ABF1 complex to test its DNA translocase activity, I tested the ability of the purified complex to restore *in vitro* NER activity to whole cell extracts prepared from Rad7/16 mutant yeast cells. It has been demonstrated that the extracts from *Δrad7* mutant strain were fully proficient in the incision step of the NER reaction *in vitro* but deficient in both excision step and repair synthesis (Reed *et al.*, 1998). In that research, repair synthesis was monitored in plasmid DNA containing N-acetyl-2-aminofluorene (AAF) adducts. In this instance, I

used instead UV irradiated pUC18 containing predominantly CPDs and 6-4 photoproducts, the major UV induced DNA damages (details described at 3.2) as the target for NER.

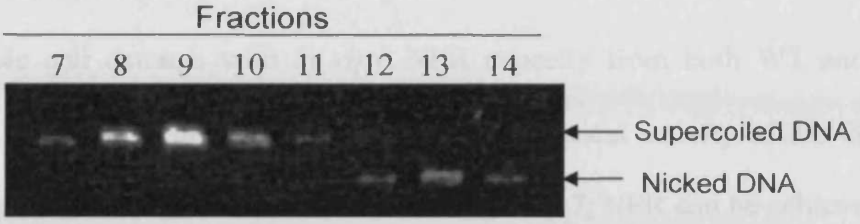

Figure 3.6. Agarose gel electrophoresis of fractions form sucrose gradient centrifuge. Picture was taken by UVP-imagine system. (DNA agarose gel electrophoresis was described at 2.5.1)

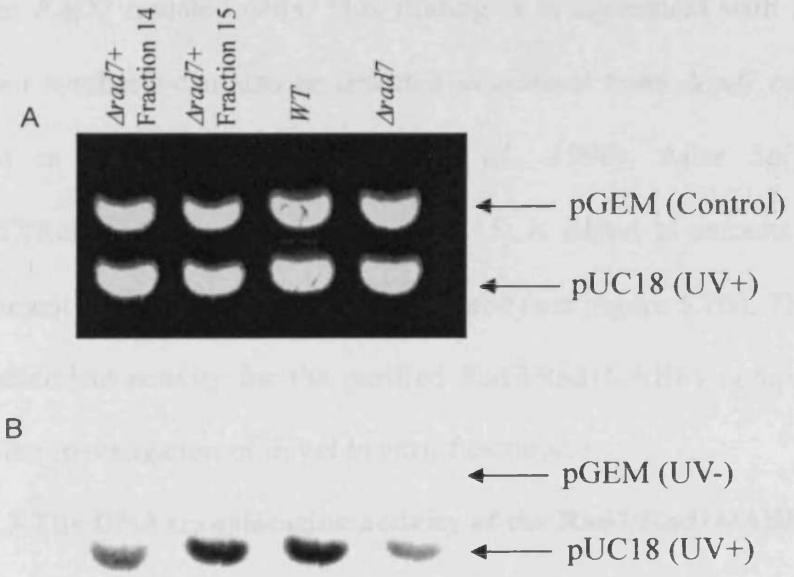

Figure 3.7 A. The plasmid DNA was visualized in gel under UV light following staining with ethidium bromide. B.DNA repair synthesis as measured by dried agarose gels. The top bands in figure A and B were un-UV irradiated plasmid DNA, pGEM, as the negtive control. The lower bands were UV-damaged pUC18.

Firstly, UV-irradiated pUC18 was purified using the method described in 3.2. UV light can induce some photoproducts that are base excision repair substrates. For example, the *E. coli* BER enzyme endonuclease III can excise these damaged bases to

result in the covalently closed circular plasmid template becoming nicked after the endonuclease III treatment (see Figure 3.6). Nicked DNA is purified from supercoiled DNA on a sucrose gradient and only supercoiled pUC18 fractions are suitable for *in vitro* NER assay and collected for this purpose.

The whole cell extracts with *in vitro* NER capacity from both WT and *Δrad7* strains were prepared as described in 3.2. The biochemical activity of the GG-NER complex was tested by *in vitro* NER. Based on Figure 3.7, NER can be achieved using the plasmid containing UV-induced damage instead of AAF adducts. Compared with the extracts from the wild type strain, a low NER activity was detected with extracts from *RAD7* mutated cells. This finding is in agreement with a previous report that repair synthesis can also be detected in extracts from *Δrad7* cells, but at lower level than in wild type cells (Reed *et al.*, 1998). After 5μl (50ng) of purified Rad7/Rad16/ABF1 complex (fraction 15) is added to extracts from a *Δrad7* strain, deficient NER in these extracts is restored (see Figure 3.7B). Thus this assay shows a biochemical activity for the purified Rad7/Rad16/ABF1 complex in NER, allowing further investigation of novel *in vitro* function(s).

3.3.3 The DNA translocation activity of the Rad7/Rad16/ABF1 complex

The triple-helix strand displacement assay employed in this chapter depends on the propensity for a homopurine–homopyrimidine repeat to form a three-strand triple helix (H-DNA) with a complementary homopyrimidine oligonucleotide at moderately low pH (pH5.5) (Saha *et al.*, 2002). The triple helix can remain stable when the pH is shifted to near neutral (pH7-8). However, if the third strand is displaced somehow, it will not reform a triple-helix at neutral pH. It has been reported that the homopyrimidine oligonucleotide occupies the major groove of the mirror repeat in the triple helix, with each base of the oligonucleotide forming a Hoogsteen base pair with

the Watson–Crick base pairs (van Dongen *et al.*, 1999). Therefore, when a DNA translocase proceeds through the triple-helix, the third strand (the homopyrimidine oligonucleotide) will become separated from the duplex since it is bound to the duplex by weaker Hoogsteen base pairs.

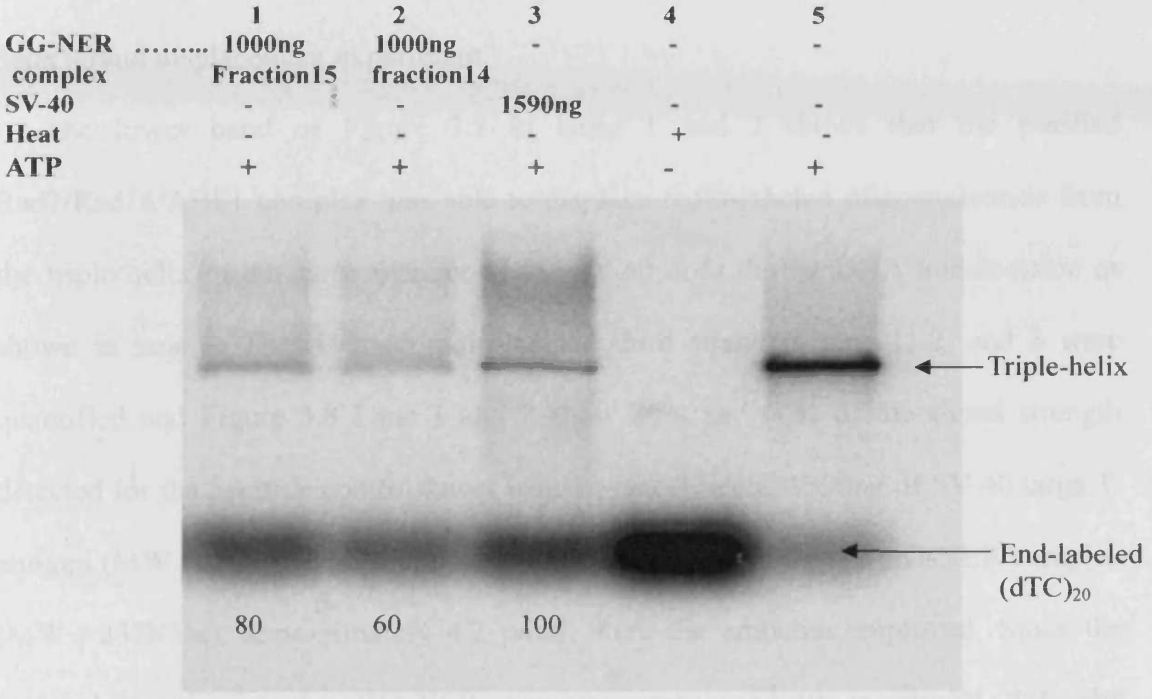

Figure 3.8. The purified Rad7/Rad16/ABF1 complex displace a triple helix. The duplex was prepared as described in 3.2. The third strand, consisting of a 40-nt single-stranded homopyrimidine repeat $(dTC)_{20}$, was end-labeled with [γ-^{32}P]ATP at the 5' end. Triple helices were centre-positioned on a 190bp duplex. After the reaction was finished, the solution was separated on 15% polyacrylamide gel.

Displacement of the third strand from a triple-helix has been used to show the translocation activity of the SV-40 large T-antigen helicase, so we have used the SV-40 system as our positive control (Kopel *et al.*, 1996). In this case a triple helix of 40 bp has been formed that is located centrally on a 190-bp double-stranded DNA, using γ-^{32}P end-labeled $(dTC)_{20}$. The third strand (γ-^{32}P radio-labeled $(dTC)_{20}$) can be totally released when the triple helix is heated briefly at 90°C (Shown in Figure 3.8 lane 4).

Following the final step of purification by glycerol gradient centrifugation, the Rad7/Rad16/ABF1 complex fractions were detected by anti-Rad7 Western blotting. The NER activity of the fractions 14 and 15 was examined by the *in vitro* NER assay as described earlier. Results showed these fractions rescued the defective NER activity in a whole cell extract (WCE) prepared from *Δrad7* (and/or *Δrad16*, *Δrad7/ Δrad16*) mutant strains (see 3.3.2). These two fractions were used to perform the triple helix strand displacement experiment.

The lower band of Figure 3.8 in lanes 1 and 2 shows that the purified Rad7/Rad16/ABF1 complex was able to displace radio-labeled oligonucleotide from the triple helix in the same manner as the SV-40 does during DNA translocation as shown in lane 3. The released radio-labeled third strand in lane 1, 2, and 3 were quantified and Figure 3.8 Lane 1 and 2 show 80% and 60% of the signal strength detected for the positive control lower band in lane 3. Here, 1590ng of SV-40 large T-antigen (MW ~100KDa) approximately 15.9 pmol, and 1000ng of GG-NER complex (MW ~237KDa), approximately 4.2 pmol, were the amounts employed. Since the molecular ratio of the GG-NER complex versus SV40 is almost 1:4, the Rad7/Rad16/ABF1 complex performs the translocase activity with a high efficiency. Strand displacement was dependent on the presence of ATP.

To test whether the translocase activity of the GG-NER complex requires the hydrolysis of ATP, the triple-helix strand displacement experiment was carried out with ATP or ATPγS, which is an analogue of ATP and cannot be hydrolyzed by ATPases (Figure 3.9). When ATPγS replaced ATP, in lane 2 and lane 4 no released third strands were observed, indicating that the GG-NER complex requires the hydrolysis of ATP to support its translocation activity.

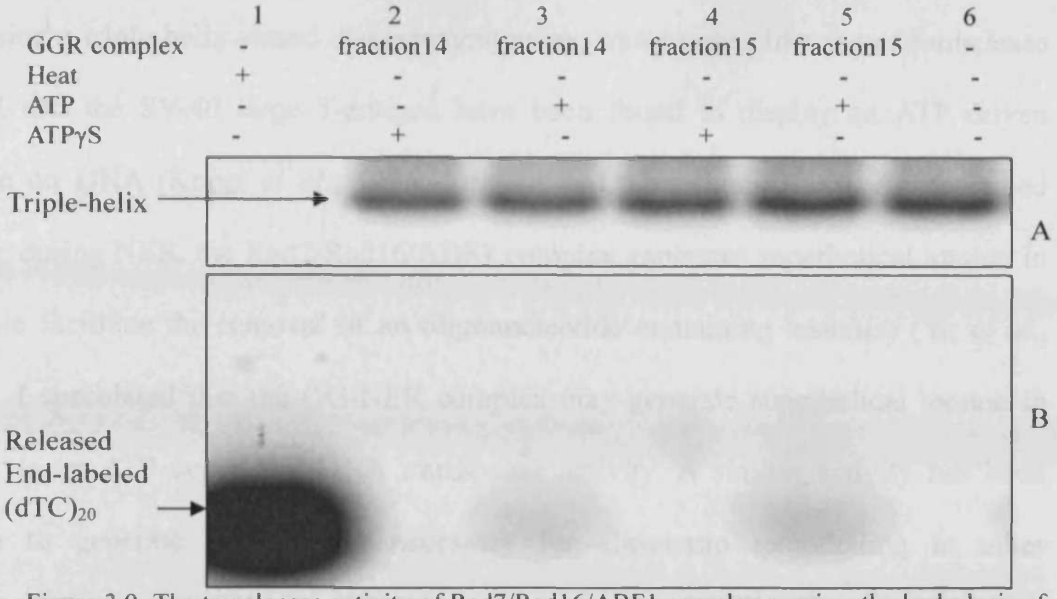

Figure 3.9. The translocase activity of Rad7/Rad16/ABF1 complex requires the hydrolysis of ATP. In lane 2 and lane 4 ATPγS, an analogue of ATP, replaced ATP. Panel A shows the triple-helix band (short exposure), panel B shows the released $d(TC)_{20}$ oligo form the triple-helix (long exposure).

Therefore, I conclude, that the purified Rad7/Rad16/ABF1 complex exhibits an ATP-dependent DNA translocase activity *in vitro*.

3.4 Discussion

In yeast Rad7 and Rad16 specifically function in the GG-NER pathway, and with ABF1 form a stable complex both *in vivo* and *in vitro* (Wang *et al.*, 1997; Reed *et al.*, 1998). The Rad16 protein has two ring finger motifs and is a homologue of Snf2 protein. Moreover, the ABF1 protein can also bind to the ABF1 DNA recognition sequence found at numerous sites throughout the yeast genome. Reed *et al* revealed that *Δrad7* and *Δrad16* mutants are proficient in NER-dependent DNA incision both *in vivo* and *in vitro*, suggesting that neither of them are essential elements in the early damage recognition stage of NER (Reed *et al.*, 1998). Therefore, instead of the GG-NER complex acting as a DNA damage sensor as previously suggested, I considered the possibility that the ATPase motors of Rad16 in the complex were utilised to perform a DNA translocase function which could generate supehelical torsion in the

DNA during GG-NER.

Using a triple helix strand displacement assay, translocases like the endonuclease EcoAI and the SV-40 large T-antigen have been found to display an ATP driven motion on DNA (Kopel *et al.*, 1996; Firmam and Szczelkum 2000). As described earlier, during NER, the Rad7/Rad16/ABF1 complex generates superhelical torsion in DNA to facilitate the removal of an oligonucleotide containing lesion(s) (Yu *et al.*, 2004). I speculated that the GG-NER complex may generate superhelical torsion in DNA via an ATP-dependent DNA translocase activity. A similar activity has been shown to generate supercoiling necessary for chromatin remodelling in other SWI/SNF type complexes such as RSC (Saha *et al.*, 2002). By monitoring the displacement of the third strand, a radio-labeled homopyrimidine oligonucleotide $(dTC)_{20}$, the purified Rad7/Rad16/ABF1 complex exhibits a similar strand displacement activity as the SV-40 large T-antigen does under similar conditions. It is possible this complex's motion on DNA plays a role in a number of aspects in NER. For example, it may facilitate excision (Yu *et al.*, 2004) and may enable histone H3 acetylation pre-excision (Teng *et al.*, in press).

Chapter 4
The UV-dependent ubiquitination and degradation of Rad4 requires a novel Rad7 E3 ubiquitin ligase

4.1 Introduction

The fundamental action of DNA repair pathways is to maintain the integrity of the genome, although the overall development of the organism including aging and development of the immune system are also influenced by these processes. NER is a major DNA repair pathway capable of removing a broad spectrum of DNA damage caused by radiation and chemicals. There are two NER sub-pathways, transcription coupled NER (TC-NER) and global genome NER (GG-NER). DNA damage is repaired by TC-NER in transcriptionally active regions, and repaired by GG-NER in non-transcribed strands and silent regions of the genome (Friedburg *et al.*, 1995; 2006; Reed and Waters, 2003; Reed *et al.*, 2005).

In the yeast *S. cerevisiae*, Rad7 and Rad16 are reported to function uniquely in the GG-NER pathway (Bang *et al.*, 1992; Reed *et al.*, 1996; Reed *et al.*, 1998). The Rad7 and Rad16 proteins are specifically involved in the removal of lesions from non-transcribed regions of the genome *in vivo*. Reed *et al.* have demonstrated that Rad7 and Rad16 are required at a stage following DNA damage incision (Reed *et al.*, 1998), and more recently Yu *et al.* have shown that these proteins are involved in generating superhelical torsion in DNA which facilitates excision of the DNA damage (Yu *et al.*, 2004). Rad16 protein belongs to the SWI2/SNF2 superfamily of proteins, several of which have been shown to be ATPases involved in chromatin remodeling. The autonomously replicating sequence-binding factor 1 protein (ABF1) is an abundant DNA-binding protein, and ABF1-binding affects the efficiency of NER in yeast (Reed *et al.*, 1999). All of these findings appear to relate to a core NER function

of Rad7/Rad16/ABF1 complex in promoting oligonucleotide excision of the damaged DNA during GG-NER, since defects in any of these activities result in a UV sensitive phenotype. A new additional and distinct function of Rad7/Rad16 is reported in this chapter as a result of studying the role of the ubiquitin proteasome pathway (UPP) in NER.

The identification of an ubiquitin-like (Ubl) domain present at the N-terminus of the Rad23 DNA repair protein provided circumstantial evidence linking NER and the UPP (Watkins *et al.*, 1993). The functional significance of the Ubl domain of Rad23 in NER was demonstrated by a deletion of that region which resulted in impaired repair activity. The link between NER and the UPP was further strengthened by the observation that this defect could be restored by the replacement of the ubl sequence of Rad23 with the actual ubiquitin sequence. Unexpectedly, the domain did not promote protein degradation of Rad23, suggesting a possible non-proteolytic function of Rad23 in NER (Watkins *et al.*, 1993).

However, Schauber *et al.* showed a direct physical association between Rad23 and the 26S proteasome and suggested that the UPP regulates NER through the Ubl domain of Rad23 by a proteolysis-dependent mode. However the short half-life of Rad23 in Schauber's work was later understood to be caused by the epitope-tag placed on Rad23 (Watkins *et al.*, 1993; Schauber *et al.*, 1998). After it was established that native Rad23 was not targeted for degradation by the proteasome in response to UV, attention had turned to the Rad4 NER protein as being an alternative potential target for ubiquitin dependent degradation by the proteasome (Lommel *et al.*, 2000b). In *S. cerevisiae* Rad4 plays an essential role in both RNA pol II-dependent TC-NER and GG-NER. It binds with Rad23 to form a stable complex *in vivo* and appears to participate in the early stage of NER, recognition of damage (Bardwell *et al.*, 1994;

Jansen *et al.*, 1998; Guzder *et al.*, 1998). The authors noted that apparently overexpression of Rad4 results in higher NER activity, suggesting that in undamaged cells, Rad4 was ubiquitinated and constitutively degraded by the proteolytic activity of the proteasome. However, in response to UV it was suggested that Rad4 became transiently stabilized, resulting in accumulation of Rad4 that in some way enhanced NER. The model suggested that proteolytic degradation of Rad4 by the proteasome negatively regulates NER. In yeast, it had been shown that two protein domains within Rad23 known as Uba domains could act as protein stabilisation signals. These domains could possibly promote the stability of a proteolytic substrate by blocking the formation of polyubiquitin chains on its surface (Ortolan *et al.*, 2000; Bertolaet *et al.*, 2001b; Chen *et al.*, 2001). Recently, it was discovered that as well as the possibility of the Uba domain acting in *trans*, these domains can function in *cis* and apparently control the proteolytic turnover of Rad23 protein itself (Heessen *et al.*, 2005). At present it remains unclear whether the Uba domains of Rad23 contribute to maintaining the steady levels of Rad4. The initial reports on Rad4 stability in response to UV in yeast were apparently supported by the observation in mice that the Rad4 homologue, XPC, accumulated after DNA damage. The accumulation of XPC was suggested to cause enhanced NER (Ng *et al.*, 2003). This study also revealed that the absence of hHR23 resulted in lower steady levels of XPC protein. It was predicted that the primary function of hHR23 in NER was to stabilize XPC and maintain the steady state level of XPC at an optimal level for NER. However, it was later shown that overexpression of Rad4 protein does not lead to enhanced NER (Xie *et al.*, 2004). Moreover, it became clear that proficient NER requires the Rad23 protein to do more that stabilise Rad4, based on the following; the R4B domain of Rad23 was required for stable interaction of Rad4 with Rad23 and this was thought to affect the stability

of the Rad4 protein. So in Rad23-R4B mutants the steady state level of Rad4 decreased to a lower level than that in WT. If the primary function of Rad23 is stabilization of Rad4, this strain should have demonstrated UV sensitivity similar to a *rad23* deletion strain. In fact, this strain only displayed a slight UV sensitivity (Ortolan *et al.*, 2004). These flaws found in the proteolytic hypothesis prompted a closer examination of a nonproteolytic function for the 19S and Rad23, and previously shown to be required for proficient NER (Reed and Gillette, 2007).

A non-proteolytic activity of the proteasome for NER was first demonstrated by Russell and Reed *et al* (Russell *et al.*, 1999). These authors revealed that complete inhibition of the proteolytic activity of the 26S proteasome did not affect NER *in vitro*, whereas targeted interventions to the 19S activity using two distinct approaches (chemical and antibody inhibition), did affect repair. The non-proteolytic function of 19S RC on NER was thought to include a molecular chaperone activity to alter the conformation of certain NER proteins to facilitate the NER reaction. It was suggested that the Ubl domain of Rad23 recruited the 19S RC to the DNA damage site. Further studies on the 19S RC revealed that even in the absence of Rad23, the 19S continued to affect NER and UV survival *in vivo* (Gillette *et al.*, 2001). So, the Ubl domain of Rad23 didn't simply recruit the proteasome to the NER machinery, but rather mediated functional interactions between the two pathways. It was shown that the UV sensitivity and defective NER of a *Δrad23* strain were significantly suppressed by introducing an additional *sug* (Rpt4 or Rpt6) mutation. In contrast, in a *Δrad23*/20S double mutation strain, UV sensitivity did not alter even though the proteolytic activity of the proteasome was severely defective. Furthermore, the rescue of UV sensitivity associated with the *Δrad23* deletion was allele specific, since mutations of other AAA-family ATPase subunits such as Cim5 did not rescue the *Δrad23*

phenotype. A model of non-proteolytic function on NER was described; the 19S RC negatively regulates NER and Rad23 acts to suppress the negative regulation of 19S RC. One of the groups that originally proposed the proteolytic model, recently recognized that a non-proteolytic function of the Ubl domain in Rad23 is likely required for proficient NER (Ortolan *et al.*, 2004).

After the non-proteolytic interaction of both Rad23 and 19S RC had been demonstrated, it became important to consider whether a ubiquitination (E2/E3) activity was also involved in the 19S/Rad23 coupled activity on NER. The progress made in understanding the role of the proteasome in TC-NER research revealed that the ubiquitin targeting pathway played an important role. During TC-NER, RNA pol II is targeted for ubiquitination and degradation and is differentially modified in response to DNA damage (Woudstra *et al.*, 2002). DNA damage causes stalling of RNA pol II during transcription, which is thought to recruit the NER machinery. RNA pol II stalling either by DNA damage or transcription pausing induces Def1 dependent ubiquitination and degradation by the 26S proteasome of the largest subunit of RNA pol II (Rpb1) in yeast (Huibregtse *et al*, 1997; Beaudenon *et al.*, 1999; Somesh *et al.*, 2005). The Ubc5/Ubc4 and Rsp5 have been identified as the E2 and E3 enzymes that catalyse RNA pol II ubiquitination in yeast (Huibregtse *et al*, 1997; Beaudenon *et al.*, 1999). Recruitment of the entire 26S proteasome to sites of stalled polymerases may also play a role in resolving these complexes (Gillette *et al.*, 2004). It is clear that the proteolytic function of the proteasome plays a role in TC-NER, since the degradation of key transcription components are dependent on the activity of the proteasome. However, it should be stressed that in yeast, defective TC-NER caused by mutation of the Rad26 gene does not cause a UV sensitive phenotype. Therefore the proteolytic function of the proteasome during TC-NER and its nonproteolytic function during

GG-NER are distinct. Significantly it has been reported that specific mutants of the ubiquitin targeting do exhibit a UV sensitive phenotype suggesting that the ubiquitin targeting pathway may also participate in GG-NER (Ortolan *et al.*, 2004).

If the ubiquitin targeting pathway is involved in GG-NER, I speculated that an E3 ubiquitin ligase might play a role, and that one or several NER protein(s) could be targeted for ubiquitination. I noted some important new findings relating to Rad7 that provided useful clues. It was previously recognized that Rad16 contained a C_3HC_4 RING finger motif (Ramsey *et al.*, 2004), typical of those found in certain classes of E3 ubiquitin ligase, and that Rad7 and Rad16 interacted both *in vitro* and *in vivo*. A novel SOCS motif in Rad7 was found and an interaction between Rad7 and Elc1. In combination these observations suggested that these factors might constitute a novel E3 ubiquitin ligase involved in GG-NER (Ho *et al.*, 2002). In mammalian cells the SOCS box motif was first identified in the suppressor of the cytokine signaling (SOCS) family of proteins, but many proteins in other families also contained a C-terminal SOCS box (Kile *et al.*, 2002). Many SOCS family proteins contain an additional central SH2 domain known to be a protein-protein interaction domain. The leucine-rich repeat domain (LLR) of the Rad7 protein also acts as a protein/protein interaction domain, and it is now clear that many SOCS proteins contain one of a number of different types of protein/protein interaction domain. In mammalian cells SOCS box proteins like SOCS-1 and VHL, together with a cullin family protein, a RING-finger protein and elongin C, function as an E3 ubiquitin ligase (Kamura *et al.*, 2001; Kile *et al.*, 2002). In yeast, the archetypical cullin-RING ubiquitin ligase is the largest known class of ubiquitin ligases (Petroski and Deshaies, 2005). The binding partner of the SOCS box protein Rad7, Rad16, has a C_3HC_4 RING-finger motif (Bang *et al.*, 1992; Prakash and Prakash, 2000; Ramsey et al., 2004). Furthermore an

interaction between Rad7 and Rad4 proteins mediated by the LRR region of Rad7 has been reported previously (Wang *et al.*, 1997). It has been reported that the protein that binds with the protein/protein interaction domain of SOCS proteins is often the target for ubiquitination. Therefore, I reasoned that Rad4 was a possible target for a putative novel E3 ubiquitin ligase containing Rad7/Rad16, an unknown cullin and a elongin protein, possibly Elc1, based on protein-protein interaction studies (Ho *et al.*, 2002). The possible E3 ligase function of the RING-finger domain in Rad16 also attracted another group's attention. Although this group did not have direct evidence they suggested, based on genetic data that Rad7/Rad16 and Elc1 could be an E3 ubiquitin ligase (Ramsey *et al.*, 2004). However, this parallel research was used to supported the idea that NER repair activity was regulated by controlling the steady level of Rad4 protein (a proteolytic model) even though their genetic data did not support this notion.

In this chapter, I investigated how this putative novel E3 ligase affected the stability of native Rad4 protein in yeast cells and examined the steady state level of Rad4 in response to UV. I revealed there is a low level of mRNA of *RAD4* in the Δ*rad23* mutant compared with the WT strain. Since the half life of Rad4 is around 3 to 4 hours, the low steady state level of Rad4 in the Δ*rad23* mutant may be caused by the low transcription level of *RAD4*. Moreover, I demonstrated that Rad4 is targeted for degradation by the 26S proteasome following UV radiation and I showed that a novel Rad7 containing E3 ubiquitin ligase, including Rad7, Rad16, Elc1 and the newly identified Cul3, ubiquitinates Rad4 following UV. The physical interaction between those components of the Rad7 E3 ligase complex was confirmed by an anti-Rad7 immunoprecipitation assay and western blotting. Moreover, Rad16, Elc1 and Cul3 were co-purified with 6His-tagged Rad7 after several steps of

chromatographic purification. Under an *in vitro* ubiquitination reaction condition, Rad4, expressed *in vitro*, was ubiquitinated by the Rad7 E3 ligase complex.

4.2 Materials and methods

The yeast strains used in this study were, WCG4a (WT), YH129/14 (*pre1-1 pre4-1*). Research Genetics parental strain BY4741, 2782 (Δ*elc1*), 1982(Δ*ela1*), 4633 (Δ*cul3*). Sc507 (WT), Sc507R7 (Δ*rad7*) and Sc507R23 (Δ*rad23*); they were described in Chapter 2. Creation of the Rad7 SOCS box mutation was achieved by site directed mutagenesis of the WT *RAD7* gene cloned in pRS314 as described in Chapter 2. Two point mutations were made resulting in the amino acid substitutions, L168A and C172A within the conserved SOCS box domain.

Purification of His-tagged Rad7

Almost 100g wet weight of cells were used to purify the 6His-tagged Rad7 protein with the protocol described in 2.9. The peak fractions of mono-Q, with nearly a 15,000 fold enrichment of Rad7/Rad16, were used for the ubiquitination reaction *in vitro*.

Expression of Rad4 protein *in vitro*

The PCR generated template was made for the TNT®T7 PCR Quick protein *in vitro* expression system. Two primers were designed to generate the Rad4 coding sequence;

Forward:5'AAGAGTACTTAATACGACTCACTATAGGAACAGCCACCATGAA
TGAAGACCTGCCCAA3'

Reverse:5'TTTTTTTTTTTTTTTTTTTTTTTTTTTTTTTAATCAGTCTGATTCCTC
TGACATCT3'.

Then the *in vitro* expression was carried out as described in 2.12.

Immunoprecipitations

Following immunoprecipitations, as described in 2.13 with Anti-Rad4 antibody, and Anti-Rad7 respectively, proteins were separated by 8% SDS-PAGE gel electrophoresis.

Western blot assay

The preparation of WCE was described in 2.10 and Western blot analysis was described in 2.15. Anti-ubiquitin antibody (Boston Biochem) was generated by genetic immunization as described (Barry and Johnston, 1997). Details of anti-Rad4 (Affiniti Research Products Limited) were described in 2.18. Commercially available anti-myc antibody was purchased from Sigma-Aldrich.

Northern blot assay

The preparation of the total RNA extract was described in 2.6.1 and Northern blot analysis was described in 2.6. The primers used in this chapter are shown below;

Actin_NTS: biotin-GCCGGTTTTGCCGGTGACG

Actin_TS: CCGGCAGATTCCAAACCCAAAA

Upper_Rad4(NTS25): biotin-ACTGATCGAAGTTTTTGCACCAACGATGATA

Lower_Rad4(TS25): CATAAAATCCGAATAATCCTCCCCG

Ubiquitination reaction *in vitro*

The ubiquitination reaction contains 1μg E1 (Yeast), 1μg hUbc4a, 1μg hUbc4b, 1.3μg hUbc4c, 0.1 μg GG-NER complex, 6μl 5× Reaction buffer (20mM $MgCl_2$, 200mM KCl 180mM Tris pH8.0), 6μl ATP (20mM), 2μl of TNT-expressed Rad4 protein or an empty vector control. The ubiquitylation reaction is initiated by adding 5μg ubiquitin then ddH_2O to total volume of 30μl. It is incubated at 28°C for 60 minutes. After the reaction is finished appropriate 100× protease inhibitors solution and the same volume of 2× SDS-PAGE loading buffer was added to the reaction

mixture. Then, all proteins in this reaction mixture were denatured at 60°C for 20 mins and separated by 8% SDS-PAGE gel electrophoresis.

4.3 Results

4.3.1 The steady state level of cellular Rad4 protein in the absence of UV damage

It was suggested that the turn over of Rad4 by the proteasome was inhibited after exposure of cells to UV light, resulting in the accumulation of Rad4 that somehow enhanced NER. Before I examined the affect of UV on Rad4 steady state levels, the half-life of Rad4 without UV irradiation was measured. Previous researchers used an epitope-tagged Rad4 protein, but here I used an antibody against endogenous Rad4 to measure the half-life of Rad4 by measuring its level in the absence of UV treatment after blocking *de novo* protein synthesis with cycloheximide. Based on the result shown in Fig3.1 A, no detectable decrease of Rad4 levels was found after 3 hours following cycloheximide treatment. This showed that native Rad4 possesses a half-life longer than 3 hours. It was previously reported that in the absence of Rad23 protein, over expressed HA-Rad4 is a short-lived protein (Ortolan *et al.*, 2004) and the lower steady levels of Rad4 observed was due to Rad4 protein being degraded rapidly. Several studies revealed that the Rad23 (hHR23B in human) protein stabilized the endogenous Rad4 (XPC in human cells) protein in normal growth conditions (Xie *et al.*, 2004; Ortolan *et al.*, 2004; Ng *et al.*, 2003). However, XPC has now been confirmed to have a half-life of over 6 hours (Okuda *et al.*, 2004).

To examine whether the half-life of Rad4 alters in absence of Rad23, the half-life of Rad4 protein in a *Δrad23* mutant strain was measured using the same method as the WT strain. The data, shown in Figure 4.1B, indicates that the half-life of native Rad4 protein remains the same in the absence of its interacting partner Rad23. To determine

whether the relative steady state level of Rad4 between a wildtype and a *Δrad23* mutant strain is different, I prepared whole cell extracts from the two strains under normal growth conditions.

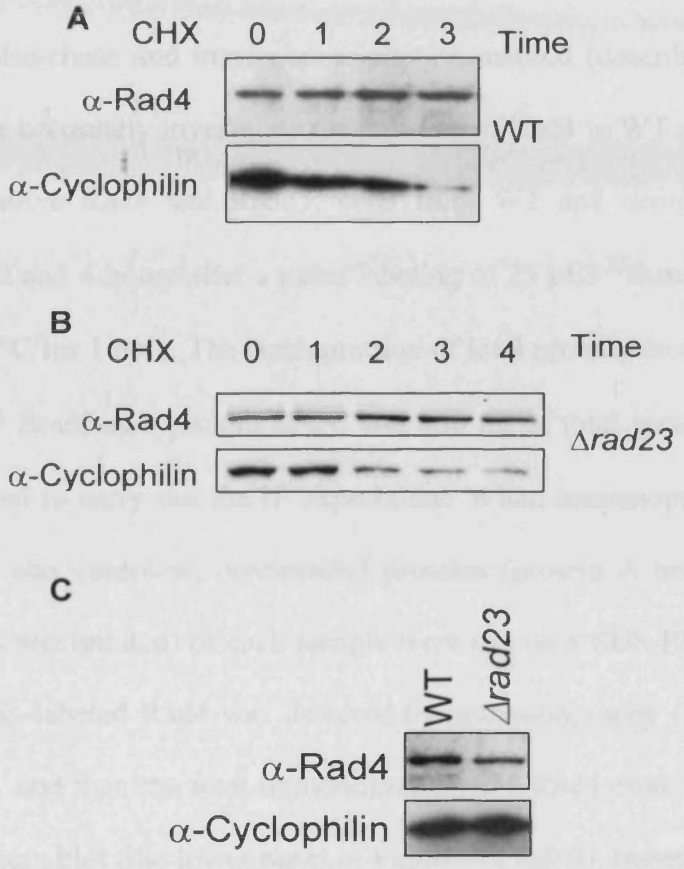

Figure 4.1. **A**. Anti-Rad4 western blot of WGC4a [WT] extracts from a strain grown in the protein synthesis inhibitor cycloheximide for the time indicated [hours] along with an anti-cyclophilin control of the same blot. **B.** Anti-Rad4 western blot of *Δrad23* extracts from a strain grown in the protein synthesis inhibitor cycloheximide for the time indicated [hours] along with an anti-cyclophilin control of the same blot. C.Anti-Rad4 western blot showing relative steady state levels of Rad4 in a wildtype and *Δrad23* mutant strain. Bottom panel shows anti-cyclophilin loading control. *ACT1* transcript levels are shown as a loading control.

I measured the concentration of total proteins by a protein assay using Bradford's reagent. 50 μg of total protein was loaded from the two samples. From figure 4.1C, it can be seen that the level of Rad4 protein is significantly decreased in

the *Δrad23* mutant strain and this confirms observations from previous studies. However, whether the reduced Rad4 level in *Δrad23* mutant strain is due to increased degradation of Rad4 protein in the absence of Rad23 required further investigation.

4.3.2 Pulse-chase experiment to measure the half-life of Rad4 protein without UV damage

A coupled pulse-chase and immunoprecipitation method (described at 2.17) was employed to more accurately investigate the half-life of Rad4 in WT and *Δrad23* cells. In the case of native Rad4 and Rad23, cells from WT and *Δrad23* strains were collected at 0, 1, 2 and 4 hours after a pulse labeling of 25 μCi ^{35}S-methionine per ml was applied at 30°C for 1 hour. The concentration of total proteins in each sample was then measured by Bradford's protein assay, and 400 μg of total proteins and 5 μl of antibody were used to carry out the IP experiment. When immunoprecipitation with α-Rad4 antibody was complete, precipitated proteins (protein A beads pellets) and supernatant (TCA precipitated) of each sample were run on a SDS-PAGE gel side by side. The ^{35}S radio-labeled Rad4 was detected by autoradiography (the top panel of Figure 4.2 A&B), and then the total immunoprecipitated Rad4 protein was measured by anti-Rad4 western blot (the lower panel of Figure 4.2 A&B). Based on figure 4.2 C, the half-life of native Rad4 protein in the wild type strain is between 3 and 4 hours with Rad23 protein present. In the absence of Rad23 protein, the half-life of Rad4 protein does not alter significantly.

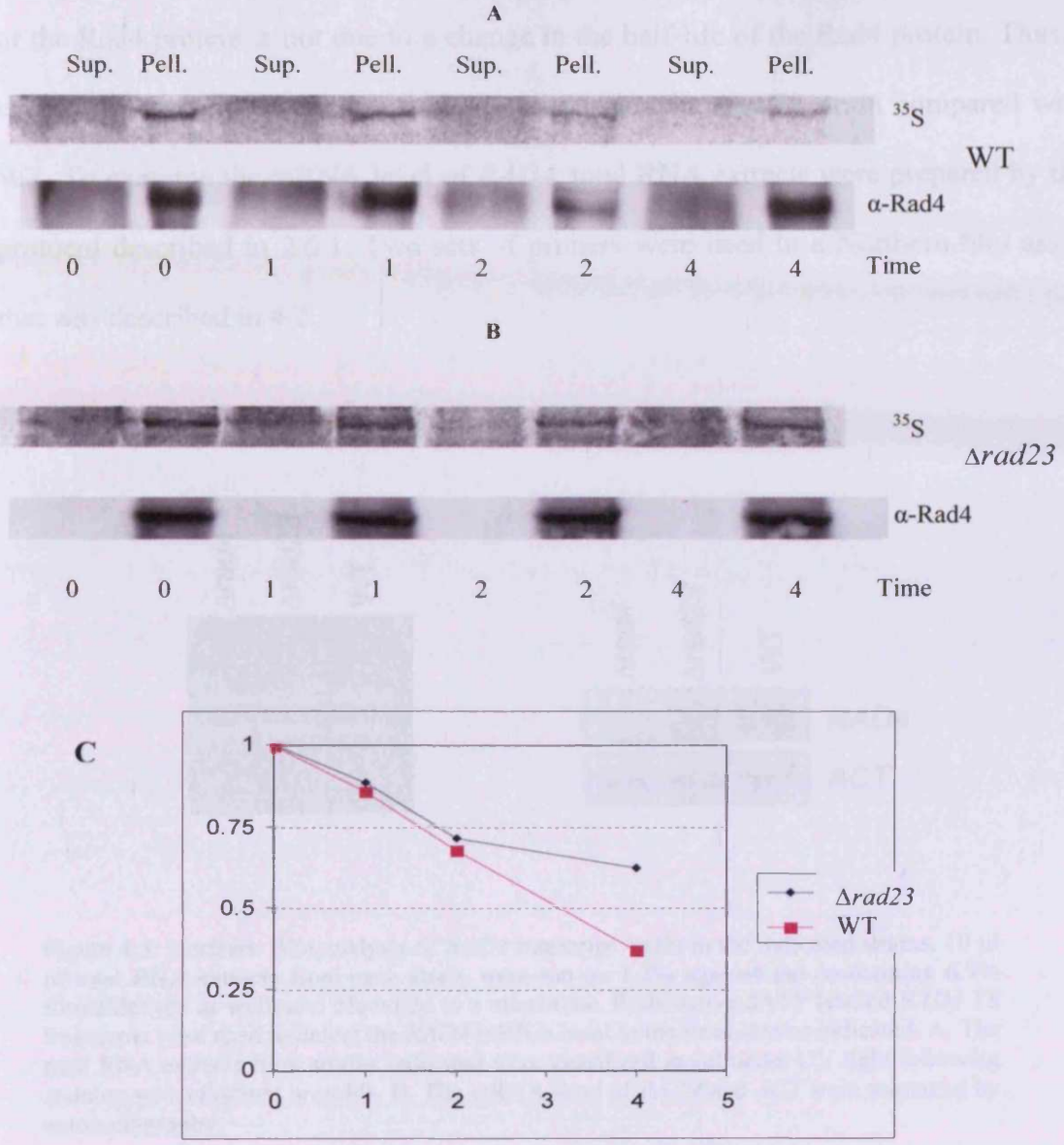

Figure 4.2. A&B. Rad4 stability is not altered in a Δ*rad23* strain. Pulse chase treatment with 35S labeled methionine followed by immunoprecipitation with anti-Rad4 antibody. (Sup.-supernatant Pell.-Pellet) A) WT B) Δ*rad23* (Reduced levels of Rad4 in the Δ*rad23* strain accounts for the higher background in the 35S exposure) C) Quantitation of data from A and B (normalized against Rad4 levels)

4.3.3 Measuring the *RAD4* mRNA level in *Δrad23* mutant and WT

Although the steady level of Rad4 is lower in *Δrad23* than that in WT, this is not due to a reduced stability of Rad4. Since the half-life of the Rad4 protein remains

similar in the two strains. In other words, the contribution of Rad23 to the steady level of the Rad4 protein is not due to a change in the half-life of the Rad4 protein. Thus, I speculated that the production of Rad4 might alter in *Δrad23* strain compared with WT. To examine the mRNA level of *RAD4*, total RNA extracts were prepared by the protocol described in 2.6.1. Two sets of primers were used in a Northern blot assay that was described in 4.2.

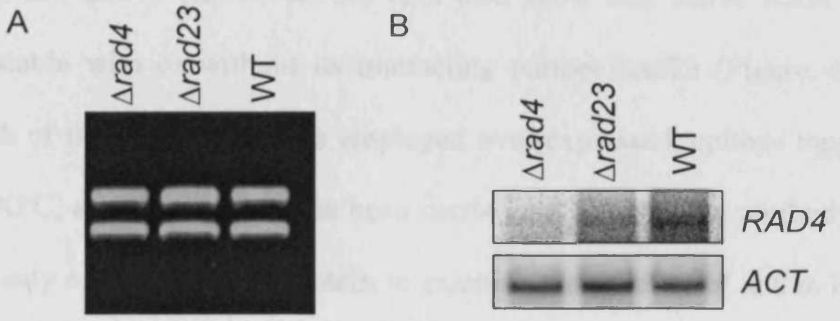

Figure 4.3. Northern Blot analysis of *RAD4* transcript levels in the indicated strains. 10 μl of total RNA extracts from each strain were run on 1.2% agarose gel (containing 6.7% formaldehyde as well) and bloted on to a membrane. Radioactive dATP labeled *RAD4* TS fragments were used to detect the *RAD4* mRNA level in the three strains indicated. A. The total RNA extracts from strains indicated were visualized in gel under UV light following staining with ethidium bromide. B. The mRNA level of *RAD4* and *ACT* were measured by autoradiography.

Figure 4.3A shows the total RNA extracts from three strains, which are *Δrad4*, *Δrad23* and WT, were equally loaded. Northern blotting analysis revealed that Rad4 transcript levels are significantly reduced in *Δrad23* cells compared with WT cells (Figure 4.3B), demonstrating that the reduced level of Rad4 protein in the *Δrad23* strain is caused predominantly by the reduced mRNA level of the *RAD4* gene. In a later chapter of the thesis I describe my experiments which investigate whether Rad23 plays a role in transcription regulation of a subset of genes involved in the response to

DNA damage.

4.3.4 Rad4 is degraded by the UPP in response to UV

It was suggested that following exposure of cells to UV irradiation, the proteolytic degradation of Rad4 is attenuated, resulting in accumulation of this repair factor and enhanced NER (Lommel *et al.*, 2002). A similar model was originally proposed for the Rad4 homologue, XPC (Ng *et al.*, 2003). More recent evidence using an antibody to the endogenous protein suggests that XPC is stable with a half-life of over six hours (Okuda *et al.*, 2004). Moreover, our data also show that native Rad4 protein also remains stable with or without its interacting partner Rad23 (Figure 4.1A and B). Since both of these earlier reports employed over-expressed, epitope tagged versions of Rad4/XPC, an investigation has been carried out by using an antibody specific to endogenously expressed Rad4 protein to examine the stability of native Rad4 protein following exposure of cells to UV light.

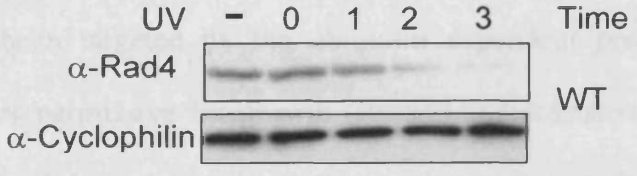

Figure 4.4. Anti-Rad4 western blot of WGC4a (WT) extracts from a strain either unirradiated [-] or UV irradiated (100J) and allowed to recover for the times indicated (hours), along with an anti-cyclophilin control of the same blot.

In contrast to earlier studies which used ectopically expressed Rad4, I found that endogenously expressed Rad4 protein is not stabilized after UV treatment, rather it is rapidly degraded following exposure to UV light. Without UV radiation, a steady level of Rad4 is observed, and the half-life of Rad4 is over 3 hours, as shown

following incubation of cells with the protein synthesis inhibitor cycloheximide (see Figure 4.1 A). Figure 4.4 (top) shows the decrease in steady state levels of Rad4 protein over a three-hour period following exposure of wild type cells to UV radiation. The steady state level of cyclophilin remains unchanged following exposure of cells to UV light Figure 4.4 (bottom).

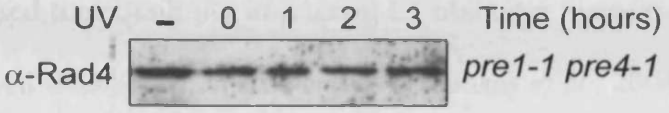

Figure 4.5. Anti-Rad4 western blot of *pre 1-1, pre 4-1* extracts from cells either unirradiated [-] or UV irradiated (40J) and allowed to recover for the times indicated [hours].

Using an isogenic strain carrying conditional mutations in two subunits of the 20S proteasome (*pre1-1*, *pre4-1*), I confirmed that the UV dependent degradation of Rad4 protein is mediated by the proteolytic activity of the 26S proteasome. This temperature sensitive strain shows a marked decrease in the ability to degrade proteins that have been targeted by the ubiquitin dependent proteolytic pathway even at temperatures permissive for growth (Russell and Johnston, 2001). Figure 4.5 shows that in the *pre1-1*, *pre4-1* strain, Rad4 protein steady state levels do not alter following exposure to UV light. From the above data it can be concluded that Rad4 protein is targeted for degradation by the UPP after UV irradiation.

4.3.5. UV dependent degradation of Rad4 requires a novel cullin based E3 ubiquitin ligase

A recent publication showed that the homologue of Rad4, XPC, is a substrate of a novel cullin-based E3 ubiquitin ligase consisting of a cullin, a RING finger protein, adaptors, and a substrate recognition protein (Sugasawa *et al.*, 2005). Moreover, the

RING domains of Rag1 and Rad5, which are both components of multisubunit E3 ubiquitin ligase complexes, are homologous to the Rad16 RING domain (Ulrich *et al.*, 2003; Yurchenko *et al.*, 2003). Direct evidence has been found that the human homologue of Elc1 is a component of an E3 ubiquitin ligase that contains a RING domain subunit (Ho *et al.*, 2002; Tyers and Rottapel, 1999). Elc1 is physically associated with the Rad7/Rad16 complex (Ramsey *et al.*, 2004; Ho *et al.*, 2002). These findings raised the possibility of a novel E3 ubiquitin ligase function of Rad16 in addition to its well established ATPase activity (Ramsey *et al.*, 2004).

Other cullin-based E3 ubiquitin ligases have a specific component which functions as a substrate specific adaptor, the protein targeted for ubiquitination usually interacting with the adaptor though a protein-protein interacting domain such as an SH2 domain or a leucine rich repeat (LRR) motif. Previous protein-protein interaction studies predicted that Rad4 might be a primary target for this putative Rad7 containing E3 ligase, since it was shown that the LRR domain of Rad7 is required for a two-hybrid interaction between Rad7 and Rad4 (Pintard *et al.*, 2004; Wang *et al.*, 1997).

Since the Rad7 protein is a SOCS box protein, I reasoned that the Rad7 E3 ligase was a novel member of the cullin based Elongin-Cullin-Socs-box (ECS) type E3 ubiquitin ligases, a subclass of the Skp1-Cullin-F-box (SCF) type family of ubiquitin ligases. To determine the components of the putative novel Rad7 E3 ligase, several mutants defective in multiple predicted components of the novel Rad7 E3 ligase were tested.

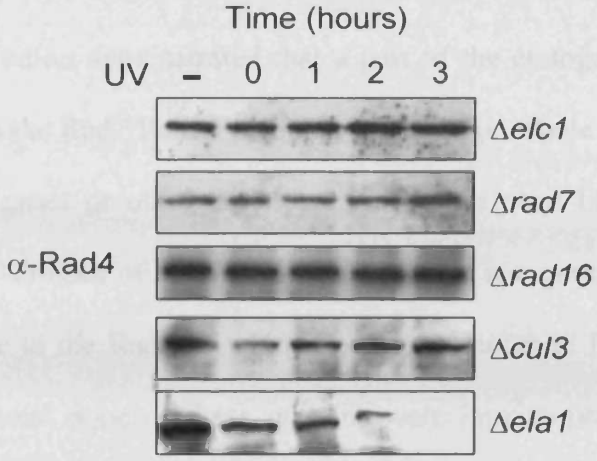

Figure 4.6. Deletion of genes encoding the ECS ligase components results in stabilization of Rad4 post UV. Anti-Rad4 western blots of extracts from Research Genetics mutant strains listed either unirradiated [-] or UV irradiated and allowed to repair for the times indicated (hours).

Mutations were introduced into predicted components of the novel Rad7 E3 ligase to measure their effect on Rad4 stability, to see if the effect on the UV-dependent degradation of endogenous Rad4 was lost, therefore identifying the components necessary to degrade Rad4 after UV. A number of cullin mutants were examined and only *CUL3* was required for the degradation of Rad4 protein following UV irradiation, as shown in Figure 4.6. Deletion of an unrelated SOCS box gene, *ELA1*, did not result in the stabilization of Rad4 protein after UV (Figure 4.6 bottom). From the above, deletion of genes which encode the Rad7/Rad16 complex, the previously identified Elc1 and the Cul3 (cullin) blocked the UV-dependent degradation of Rad4 protein, suggesting that those proteins are all components of the novel Rad7 E3 ubiquitin ligase.

4.3.6 Physical interaction between components of the novel Rad7 E3 ubiquitin ligase

Specific co-immunoprecipitation with anti-Rad7 antibody was carried out to

identify whether there is a physical interaction between components of the Rad7 E3 ligase. Although some level of Elc1 and Cul3 still exist in the supernatant, reciprocal immunoprecipitation demonstrated that a part of the endogenous Elc1 and Cul3 are associated with the Rad7/Rad16 complex in wild type whole cell extracts. Since other E3 ubiquitin ligases or other functional complexes need Elc1 and Cul3 for proper function in the absence of Rad7/Rad16 complex, it is a possible that only a subset of them contribute to the Rad7 E3 ubiquitin ligase (shown in Figure 4.7 left side). In a control experiment none of these proteins were immunopreciptated when using an extract from *Δrad7* (shown at Figure 4.7 right side). The detection of Cul3, Elc1 and

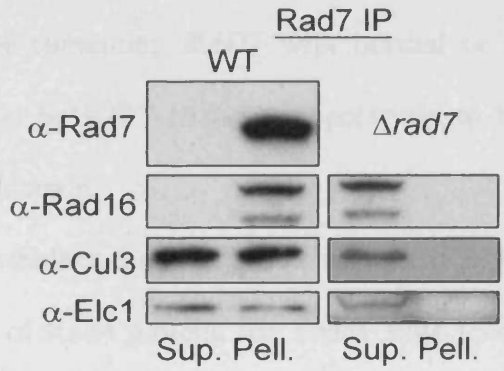

Figure 4.7 Characterization and activity of the Rad7 ECS E3 ligase. Co-immunoprecipitation of ECS ligase components with Rad7. Western blot of Rad7 immunoprecipitation probed with the antibodies listed. [Sup. Supernatant, Pell. Pellet]. Wildtype (WT) extract is on left, control extract (*Δrad7*) lacking Rad7 protein is on right.

Rad16 proteins co-precipitating with Rad7 protein further suggests that this complex is a member of the cullin based family of E3 ubiquitin ligases.

4.3.7. The SOCS box domain of Rad7 is required for UV-dependent degradation of Rad4

Since Rad7 plays a crucial role in the GG-NER pathway, in order to investigate the role of this novel ubiquitin ligase function, mutations were introduced into the conserved SOCS box domain shown as follows:

Rad7 SOCS Domain

A A
165 VSSLQSLCITKISENISKWQK.....LGGVSTA-NLNNLAKAL 217

Among the amino acid sequence of the SOCS box domain of Rad7, alanine mutations were introduced into two conserved residues (underlined). The mutant known as psocs is noted with the mutated residues in bold. pRAD7 and psocs strains were made by Simon H Reed. Briefly, the *RAD7* and socs-*RAD7* were obtained by PCR. The sequences of the two PCR products are the same except for the SOCS box region. Then, two PCR products were inserted into a plasmid pRS314 respectively. The pRS314 containing *RAD7* with normal or mutated SOCS box domain were transferred to Sc507R7 (Δ*rad7*) respectively to make a wild type (pRAD7) and a psocs mutant strain.

To test whether the SOCS box mutated Rad7 protein affects the UV-dependent degradation of Rad4 protein, the steady state level of Rad4 was measured followed UV treatment in WT (pRAD7) and psocs cells.

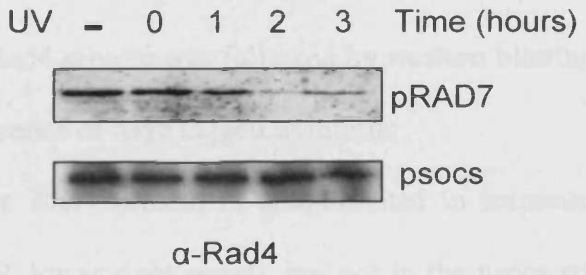

Figure 4.8. Post UV steady state levels of Rad4 shown by anti-Rad4 western blot. The cells were either unirradiated [-] or UV irradiated and allowed to repair for the times indicated (hours). Top panel, extracts from a Sc507 derived *rad7* deleted yeast strain transformed with a centromeric vector expressing wild type Rad7 (top panel pRAD7) or SOCS box domain mutant (bottom panel psocs) from the endogenous Rad7 promoter.

Figure 4.8 shows that the steady state level of Rad4 protein remains stable after

UV treatment in the psocs strain (Figure 4.8 bottom panel) whilst the UV-dependent degradation still happens in the pRAD7 (WT) strain (Figure 4.8 top panel). This result not only confirmed that the UV-dependent degradation of Rad4 protein requires the SOCS-box protein Rad7, but it also characterized the crucial role of the SOCS box domain in the degradation of Rad4 protein after UV.

4.3.8. The UV-dependent ubiquitination of Rad4 is absent in a psocs mutant strain

Previous evidence shows that the UV-dependent degradation of endogenous Rad4 protein needs activity of the novel cullin-based E3 ubiquitin ligase consisting of Rad7, Rad16, Elc1 and Cul3. Mutations in the conserved SOCS box domain of Rad7 result in the stable steady level of Rad4 after UV treatment, suggesting that this domain is crucial for the activity of the novel cullin-based E3 ubiquitin ligase. To determine whether the Rad7 E3 ligase is required to change the ubiquitination status of Rad4 after UV irradiation, I immuno-precipitated Rad4 protein in a strain expressing Myc epitope tagged ubiquitin protein (Hochstrasser *et al.*, 1991) and either wild type Rad7 (pRAD7), or the SOCS box mutated Rad7 (psocs) proteins (A plasmid expressing Myc-tagged ubiquitin was introduced into pRAD7 and psocs respectively). Immunoprecipitation of Rad4 protein was followed by western blotting with anti-Myc antibody to detect the presence of Myc tagged ubiquitin.

Figure 4.9 shows that Rad4 protein is ubiquitinated in response to UV in the pRAD7 strain (Figure 4.9, lower right panel), but not in the psocs strain (Figure 4.9 lower left panel). Reprobing the same blot with anti-Rad4 antibody confirmed the position of Rad4 protein (Figure 4.9 upper left and right panels). The higher background in anti-myc blotting may be caused by the non-specific binding with protein A beads and the sensitivity of anti-myc antibody.

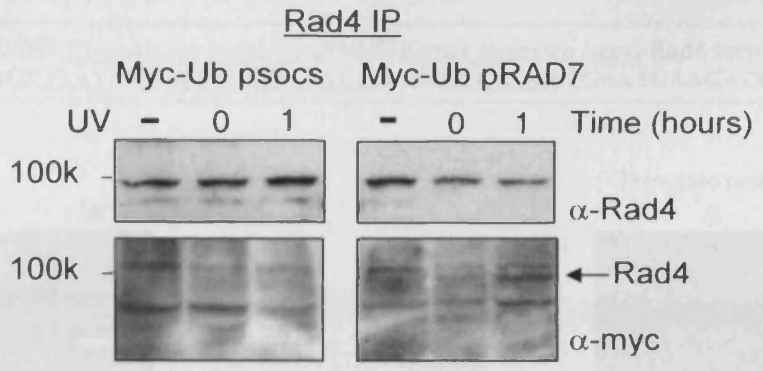

Figure 4.9. The ubiquitination status of Rad4 at 0 and 1 hour post UV in the wild type (pRad7), and SOCS box mutated (psocs) strains expressing Myc tagged ubiquitin. These strains were either unirradiated [-] or UV irradiated and allowed to repair for 0 or 1 hour, lower panel. Rad4 was immunoprecipitated from the extracts and then blotted with anti-Myc antibody. The upper panel shows the same blot probed with Rad4 antibody.

This result demonstrates that *in vivo* the cellular ubiquitination of Rad4 protein dependents on the activity of the Rad7 E3 ubiquitin ligase in response to UV light. Furthermore, the conserved SOCS box domain of Rad7 is necessary for the ubiquitination of Rad4 by this novel E3 ubiquitin ligase.

4.3.9. *In vitro* expression of the Rad4 protein

It was reported that Rad4 protein confers toxicity to *E. coli* (Wei and Friedberg, 1998), so in order to obtain Rad4 substrate I employed an *in vitro* transcription and translation system, the TNT® T7 PCR Quick for PCR DNA system, to express Rad4 protein. Since the efficiency of this TNT *in vitro* expression system dramatically decreased when it is used for expressing a protein with a high molecular weight (MW), the protocol provided by Promega company was modified specifically for Rad4, with a MW of 87kDa. Otherwise, the Rad4 protein cannot be expressed or is expressed at an unacceptably low efficiency by this kit.

A

5'-*NNNNNNNNN*-T7 promoter sequence-*NNNN*-Kozak sequence (part)-Rad4 forward primer
5'-*AAGAGTACT*TAATACGACTCACTATAGG*AACA*GCCACCATGAATGAAGACCTGCCCAA-3'

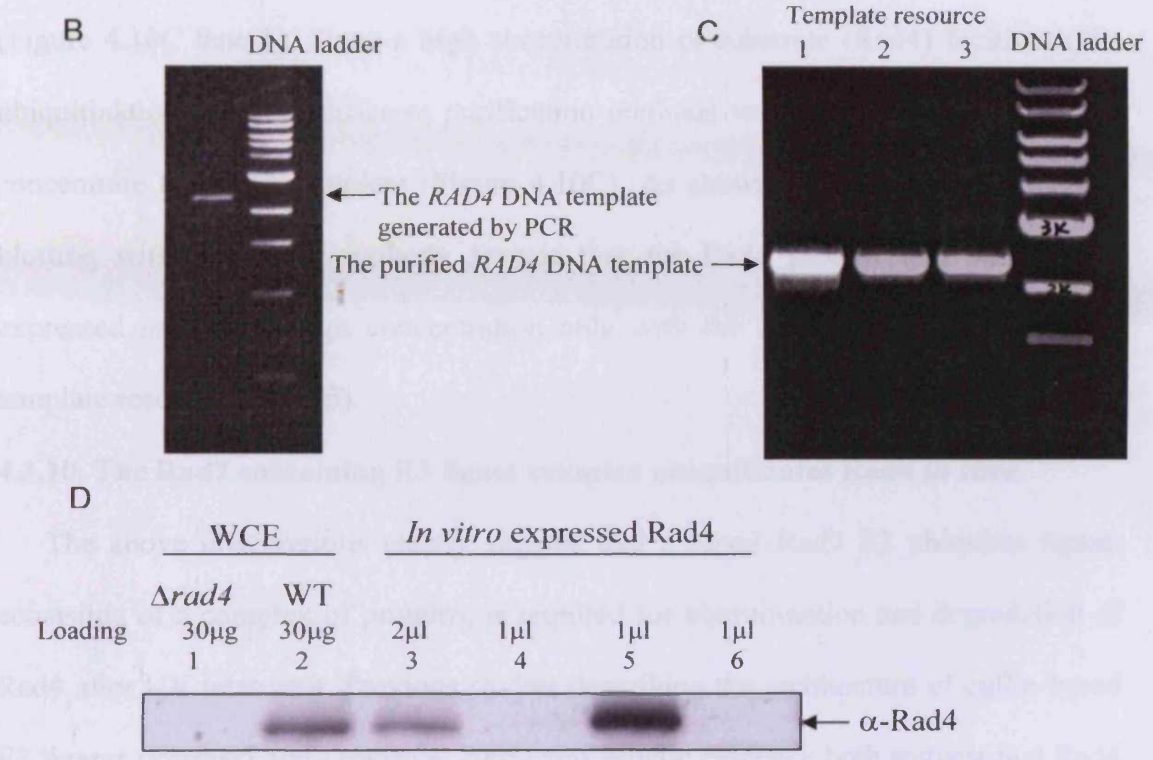

Figure 4.10. The Rad4 protein *In vitro* expression experiment. A. The structure and containing elements of the 5'-Primer. B. The PCR-generated DNA template was visualized in gel under UV light following staining with ethidium bromide. C. The *RAD4* DNA template was visualized by the same method used in Figure B. The *RAD4* DNA templates purified from different methods were named template resource 1, 2 and 3 respectively. (Template resource 1 [Lane 1]- a normal phenol/chloroform purification and an ethanol precipitation; template resource 2 [Lane 2]- an ethanol precipitation; template resource 3 [Lane 3]- QIAGEN PCR purification kit). D. The anti-Rad4 western blot analysis followed Rad4 *In vitro* expression experiment. The total proteins of 30μg (5μl) loading in lane 1 and 2 are same. In lane 3, 4, 5 and 6, the components of reaction were same except for the resource of the *RAD4* DNA template (Lane3-PCR generated DNA template; Lane4-template resource 1; Lane5-template resource 2; Lane6-template resource 3).

Using this system, a PCR generated DNA template is created and this is suitable for transcription and translation *in vitro*. The designation of the 5'-primer was shown in Figure 4.10A while the 3'-primer was created without any alteration according to the manual provided by Promega. In this study, the genomic DNA extracted from a wild type strain is used as the PCR template. However, under optimized conditions, the efficiency of PCR still remains low with this set of long primers (Figure 4.10B

left). Since a limited volume of the PCR-generated *RAD4* DNA template can be added to the *in vitro* expression reaction (described in 2.12), without further purification of this template the Rad4 protein was successfully expressed, but only at a low yield (Figure 4.10C lane 3). Since a high concentration of substrate (Rad4) facilitates the ubiquitination reaction, different purification methods were employed to purify and concentrate the DNA template (Figure 4.10C). As shown in Figure 4.10D, western blotting with anti-Rad4 antibody reveals that the Rad4 protein was successfully expressed *in vitro* at high concentration only with the *RAD4* DNA template from template resource 2 (lane5).

4.3.10. The Rad7 containing E3 ligase complex ubiquitinates Rad4 *in vitro*

The above observations clearly suggest that a novel Rad7 E3 ubiquitin ligase, consisting of a complex of proteins, is required for ubiquitination and degradation of Rad4 after UV treatment. Previous studies describing the architecture of cullin-based E3 ligases (Petroski and Deshaies, 2005) and genetic evidence both suggest that Rad4 is a primary target of this E3 ligase (Pintard *et al.*, 2004; Wang *et al.*, 1997).

I next examined the biochemical activity of the Rad7 E3 ubiquitin ligase *in vitro*. Since the E1 (ubiquitin activator) and E2 (ubiquitin conjugate enzyme (UBC)) are often required for activation during the ubiquitin targeting stage of the UPP, E1 (yeast) and 3 E2 human homologues: hUbc4a, hUbc4b, and hUbc4c, were selected to perform this experiment. The reagents used in this experiment were either commercially available or generated in our laboratory. The normal expressed Rad7 E3 ubiquitin ligase in yeast was purified through several chromatographic steps (shown in Figure 4.11) following the protocol described in 2.9 (details see 3.3.1).

In order to purify the E3 ligase complex, a strain expressing epitope tagged (6His) Rad7 protein was used (Reed *et al.*, 1998). I estimate that during the multiple

chromatographic steps of the purification nearly a 15,000 fold enrichment of Rad7/Rad16 is achieved. As shown at Figure 4.11, Cul3 and Elc1 proteins co-purify with Rad7 and Rad16 proteins through a number of chromatographic steps that include Ni-NTA, p-11, DEAE Sephacel and Mono-Q columns. Western blotting showed that peak fractions eluted from the mono-Q column of the Rad7 protein

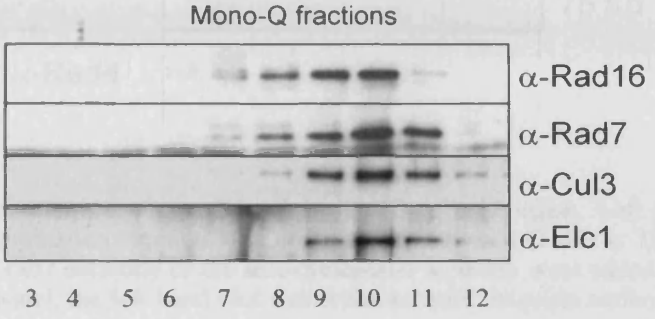

Figure 4.11. Purification of the Rad7 ECS ligase. A.Western blot of Mono-Q fractions probed with the antibodies listed.

purification (Reed *et al.*, 1998), contain Rad7, Rad16, Elc1 and Cul3 proteins. Since concentrations of Rad7, Rad16, Elc1 and Cul3 are high in the peak fraction (fraction 10), material from fraction 10 is used in subsequent ubiquitination experiment.

I tested the ability of the purified E3 ligase containing Rad7, Rad16, Elc1 and Cul3 to ubiquitinate Rad4 *in vitro*. In addition to the putative E3 ubiquitin ligase, E1 and E2 enzymes were also added in order to provide a complete complement of enzymes necessary for the ubiquitin activation stages of the ubiquitin proteasome pathway (Details of reaction conditions are described in 2.16). To avoid possible degradation of Rad4 protein, the reaction products are finally run on SDS-PAGE gels immediately followed by adding appropriate protease inhibitors.

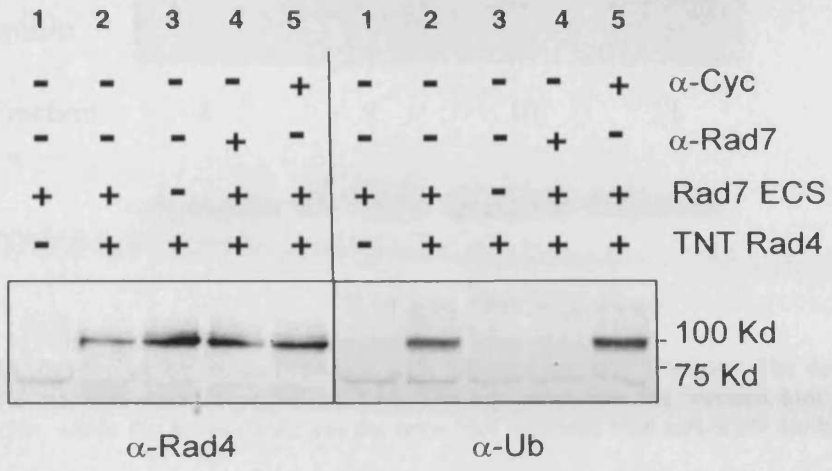

Figure 4.12. *In vitro* ubiquitination of Rad4 by purified Rad7 ligase. Left panel, anti-Rad4 western blot of ubiquitination reaction with components indicated (TNT- is TNT reaction with control vector) Anti-rad7 antibody or the anti-cyclophilin antibody were added in lanes 4 and 5 respectively. Right panel, the left hand blot was reprobed with ubiquitin antibody. Approximate MW markers indicated on left.

The details of this biochemical reaction were described as 2.16. As Shown in figure 4.12, in the *in vitro* reaction conditions described, the ubiquitination status of Rad4 protein changed (lane 2 and 5 at right panel of Figure 4.12) showing that the ubiquitination of Rad4 protein is successful when the Rad7 E3 ligase complex is added to the reaction. Comparing lane 4 and lane 5, when a Rad7 specific antibody was added to the reaction, the activity of the Rad7 E3 ubiquitin ligase is lost (due to antibody inhibition), resulting in no ubiquitination of Rad4 protein. A non-specific antibody, anti-cyclophilin antibody, did not inhibit the ubiquitination reaction. I conclude that since the ubiquitin ligase is specifically inhibited by anti-Rad7, the ubiquitin ligase function was dependent specifically on the E3 ligase complex and it was not an unrelated contaminant that may have been present in the purified E3 ligase.

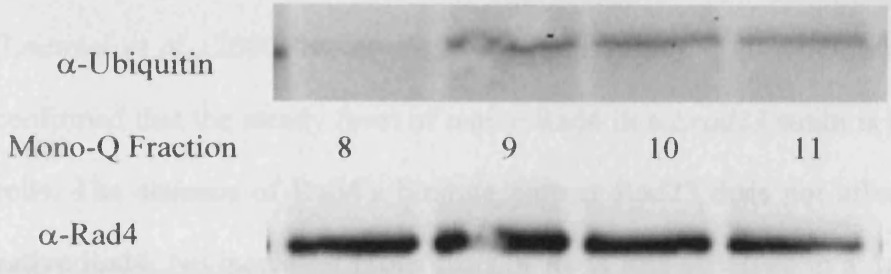

Figure 4.13. *In vitro* ubiquitination reaction with different mono-Q fractions. The details of this biochemical reaction were described as 2.16. The top panel was the western blot probe with anti-ubiquitin, whilst the lower panel was the same blot reprobed with anti-Rad4 antibody.

After the activity of the Rad7 E3 ligase complex (Fraction 10) was confirmed, the ubiquitination reaction of Rad4 was performed with different Mono-Q fractions. Examination of both Figures 4.11 and Figure 4.13, explains why the ubiquitination of Rad4 protein fails when fraction 8 is used (Figure 4.13), since this fraction lacks Elc1 protein or its concentration is significantly reduced. Low concentration of Rad16 in fraction 11 caused the decreased ubiquitination efficiency comparing with fraction 10. This result provides evidence that an efficient Rad4 ubiquitination reaction requires all identified components of the Rad7 E3 ubiquitin ligase.

From evidences both *in vivo* and *in vitro*, it is clear that the novel Rad7 E3 ubiquitin ligase, including Rad7, Rad16, Elc1 and Cul3, are required for the UV-dependent degradation and ubiquitination of Rad4 protein in yeast.

4.4 Discussion

In this chapter, my investigations reveal that the native Rad4 protein behaves differently compared to with over expressed epitope-tagged Rad4 protein in both WT and Δ*rad23* strains. It has been reported that over-expressed HA-Rad4 is a short lived protein and without its binding partner Rad23 protein, increased turn over of tagged

Rad4 protein caused its steady level to be lower in a Δ*rad23* strain than in WT (Lommel *et al.*, 2000; Ng *et al.*, 2003; Ramsey *et al.*, 2004; Ortolan *et al.*, 2004). I confirmed that the steady level of native Rad4 in a Δ*rad23* strain is lower than in WT cells. The absence of Rad4's binding partner Rad23 does not affect the half-life of native Rad4. No increased proteolysis of Rad4 was observed in a Δ*rad23* strain. This observation shows that the half life of native Rad4 is not significantly influenced by Rad23.

Interestingly, my data reveal that the *RAD4* mRNA level decreased in a Δ*rad23* strain compared with WT, suggesting Rad23 may play a role in transcription. The possible role of Rad23 in transcription will be discussed in Chapter 6.

From the results in this section I conclude that the ubiquitination and degradation of Rad4 protein in *S. cerevisiae* requires a novel Rad7 E3 ubiquitin ligase, consisting of Rad7, Rad16, Elc1 and Cul3. Genetic data were reported that a Rad7 containing complex, including Rad7, Rad16 and Elc1, might act as an E3 ubiquitin ligase (Ramsey *et al.*, 2004). However, in that report neither direct evidence showing ubiquitin ligase activity nor a cullin component was identified as part of a putative E3 ligase complex. The evidence in this chapter supported the fact that Rad7 is a part of an ECS E3 ligase complex and that a Cullin (Cul3) is also involved. My observations show that these proteins included in the Rad7 E3 ubiquitin ligase can co-IP and co-purify. The *in vitro* ubiquitination reaction and a direct Rad4-IP experiment all provide direct evidence supporting the notion that Rad4 is a target for ubiquitination by the Rad7 ECS E3 ligase complex both *in vitro* (Figure 4.12) and *in vivo* (Figure 4.9). Moreover, Rad7 protein has SOCS box homology in a one domain of the protein and was previously reported to be a SOCS box protein (Ho *et al.*, 2003). I demonstrate that the novel Rad7 E3 ubiquitin ligase is a novel member of the cullin

based Elongin-Cullin-Socs-box (ECS) type E3 ubiquitin ligases, a subclass of the Skp1-Cullin-F-box (SCF) type family of ubiquitin ligases. Since Rad7 possesses a Leucine Rich Repeat (LRR) motif, a specific protein-protein interaction domain, the role of Rad7 in this ECS ligase is as the substrate adapter and it mediates ubiquitin ligase activity (Kobe, *et al.*, 1994; Wang, *et al.*, 1997; Ho, *et al.*, 2002). Mutation in the conserved SOCS domain of Rad7 protein results in failure of the UV-dependent ubiquitination and degradation of Rad4 protein, and this confirmed that the SOCS-box protein, Rad7, is an essential component for the E3 complex acting as its ubiquitin ligase activity.

Chapter 5
Distinct functions of the ubiquitin-proteasome pathway influence nucleotide excision repair

5.1 Introduction

In *S. cerevisiae*, Rad6, the key component of the Rad6-dependent post-replication DNA repair pathway, also acts as an ubiquitin-conjugating enzyme (E2) (Jentsch *et al.*, 1987). This observation was the first evidence revealing an interaction between the ubiquitin-proteasome pathway (UPP) and DNA repair pathways. Among several DNA repair pathways, nucleotide excision repair (NER) removes a broad spectrum of DNA damage caused by radiation and chemicals including the cyclobutane pyrimidine dimers (CPD) caused by UV light. There are two NER sub-pathways, transcription coupled NER (TC-NER) and global genome NER (GG-NER) (Friedberg *et al.*, 1995; 2006; Reed and Waters, 2003; Reed, 2005). From the studies described in Chapter 4, it would appear that regulation of the UPP in NER is required for optimal NER. Although the highly conserved core components of the NER machinery have all been identified and cloned, NER protein(s) that mediate interaction(s) with other pathways, like the ubiquitin proteasome pathway (UPP), are poorly understood (Aboussekhra *et al.*, 1995; Guzder *et al.*, 1995; Reed, 2005; Reed and Gillette, 2007).

The ubiquitin like (Ubl) domain of the NER protein Rad23 is required for proficient NER and does not promote protein degradation of Rad23 (Watkins *et al.*, 1993). This finding suggested that a non-proteolytic function of Rad23 may be involved in promoting proficient NER. However, the subsequent identification of an interaction between NER and the UPP through the ubl domain of Rad23 (Schauber *et al.*, 1998) led to the suggestion of a proteolytic role for the proteasome in NER. Two factors contributed to this notion; the epitope tagged Rad23 used in this research was

rapidly degraded by the proteasome, and Rad23 suppresses the toxicity of overexpressed Rad6 (Ubc2) and Ubr1 in yeast, a genetic screen that was intended to identify *bone fide* substrates of the ubiquitin targeting pathway (Schauber *et al.*, 1998; Ortolan *et al.*, 2000). In Chapter 4, the Rad23 mediated regulation of the UPP in NER via a proteolytic and non-proteolytic model was discussed in detail. In summary, a key component of the proteasome, the 19S RC, negatively regulates NER and Rad23 acts to attenuate the negative regulation of 19S RC. Moreover, the primary function of Rad23 is not stabilization of Rad4 protein (Russell *et al.*, 1999; Gillette *et al.*, 2001; Ortolan *et al.*, 2004; Xie *et al.*, 2004). Additionally, it seems that the proteolytic function of the proteasome may play a role in TC-NER, since the degradation of key transcription components are dependent on the activity of the proteasome (Huibregtse *et al*, 1997; Beaudenon *et al.*, 1999; Woudstra *et al.*, 2002; Somesh *et al.*, 2005), but the effect of TC-NER on UV survival in yeast is relatively small (the *Δrad26* strain is not UV sensitive).

In the previous chapter, I demonstrated that Rad4 is targeted for degradation by the 26S proteasome following UV radiation. Furthermore, in the absence of UV the native Rad4 protein is stable with a half-life over 3 hours. My observations show that a novel cullin-based E3 ubiquitin ligase, consisting of Rad7, Rad16, Cul3 and Elc1, ubiquitinates Rad4 following UV *in vivo* and *in vitro*. Moreover, mutations in the conserved SOCS domain of Rad7 protein result in failure of the UV-dependent ubiquitination and degradation of Rad4 protein, supporting the notion that Rad7 is an essential component in the novel E3 ligase. Therefore, the Rad7 containing ECS ligase is a novel member of the cullin based Elongin-Cullin-Socs-box (ECS) type E3 ubiquitin ligases.

In this chapter, how the ECS ligase affects the UV survival and NER was

examined. The results in this chapter show that cellular survival after UV correlates with the ubiquitination of Rad4, but not its subsequent degradation. In the absence of Rad23, the ECS complex influences cellular UV survival. Moreover, I examined whether this newly identified E3 ligase functions in the same pathway as the previously identified Rad23/19S RC function in NER. I speculated that the non-proteolytic activity of the Rad23/19S RC interaction could include a requirement for an ubiquitination event regulated by an E3 ligase. My results indicate that the novel E3 ligase and the Rad23/19S RC function are in separate pathways. The Rad7 containing E3 ligase is required for inducible NER in a region of *MAF2* by a method measuring the lesion removal at nucleotide level. This suggests that this ECS ligase is involved in regulating a component of the NER pathway that requires *de novo* protein synthesis.

5.2 Materials and methods

Yeast strains and plasmids

The yeast strains used in this study were, WCG4a (WT), Sc507 (WT), Sc507R7 (Δ*rad7*) and Sc507R23 (Δ*rad23*) were described in Chapter 2. Strain Sc507 (T7-*SUG1* ade2–1 ura3–1 his3–11,15 trp1–1 leu2–3,112 can1–100) was derived from Sc342 (same as W3031A) (MATa ade2–1 trp1–1 leu2–3, 112 his3–11, 15 ura3–1 can1–100) and was constructed by inserting a bacteriophage T7 epitope S10 at the amino terminus of the wild-type *SUG1* gene. Creation of the Rad7 SOCS box mutation was achieved by site directed mutagenesis of the WT *RAD7* gene cloned in pRS314 as described in Chapter 4.

The *sug2-1*/Δ*rad23* (WH201R23) was derived from W3031A (Gillette *et al.*, 2001). The *RAD7* gene in WH201R23 was deleted and then transformed with pRS314

expressing wild type or SOCS box mutated Rad7 to acquire *sug2-1*/Δ*rad23*/pRAD7 and *sug2-1*/Δ*rad23*/psocs strains respectively.

With a similar method as described above, pRAD7/Δ*rad23* and psocs/Δ*rad23* strains were derived from Sc507R23.

Precultures of strains carrying plasmids were grown in synthetic complete medium containing 0.7% yeast nitrogen base supplemented with amino acids (with selected amino acids dropped out) and 2% glucose.

Measurement of induced NER at nucleotide level

Cells were firstly treated with an initial UV dose of 20 J/m^2. After 1 hour incubation in culture medium, cells were irradiated with a second, higher UV dose (100-150 J/m^2) following the protocol described in Chapter 2 (see 2.3). Examining DNA repair at nucleotide level is also described in Chapter 2 (see 2.8).

Analysis of Rad4 protein stability and UV Survival

Yeast protein extracts were prepared by bead beating in yeast dialysis buffer as described in Chapter 2.10. Western analysis of Rad4 protein was performed using standard methods using the antibodies noted in the Results section. Anti-Rad4 antibody was raised against a specific Rad4 peptide (Affiniti Research Products Limited, see 2.18).

Post UV cellular survival was measured by plating yeast cells onto appropriate growth medium prior to UV irradiation at the doses stated (details see 2.3).

5.3 Results

5.3.1. Post UV Rad4 degradation does not correlate with UV survival

Chapter 4 revealed that UV induced ubiquitination and degradation of Rad4 protein are dependent on the Rad7 E3 ligase, the work described in this chapter asks,

what is the physiological function of this process in the cell?

To examine whether the UV induced degradation of Rad4 protein influences the cellular UV survival, firstly I tested the UV sensitivity of three strains, pRAD7, psocs and Δ*rad7* strain. The details of psocs and pRAD7 strains were described in chapter 4.3.7. Figure 4.8 indicated that the steady state Rad4 protein level remained stable after UV treatment in the psocs strain. As shown in Figure 5.1, in the *rad7* deleted strain, a significant decrease in UV survival was observed, and this result was expected (Verhage *et al.*, 1996). Surprisingly, the psocs mutant strain exhibits almost WT UV resistance similar to the pRAD7 strain (see Figure 5.1). I reasoned that the E3 ligase function of Rad7 might be distinct from Rad7's core function in the GG-NER reaction which is involved in an early stage of NER and linked to the excision of DNA damage. Alternatively, it was possible that some other protein, possibly a NER factor, might have a functional overlap with this ECS ligase, resulting in the psocs strain displaying a UV sensitivity similar to the WT strain.

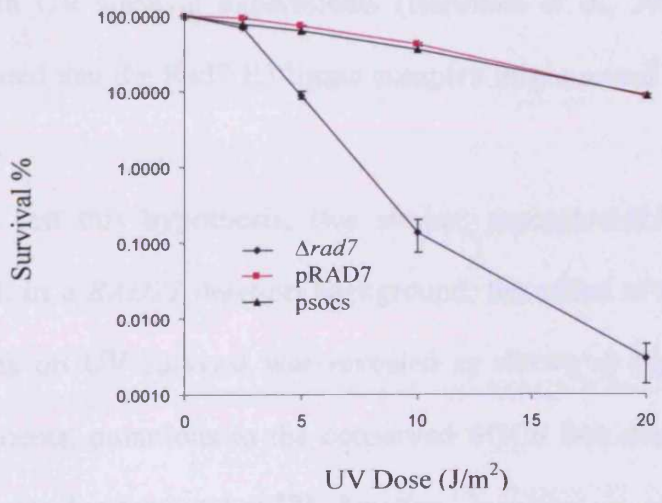

Figure 5.1. UV survival for the mutant strains listed. Post UV cellular survival assay was described in 2.3.

After cells are exposed to UV, the steady state level of Rad4 remained stable in the psocs strain whereas it decreased in the pRAD7 strain (see Figure 4.8). This differential regulation of Rad4 in psocs versus pRAD7 strains does not affect UV sensitivity (see Figure 5.1); both strains are not UV sensitive. This indicates that altering the stability of Rad4 protein in response to UV does not affect UV survival under the conditions described.

5.3.2. The Rad7 E3 ubiquitin ligase affects UV survival in the absence of Rad23

Collectively, the observations described so far show that UV dependent degradation and ubiquitination requires the Rad7 E3 ubiquitin ligase complex, but neither the ubiquitination nor the UV dependent degradation of Rad4 correlate with cellular survival following UV radiation. I considered whether a functional overlap exists between the activity of the Rad7 E3 ubiquitin ligase complex and some other NER factor creating redundancy. Since the substrate of the Rad7 E3 ligase is Rad4, I considered whether its binding partner, Rad23, may mask the role of the ligase. Especially since it has been reported that Rad23 possessed overlapping functions with Rad7 in UV survival experiments (Bertolaet *et al*, 2001a; Gillette *et al*, 2001); I speculated that the Rad7 E3 ligase complex might reveal its function in the absence of Rad23.

To test this hypothesis, two strains, psocs/Δ*rad23* and pRAD7/Δ*rad23*, were created. In a *RAD23* deletion background, the effect of the Rad7 E3 ubiquitin ligase complex on UV survival was revealed as shown as Figure 5.2A. From our earlier experiments, mutations in the conserved SOCS box domain of Rad7 protein do not disturb its fundamental NER function, resulting in a strain with wild type UV sensitivity. However, increased UV sensitivity was seen in the psocs/Δ*rad23* strain compared with the post-UV cellular survival of the pRAD7/Δ*rad23* strain (Figure

5.2A). Therefore, the defective function of the Rad7 E3 ubiquitin ligase in the psocs/Δ*rad23* strain causes increased UV sensitivity in this strain.

To further investigate this, the steady level of Rad4 protein after exposure to UV in those two strains was examined by Western blotting with anti-Rad4 antibody. As shown in Figure 5.2B, in the *RAD23* deletion background the steady level of Rad4 protein remained stable in the psocs/Δ*rad23* strain but decreased in the pRAD7/Δ*rad23* strain after UV irradiation. It is interesting to note that while the steady state level of Rad4 is lower in the pRAD7/Δ*rad23* mutant, the increased steady state level of Rad4 in the psocs/Δ*rad23* double mutant does not result in an increase in UV survival. This result is in agreement with previous findings that show inhibiting the proteolytic activity of the 26S proteasome does not significantly influence NER in a Δ*rad23* strain (Gillette *et al.*, 2001; Lommel *et al.*, 2002). Therefore, the degradation of Rad4 after UV does not contribute to UV survival.

Although the ubiquitination and degradation of Rad4 protein after UV irradiation both require the Rad7 E3 ligase activity, only the ubiquitination of Rad4 protein correlates with changes in cellular UV survival. So the specific requirement of the Rad7 containing E3 ligase for cellular survival is revealed when the *RAD23* gene is deleted, suggesting that Rad23 predominantly affects UV survival compared with the Rad7 ECS complex function. The data also demonstrate that the Rad7 containing E3 ligase and Rad23 proteins have overlapping functions in UV survival as previously suggested (Bertolaet *et al.*, 2001a; Gillette *et al.*, 2001).

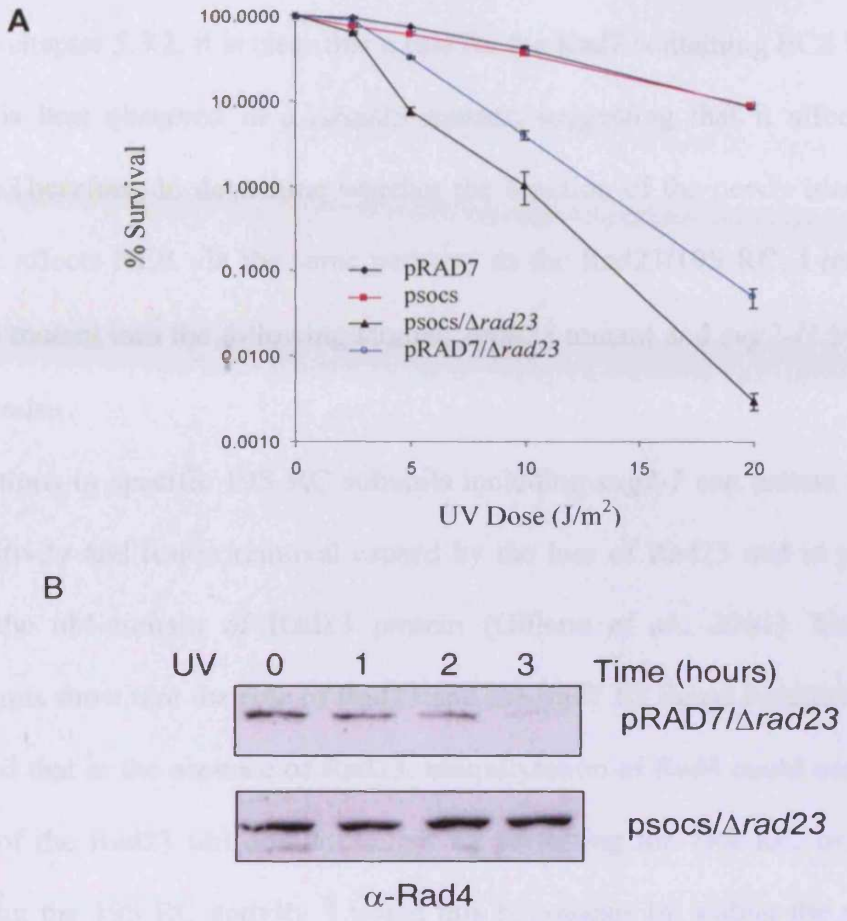

Figure 5.2. **A**. UV survival for the mutant strains listed. **B** Anti-Rad4 western blot of protein extracts prepared from pRad7/*Δrad23* (top) or psocs/*Δrad23* (bottom). Strains were UV irradiated and allowed to repair for the times indicated (hours).

In this section, I showed that the Rad7 E3 ubiquitin ligase contributes to UV survival and this can be observed clearly when Rad23 protein is absent. Moreover, although Rad4 protein is ubiquitinated and degraded after UV, only ubiquitination of Rad4 correlates with an affect on cellular UV survival, while degradation of Rad4 does not.

5.3.3 The Rad7 E3 ligase functions in a pathway different from the Rad23/19S RC activity

From chapter 5.3.2, it is clear that a role for the Rad7 containing ECS ligase in UV survival is best observed in a Δ*rad23* mutant, suggesting that it affects the NER pathway. Therefore, to determine whether the function of the newly identified Rad7 E3 ligase affects NER via the same pathway as the Rad23/19S RC, I introduced the E3 ligase mutant into the following strains; *Δrad23* mutant and *sug2-1*/*Δrad23* double mutant strains.

Mutations in specific 19S RC subunits including *sug2-1* can rescue the defect in UV sensitivity and lesion removal caused by the loss of Rad23 and in particular the loss of the ubl-domain of Rad23 protein (Gillette *et al.*, 2001). Since previous observations show that the role of Rad23 and the Rad7 E3 ligase functionally overlap, I surmised that in the absence of Rad23, ubiquitylation of Rad4 could compensate for the loss of the Rad23 ubl domain, either by recruiting the 19S RC, or functionally influencing the 19S RC activity. I tested this hypothesis by adding the *sug2-1* (19S) mutation to the UV sensitive Δ*rad23*/psocs strain. Adding the 19S RC mutation to the Δ*rad23*/psocs strain could result in a number of different outcomes. Conceivably it could have no effect on the UV survival of the Δ*rad23*/psocs strain (if the function of the E3 ligase was to recruit the 19S RC), or it could rescue UV sensitivity to the same level as the Δ*rad23*/*sug2-1* mutant strain (if the E3 ligase functionally affected the 19S activity and worked in the same pathway). Finally it could result in an intermediate UV phenotype (which would be consistent with a function that was independent of the 19S RC activity).

Figure 5.3 shows that the *sug2-1*/Δ*rad23*/psocs mutation displays an intermediate UV phenotype, partially rescuing the Δ*rad23*/psocs double mutant, but to a level less

than the Δ*rad23*/*sug2-1*strain. This observation is consistent with the Rad7 containing E3 ligase activity functioning in a pathway different from that employing the Rad23/19S activity.

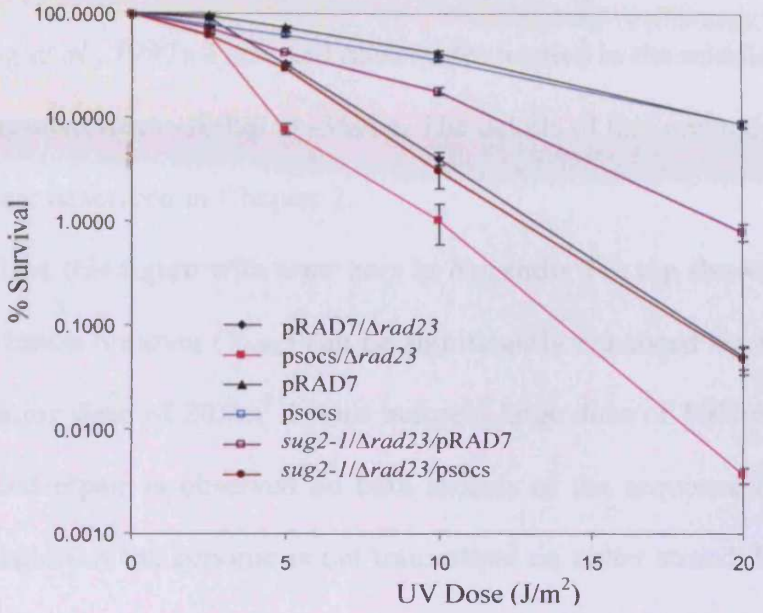

Figure 5.3. UV survival of the Sc507 derived strains listed.

5.3.4 Inducible NER requires the activity of the Rad7 E3 ligase

It has been reported that a number of yeast genes have UV-inducible promoters that share common regulatory elements and they participate in an inducible and co-regulatable repair system (Friedberg *et al.*, 2006). A rapid transcriptional induction of several DNA repair genes, including Rad2, Rad7, Rad16 and Rad23, acts in response to UV induced DNA damage and is required for proficient NER (Waters *et al.*, 1993). The induced expression of repair genes caused by DNA damage may enhance NER (Waters *et al.*, 1993). Besides the DNA repair genes, Rad9, Rad24 and other checkpoint genes are also required for inducible NER (Yu *et al.*, 2001).

Since ubiquitination of proteins can have other functions besides a signal for degradation, I speculated the ubiquitination of Rad4 might be a signal for inducible DNA repair. I investigated whether the Rad7 E3 ligase plays a role in inducible NER. In this chapter, an end-labeling strategy was employed to measure the removal of UV-induced CPDs at nucleotide resolution in the promoter region of the *S. cerevisiae MFA2* gene (Teng *et al.*, 1997). I selected nucleotides located in the middle area of the *HaeIII MFA2* fragment from -100bp to -350bp. The details of this method and its data quantification were described in Chapter 2.

Figure 5.4C (see this figure with error bars in Appendix IV) top shows that in WT cells the rate of lesion removal ($T_{50\%}$) can be significantly enhanced by exposing the cells to a stimulating dose of $20J/m^2$ 1 hour before a large dose of $100J/m^2$. It can be seen that enhanced repair is observed on both strands of the sequence investigated. This particular region of the genome is not transcribed on either strand, but an effect on repair was observed on the strand that becomes the NTS in the coding region. Figure 5.4C bottom shows the loss of inducible repair in a strain containing mutations in the SOCS box of the *RAD7* gene (psocs). Inducible repair is significantly reduced in the non-transcribed strand (NTS) in psocs strain, and to a lesser extent in the other strand.

I conclude that the Rad7 E3 ligase complex plays a role in inducible NER. Inducible NER has been shown to require transcriptional activation of several genes and *de novo* protein synthesis (Waters *et al.*, 1993). Therefore, I speculate that the Rad7 E3 ligase complex may be involved in the regulation of *de novo* protein synthesis in response to DNA damage.

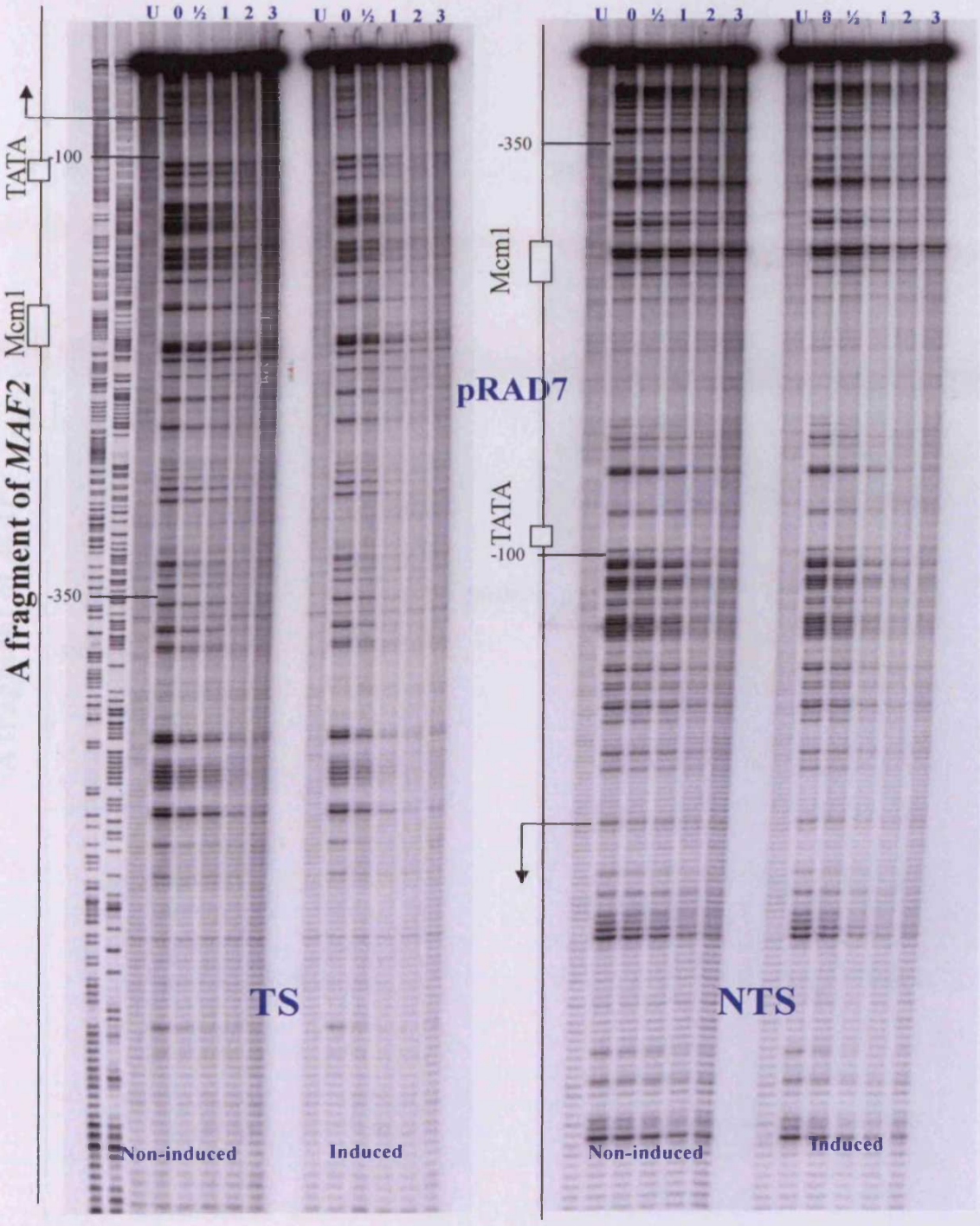

Figure 5.4A Repair of CPDs in the *MFA2* promoter in pRAD7 strains. Gels depicting CPDs in the transcribed strand (TS) and nontranscribed strand (NTS) of HaeIII restriction fragment (-516 to +83) in the *MFA2* promoter in wild-type (pRAD7) after100 J/m^2 UV irradiation (Non-induce) or an initial 20J/m^2 and a second 100 J/m^2 UV irradiation (Induced). Lane U, DNA from nonirradiated cells; lanes 0–3, DNA from irradiated cells after 0–3h of repair. Alongside the gels are symbols representing nucleosome positions, *MFA2* upstream activating sequences, and the start site of *MFA2* transcription (arrow). The selected nucleotides are from -100 to -350.

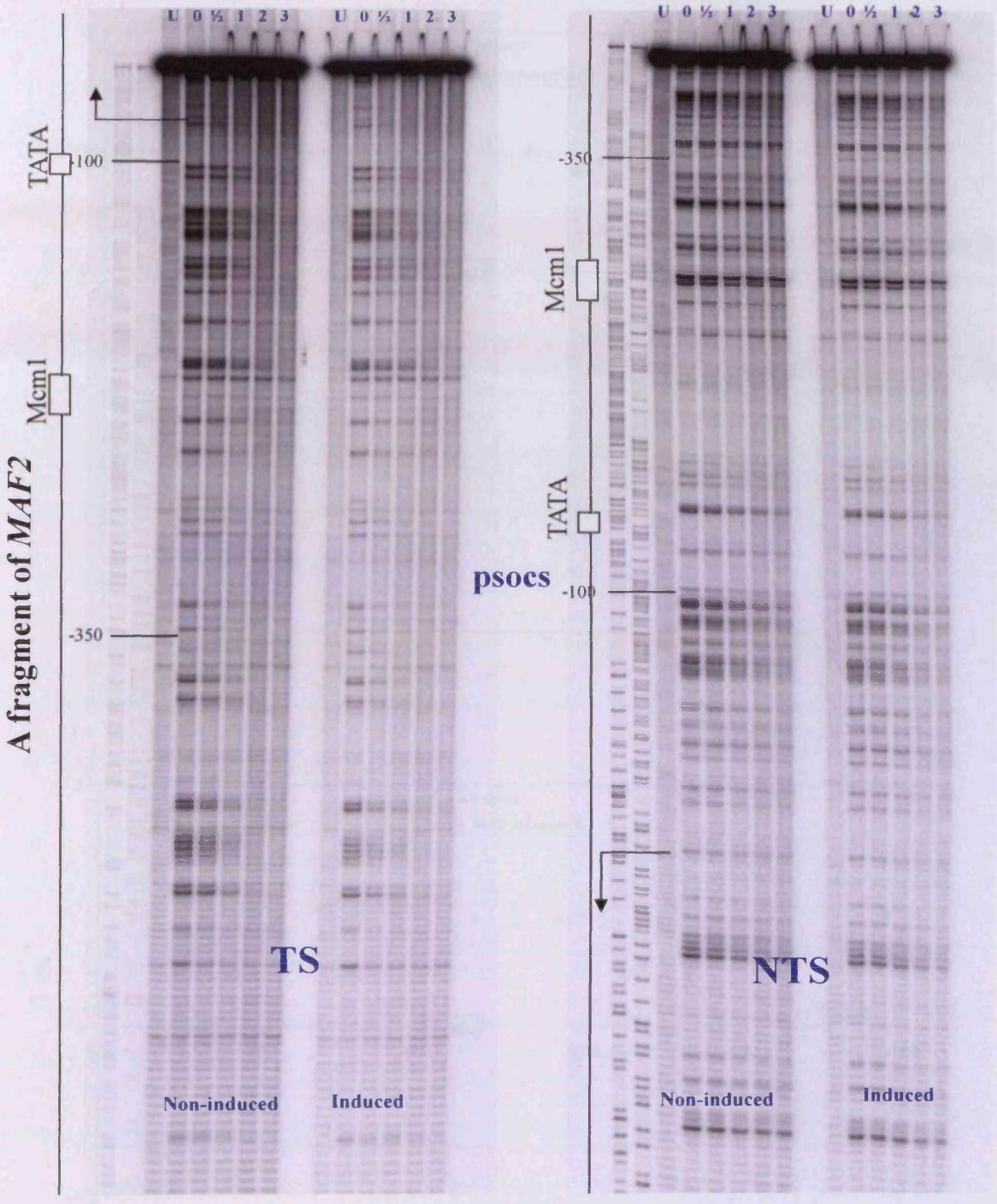

Figure 5.4B Repair of CPDs in the *MFA2* promoter in psocs strains. Gels depicting CPDs in the transcribed strand (TS) and nontranscribed strand (NTS) of HaeIII restriction fragment (-516 to +83) in the *MFA2* promoter in psocs after100 J/m^2 UV irradiation (Non-induce) or an initial 20J/m^2 and a second 100 J/m^2 UV irradiation (Induced). Lane U, DNA from nonirradiated cells; lanes 0–3, DNA from irradiated cells after 0–3h of repair. Alongside the gels are symbols representing nucleosome positions, *MFA2* upstream activating sequences, and the start site of *MFA2* transcription (arrow). The selected nucleotides are from -100 to -350.

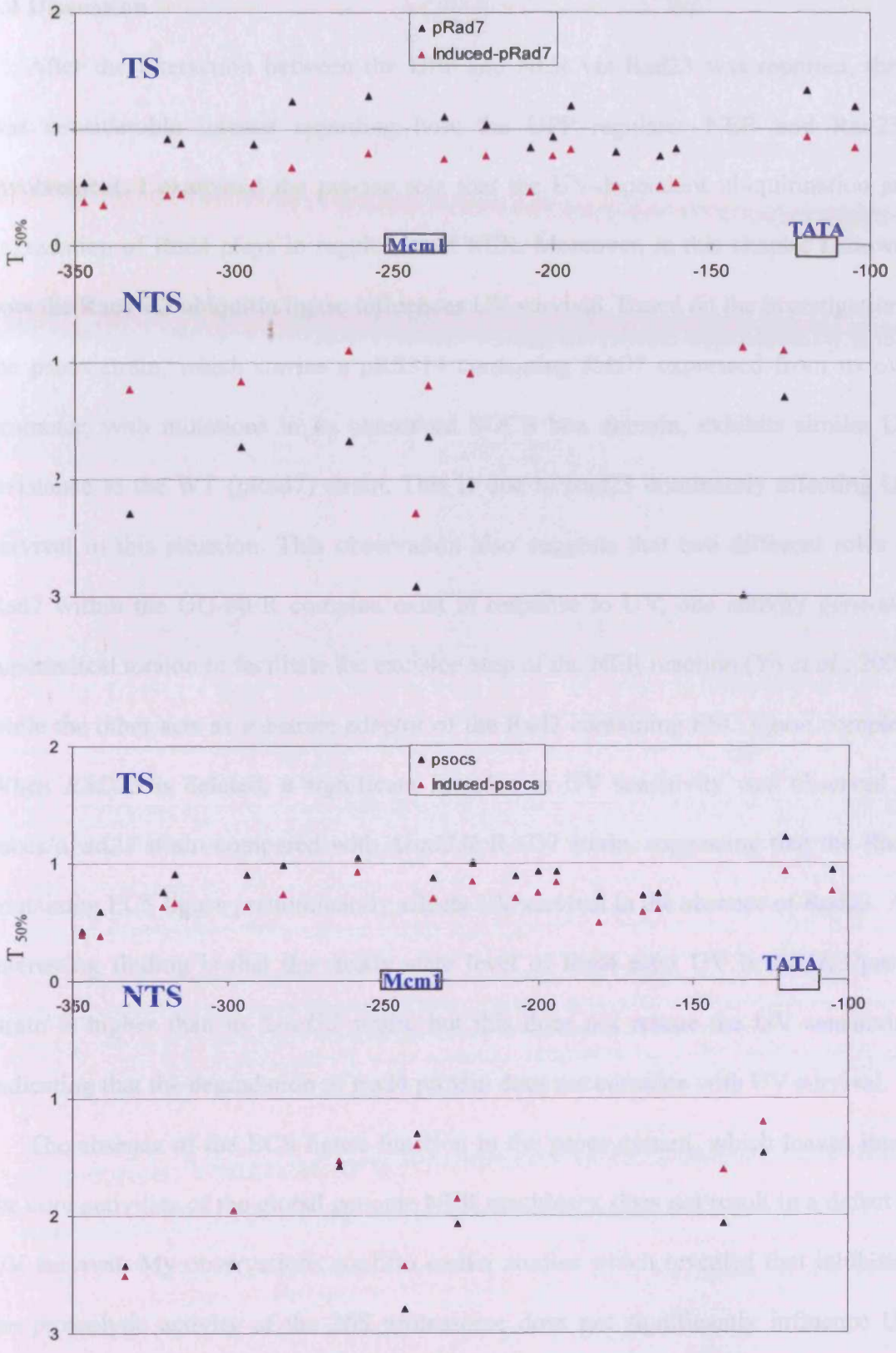

Figure 5.4C Quantification results form figure 5.4A and B. Time to remove 50% of the initial CPDs ($T_{50\%}$) at given sites. Details of quantification was described in 2.8.

5.4 Discussion

After the interaction between the UPP and NER via Rad23 was reported, there was considerable interest regarding how the UPP regulates NER and Rad23's involvement. I examined the precise role that the UV-dependent ubiquitination and degradation of Rad4 plays in regulation of NER. Moreover, in this chapter I showed how the Rad7 E3 ubiquitin ligase influences UV survival. Based on the investigations, the psocs strain, which carries a pRS314 containing *RAD7* expressed from its own promoter, with mutations in its conserved SOCS box domain, exhibits similar UV resistance to the WT (pRad7) strain. This is due to Rad23 dominantly affecting UV survival in this situation. This observation also suggests that two different roles of Rad7 within the GG-NER complex exist in response to UV; one activity generates superhelical torsion to facilitate the excision step of the NER reaction (Yu *et al.*, 2004), while the other acts as substrate adaptor of the Rad7 containing ESC ligase complex. When *RAD23* is deleted, a significant increase in UV sensitivity was observed in psocs/Δ*rad23* strain compared with Δ*rad23*/pRAD7 strain, suggesting that the Rad7 containing ECS ligase predominantly affects UV survival in the absence of Rad23. An interesting finding is that the steady state level of Rad4 after UV in Δ*rad23*/psocs strain is higher than in Δ*rad23* strain, but this does not rescue the UV sensitivity, indicating that the degradation of Rad4 protein does not correlate with UV survival.

The absence of the ECS ligase function in the psocs mutant, which leaves intact the core activities of the global genome NER machinery, does not result in a defect in UV survival. My observations confirm earlier studies which revealed that inhibiting the proteolytic activity of the 26S proteasome does not significantly influence UV survival (Gillette *et al.*, 2001). Therefore although Rad4 is ubiquitinated and degraded

in response to UV, it is only the ubiquitination of Rad4 which plays a role in UV survival. In this chapter, my data also confirms that the Rad7 E3 complex has functional overlap with Rad23 in UV survival as reported earlier (Bertolaet *et al.*, 2001a; Gillette *et al.*, 2001).

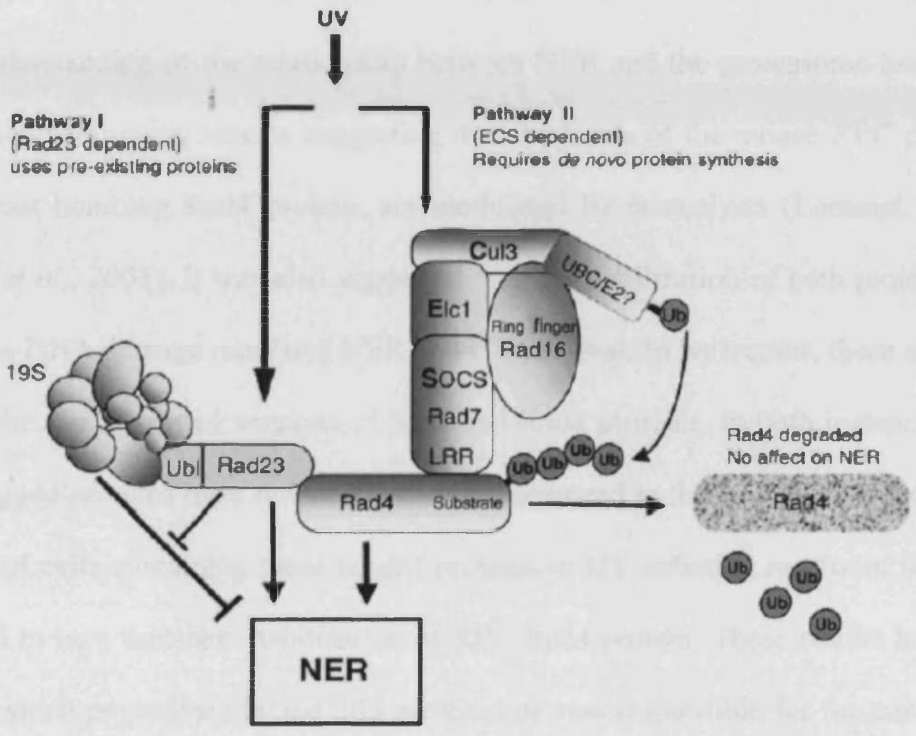

Figure 5.5 Regulation of the parallel pathways that regulate the NER response to UV. Pathway I is regulated by Rad23 and operates independently of *de novo* protein synthesis. Rad23 functions, in part, by attenuating the inhibitory effect of the 19S proteasome on the rate of lesion removal. Pathway II relies on *de novo* protein synthesis and the ubiquitination of Rad4 via the action of the ECS ligase depicted in the center of the figure. Subsequently, Rad4 is degraded via the 26S proteasome with *de novo* synthesis eventually restoring Rad4 to it's pre-UV levels. (Adapted form Gillette *et al.*, 2006 with permission)

In this chapter, my data shows that inducible NER is significantly decreased particularly for the NTS of a promoter region of *MAF2*. This suggests that the function of this ECS ligase in promoting efficient NER relates to its ability to regulate *de novo* protein synthesis following DNA damage. Based on my data and other work from our group, it has been confirmed that after exposing cells to UV radiation, the

NER response is comprised of two components, based on their requirement for *de novo* protein synthesis (Figure 5.5). Pathway I requires the interaction of Rad23 protein and the 19S RC, and functions independently of *de novo* protein synthesis. Pathway II requires the novel Rad7 containing E3 ubiquitin ligase and depends on *de novo* protein synthesis. Both pathways require distinct non-proteolytic activities of the UPP system.

An understanding of the relationship between NER and the proteasome has been made difficult following reports suggesting that the levels of the mouse XPC protein and its yeast homolog Rad4 protein, are modulated by proteolysis (Lommel *et al.*, 2002; Ng *et al.*, 2003). It was also suggested that the stabilization of both proteins in response to DNA damage regulated NER and UV survival. In both cases, these studies involved the use of tagged versions of XPC and Rad4 proteins. In both instances the epitope tagged proteins have reduced half-lives compared to the endogenous proteins. Exposure of cells containing these tagged proteins to UV radiation results in what is interpreted to be a transient stabilization of XPC/Rad4 protein. These results led to a model in which proteolysis by the 26S proteasome was responsible for the continual turnover of Rad4/XPC protein. The model suggested that following UV damage, proteolytic degradation of Rad4/XPC protein by the 26S proteasome was attenuated, resulting in accumulation of this repair factor and enhancement of NER (Lommel *et al.*, 2002; Ng *et al.*, 2003).

In contrast, my studies show that this is not the case when native Rad4 protein is studied. My results show that native Rad4 protein has a half-life of around 4 hours (Figure 4.2C). Upon UV exposure, steady state levels of Rad4 protein rapidly decrease, due to increased proteolysis by the proteasome. It is known that the Ubl domain and the Rad4 interacting domain of the Rad23 protein are functionally distinct

(Bertolaet *et al.*, 2001a; Bertolaet *et al.*, 2001b; Gillette *et al.*, 2001), and it has been suggested that the Rad4 binding domain of Rad23 protects Rad4 from degradation by the 26S proteasome. It is clear that in the absence of Rad23, steady state levels of Rad4 are reduced, but the cause of this reduced Rad4 level and whether they directly affect NER has not been established. I showed that the reduced levels of Rad4 in *RAD23* deleted cells is not due to increased proteolysis of Rad4 in these cells, but rather due to reduced production of Rad4 transcript. My results reveal the mechanism of reduced Rad4 levels in these cells. Although Rad4 protein levels are reduced in Δ*rad23* cells, stabilization of Rad4 in proteolytic defective mutants has no effect on the NER defective phenotype of a Δ*rad23* strain. Others have shown that over-expressing Rad4 in a Δ*rad23* background, has only a minor affect in rescuing UV survival (Xie *et al.*, 2004). These observations suggest that stabilization of Rad4 *per se* plays no significant role in UV survival. The relationship between steady state levels of Rad23 and it's binding partner is also observed in mammalian cells, where the lack of hHR23A/B results in lowered steady state levels of XPC (Ng *et al.*, 2003; Okuda *et al.*, 2004). However, unlike yeast, in mammalian cells the half-life of XPC decreases (Okuda *et al.*, 2004). At present it is unclear whether proteolysis plays a role in mammalian NER.

I identified Rad7, Rad16, Elc1 and Cul3 as part of an ECS type E3 ubiquitin ligase that ubiquitinates Rad4 protein following exposure of cells to UV radiation. This complex ubiquitinates Rad4 protein *in vitro*. I do not observe a ladder of ubiquitination in the *in vitro* reaction, nor *in vivo*. However, Rad4 is degraded by the 26S proteasome *in vivo*, suggesting that polyubiquitination could occur. Alternatively, recent evidence suggests that under certain circumstances proteasome dependent degradation can occur in the absence of polyubiquitination (Wang *et al.*, 2007).

Specific point mutations within the conserved SOCS domain of Rad7 protein inhibit the UV induced ubiquitination of Rad4 protein *in vivo*. My results show that the *rad7,* psocs mutation increases the UV sensitivity of a Δ*rad23* strain, even though Rad4 protein is stabilized. In contrast, stabilization of Rad4 protein in the Δ*rad23* strain, by direct inhibition of 26S proteasome proteolytic activity has no effect on NER (Gillette *et al.*, 2001). These observations show that the changes observed in the stability of Rad4 protein in response to UV do not influence NER and UV survival. Therefore it is possible to differentiate between the effect of Rad4 protein ubiquitination and Rad4 protein degradation on NER and UV survival. Ubiquitination of Rad4 protein in response to UV specifically regulates NER via a pathway that requires *de novo* protein synthesis. This event directly influences NER and UV survival. Rad4 protein is subsequently degraded by the UPP, and this event does not directly influence NER or UV survival. I suggest that this mechanism restores cellular Rad4 protein levels to the un-ubiquitinated, pre-UV state.

Chapter 6
Does the Rad7 E3 ligase regulate a component of the transcriptional response to DNA damage?

6.1 Introduction

In *S. cerevisiae*, the Rad23 protein displays multiple roles in different pathways, including NER, cell cycle and the UPP. (Biggins *et al.*, 1996; Watkins *et al.*, 1993; Gillette *et al.*, 2001; Ortolan *et al.*, 2000; Gillette *et al.*, 2006). In chapter 4 and 5, my results show that loss of the Rad23 protein does not alter the half life of the Rad4 protein but instead alters the steady state mRNA level of *RAD4*. My data also show that the post UV degradation of Rad4 does not correlate with cellular UV survival, but the UV-induced ubiquitination of Rad4 does. Furthermore, the Rad7 containing ECS ligase is required for inducible NER. The NER response to UV irradiation includes two components; pathway I functions independently of *de novo* protein synthesis and involves the non proteolytic interaction of Rad23 and the 19S that we identified previously (Gillette *et al.*, 2006). Pathway II requires *de novo* protein synthesis and the activity of the Rad7 E3 ligase is necessary for proper functioning of this pathway (Gillette *et al.*, 2006).

In chapter 4, my data demonstrates that the mRNA level of *RAD4* decreased in a Δ*rad23* mutant strain compared with a WT strain, suggesting that Rad23 could play a role in regulating transcription of certain genes. Moreover, in the absence of Rad23, the activity of the Rad7 ECS ligase is required for cellular UV survival, suggesting an overlapping function of Rad23 and this E3 ligase. So I speculated that the Rad23 protein as a component of the Rad23/Rad4 complex may play a role in regulating gene transcription of a subset of genes in response to DNA damage in addition to its proposed DNA damage recognition function. Importantly, my results described in

chapter 5 showed that the steady level of Rad4 does not affect cellular UV survival. Therefore I considered the possibility that the Rad4/Rad23 complex may affect the transcriptional regulation of other gene(s) to facilitate efficient NER.

In order to explore this possibility, we performed gene expression profiling in a strain deleted of Rad4 and Rad23. Our microarray data revealed that the transcriptional regulation of a relatively small subset of genes was affected. We noted that some of these genes appeared to be involved in the cellular response to DNA damage. One of these called *DDR2*, was originally revealed in a genetic screen for genes which showed increased transcription following exposure of cells to DNA damaging agents (McClanahan and McEntee, 1984). The inducible transcription of *DDR2* requires two transcriptional activators Msn2/Msn4, which stimulates transcription by binding to the stress-response element (STRE) in its promoter region in response to DNA damage (Schmitt and McEntee, 1996; Martinez-Pastor *et al.*, 1996). I speculated that expression of Ddr2 in response to DNA damage may be co-regulated by changes in the binding of the Rad4/Rad23 complex to the *DDR2* promoter region after DNA damage, and that changes in binding might be regulated through the ubiquitination of Rad4 by the Rad7 E3 ligase to facilitate overall NER efficiency in response to UV damage. This speculation was based on recent observations that describe how ubiquitination can influence changes in transcriptional regulation (Ferdous *et al.*, 2007).

In this chapter, I describe preliminary experiments designed to investigate how the Rad4/Rad23 complex might influence the regulation of a specific set of genes in response to DNA damage. Initially I have investigated the occupancy of Rad23 in the promoter region of *DDR2* as measured by chromatin immunoprecipitation (ChIP) assay. Early indications suggest that Rad23's occupancy at the promoter of *DDR2* is

influenced by the Rad7 E3 ligase, and is regulated in response to DNA damage.

6.2 Materials and methods

Yeast strains and plasmid

The yeast strains used in this study were, BY4741 (WT), BY4741elc1 (Δ*elc1*), and BY4741R23 (Δ*rad23*), purchased form Euroscarf . The pRAD7 and psocs strains were described in 4.2.

Chromatin immunoprecipitation (ChIP) – quantitative PCR (qPCR)

The in vivo crosslinking and sonication of chromatin extracts

Cells were grown to a density of $2\sim4\times10^7$ cells/ml, and 2.8 ml of 37% formaldehyde was added to 100 ml of the culture medium (containing at least 2×10^9 cells). The mixture was incubated at room temperature for 20 mins with occasional swirling to allow efficient DNA and protein cross-linking. The cross-linking reaction was ceased by adding 5.5 ml of 2.5M glycine to a final concentration of 0.125M. Cells were collected by centrifugation and then washed with ice-cold TBS buffer and ChIP lysis buffer. Cells were resuspended in 500 μl of ChIP lysis buffer supplemented with 12.5 μl of 20% SDS and 12 μl of 100× protease inhibitors. After 0.5 ml glass beads were added to this solution, the mixture was vortex (at the highest speed on a turboMix) at 4°C for 10-15 mins. The cell lysate was carefully collected by centrifugation. The cell lysate was sonicated by a Diagenode sonication system at the high output rate for 3-4 mins (6-8 × 0.5 min on/0.5 min off cycle). The sonicated cell lysate was spun down at 13,200 r.p.m for 15 mins at 4°C. Supernatant (chromatin extract) was transferred to a clean tube and stored at -80°C until further use.

Chromatin immunoprecipitation (ChIP)

Protein A beads were washed twice with ChIP lysis buffer and then equilibrated with ChIP lysis buffer supplemented with 0.1% BSA and 40 μg/ml single strand

salmon sperm DNA for 3 hours at 4°C. 50 µl of chromatin extracts were added to 500 µl of ChIP binding buffer (ChIP lysis buffer supplemented with 0.25% SDS and 1× protease inhibitors) and then the solution was cleaned with the equilibrated protein A beads. After removal of the protein A beads by centrifugation, the chromatin immunoprecipitation was carried out by adding 1-5 µl antibody to this cleaned solution at 4°C for overnight. 20-30µl of protein A beads slurry (ChIP lysis buffer washed twice) was added to the solution and incubated for 2-3 hours at 4°C. The protein A beads were quickly spun down and washed successively with ChIP lysis buffer, ChIP lysis buffer with an increased salt concentration (500mM NaCl), LiCl solution and TE buffer.

The protein A beads were incubated with 250 µl elution buffer at room temperature for 10 mins. Then, the supernatant was collected by centrifugation. The pellet was eluted again. The two parts of eluate were pooled together and incubated at 65°C overnight.

Subsequently the elution was treated with ribonuclease A and protease K, the DNA was purified by a standard phenol/chloroform purification or a PCR purification kit (QIAGEN). In order to precipitate the DNA, 100 µg glycogen, 1/10 volume of 3M sodium acetate (pH5.2) and 2 volume of ethanol were added to the solution. The precipitated DNA was resuspended in 50-100 µl TE buffer and stored at -20°C.

The quantitative PCR (qPCR)

Quantitative PCR was carried out with the following primer pairs;

Upper_DDR2-primer-1: TGCTCAAAGGTTTATGCCCGATGTT

Lower_DDR2-primer-1: TGCATTATTGATGTCCCATAAGGGG

Upper_DDR2-primer-2: CCCAGACACGGTTGCCAAGGCCTCG

lower_DDR2-primer-2: CGGGCATAAACCTTTGAGCATCATC

Upper_DDR2-primer-3: AGCCCTCCAAGCAAGCACGC

Lower_DDR2-primer-3: CGTGCAAAGCAGGAGCAGCG

Upper-GPG1-primer-1: GCGCCCTGTATCAAAAAGAAGCTTT

Lower-GPG1-primer -1: GGAACTTCCTCACACCGCGGTTTGT

A serial dilution of the genomic DNA from a WT (Sc507) strain was used to make a standard DNA concentration curve. Therefore, based on this standard curve all raw data acquired from real-time PCR machine was analyzed by iQ5 software (Bio-Rad).

Northern blot assay

The protocol of Northern blot was described in chapter 2. The following primers were used in this chapter;

Actin_NTS: biotin-GCCGGTTTTGCCGGTGACG

Actin_TS: CCGGCAGATTCCAAACCCAAAA

DDR2_NTS: biotin-*ACAGAT*TGCTCAAAGGTTTATGCCCGATGTT

DDR2_TS: GGTATCATCATCGTGGCAGTAAGCG

6.3 Results

6.3.1 Deletion of the *RAD23* gene affects the mRNA level of *DDR2*

To test whether the Rad23/Rad4 complex affects the transcription of the *DDR2* gene, the mRNA level in Δ*rad4*, Δ*rad23*, Δ*rad23*/Δ*rad4* mutant and wild type strains was detected by Northern blot assay (described in 2.6). In the absence of Rad23, Rad4 or Rad4/Rad23 the mRNA level of *DDR2* was significantly elevated compared with the very low levels of transcript observed in WT cells (Figure 6.1). This suggests that the Rad4/Rad23 heterodimer could influence the regulation of transcription of the DDR2 gene.

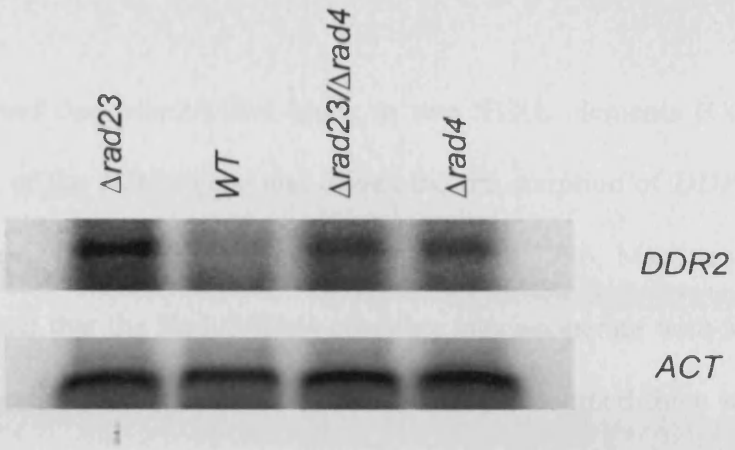

Figure 6.1. Northern blotting analysis of strains listed.

It has been reported previously that in the absence of Rad52 or after UV treatment, the transcription of *DDR2* increased (McClanahan and McEntee, 1984). The authors speculated that the Rad52 protein indirectly affects the transcription of *DDR2,* and suggested that persistent unrepaired lesions caused by the loss of Rad52 results in an increased mRNA level of *DDR2* (McClanahan and McEntee, 1984). In order to address how Rad4/Rad23 affects *DDR2*'s transcription, I chose a ChIP-qPCR method to test whether Rad4/Rad23 has a direct rather than an indirect involvement in regulating DDR2 expression. This method allowed me to examine the occupancy of Rad23 [and later Rad4] in the promoter region of *DDR2*.

6.3.2 The occupancy of Rad23 in the promoter region of *DDR2*

To measure the occupancy of Rad23 in the promoter region of *DDR2*, firstly *in vivo* crosslinking of DNA associated proteins was carried out as described in the protocol 6.2. After the chromatin extract was sonicated, the size of chromatin fragments was determined. A reverse-crosslinking treatment followed, and phenol/chloroform purification was applied to extract DNA from Δ*rad23*, Δ*elc1* (see later) and WT strains. The length of DNA fragments was checked on a 1.5% agarose

gel (Figure 6.2 A). The majority of DNA fragments were distributed from 300 bp to 500 bp in length.

It was reported that Msn2/Msn4 binds to two STRE elements (CCCCT) in the promoter region of the *DDR2* gene and drives the transcription of *DDR2* in response to DNA damage or heat shock (Schmitt and McEntee, 1996; Martinez-Pastor *et al.*, 1996). I speculated that the Rad23/Rad4 complex may cooperate with Msn2/Msn4 to control the transcriptional rate of *DDR2*. To test this, I designed three sets of primers necessary to perform qPCR (shown in figure 6.2C); one set (DDR2-primers-1) hybridises around the two STRE elements in the promoter region of the *DDR2* gene, the other two sets of primers hybridise up and downstream of the STRE elements (Figure 6.2C). The chromatin immunoprecipitation was carried out with anti-Rad23 antibody as the protocol describes in 6.2. The results from qPCR experiments with the three different sets of primers described above, are displayed in Figure 6.2B. The data demonstrate that the Rad23 protein binds to the promoter region of *DDR2*. Binding occurs predominantly in the region of the two STRE elements, where the Msn2/Msn4 transcriptional activator is known to bind to in response to DNA damage. This raises the possibility that the Rad23/Rad4 complex may co-regulate *DDR2* expression with Msn2/Msn4 after DNA damage. One possibility is that regulation occurs via an exchange of binding factors after UV exposure. My preliminary data is consistent with the idea that the Rad23 protein directly influences *DDR2*'s transcription based on the data shown in both Figure 6.1 and Figure 6.2B. I will test whether Rad4 shows similar occupancy at the promoter of *DDR2* as does Rad23, since I speculate that regulation of *DDR2* involves the Rad4/Rad23 heterodimer. This notion is currently being investigated.

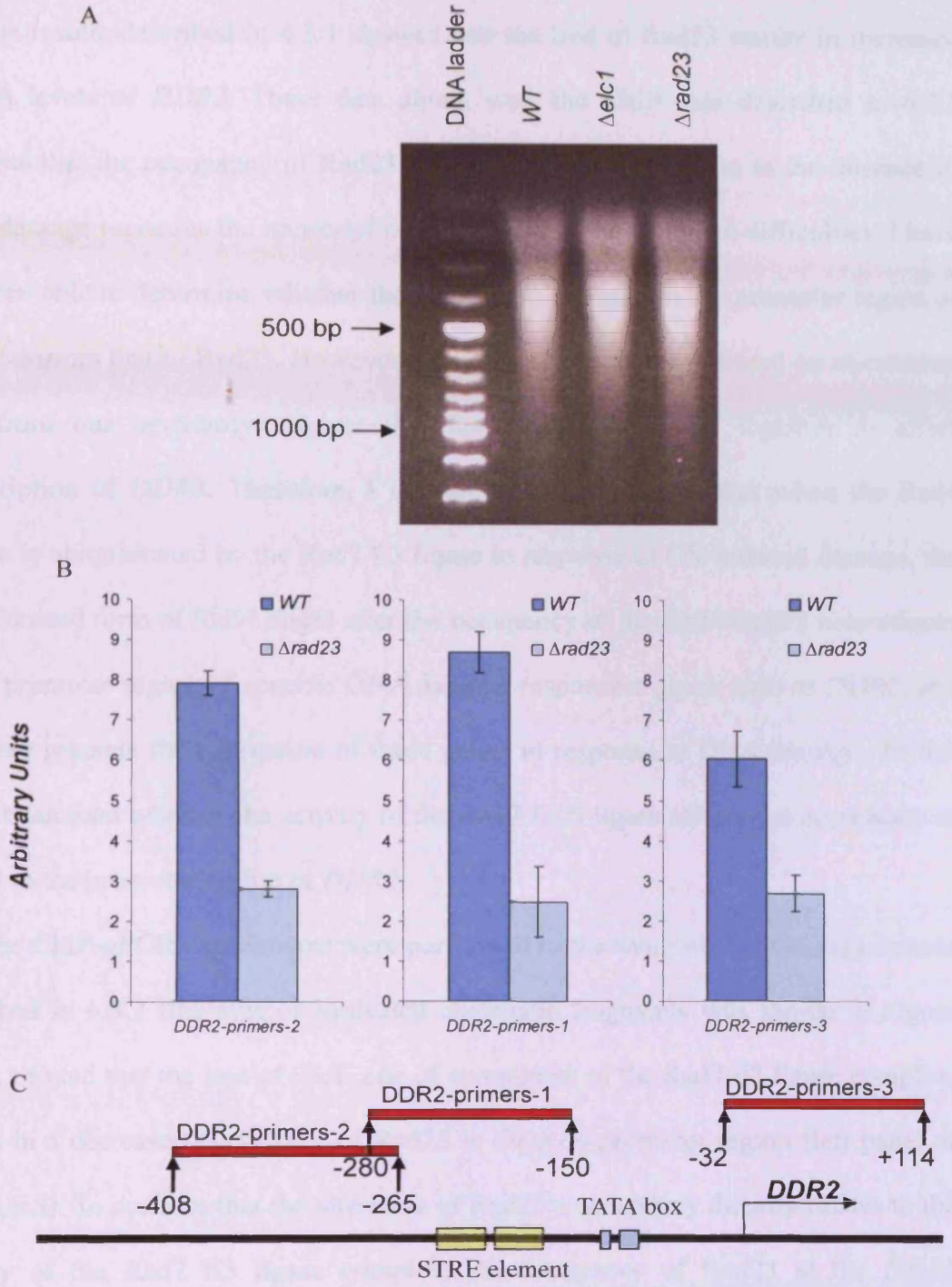

Figure 6.2. A. Gel electrophoresis of the DNA fragments isolated after chromatin crosslinking and sonication. The crosslinked chromatin extracts form Δ*elc1*, Δ*rad23* mutant and WT strains are shown. B. The qPCR results using the primer pairs listed following chromatin immunoprecipitation with anti-Rad23 antibody. The DNA sequence of each primer pair was described in 6.2. C. Location of PCR products for each of the three sets of primer pairs used for qPCR.

6.3.3 The Rad7 E3 ligase influences the occupancy of Rad23

The results described in 6.3.1 showed that the loss of Rad23 results in increased mRNA levels of *DDR2*. These data along, with the ChIP data described in 6.3.2 suggests that the occupancy of Rad23 in *DDR2*'s promoter region in the absence of DNA damage represses the transcription of *DDR2*. Due to technical difficulties, I have not been able to determine whether the occupancy of Rad4 in the promoter region of *DDR2* mirrors that of Rad23. However, preliminary observations based on microarray data from our laboratory suggest that Rad4 and Rad23 act together to affect transcription of *DDR2*. Therefore, I considered the possibility that when the Rad4 protein is ubiquitinated by the Rad7 E3 ligase in response to UV induced damage, the ubiquitinated form of Rad4 might alter the occupancy of the Rad4/Rad23 heterodimer in the promoter region of specific DNA damage responsive genes such as *DDR2*, and therefore regulate the expression of these genes in response to DNA damage. To test this, I examined whether the activity of the Rad7 ECS ligase affects the occupancy of Rad23 in the promoter region of *DDR2*.

The ChIP-qPCR experiments were performed in the same way as the experiments described in 6.3.2 (the size of sonicated chromatin fragments was shown in Figure 6.2A). I found that the loss of Elc1, one of component of the Rad7 E3 ligase complex, results in a decreased occupancy of Rad23 in *DDR2*'s promoter region (left panel of Figure 6.3). To confirm that the alteration of Rad23's occupancy directly relates to the activity of the Rad7 E3 ligase complex, the occupancy of Rad23 at the *DDR2* promoter region was also measured in both pRAD7 (WT) and psocs (E3 ligase mutant) cells (right panel of Figure 6.3). As anticipated, Rad23's occupancy in the promoter region of *DDR2* was significantly decreased in psocs cells compared with pRAD7 (WT) cells. Since I speculated that Rad23 may influence the transcription of only a

small cluster of genes, I tested the occupancy of Rad23 in the promoter region of the *GPG1* gene (as a negative control) and also examined whether Rad23 occupancy altered in the absence of Elc1. However, it was not identified as having significantly altered levels of transcription in our microarray analysis of Δ*rad4*/Δ*rad23* mutated cells. Occupancy of Rad23 at the *GPG1* promoter is very low compared to the Δ*rad23* mutant control, and does not significantly alter in the absence of Elc1 (the middle one of Figure 6.3), indicating that the E3 ligase only influences the occupancy of Rad23 in the promoter region of specific genes such as *DDR2*.

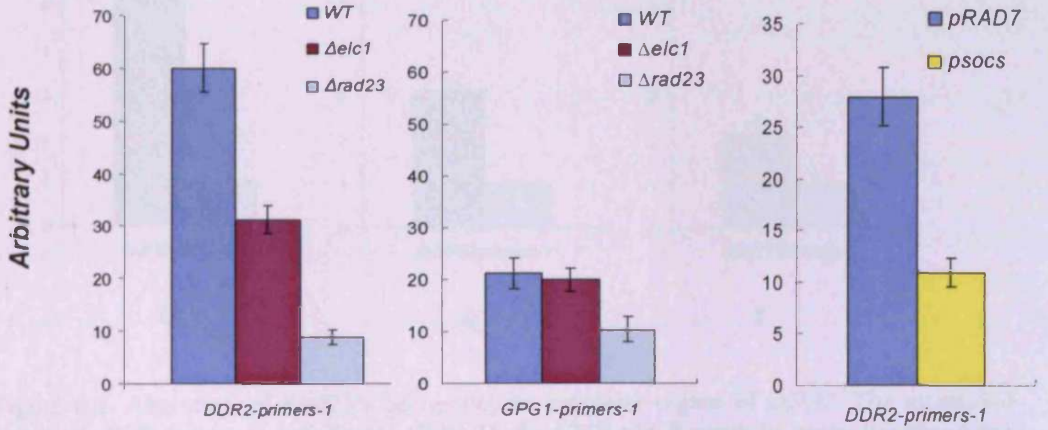

Figure 6.3. The qPCR results using the primer pairs listed following chromatin immunoprecipitation with anti-Rad23 antibody.

6.3.4 Rad23's occupancy in the promoter region of *DDR2* decreased in response to UV

The same assay was employed [with minor modifications to adjust for the effect of UV on the cells] to test whether the Rad23's occupancy alters in response to UV. The result of anti-Rad23 ChIP-qPCR experiments using chromatin extracts from Δ*rad23* cells collected at 0 and 1 hour after UV treatment or without UV treatment (U) was measured and arbitrarily set as background level binding. Next the same assay was performed using chromatin extracts from WT cells. The values obtained from the

wild type extracts were divided by the corresponding background levels to obtain the enrichment ratio. The ratio determines the extent to which the Rad23 protein binds to the promoter region of *DDR2*.

The occupancy of Rad23 in *DDR2*'s promoter region decreased in response to UV (see Figure 6.4). This corresponds with increased *DDR2* transcription after cells are exposed to UV (McClanahan and McEntee, 1984).

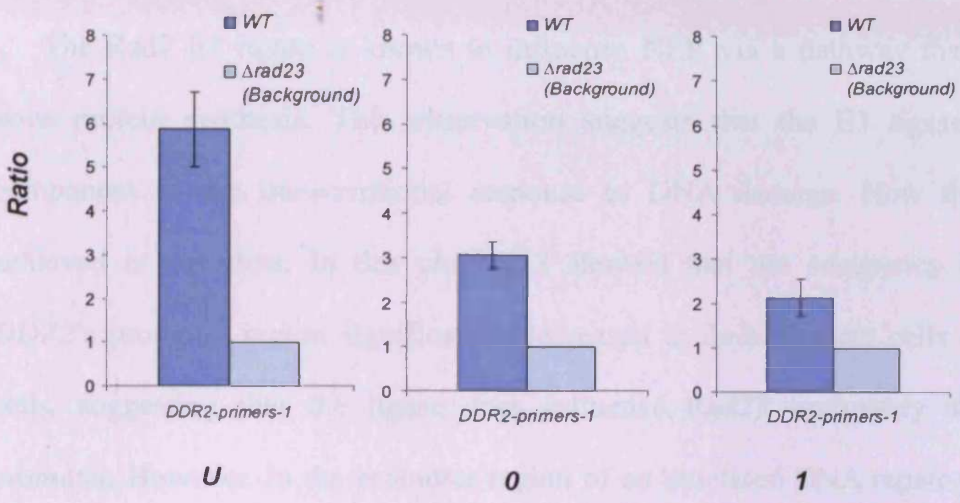

Figure 6.4. Alteration of Rad23's occupancy in promoter region of *DDR2*. The quantified result of qPCR followed anti-Rad23 ChIP. U, the ChIP-qPCR result by suing the chromatin extracts from nonirradiated cells; 0–1, the ChIP-qPCR result by using the chromatin extracts from irradiated cells after 0–1h of repair.

6.4. Discussion

In chapter 4, my data demonstrated that the mRNA level of *RAD4* decreased in a Δ*rad23* mutant strain compared with the WT strain, raising the possibility of Rad23 being involved in the regulation of the transcription of certain genes. In this chapter my results showed that the mRNA level of *DDR2* also is affected by the Rad23 protein. Furthermore, I showed the occupancy of Rad23 at the promoter region of *DDR2* in the absence of DNA damage. Although the increased mRNA level may result from an increased rate of transcription initiation, a decreased rate of processing of mRNA degradation, or both, my data support the notion that Rad23 directly affects

the rate of transcription.

After the total RNA extracts from Δ*rad23*, Δ*rad23*/Δ*rad4*, and WT strains were analyzed by microarray analysis, it was revealed that the transcription of a cluster of stress response genes are significantly altered in the absence of Rad23 or the Rad4/Rad23 complex (data not shown). One of these genes, *DDR2* was selected to investigate the possible occupancy of Rad23 at its promoter region, in order to test whether Rad23 directly influences the transcriptional regulation of *DDR2*.

The Rad7 E3 ligase is known to influence NER via a pathway that requires *de novo* protein synthesis. This observation suggests that the E3 ligase regulates a component of the transcriptional response to DNA damage. How this might be achieved is not clear. In this chapter, I showed that the occupancy of Rad23 in *DDR2*'s promoter region significantly decreased in Δ*elc1* mutant cells and in psocs cells, suggesting that the ligase does influence Rad23 occupancy at the *DDR2* promoter. However, in the promoter region of an unrelated DNA repair gene, *GPG1*, the occupancy of Rad23 is not detected is not significantly altered by the Rad7 E3 ligase. These preliminary observations leave a number of significant questions that remain to be determined. For example, it is not clear whether the alteration of Rad23's occupancy at the promoter of *DDR2* in response to UV is directly responsible for elevated *DDR2* transcription. The half-life of *DDR2*'s mRNA in a WT strain and a Δ*rad23* strain need be detected to answer whether Rad23 directly affects the transcription of *DDR2*. I also need to determine how Rad23 occupancy at the *DDR2*'s promoter is altered in response to DNA damage, and whether Rad4 and in particular the ubiquitination of Rad4 plays a role. Future work will focus on addressing these questions.

Chapter 7

General discussion and future experiments

The work presented in this thesis focused on the role of the Rad7/Rad16/ABF1 complex (GG-NER complex) in the NER pathway. Firstly, I showed that the Rad7/Rad16/ABF1 complex displays a DNA translocase activity on DNA that is necessary for its fundamental core NER function in generating superhelical torsion in DNA. This activity is necessary for efficient oligonucleotide excision of DNA damage during NER.

A novel Rad7 containing complex, consisting of Rad7, Rad16, Cul3 and Elc1, exhibits an E3 ubiquitin ligase activity after UV-irradiation. A conserved SOCS box domain and a LRR domain exist in the Rad7 protein which acts as the target adaptor in this Elongin-Cullin-Socs box (ECS) ligase complex. UV-dependent ubiquitination of Rad4, a physiological target of this novel ECS ligase, directly contributes to enhanced repair and UV cellular survival but the subsequent degradation of Rad4 does not. In the absence of the Rad23 protein, the Rad7 ECS ligase regulates NER in a pathway different from that employing the Rad23/proteasome 19S regulatory complex (19S RC). Therefore, the ubiquitin proteasome pathway (UPP) regulates NER via two distinct mechanisms.

Finally, the loss of Rad23 results in an altered steady state level of transcription of *RAD4* and a small subset of other genes including *DDR2*. How Rad23 influences the transcription of a subset of genes has been investigated by measuring the occupancy of Rad23 in the promoter region of *DDR2* and determining how this occupancy is altered in response to UV damage, and by the Rad7 E3 ligase complex.

7.1 The Rad7/Rad16/ABF1 complex displays an ATP-dependent DNA translocase activity

In yeast, two specific GG-NER functioning proteins, Rad7 and Rad16, bind tightly as a complex and do not have identified human homologues (Bang *et al.*, 1992; Verhage *et al.*, 1994; Wang *et al.*, 1997). Based on the existence of two ring finger motifs in the Rad16 protein and the specifically UV-damaged DNA binding characteristics of the Rad7/Rad16 complex, the Rad7/Rad16 (NEF4) complex has been assumed to be a DNA damage sensor (Guzder *et al.*, 1997; 1998). However, in the absence of Rad7 or Rad16, the incision stage of NER operates proficiently both *in vitro* and *in vivo* (Reed *et al.*, 1998). Moreover, the Rad7/Rad16 complex is involved in the removal of the oligonucleotide containing the damage (Reed *et al.*, 1998). It has been found that the superhelicity generated by Rad7/Rad16/ABF1 complex can facilitate the removal of the excised oligonucleotide (Yu *et al.*, 2004), indicating that the complex predominantly facilitates oligonucleotide excision.

It has been shown that the ATPase motors of the SWI/SNF family complexes can generate superhelical torsion and often do so by a DNA translocase activity (Havas *et al.*, 2000; Saha *et al.*, 2002; Durr *et al.*, 2005). I tested whether the Rad7/Rad16/ABF1 complex possessed DNA translocase activity, to determine how superhelical torsion is generated by this complex of proteins. By using a triple-helix strand displacement assay, the purified GG-NER complex and the SV-40 large antigen, a known DNA translocase, the DNA translocase activity was examined. My observations show that the Rad7/Rad16/ABF1 complex releases the radio-labeled third strand from a triple-helix in a similar fashion to the SV-40 large antigen. When SγATP, which is a homologue of ATP and cannot be hydrolysed, replaces ATP, the GG-NER complex lost its translocase activity. Therefore, I demonstrate that the Rad7/Rad16/ABF1

complex exhibits the ATP-dependent DNA translocase activity.

7.2 UV-dependent ubiquitination and degradation of Rad4 requires the Rad7 E3 ligase complex

Firstly, the stability of native Rad4 protein under normal conditions has been examined in a wild type strain and a *Δrad23* strain by using an antibody specific to endogenously expressed Rad4 protein. It has been suggested that Rad23 stabilizes overexpressed epitope-tagged Rad4 by preventing its proteolysis, and therefore Rad4 is rapidly degraded when Rad23 is absent (Lommel *et al.*, 2002; Ortolan *et al.*, 2004). It was suggested that the primary function of Rad23 is to stabilize Rad4 protein. However, in my study I showed that the steady state level of endogenous Rad4 protein remains stable over a 3-hour period following incubation of cells with the protein synthesis inhibitor cycloheximide in both WT and *Δrad23* strains. Moreover, in a pulse-chase experiment, a more accurate method for measuring the half life of proteins, the half-life of Rad4 has been found to be between 3 and 4 hours both in WT and *Δrad23* strains, consistent with the observations made in the cycloheximide experiment. The steady state level of a protein is the result of a combination of the production and turnover of the protein. By the northern blotting analysis, I showed that the lower mRNA level of *RAD4* gene in the *Δrad23* strain compared with the WT strain is the primary cause of the low Rad4 protein level in *Δrad23* cells.

It has been reported that tagged Rad4/XPC protein is further stabilized following the exposure of cells to UV light (Lommel *et al.*, 2002; Ng *et al.*, 2003). It was suggested that the proteolytic degradation of Rad4 is somehow attenuated after UV and this results in accumulation of XPC/Rad4 and enhanced NER. However, these studies were carried out using an over-expressed, epitope-tagged version of

Rad4/XPC. I examined whether the same phenomenon occurred following UV treatment of yeast cells expressing native Rad4. My observations showed that the endogenous Rad4 protein is rapidly degraded following exposure to UV light, though native Rad4 in the absence of DNA damage is stable with a half-life of over 3 hours. In a strain carrying mutations in two subunits of the 20S proteasome (*pre1-1, pre4-1*), the steady state level of endogenous Rad4 protein does not alter following UV radiation, so I conclude that UV-dependent degradation of Rad4 is mediated by the proteolytic activity of the 26S proteasome.

A recent report suggests that, in addition to the fundamental core NER function, the Rad7/Rad16 complex in concert with Elc1 may act as an ubiquitin E3 ligase which controls an activity outside the core GG-NER function of Rad7/Rad16 (Ramsey *et al.*, 2004). Our data confirmed the notion that Rad7, Rad16 and Elc1 are components of an E3 ligase and I showed that Cul3 is a newly identified component of the Rad7 E3 ligase. Since cullin-based E3 ubiquitin ligases include a specific component that acts as a substrate-specific adaptor, the putative interaction between Rad7 and Rad4 through the leucine-rich repeat (LRR) motif in Rad7 protein, raises the possibility that Rad4 is a target of the newly identified Rad7 E3 ligase (Wang *et al.*, 1997; Pintard *et al.*, 2004). By careful analysis of amino acid sequence, Rad7 was identified as a SOCS box-containing protein (Ho *et al.*, 2002). Therefore, the Rad7 E3 ligase complex consists of Rad7, Rad16, Elc1 and Cul3, and this complex is a novel member of the Elongin-Cullin-Socs-box (ECS) type ubiquitin ligase, a subclass of the Skp1-Cullin-F-box (SCF) type family of ubiquitin ligases. I showed that all four components of the newly identified Rad7 ECS ligase are required for the UV-dependent degradation of Rad4 protein and the physical interaction among the four components of the Rad7 ECS ligase complex was identified using

immunoprecipitation with anti-Rad7 antibody and Western blotting. In this instance all of the Rad16 protein and a fraction of total Elc1 and Cul3 co-precipitates with Rad7 protein in the WT extracts. None of these proteins immunoprecipitate in the *Δrad7* extracts. Collectively, the UV-dependent degradation of Rad4 protein requires the newly identified Rad7 ECS ubiquitin ligase, which includes Rad7, Rad16, Elc1 and Cul3.

By introducing three point mutations into the conserved SOCS-box domain of Rad7, I predicted that the activity of Rad7 containing E3 ligase complex would be dramatically reduced. I observed that in the psocs strain that expresses the SOCS box-mutated Rad7 protein, the UV-dependent degradation of Rad4 protein does not occur, indicating the crucial role of the Rad7 SOCS box domain in the degradation of Rad4 protein following UV treatment.

To determine whether the Rad4 protein is ubiquitinated by the newly identified Rad7 ECS ligase complex, a plasmid that expresses Myc-tagged ubiquitin protein was transferred into psocs and pRad7 strains respectively (Hochstrasser *et al.*, 1991). For each strain, extracts from untreated cells and UV irradiated cells with 0 or 1 hour repair times were analyzed by immunoprecipitation coupled with western blotting. Only in the pRad7 (WT) strain did the ubiquitination status of Rad4 change after one hour repair time following UV treatment. In contrast, no UV-dependent ubiquitination of Rad4 was seen in the psocs strain. In conclusion, *in vivo*, for the ubiquitination and degradation of Rad4 protein following UV radiation, all components of the Rad7 ECS ubiquitin ligase complex are required.

To confirm our *in vivo* findings, ubiquitination of Rad4 protein was investigated *in vitro*. Since *RAD4* is toxic to *E. coli* (Wei and Friedberg, 1998), Rad4 protein was expressed *in vitro* using a transcription/translation coupled system and identified by

Western blotting probed with anti-Rad4 antibody. Our previous observations confirmed that physical interaction exists among the four components of the Rad7 ECS ligase complex; all components were copurified through multiple chromatographic steps. With a previously reported method, the 6-His tagged Rad7 protein has been purified and enriched approximately 15,000-fold (Reed *et al.*, 1998). After several chromatographic steps, the newly identified components Cul3, Elc1 and Rad16 are all detected in the same mono-Q fractions. Using the peak mono-Q fraction, *in vitro* expressed Rad4 was ubiquitinated under the reaction conditions described, while the ubiquitination reaction was inhibited with an additional antibody specific to Rad7. Furthermore, a fraction lacking Elc1 also lost the capacity to support the ubiquitination of Rad4 protein. Hence, these observations confirmed that the ubiquitin ligase function was directly related to the Rad7 E3 ligase complex.

7.3 Distinct functions of the ubiquitin-proteasome pathway influence nucleotide excision repair

To investigate the physiological function of the UV-dependent ubiquitination and degradation of Rad4 protein, the cellular UV survival has been determined in a variety of mutants. Within this series of mutants, the psocs strain exhibits near normal levels of UV survival, similar to the pRad7 (WT) strain. This suggests that altering the stability of Rad4 protein in response to UV does not affect UV survival. Moreover, my observations demonstrate that the SOCS box-mutated Rad7 protein possesses normal core NER function, but loses the function of the E3 ubiquitin ligase. In the absence of Rad23 protein, the activity of the Rad7 ECS ubiquitin ligase is uncovered and plays a role in cellular UV survival. In the *RAD23* deletion background, an additional mutation to the SOCS box domain of Rad7 protein cause a further decrease in UV survival, despite the fact that the steady level of Rad4 protein is increased in

psocs/*Δrad23* strain, and is higher than that in the *Δrad23* strain. Hence, it can be deduced that the UV-dependent degradation of Rad4 does not correlate with UV survival but the UV-dependent ubiquitination of Rad4 does.

To detect whether the Rad7 E3 ligase complex also functioned in the same pathway as the 19S RC, a mutation of 19S RC (*sug2-1*) was added to the *Δrad23*/psocs strain. It is known that the defective NER and UV survival caused by the loss of Ubl domain of Rad23 can be rescued by additional mutations in specific 19S RC subcomponents, including the *sug2-1* mutant (Gillette *et al.*, 2001). My data showed that the UV sensitivity of *sug2-1*/*Δrad23*/psocs strain is intermediate between the *sug2-1*/*Δrad23* strain and the *Δrad23*/psocs strain. The partially rescued UV survival of the *Δrad23*/ *sug2*-1/psocs strain indicates that the Rad7 E3 ubiquitin ligase complex regulates NER in a pathway different from that of the Rad23/19S RC activity described previously.

To test whether the ubiquitination of Rad4 plays a role in inducible NER, an end-labeling strategy developed by our group was employed to examine lesion removal at the nucleotide level in a selected region of the gene, namely part of the *MFA2* gene (Teng *et al.*, 1997). My results showed that inducible NER is decreased in the psocs strain compared with the WT strain. Since *de novo* protein synthesis is involved in inducible NER, I speculate that the function of the Rad7 E3 ubiquitin ligase complex and the ubiquitination Rad4 may regulate the inducible NER pathway.

It has been accepted widely that the combined action of the UPP and NER results in efficient DNA repair and UV survival (Bertolaet *et al.*, 2001b; Gillette *et al.*, 2001; Lommel *et al.*, 2002; Ng *et al.*, 2002; Ramsey *et al.*, 2004; Russell *et al.*, 1999; Schauber *et al.*, 1998; Sweder and Madura, 2002). When Rad4/XPC is over expressed and epitope-tagged, Rad23 was thought to regulate NER by stabilizing short-lived

Rad4/XPC. Furthermore, it was suggested that UV-induced damage can result in the further stabilization of Rad4/XPC, causing the accumulation of it, and subsequent enhanced NER (Lommel *et al.*, 2002; Ng *et al.*, 2003). This model result in a number of following specific predictions:

(1) Rad23 is primarily responsible for stabilizing Rad4/XPC in cells.

(2) Stably expressing Rad4 in *Δrad23* cells should rescue the UV phenotype of *Δrad23* cells.

It is now clear that this is not the case (Xie, *et al.*, 2004; Ortolan *et al.*, 2004). In contrast, in cells which normally express native Rad4 protein, the regulatory function of Rad23 does not relate to stabilization of Rad4 protein since it is inherently stable, with a half life of around 4 hours. Partially based on my data a new model was introduced in this chapter; NER pathway I is regulated by the Rad23 mediated nonproteolytic activity of the 19S RC while NER pathway II relies on both the activity of the Rad7 E3 ubiquitin ligase complex and *de novo* protein synthesis. Furthermore, NER is predominantly controlled by pathway I, so losing the activity of the Rad7 ECS ligase does not dramatically affect the rate of lesion removal and cellular UV survival.

7.4 The occupancy of Rad23 in the promoter region of *DDR2*

In the absence of Rad23, the mRNA level of a DNA damage response gene, *DDR2*, elevated as revealed by the Northern blotting. Furthermore, the occupancy of Rad23 in the promoter region of *DDR2*, around the two STRE elements, was confirmed by the ChIP-qPCR assay. In chapter 4, I showed a lower mRNA level of *RAD4* in *Δrad23* cells compared with WT cells. Although the half life of mRNA decreasing also results in a reduced steady state level of mRNA, my data in both of chapter 4 and 6 strongly suggest Rad23 directly affects the transcription of *DDR2*.

To reveal the relationship between the Rad7 E3 ligase complex and *de novo* protein synthesis, Rad23's occupancy in the promoter region of *DDR2* was measured in several strains. Interestingly, Rad23's occupancy is significantly decreased in the absence of Elc1 in the promoter region of the *DDR2* gene. Furthermore, the occupancy of Rad23 significantly decreased in SOCS box mutant cells in the promoter region of *DDR2* compared with pRAD7 cells, suggesting the Rad7 E3 ligase affects *do novo* protein synthesis possibly by altering Rad23's occupancy in the regulatory regions of a small cluster of genes.

7.5 Further experiments

My studies have stimulated several important new research topics that will be explored during future studies.

One important question to answer, in my view, is focused on the functional difference between Rad4 protein and ubiquitinated Rad4 protein. In humans, the ubiquitination of XPC (human homologue of Rad4) by the UV-DDB complex results in alteration of XPC's DNA binding properties. It has been suggested that ubiquitination of DDB following UV eliminates its capacity to bind to DNA containing 6-4PP damage. In contrast, ubiquitinated XPC acquired a stimulated damaged DNA binding capacity without changing its binding specificity (Sugasawa *et al.*, 2005). In yeast Rad4 plays an essential role in both TC-NER and GG-NER of RNA pol II transcribed genes, while in human cells XPC is a dispensable element for TC-NER. So, the precise significance of the functional alteration of ubiquitinated Rad4 protein and how this relates to ubiquitination of XPC in human cells remain unclear. Based on a previous report, the ubiquitination of Rad4 protein likely plays a role in a UV response that requires *de novo* protein synthesis, since pathway II relies on both the ubiquitination of Rad4 protein, and *de novo* protein synthesis (Gillette *et*

al., 2006). Further investigation into the biological properties of Rad4 protein and the ubiquitinated Rad4 protein will likely enhance our understanding of how Rad4 functions during NER.

How the UPP/19S RC applies its negative influence on NER or the rate of lesion remove is not clear at present. It has been suggested that the UPP may regulate NER by turning over the NER components like Rad4, while Rad23 prevents Rad4 degradation. However, the stable existence of Rad4 protein in *Δrad23* strain has been confirmed directly in our studies, indicating that the negative regulation of the UPP operates through a nonproteolytic way. Although the Rad23 mediated 19S RC regulation is required for optimal NER, in the absence of Rad23 a negative influence of the UPP/19S RC on NER still exists. So in the *RAD23* deletion background additional mutations to 19S RC, like *sug2-1*, can partly rescue the defected NER. Hence, in the absence of Rad23 protein, whether a physical interaction between the NER components and the 19S RC, or the UPP still exists may be examined by co-immunoprecipitation coupled with western blotting. It is possible that the 19S RC interacts with ubiquitinated NER proteins following UV radiation and thereby negatively regulates the NER processing. Hence, experiments should also be carried out following exposure of cells to UV light.

I demonstrated that Rad4 protein is not rapidly degraded in the absence of its binding partner Rad23. Moreover, a recent report suggested that the degradation of overexpressed HA-tagged Rad4 protein is slightly reduced in a *Δrad23* deleted strain compared with the WT strain (Ju and Xie, 2006). In *Δrad23* cells, the low steady state level of Rad4 protein results from the reduced mRNA level of *RAD4*. Therefore, whether Rad4/Rad23 complex directly plays a role in transcription or UV-induced transcription of NER genes including *RAD4* becomes an important issue. I have

performed microarray experiments and showed that the transcription level of a small subset of genes, most of them stress response genes, was different from the WT and the *Δrad23* mutant strains. The Rad23's occupancy in the regulatory regions of *DDR2*, one of these genes, is influenced by the Rad7 E3 ligase complex. Whether the ubiquitination of Rad4/the Rad7 E3 ligase is directly responsible for induced transcription of a cluster of genes is a current focus of our research. However, to answer whether the occupancy of Rad23 in the promoter region of *DDR2* influences its transcription, further investigation is required.

Appendix I

Growth media and solution

AI-1 Growth media

All media used in this thesis had been autoclaved for 20-30min at 15psi.

Yeast Complete (YC)

16g Glucose; 20ml YC Stock solution. Made up to 400ml with H_2O. YC slopes and plates were obtained by supplementing this medium with 8g Bacto-Agar [Difco Laboratories, USA].

Yeast Synthetic complete (drop our) (SC and SC-drop out)

4g Difco yeast nitrogen base; 12g Glucose; 0.5g SC mixture or SC-drop out mixture; 600 ml d-water. SC plates or SC-drop out plates were obtained by supplementing this medium with 10g Bacto-Agar [Difco Laboratories, USA].

The ingredient of amino acid for SC (SC-drop out) mixture

Ademine hemisulfate 2g; Arginine HCl 2g; Histidine HCl 2g; Isoleucine 2g; Leucine 2g; Lysine HCl 2g; Methionine 2g; Phenylalanine 3g; Serine 2g; Threonine 2g; Tryptophan 3g; Tyrosine 2g; Uracil 1.2g; Valine 9g. In this thesis, SC-drop out mixture obtained by without adding a certain ingredient or ingredients.

YC Stock solution

240g Mycological peptone; 400g Yeast extract; 40g Casein hydrolysate; 1g F-inositol; 200mg Nicotinic acid; 200mg Riboflavin; 200mg Calcium pantothenate; 200mg Aneurin hydrochloride; 100mg Para-amino benzoic acid; 16 mg Pyridoxine; 0.5mg Biotin; 100ml Chloroform. Made up to 5000ml with H_2O.

YPD medium

2g Yeast extract; 1g Bacto-Peptone and 4g Glucose. Made up to 200ml with H2O. YPD slopes and plates were obtained by added with 4g Bacto-Agar.

AI-2 Stock Solutions

0.5M EDTA (pH0.8)

EDTA • Na_2 • $2H_2O$	186.1g
H_2O	800ml

Stir vigorously on a magnetic stirrer. Adjust the pH to 8.0 with NaOH (~20g of NaOH pellets). Add H_2O to make 1 litre.

1M Tris

Tris base	121.1g

H_2O	800ml

Adjust the pH to the desired value by adding concentrated HCl. Add H_2O to make 1 litre.

pH	HCl
7.4	70ml
7.6	60ml
8.0	42ml

TE Buffer

Tris-HCl, pH7.5	10mM
EDTA, pH8.0	1mM

3M Sodium acetate (pH5.2)

Sodium acetate • $3H_2O$	408.1g
H_2O	800ml

Adjusted the pH to 5.2 with glacial acetic acid. Add H2O to make 1 litre.

5M NaCl

NaCl	292.2g
H_2O	up to 1 litre

10% SDS (Sodium dodecyl sulphate)

SDS (electrophoresis grade)	100g
H2O	900ml

Heat to 68°C to assist dissolution. Adjust the pH to 7.2 by adding a few drops of concentrated HCl. Make up the volume to 1 litre with H_2O.

20×SSC

NaCl (3 M)	175.3 g
Sodium citrate dihydrate (0.3 M)	88.2 g
H_2O	800 ml

Adjust the pH to 7.0 with HCl. Make up the volume to 1 litre with H_2O.

1M Phosphate solution

Na_2HPO_4	71 g
H_3PO_4 (85%)	4 ml
H_2O	up to 1000 ml.

Phosphate Buffered Saline (PBS)

NaCl	8 g
KCl	0.2 g
Na_2HPO_4	1.44 g
KH_2PO_4	0.24 g
H_2O	800 ml

Adjust the pH to 7.4 with 5 M NaOH. Add H_2O to 1 litre.

1 M DTT (Dithiothreitol)

DTT	3.09 g

Dissolved in 20 ml of 0.01 M sodium acetate (pH 5.2). Sterilise by filtration. Do not autoclave DTT or solutions containing DTT.

AI-3. Solutions for DNA and RNA extraction

SEC Buffer

Sorbitol	1.0 M
EDTA	100 mM
Citrate Phosphate buffer (pH 5.8)	10 mM

Sorbitol solution

Sorbitol	0.9 M
Tris·HCl (pH 8.0)	100 mM
EDTA	100 mM

DNA Lysis Buffer

Urea	4 M
NaCl	200 mM
Tris-HCl (pH 8.0)	100 mM
CDTA	10 mM
n-Lauroyl Sarcosine	0.5% (w/v)

RNA Lysis Buffer

Tris-HCl (pH 7.5)	10 mM
EDTA (pH 8.0)	10mM
SDS	0.5%

AI-4. Solutions for electrophoresis (DNA&RNA)

50× TAE

2 M Tris base	242 g
1 M Sodium Acetate·$3H_2O$	136 g
50 mM EDTA·Na_2·$2H_2O$	19 g

Adjust to pH7.2 with glacial acetic acid. Add H_2O to make 1 litre.

10× TBE

Tris base	108 g
Boric acid	55 g
$Na_2EDTA·2H_2O$	9.3 g

Add H_2O to 1 litre.

Denaturing running buffer

NaOH	36 mM
EDTA	1 mM.

Non denaturing loading buffer

Ficoll	10%
SDS	0.5%
Bromophenol Blue	0.06%

Made up in 1× TAE.

Denaturing loading buffer

NaOH	50 mM
EDTA	1 mM
Ficoll	2.5%
Bromocresol Green	0.025%

Sequencing gel-loading buffer

Deionized formamide	95%
EDTA (pH 8.0)	20 mM
Xylene cyanol FF	0.05%
Bromophenol blue	0.05%

Neutralising gel washing buffer

Tris-HCl (pH7.5)	1 M
NaCl	1.5 M

Fixative solution for sequencing gel

Methanol (15%)	600 ml
Acetic acid (5%)	200 ml

Add H_2O to make 4 litres.

AI-5. Solutions for Northern Blotting

10× FA gel buffer

3-[N-Morpholino]propanesulfonic acid (MOPS) (free acid)	200 mM
Sodium acetate	50 mM
EDTA	10 mM

Adjust pH to 7.0 with NaOH.

1× FA gel running buffer

10× FA gel buffer	100 ml
37% (12.3) Formaldehyde	20 ml
RNase-free water	880 ml

5× RNA loading buffer

Saturated aqueous bromophenol blue	16 µl
0.5 M EDTA, pH 8.0	80 µl
37% (12.3) formaldehyde	720 µl
formamide	3 ml
10× FA gel buffer	4 ml
Add RNase-free water to 10 ml	

10× MOPS buffer

Morpholinopropanesulphonic acid (0.4 M)	83.7 g
Sodium Acetate·H_2O (0.1 M)	13.6 g
EDTA·Na_2·$2H_2O$ (10 mM)	1.87 g

Adjust pH to 7.2 with NaOH. Add H_2O to make to 1 litre.

(Pre)hybridisation solution for RNA

Phosphate solution (1M)	5 ml
SDS (20%)	3.5 ml
BSA	0.25 mg
EDTA (0.5M, pH 8.0)	20 µl
H_2O	up to 10 ml.

Probe stripping solution

SSC (20x)	2.5 ml
SDS (10%)	50 ml
H_2O	up to 500 ml

AI-6. Solutions for protein purification and whole cell extraction preparation

Extraction Buffer A

Hepes pH7.3	40 mM
NaCl	350 mM (0-1000mM)
Tween 20	0.1% (v/v)
Glycerol	10% (v/v)
DTT	1mM (adding before use)

Hypotonic Buffer A

Tris-HCl, pH8.0	10 mM
EDTA	1 mM
DTT	5 mM (adding before use)

Sucrose solution

Tris-HCl, pH8.0	50 mM
$MgCl_2$	10 mM
Sucrose	25% (w/w)
Glycerol	50% (v/v)
DTT	2 mM (adding before use)

Yeast Dialysis Buffer

Hepes pH7.6	40 mM
$MgSO_4$	10 mM
EGTA	10 mM
Glycerol	20% (v/v)
DTT	5 mM (adding before use)

100× Protease Inhibitors in ethanol

Benzamidine	30 mg/ml
Pepstatin	100 μg/ml
Leupeptin	100 μg/ml
Chymostatin	100 μg/ml
Antipain	100 μg/ml
PMSF	100 mM

AI-7. Solutions for Western Blotting

5× SDS-PAGE Running Buffer

Tris-base	15.1g
Glycine	94 g (72g)
SDS (Electrophoresis grade)	5 g
dd-water	up to 1000ml

2× SDS-PAGE Loading Buffer

Tris-HCl pH6.8	100 mM
DTT	200 mM
SDS (Electrophoresis grade)	4%
Glycerol	20%
Bromophenol	0.2%

10× TBST Buffer

Tris-HCl pH7.6	200 mM
NaCl	1.37 M
Tween 20	1% (v/v)

SDS-PAGE resolution gel 8% (1 gel)

40% Acrylamide/Bis	1.5 ml
1.5M Tris-base pH8.8	1.8 ml
Temed	5 µl
10% SDS	75 µl
10% APS	38 µl
dd-water	4 ml

SDS-PAGE Stacking gel (1 gel)

40% Acrylamide/Bis	0.5 ml
1.5M Tris-base pH6.8	0.65 ml
Temed	10 µl
10% SDS	50 µl
10% APS	50 µl
dd-water	3.2 ml

Western Transfer Buffer

Tris-base	12.12 g
Glycine	45.2 g
Methanol	800 ml
d-Water	up to 4L

AI-8. Solutions for NER *in vitro.*

NER Buffer

Hepes-KOH pH7.8	45 mM
$MgCl_2$	7.4 mM
DTT	0.9 mM
EDTA	0.4 mM
Phosphocreatine	40 mM
Glycerol	4%
BSA	100 µg/ml
REG 8000	5%

5×dNTP mixture for dC*TP

dCTP	20 µM
dATP	200 µM
dTTP	200 µM
dGTP	200 µM

AI-9. Solutions for the chromatin immunoprecipitation.

ChIP lysis buffer

50mM	Hepes-KOH, pH7.5
140mM	NaCl
1mM	EDTA
1%	Triton X-100
0.1%	Sodium deoxycholate

LiCl solution

10mM	Tris-HCl
250mM	LiCl
1mM	EDTA
0.5%	Igapel CA-630
0.5%	Sodium dèoxycholate

Elution buffer

1%	SDS
0.1M	$NaHCO_3$

Proteinase K buffer

10mM	Tris-HCl
5mM	EDTA
0.5%	SDS

Cell survival as a function of UV dose

AII. 1 Data of Figure 5.1 and 5.2A. (All strains were generated from SC507)

pRAD7 (WT)								
UV Dose	Exp-1	Percent (%)	Exp-2	Percent (%)	Exp-3	Percent (%)	Avg. (percent)	Standard deviation
0	172.3	100.0000	193.3	100.0000	212	100.0000	100.0	0
2.5	157	91.1201	186.3	96.3787	198	93.3962	93.6	2.63
5	127.6	74.0569	142	73.4609	153.3	72.3113	73.3	0.887
10	68	39.4660	84.6	43.7662	87.6	41.3208	41.5	2.157
20	15	8.7057	15.3	7.9152	19.3	9.1038	8.57	0.605

Δrad7								
UV Dose	Exp-1	Percent (%)	Exp-2	Percent (%)	Exp-3	Percent (%)	Avg. (percent)	Standard deviation
0	108	100.0000	117	100.0000	112	100.0000	100.0	0
2.5	75	69.4444	77.6	66.3248	79	70.5357	68.7683	2.19
5	10.8	10.0000	9.6	8.2051	9.3	8.3036	8.8362	1.01
10	0.133	0.1231	0.096	0.0821	0.23	0.2054	0.1369	0.0628
20	0.003	0.0028	0.0053	0.0045	0.0016	0.0014	0.0029	0.00156

psocs								
UV Dose	Exp-1	Percent (%)	Exp-2	Percent (%)	Exp-3	Percent (%)	Avg. (percent)	Standard deviation
0	167	100.0000	195.3	100.0000	203.3	100.0000	100.0	0
2.5	130	77.8443	149.6	76.6001	151	74.2745	76.2	1.81
5	106	63.4731	123.3	63.1336	119.3	58.6818	61.8	2.67
10	56.6	33.8922	71	36.3543	75	36.8913	35.7	1.60
20	13.7	8.2036	16.3	8.3461	19.6	9.6409	8.73	0.79

pRAD7/*Δrad23*								
UV Dose	Exp-1	Percent (%)	Exp-2	Percent (%)	Exp-3	Percent (%)	Avg. (percent)	Standard deviation
0	53	100.0000	96	100.0000	104.6	100.0000	100.0000	0
2.5	48	90.5660	88.3	91.9792	87	83.1740	88.5731	4.73
5	17.3	32.6415	29.6	30.8333	34.6	33.0784	32.1844	1.19
10	1.8	3.3962	4	4.1667	4.63	4.4264	3.9964	0.536
20	0.026	0.0491	0.036	0.0375	0.066	0.0631	0.0499	0.0128

psocs/*Δrad23*								
UV Dose	Exp-1	Percent (%)	Exp-2	Percent (%)	Exp-3	Percent (%)	Avg. (percent)	Standard deviation
0	43.3	100.0000	110.6	100.0000	113	100.0000	100.0000	0
2.5	28.3	65.3580	70.3	63.5624	68	60.1770	63.0324	2.63
5	2.89	6.6744	8.6	7.7758	9.3	8.2301	7.5601	0.800
10	0.433	1.0000	3.6	3.2550	2	1.7699	2.0083	1.146
20	0.001	0.0023	0.004	0.0036	0.0033	0.00292	0.0029	0.000654

Data of Figure 5.3. (All strains were generated form SC507)
Cellular UV survial of pRAD7, psocs, pRAD7/*Δrad23*, psocs/*Δrad23* used in Figure 5.3 was shown above.

sug2-1/Δ*rad23*/pRAD7								
UV Dose	Exp-1	Percent (%)	Exp-2	Percent (%)	Exp-3	Percent (%)	Avg. (percent)	Standard deviation
0	196.3	100.0000	212.3	100.0000	191.6	100.0000	100.0000	0
2.5	142	72.3383	153	72.0678	141.3	73.7474	72.7178	0.901824
5	83.3	42.4350	89	41.9218	81	42.2756	42.2108	0.262678
10	36.33	18.5074	40.6	19.1239	31.3	16.3361	17.9891	1.46436
20	1.33	0.6775	2.03	0.9562	1.43	0.7463	0.7934	0.145156

sug2-1/Δ*rad23*/psocs								
UV Dose	Exp-1	Percent (%)	Exp-2	Percent (%)	Exp-3	Percent (%)	Avg. (percent)	Standard deviation
0	160.6	100.0000	154.3	100.0000	167	100.0000	100.0000	0
2.5	100.6	62.6401	94.6	61.3091	101.3	60.6587	61.5360	1.010
5	49	30.5106	43	27.8678	53.6	32.0958	30.1581	2.136
10	4.66	2.9016	3.3	2.1387	7	4.1916	3.0773	1.0377
20	0.051	0.0318	0.083	0.0538	0.096	0.0575	0.0477	0.0139

Appendix III. Data form experiments for CPD removal in the *MAF2* at nucleotide level
[Data for Figure 5.4 A, B, &C]

psocs-TS Exp-1

CPD Position	Repair time					Adjusted signal remaining					$T_{50\%}$
						Repair time					
	0	0.5	1	2	3	0	0.5	1	2	3	
Top	1101157	1114781	1115050	1193882	1055496						
-105	10105.33	7271.595	4223.377	1872.245	1394.634	1.00	0.74	0.46	0.20	0.17	**0.9**
-120	9661.596	8039.472	5039.037	3276.303	1938.057	1.00	0.86	0.57	0.36	0.24	**1.25**
-161	29938.59	18453.77	8289.756	1933.258	1540.333	1.00	0.64	0.30	0.07	0.06	**0.71**
-166	11529.67	6951.499	3356.886	2526.646	1432.562	1.00	0.62	0.32	0.23	0.15	**0.67**
-180	36097.42	21779.75	9718.855	1955.947	2816.15	1.00	0.62	0.30	0.06	0.09	**0.67**
-194	7533.972	5169.67	2764.74	735.458	1019.225	1.00	0.71	0.40	0.10	0.16	**0.8**
-200	14898.19	10663.19	5563.197	1808.18	924.533	1.00	0.74	0.41	0.13	0.07	**0.85**
-207	9959.96	7190.262	3548.669	2693.848	840.602	1.00	0.75	0.39	0.29	0.10	**0.85**
-221	5793.07	4398.517	2584.273	2070.722	1449.132	1.00	0.79	0.49	0.38	0.30	**0.95**
-234	8673.129	6147.15	2599.774	1827.995	1247.929	1.00	0.73	0.33	0.22	0.17	**0.75**
-258	22272.9	21956.66	8924.563	4705.444	2030.929	1.00	1.02	0.44	0.22	0.11	**0.94**
-282	7879.622	6775.694	3223.344	2552.524	1732.167	1.00	0.89	0.45	0.34	0.26	**1.02**
-294	6440.052	5581.292	2745.236	1530.646	1212.695	1.00	0.90	0.47	0.25	0.23	**0.95**
-317	2474.635	1783.52	1047.995	692.497	465.85	1.00	0.75	0.46	0.30	0.23	**0.9**
-321	2533.574	1154.203	600.103	341.315	229.288	1.00	0.53	0.29	0.16	0.12	**0.68**
-341	5566.81	3116.483	2154.664	2462.331	2056.021	1.00	0.58	0.42	0.47	0.44	**0.62**
-347	3874.185	1547.185	1376.89	1616.224	1408.228	1.00	0.41	0.39	0.44	0.44	**0.4**
Sum	1296389	1268750	1215679	1279160	1126709						
Ratio	1.00	0.98	0.94	0.99	0.87						

psocs-TS Exp-2

CPD Position	Repair time					Adjusted signal remaining (Repair time)					$T_{50\%}$
	0	0.5	1	2	3	0	0.5	1	2	3	
Top	278236.3	244629.9	247904.3	339683.2	240429.6						
-105	3974.34	2514.248	1389.47	1033.178	572.957	1.00	0.77	0.45	0.25	0.20	**0.98**
-120	3347.618	2366.169	1431.387	1042.216	683.958	1.00	0.86	0.55	0.30	0.28	**1.20**
-161	10553.47	5656.167	2933.597	1697.547	986.473	1.00	0.65	0.36	0.16	0.13	**0.77**
-166	3635.305	2011.508	965.288	666.669	422.297	1.00	0.67	0.34	0.18	0.16	**0.78**
-180	13698.67	7538.812	3562.724	2087.357	1188.574	1.00	0.67	0.33	0.15	0.12	**0.77**
-194	2383.355	1938.341	971.994	1054.828	442.999	1.00	0.98	0.52	0.43	0.26	**1.05**
-200	4352.316	2729.114	1632.287	1006.174	469.923	1.00	0.76	0.48	0.22	0.15	**1.00**
-207	4133.779	2724.89	1478.211	1020.304	668.719	1.00	0.80	0.46	0.24	0.22	**0.93**
-221	1934.725	1487.574	720.194	741.851	556.173	1.00	0.93	0.48	0.37	0.40	**1.05**
-234	2981.854	2002.002	1028.61	759.606	424.917	1.00	0.81	0.44	0.25	0.20	**1.00**
-258	8023.952	5325.832	3285.33	2444.853	1382.035	1.00	0.80	0.52	0.30	0.24	**1.15**
-282	2105.36	1389.284	754.931	781.06	501.966	1.00	0.80	0.46	0.36	0.33	**0.95**
-294	2074.74	1222.967	722.159	817.801	558.811	1.00	0.71	0.45	0.38	0.37	**0.85**
-317	1321.739	791.183	425.988	313.549	171.127	1.00	0.72	0.41	0.23	0.18	**0.90**
-321	1216.274	716.988	414.091	296.488	138.316	1.00	0.71	0.44	0.24	0.16	**0.82**
-341	1358.285	624.265	343.846	327.215	269.983	1.00	0.56	0.32	0.23	0.28	**0.56**
-347	854.998	323.948	155.588	54.563	27.615	1.00	0.46	0.23	0.06	0.04	**0.45**
Sum	346187.1	285993.2	270120	355828.4	249896.4						
Ratio	1.00	0.83	0.78	1.03	0.72						

Induced psocs-TS Exp-1

CPD Position	Repair time					Adjusted signal remaining					$T_{50\%}$
						Repair time					
	0	0.5	1	2	3	0	0.5	1	2	3	
Top	443270.9	426164.2	556938.8	638687.4	484796.5						
-105	5182.295	2793.106	2298.731	1450.989	1081.061	1.00	0.61	0.40	0.23	0.22	**0.75**
-120	5047.1	3526.501	2717.53	1692.734	1082.188	1.00	0.79	0.49	0.27	0.23	**0.98**
-161	13055.33	6373.508	3821.866	1602.802	894.695	1.00	0.55	0.27	0.10	0.07	**0.57**
-166	5404.195	2394.389	1544.47	1111.076	727.644	1.00	0.50	0.26	0.17	0.14	**0.55**
-180	17798.94	7791.37	4468.098	2063.448	1195.122	1.00	0.49	0.23	0.09	0.07	**0.50**
-194	3068.81	1884.945	1373.406	887.067	661.477	1.00	0.69	0.41	0.23	0.23	**0.79**
-200	6235.813	3915.019	2472.121	1182.483	343.854	1.00	0.71	0.36	0.15	0.06	**0.75**
-207	5198.777	2886.706	1735.763	1013.669	827.542	1.00	0.63	0.30	0.16	0.17	**0.72**
-221	2649.361	1816.933	1363.289	1109.536	754.663	1.00	0.77	0.47	0.34	0.31	**0.90**
-234	3953.132	2139.307	1270.626	859.336	563.685	1.00	0.61	0.29	0.18	0.15	**0.65**
-258	9886.987	6176.346	4555.511	2617.126	965.903	1.00	0.70	0.42	0.21	0.11	**0.90**
-282	3180.1	1837.519	1436.359	1471.796	1124.972	1.00	0.65	0.41	0.38	0.38	**0.75**
-294	3162.741	1609.821	1285.812	947.139	713.961	1.00	0.57	0.37	0.24	0.24	**0.63**
-317	1632.945	871.165	532.68	392.443	244.384	1.00	0.60	0.30	0.20	0.16	**0.63**
-321	1694.719	895.489	687.982	689.171	497.627	1.00	0.60	0.37	0.33	0.32	**0.65**
-341	2758.317	1068.395	1029.585	829.662	597.795	1.00	0.44	0.34	0.24	0.23	**0.45**
-347	1726.856	727.706	660.661	444.176	457.893	1.00	0.47	0.35	0.21	0.29	**0.75**
Sum	534907.3	474872.4	590193.2	659052.1	497530.9						
Ratio	1.00	0.89	1.10	1.23	0.93						

Induced psocs-TS Exp-2

CPD Position	Repair time					Adjusted signal remaining					$T_{50\%}$
						Repair time					
	0	0.5	1	2	3	0	0.5	1	2	3	
Top	164862.4	199420.5	227377.3	184329.3	203883.6						
-105	2152.097	1466.21	867.125	430.281	441.077	1.00	0.62	0.34	0.22	0.20	**0.78**
-120	1967.165	1513.758	911.526	468.884	474.085	1.00	0.70	0.39	0.26	0.24	**0.88**
-161	5785.144	3396.288	1793.508	784.869	817.045	1.00	0.54	0.26	0.15	0.14	**0.65**
-166	2161.677	1194.628	646.637	279.316	292.194	1.00	0.50	0.25	0.14	0.13	**0.62**
-180	8097.193	4441.173	2194.533	881.424	794.067	1.00	0.50	0.23	0.12	0.10	**0.5**
-194	1687.142	1256.876	820.243	391.711	323.903	1.00	0.68	0.41	0.25	0.19	**0.9**
-200	2781.464	1940.325	1090.786	434.127	377.976	1.00	0.64	0.33	0.17	0.13	**0.75**
-207	2738.707	1698.183	1063.636	469.355	491.613	1.00	0.57	0.33	0.18	0.18	**0.7**
-221	1413.532	962.568	553.117	355.624	279.072	1.00	0.62	0.33	0.27	0.19	**0.8**
-234	1965.441	1394.689	735.673	243.536	249.521	1.00	0.65	0.32	0.13	0.12	**0.75**
-258	5186.357	4181.304	2684.975	1057.166	864.324	1.00	0.74	0.44	0.22	0.16	**0.95**
-282	1385.347	916.748	478.13	337.812	425.743	1.00	0.60	0.29	0.26	0.30	**0.72**
-294	1332.348	788.026	528.907	422.716	412.622	1.00	0.54	0.34	0.34	0.30	**0.65**
-317	771.503	477.461	268.659	120.073	126.578	1.00	0.56	0.30	0.17	0.16	**0.7**
-321	720.647	421.435	280.084	203.414	175.569	1.00	0.53	0.33	0.30	0.24	**0.62**
-341	766.84	303.367	228.395	125.8	212.455	1.00	0.36	0.25	0.18	0.27	**0.36**
-347	380.837	145.434	71.088	34.544	113.165	1.00	0.35	0.16	0.10	0.29	**0.35**
Sum	206155.8	225919	242594.3	191370	210754.6						
Ratio	1.00	1.10	1.18	0.93	1.02						

psocs-NTS Exp-1

CPD Position	Repair time					Adjusted signal remaining					$T_{50\%}$
						Repair time					
	0	0.5	1	2	3	0	0.5	1	2	3	
Top	701017.2	678075.7	697808.1	861433.6	769784.1						
-333	4758.027	4047.745	3305.561	2620.668	1846.826	1.00	0.89	0.72	0.47	0.38	**1.85**
-298	17570.98	15710.26	12796.78	10966.45	7106.299	1.00	0.93	0.75	0.54	0.39	**2.20**
-264	5943.571	5062.326	2946.4	1792.243	1121.15	1.00	0.89	0.51	0.26	0.18	**1.05**
-243	12811.56	12475.48	10006.96	8751.494	6092.559	1.00	1.02	0.81	0.59	0.46	**2.60**
-239	10055.45	7796.106	5007.737	3089.077	1560.221	1.00	0.81	0.52	0.26	0.15	**1.05**
-226	1889.448	1950.771	1518.255	1198.393	770.867	1.00	1.08	0.83	0.54	0.40	**2.40**
-140	4146.409	3432.04	3017.804	2167.691	1719.641	1.00	0.86	0.75	0.45	0.40	**1.95**
-127	8694.78	6501.191	4396.054	2284.031	1437.616	1.00	0.78	0.52	0.23	0.16	**1.05**
Sum	766887.4	735051.6	740803.7	894303.7	791439.3						
Ratio	1.00	0.96	0.97	1.17	1.03						

psocs-NTS Exp-2

CPD Position	Repair time					Adjusted signal remaining (Repair time)					$T_{50\%}$
	0	0.5	1	2	3	0	0.5	1	2	3	
Top	385400.1	355916.2	332883.5	462463.1	484970.3						
-333	3984.828	3642.487	2533.359	2718.539	2570.434	1.00	1.00	0.77	0.61	0.56	**3.00**
-298	15762.86	13395.94	10227.97	10228.36	8517.006	1.00	0.93	0.78	0.58	0.47	**2.65**
-264	6344.558	5688.87	4015.669	3613.161	2337.27	1.00	0.98	0.76	0.51	0.32	**2.10**
-243	12689.86	10896.91	8448.537	9500.422	8361.648	1.00	0.94	0.80	0.67	0.57	**3.00**
-239	8849.111	7087.234	4604.432	3909.347	2888.897	1.00	0.88	0.63	0.40	0.28	**1.55**
-226	2791.924	2342.785	1516.348	1386.786	926.435	1.00	0.92	0.66	0.44	0.29	**1.75**
-140	3987.992	3337.955	2429.436	2481.002	1611.634	1.00	0.92	0.74	0.56	0.35	**2.20**
-127	6673.049	5303.778	3349.73	2430.543	1619.879	1.00	0.87	0.61	0.33	0.21	**1.89**
Sum	446484.3	407612.1	370009	498731.3	513803.5						
Ratio	1.00	0.91	0.83	1.12	1.15						

Induced psocs-NTS Exp-1

CPD Position	Repair time					Adjusted signal remaining					$T_{50\%}$
						Repair time					
	0	0.5	1	2	3	0	0.5	1	2	3	
Top	252753.6	252712	341614.4	439452.7	360270.9						
-333	2119.877	1913.928	2145.498	2179.1	1548.174	1.00	0.92	0.78	0.64	0.56	**3.00**
-298	9133.77	7742.413	8621.717	7387.878	4522.212	1.00	0.87	0.73	0.50	0.38	**2.05**
-264	3118.928	2568.178	2513.301	1608.656	864.694	1.00	0.84	0.62	0.32	0.21	**1.40**
-243	7155.933	6043.313	7184.758	6167.537	3709.39	1.00	0.86	0.78	0.53	0.40	**2.20**
-239	5079.146	4058.078	4171.747	2375.09	1472.602	1.00	0.82	0.63	0.29	0.22	**1.30**
-226	1539.27	1072.825	1311.001	771.962	469.198	1.00	0.71	0.66	0.31	0.23	**1.30**
-140	2893.329	2071.571	2005.36	1639.855	1589.622	1.00	0.73	0.54	0.35	0.42	**1.10**
-127	3544.167	2942.448	2356.19	1539.749	1008.073	1.00	0.85	0.51	0.27	0.22	**1.25**
Sum	287338.1	281124.7	371923.9	463122.5	375454.9						
Ratio	1	0.98	1.29	1.61	1.31						

Induced psocs-NTS Exp-2

CPD Position	Repair time					Adjusted signal remaining					$T_{50\%}$
						Repair time					
	0	0.5	1	2	3	0	0.5	1	2	3	
Top	227163	242203.4	265302.7	234806.7	253178						
-333	2904.418	2690.395	2137.976	1344.162	1359.586	1.00	0.89	0.67	0.49	0.47	**2.00**
-298	10555.74	9490.675	7873.694	4349.139	3555.804	1.00	0.86	0.68	0.44	0.34	**1.85**
-264	4533.574	3914.135	3383.098	1825.407	1378.327	1.00	0.83	0.68	0.43	0.30	**1.65**
-243	8423.835	8276.5	7652.622	4791.684	3765.698	1.00	0.94	0.82	0.60	0.45	**2.65**
-239	5227.033	4850.027	3447.652	2074.255	1428.206	1.00	0.89	0.60	0.42	0.27	**1.50**
-226	1735.008	1927.728	1402.177	999.905	679.01	1.00	1.06	0.73	0.61	0.39	**2.40**
-140	2926.99	2562.43	1869.347	1460.27	1195.961	1.00	0.84	0.58	0.53	0.41	**2.12**
-127	4142.043	3611.179	2404.678	1010.674	702.156	1.00	0.83	0.53	0.26	0.17	**1.15**
Sum	267611.6	279526.5	295473.9	252662.2	267242.7						
Ratio	1.00	1.04	1.10	0.94	1.00						

pRAD7-TS Exp-1

CPD Position	Repair time					Adjusted signal remaining					$T_{50\%}$
						Repair time					
	0	0.5	1	2	3	0	0.5	1	2	3	
Top	694040.6	607213.2	680680.5	890908.7	1061732						
-105	12180.94	7850.516	6092.825	2827.986	2629.597	1.00	0.79	0.59	0.22	0.18	**1.15**
-120	10300.2	6636.561	4532.572	2848.524	2862.768	1.00	0.79	0.52	0.27	0.23	**1.12**
-161	30114.56	16530.98	10460.28	5084.371	4079.934	1.00	0.68	0.41	0.16	0.11	**0.85**
-166	11013.68	5422.011	2710.667	1833.996	1895.567	1.00	0.61	0.29	0.16	0.14	**0.70**
-180	38540.18	21529.05	10743.24	5301.828	4224.422	1.00	0.69	0.33	0.13	0.09	**0.77**
-194	6943.933	4306.915	3139.085	2130.905	2146.782	1.00	0.76	0.54	0.29	0.25	**1.13**
-200	12296.19	7675.202	4308.068	2356.537	1470.302	1.00	0.77	0.42	0.18	0.10	**0.92**
-207	13831.62	7488.646	3847.291	2493.794	2337.058	1.00	0.67	0.33	0.17	0.14	**0.77**
-221	6244.849	3765.379	2429.304	1854.367	1947.93	1.00	0.74	0.46	0.28	0.25	**1.02**
-234	9866.923	6459.825	4935.519	2267.604	2174.47	1.00	0.81	0.59	0.22	0.18	**1.16**
-258	25054.2	18721.45	13483.9	8970.205	6391.23	1.00	0.92	0.64	0.34	0.21	**1.50**
-282	5917.06	4366.35	2880.305	1917.704	1927.628	1.00	0.91	0.58	0.31	0.27	**1.35**
-294	6337.957	3475.286	2088.962	1597.437	2101.067	1.00	0.68	0.39	0.24	0.27	**0.85**
-317	4032.021	2519.758	1463.819	837.554	952.083	1.00	0.77	0.43	0.20	0.19	**0.82**
-321	3709.583	1984.145	1275.576	863.171	852.444	1.00	0.66	0.41	0.22	0.19	**0.85**
-341	5154.277	2177.311	1231.603	1052.28	1437.145	1.00	0.52	0.28	0.20	0.23	**0.54**
-347	2973.346	1301.552	637.957	1362.095	998.711	1.00	0.54	0.25	0.44	0.27	**0.56**
Sum	898552.1	729424.2	756941.4	936509	1102161						
Ratio	1.00	0.81	0.84	1.04	1.23						

pRAD7-TS Exp-2

CPD Position	Repair time					Adjusted signal remaining					$T_{50\%}$
						Repair time					
	0	0.5	1	2	3	0	0.5	1	2	3	
Top	1056566	1180397	1198262	1334893	1297667						
-105	10973.48	10213.19	6609.754	2665.598	1666.389	1.00	0.86	0.58	0.22	0.14	**1.21**
-120	9793.132	10019.9	6421.418	4648.206	4045.841	1.00	0.95	0.63	0.43	0.39	**1.53**
-161	31569.28	25748.32	12207.76	5057.81	1395.432	1.00	0.75	0.37	0.14	0.04	**0.80**
-166	12582.73	9134.572	4606.961	2809.433	1626.248	1.00	0.67	0.35	0.20	0.12	**0.82**
-180	36475.89	31974.96	14030.51	4228.158	1922.179	1.00	0.81	0.37	0.10	0.05	**0.82**
-194	7153.989	8786.408	4658.217	1505.153	1474.374	1.00	1.14	0.63	0.19	0.19	**1.25**
-200	15722.24	14377.35	7697.44	3709.661	845.776	1.00	0.85	0.47	0.21	0.05	**0.95**
-207	10706.93	9062.48	4980.007	2636.068	1874.445	1.00	0.78	0.45	0.22	0.16	**0.90**
-221	7174.405	6740.405	4422.369	3635.021	3233.591	1.00	0.87	0.60	0.46	0.42	**1.05**
-234	8870.564	8621.843	4669.811	2733.905	2499.728	1.00	0.90	0.51	0.28	0.26	**1.04**
-258	26165.56	28785.14	14148.59	6998.314	3107.491	1.00	1.02	0.53	0.24	0.11	**1.06**
-282	8922.038	10160.48	4805.769	3273.744	2482.095	1.00	1.00	0.52	0.33	0.26	**1.12**
-294	7910.293	6749.371	3724.436	3458.273	2489.22	1.00	0.79	0.46	0.39	0.29	**0.88**
-317	2421.547	2148.083	1184.27	826.507	536.625	1.00	0.82	0.47	0.31	0.21	**0.93**
-321	2352.781	2039.831	1195.362	1012.022	584.84	1.00	0.80	0.49	0.39	0.23	**0.97**
-341	4944.213	2568.478	1345.407	1434.01	1426.679	1.00	0.48	0.26	0.26	0.27	**0.47**
-347	3506.294	1918.734	637.58	312.896	199.518	1.00	0.51	0.18	0.08	0.05	**0.52**
Sum	1263812	1369447	1295608	1385838	1329077						
Ratio	1.00	1.08	1.03	1.10	1.05						

Induced pRAD7-TS Exp-1

CPD Position	Repair time					Adjusted signal remaining					$T_{50\%}$
						Repair time					
	0	0.5	1	2	3	0	0.5	1	2	3	
Top	638113.6	415065	330666.1	416227.2	747116.8						
-105	10570.62	3945.542	1723.198	1228.208	1431.095	1.00	0.65	0.38	0.23	0.15	**0.79**
-120	8319.105	3327.773	1563.043	1110.736	1407.731	1.00	0.70	0.44	0.26	0.19	**0.85**
-161	27879.71	8333.45	3094.378	1759.895	2096.951	1.00	0.52	0.26	0.12	0.08	**0.54**
-166	9432.81	2607.258	970.434	709.06	980.215	1.00	0.48	0.24	0.15	0.11	**0.48**
-180	35830.59	10428.21	3443.095	1449.585	1683.089	1.00	0.51	0.23	0.08	0.05	**0.52**
-194	7598.992	2725.518	1077.392	588.822	328.222	1.00	0.63	0.33	0.15	0.05	**0.68**
-200	11686.88	4309.402	1527.968	605.978	879.417	1.00	0.64	0.31	0.10	0.08	**0.72**
-207	15072.62	4136.475	1461.952	1052.083	849.201	1.00	0.48	0.23	0.14	0.06	**0.47**
-221	6087.89	2159.736	847.408	458.422	1078.718	1.00	0.62	0.33	0.15	0.19	**0.7**
-234	10881.32	3697.118	1392.891	710.254	831.715	1.00	0.59	0.30	0.13	0.08	**0.63**
-258	27563.79	10695.93	4636.388	2837.158	3104.942	1.00	0.68	0.40	0.20	0.12	**0.76**
-282	7268.767	2411.024	1002.629	822.843	1346.038	1.00	0.58	0.33	0.22	0.20	**0.62**
-294	6754.076	1929.943	823.692	1002.852	1696.378	1.00	0.50	0.29	0.29	0.27	**0.5**
-317	4851.066	1372.565	419.167	331.503	507.399	1.00	0.49	0.20	0.13	0.11	**0.5**
-321	4214.562	1130.59	476.755	490.846	615.194	1.00	0.47	0.27	0.23	0.16	**0.45**
-341	4285.453	837.184	408.669	531.256	494.81	1.00	0.34	0.22	0.24	0.13	**0.34**
-347	2510.298	558.921	249.38	459.172	659.896	1.00	0.39	0.23	0.35	0.29	**0.38**
Sum	838922.2	479671.6	355784.5	432375.8	767107.8						
Ratio	1.00	0.57	0.42	0.52	0.91						

Induced pRAD7-TS Exp-2

CPD Position	Repair time					Adjusted Signal remaining					$T_{50\%}$
						Repair time					
	0	0.5	1	2	3	0	0.5	1	2	3	
Top	541239.1	849055.5	842135.2	841993.7	917548.6						
-105	5899.577	5319.492	4293.902	1660.733	957.484	1.00	0.63	0.53	0.21	0.11	**0.88**
-120	5409.792	5255.367	3872.557	1888.228	1550.114	1.00	0.67	0.52	0.26	0.20	**1.02**
-161	16963.06	12906.36	3994.816	2232.438	2107.971	1.00	0.53	0.17	0.10	0.09	**0.53**
-166	6556.112	4837.833	3555.457	1402.826	1110.908	1.00	0.51	0.40	0.16	0.12	**0.53**
-180	23115.56	16503.56	2830.511	2022.836	1519.249	1.00	0.50	0.09	0.07	0.05	**0.5**
-194	4473.907	4577.213	3185.237	1152.802	904.772	1.00	0.71	0.52	0.19	0.14	**0.97**
-200	8510.653	8092.126	5180.152	916.626	535.538	1.00	0.66	0.44	0.08	0.04	**0.82**
-207	7062.778	4876.123	3364.873	1080.879	1065.423	1.00	0.48	0.35	0.11	0.10	**0.46**
-221	4373.027	3814.91	3501.434	1340.838	1177.869	1.00	0.61	0.58	0.23	0.19	**0.85**
-234	5230.232	4618.459	3525.058	999.012	868.375	1.00	0.61	0.49	0.14	0.11	**0.85**
-258	11979.13	12461.67	5487.73	2705.095	1686.917	1.00	0.72	0.34	0.17	0.10	**0.82**
-282	3987.775	4112.858	1731.076	1514.539	1688.527	1.00	0.72	0.32	0.29	0.29	**0.71**
-294	4102.372	3216.723	2293.709	1231.949	1466.619	1.00	0.54	0.41	0.23	0.25	**0.58**
-317	1957.472	1143.597	894.102	400.036	445.288	1.00	0.41	0.33	0.15	0.16	**0.38**
-321	1823.772	1081.091	1007.723	818.835	597.315	1.00	0.41	0.40	0.34	0.23	**0.42**
-341	2650.954	1332.624	1164.264	712.194	738.332	1.00	0.35	0.32	0.20	0.19	**0.35**
-347	1650.615	940.069	634.067	398.365	349.608	1.00	0.40	0.28	0.18	0.15	**0.38**
Sum	656985.9	944145.6	892651.9	864471.9	936318.9						
Ratio	1.00	1.44	1.36	1.32	1.43						

pRAD7-NTS Exp-1

CPD Position	Repair time					Adjusted signal remaining					$T_{50\%}$
						Repair time					
	0	0.5	1	2	3	0	0.5	1	2	3	
Top	1113115	888428.8	875029.7	915026.1	1133788						
-333	15124.23	10389.43	8894.407	4965.071	6474.544	1.00	0.87	0.77	0.43	0.47	**2.05**
-298	56507.63	41425.38	33380.73	20383.51	19781.26	1.00	0.93	0.78	0.47	0.38	**1.9**
-264	21018.8	16876.27	13065.58	8331.748	8107.626	1.00	1.02	0.82	0.52	0.42	**2.1**
-243	44917.76	32680.01	30501.3	26039.45	27013.25	1.00	0.92	0.89	0.76	0.65	**4.2**
-239	31966.87	23079.11	18162.77	12667.97	9763.777	1.00	0.91	0.75	0.52	0.33	**2.1**
-226	10003.64	7582.351	6909.491	3576.813	3994.355	1.00	0.96	0.91	0.47	0.43	**1.9**
-140	11991	7643.857	5633.158	5298.15	5511.153	1.00	0.81	0.62	0.58	0.50	**3**
-127	21362.3	13926.16	9866.794	5402.707	3501.272	1.00	0.83	0.61	0.33	0.18	**1.35**
Sum	1326007	1042031	1001444	1001692	1217935						
Ratio	1	0.79	0.76	0.76	0.92						

pRAD7-NTS Exp-2

CPD Position	Repair time					Adjusted signal remaining					$T_{50\%}$
						Repair time					
	0	0.5	1	2	3	0	0.5	1	2	3	
Top	684237.2	865002	839425	942086.9	899973.7						
-333	4877.569	5585.357	3815.327	3649.484	2936.71	1.00	0.91	0.66	0.57	0.49	**2.55**
-298	18003.58	20117.67	13976.64	8344.824	5812.384	1.00	0.89	0.65	0.36	0.26	**1.55**
-264	5717.876	6112.704	3356.826	3023.101	2911.876	1.00	0.85	0.49	0.41	0.41	**1.25**
-243	12931.12	16192.72	14196.73	11482.25	7562.785	1.00	1.00	0.92	0.68	0.47	**2.85**
-239	11108.81	11764.5	7283.399	3448.692	2143.899	1.00	0.85	0.55	0.24	0.16	**1.18**
-226	2084.63	2527.651	1973.821	1300.309	942.53	1.00	0.97	0.80	0.48	0.37	**1.88**
-140	3413.48	3836.691	2721.613	2589.543	2290.715	1.00	0.90	0.67	0.58	0.54	**3.00**
-127	7438.581	8242.405	4941.698	2707.553	1722.329	1.00	0.88	0.56	0.28	0.19	**1.25**
Sum	749812.9	939381.7	891691	978632.7	926296.9						
Ratio	1.00	1.25	1.19	1.31	1.24						

Induced pRAD7-NTS Exp-1

CPD Position	Repair time					Adjusted signal remaining					$T_{50\%}$
						Repair time					
	0	0.5	1	2	3	0	0.5	1	2	3	
Top	761907.4	672659.6	459318.8	543950.2	761244.8						
-333	10550.77	6653.859	2805.537	2028.262	2744.34	1.00	0.74	0.48	0.31	0.30	**1.0**
-298	41588.8	29857.68	13225.97	9321.075	9439.103	1.00	0.84	0.58	0.36	0.26	**1.18**
-264	20029.72	12699.31	5358.617	2457.886	2711.274	1.00	0.75	0.49	0.19	0.16	**0.95**
-243	30903.65	22524.91	12978.43	10402.65	10889.71	1.00	0.86	0.76	0.53	0.41	**2.25**
-239	21764.96	16155.89	7393.702	4576.465	4475.37	1.00	0.87	0.62	0.33	0.24	**1.35**
-226	8100.861	6046.948	2661.993	1566.947	1494.328	1.00	0.88	0.60	0.31	0.21	**1.25**
-140	8537.8	3946.681	1833.812	1853.316	3012.841	1.00	0.54	0.39	0.34	0.41	**0.7**
-127	14508.35	7959.294	3048.137	1618.343	1837.808	1.00	0.65	0.38	0.18	0.15	**0.8**
Sum	917892.3	778504.2	508625	577775.1	797849.6						
Ratio	1	0.85	0.55	0.63	0.87						

Induced pRAD7-NTS Exp-2

CPD Position	Repair time					Adjusted signal remaining					$T_{50\%}$
						Repair time					
	0	0.5	1	2	3	0	0.5	1	2	3	
Top	322942.3	453309.7	558148.2	493649.4	526053						
-333	3135.712	3352.171	3199.208	1759.982	1187.511	1.00	0.79	0.62	0.40	0.26	**1.45**
-298	12292.96	12572.96	11057.66	5141.82	4290.407	1.00	0.75	0.55	0.30	0.24	**1.15**
-264	3978.011	3440.397	2633.988	1174.203	430.267	1.00	0.64	0.41	0.21	0.07	**0.85**
-243	9100.969	11412.82	11647.43	7531.017	4751.188	1.00	0.92	0.78	0.59	0.35	**2.35**
-239	6833.367	7079.744	5843.988	2363.552	1605.509	1.00	0.76	0.52	0.25	0.16	**1.05**
-226	2177.112	1883.281	1762.451	993.548	711.703	1.00	0.64	0.50	0.32	0.22	**0.95**
-140	2310.762	2217.6	1988.835	1907.104	1424.896	1.00	0.71	0.53	0.59	0.42	**1.05**
-127	4374.7	4373.362	3555.552	1180.837	894.265	1.00	0.73	0.50	0.19	0.14	**0.99**
Sum	367145.9	499642	599837.3	515701.5	541348.8						
Ratio	1	1.36	1.63	1.40	1.47						

	St Dev of $T_{50\%}$			
TS Position	psocs	Induced-psocs	pRad7	Induced-pRad7
-105	0.056569	0.02121	0.042426	0.06364
-120	0.035355	0.07071	0.29	0.12
-161	0.042426	0.05657	0.035355	0.007071
-166	0.077782	0.0495	0.084853	0.035355
-180	0.070711	0	0.035355	0.014142
-194	0.176777	0.07778	0.084853	0.205061
-200	0.106066	0	0.021213	0.070711
-207	0.056569	0.01414	0.091924	0.007071
-221	0.070711	0.07071	0.021213	0.106066
-234	0.176777	0.07071	0.084853	0.155563
-258	0.148492	0.03536	0.247487	0.042426
-282	0.049497	0.02121	0.162635	0.06364
-294	0.070711	0.01414	0.021213	0.056569
-317	0	0.0495	0.077782	0.084853
-321	0.098995	0.02121	0.084853	0.021213
-341	0.042426	0.04243	0.049497	0.007071
-347	0.035355	0.07071	0.028284	0
NTS Position	psocs	Induced-psocs	pRad7	Induced-pRad7
-333	0.813173	0.70711	0.353553	0.318198
-298	0.318198	0.141421	0.247487	0.021213
-264	0.742462	0.176777	0.601041	0.070711
-243	0.282843	0.318198	0.106066	0.070711
-239	0.353553	0.141421	0.650538	0.212132
-226	0.459619	0.777817	0.19799	0.212132
-140	0.176777	0.721249	0	0.247487
-127	0.59397	0.070711	0.070711	0.13435

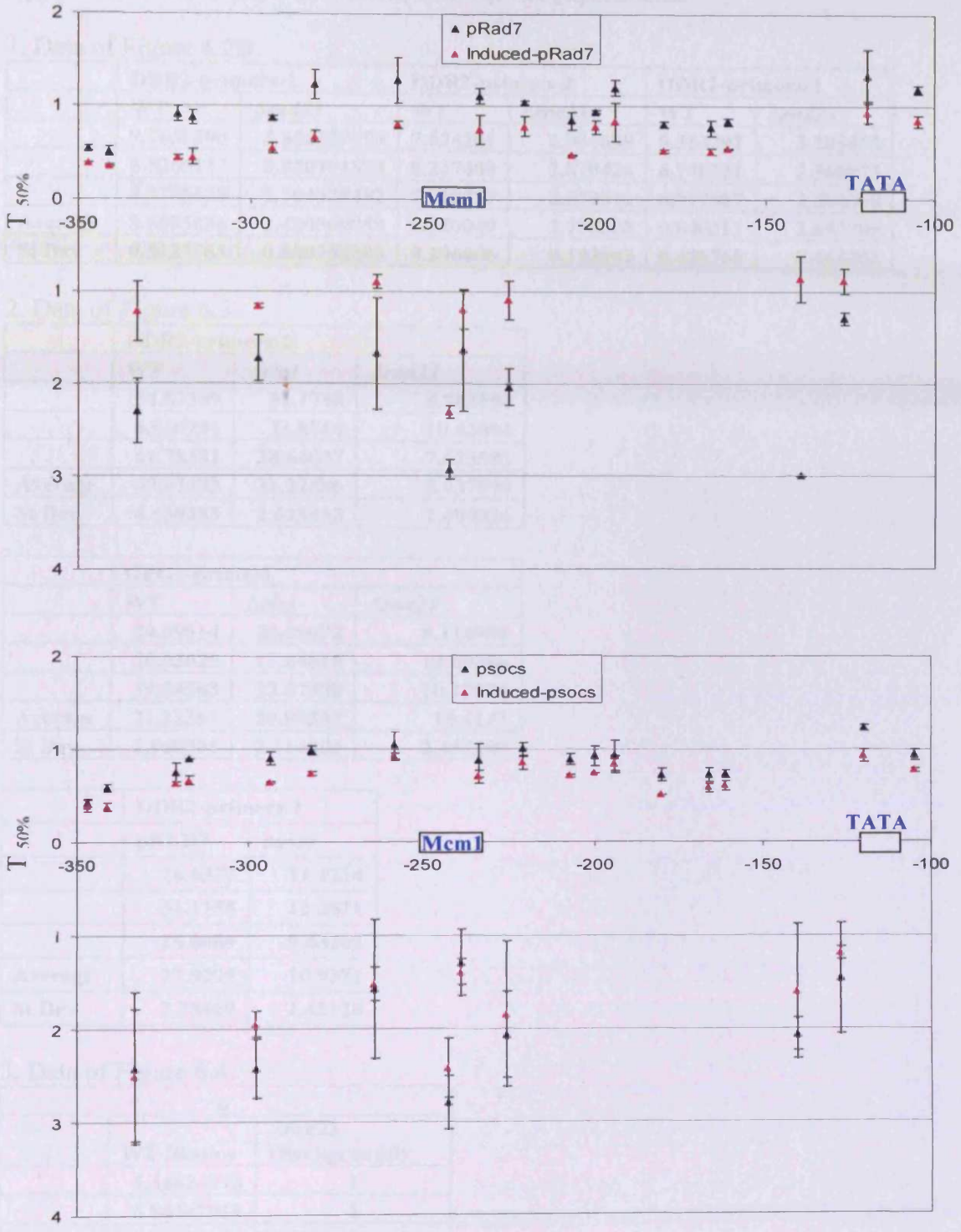

Figure 5.4C (with error bars) Quantification results form figure 5.4A and B. Time to remove 50% of the initial CPDs ($T_{50\%}$) at given sites. Details of quantification was described in 2.8.

Appendix IV. Data from anti-Rad23 ChIP-qPCR experiments.

1. Data of Figure 6.2B.

	DDR2-primers-1		DDR2-primers-2		DDR2-primers-3	
	WT	Δ*rad23*	WT	Δ*rad23*	WT	Δ*rad23*
	9.2636296	3.856439799	7.624201	2.944688	5.363292	3.205472
	8.5265137	0.820791893	8.217408	2.870424	6.740251	2.568073
	8.2785625	2.764475482	7.918537	2.579512	6.017407	2.304569
Average	8.6895686	2.480569058	7.920049	2.798208	6.040317	2.692705
St Dev	0.5123763	0.880750385	0.296606	0.193002	0.688765	0.463202

2. Data of Figure 6.3.

	DDR2-primers-1		
	WT	*Δelc1*	*Δrad23*
	54.83309	31.1748	8.763154
	63.60791	33.8714	10.42694
	61.78381	28.64037	7.623583
Average	60.07493	31.22886	8.937894
St Dev	4.630283	2.615933	1.409826

	GPG1-primers		
	WT	Δ*elc1*	Δ*rad23*
	24.59514	20.09072	8.114986
	20.03025	17.84618	13.00386
	19.04563	22.07308	10.12524
Average	21.22367	20.00333	10.4147
St Dev	2.960991	2.114805	2.457259

	DDR2-primers-1	
	pRAD7	psocs
	26.6372	11.1214
	31.1155	12.2571
	26.0089	9.43262
Average	27.9205	10.9371
St Dev	2.78469	1.42126

3. Data of Figure 6.4.

u		
	WT (Ratio)	Δ*rad23* (Background)
	5.34824973	1
	6.84447918	1
	5.40546141	1
Average	5.86606344	
St Dev	0.84781561	

0		
	WT (Ratio)	Δ*rad23* (Background)
	2.718916707	1
	3.286839952	1
	3.174671713	1
Average	3.060142791	
St Dev	0.300785403	

1		
	WT (Ratio)	Δ*rad23* (Background)
	2.152001658	1
	2.54709718	1
	1.707922256	1
Average	2.135673698	
St Dev	0.419825666	

Appendix V.
My contributions to the EMBO paper published in 2006 (Gillette *et al.*, 2006) as follow:

1. Experimental works described in Figure 1.
2. Experimental works described in Figure 2.
3. Experimental works described in Figure 3 C, D and E.
4. Experimental works described in Figure 4 A and B.
5. Experimental work described in Figure 5 B.

The EMBO Journal (2006), 1 10 | © 2006 European Molecular Biology Organization | All Rights Reserved 0261-4189/06
www.embojournal.org

THE EMBO JOURNAL

Distinct functions of the ubiquitin–proteasome pathway influence nucleotide excision repair

Thomas G Gillette[1], Shirong Yu[2], Zheng Zhou[2], Raymond Waters[2], Stephen Albert Johnston[1] and Simon H Reed[2,*]

[1]The Center for Biomedical Inventions, Medicine and Microbiology, University of Texas Southwestern Medical Center, Dallas, TX, USA and [2]Department of Pathology, School of Medicine, Cardiff University, Cardiff, UK

The Rad23/Rad4 nucleotide excision repair (NER) protein complex functions at an early stage of the NER reaction, possibly promoting the recognition of damaged DNA. Here we show that Rad4 protein is ubiquitinated and degraded in response to ultraviolet (UV) radiation, and identify a novel cullin-based E3 ubiquitin ligase required for this process. We also show that this novel ubiquitin ligase is required for optimal NER. Our results demonstrate that optimal NER correlates with the ubiquitination of Rad4 following UV radiation, but not its subsequent degradation. Furthermore, we show that the ubiquitin–proteasome pathway (UPP) regulates NER via two distinct mechanisms. The first occurs independently of *de novo* protein synthesis, and requires Rad23 and a nonproteolytic function of the 19S regulatory complex of the 26S proteasome. The second requires *de novo* protein synthesis, and relies on the activity of the newly identified E3 ubiquitin ligase. These studies reveal that, following UV radiation, NER is mediated by nonproteolytic activities of the UPP, via the ubiquitin-like domain of Rad23 and UV radiation-induced ubiquitination of Rad4.

The EMBO Journal advance online publication, 4 May 2006; doi:10.1038/sj.emboj.7601120

Subject Categories: proteins; genome stability & dynamics

Keywords: DNA repair; NER; proteasome; ubiquitin; yeast

Introduction

The ubiquitin–proteasome pathway (UPP) is the major pathway for degradation of cellular proteins (Pickart, 2004). This occurs through two discrete steps: covalent attachment of multiple ubiquitin molecules (conjugation) to target proteins, and subsequent degradation of the tagged proteins by the 26S proteasome (comprised of the catalytic 20S core and the 19S regulator) (Glickman and Ciechanover, 2002). This canonical role of the UPP is associated with housekeeping functions, regulation of protein turnover, and antigenic-peptide generation (Ciechanover and Ben-Saadon, 2004). More recently, it has become evident that both components of this pathway have noncanonical (nonproteolytic) functions that include the regulation of transcription (Ferdous *et al*, 2001, 2002; Salghetti *et al*, 2001; Gonzalez *et al*, 2002; Gillette *et al*, 2004), endocytosis (Strous and Govers, 1999), and DNA repair (Russell *et al*, 1999; Gillette *et al*, 2001; Dupre *et al*, 2004).

Nucleotide excision repair (NER) removes lesions in DNA caused by ultraviolet (UV) light. This process requires the coordinated activity of over 30 proteins, the majority of which are conserved from yeast to man. Defective NER has been documented in the hereditary cancer-prone disease *Xeroderma pigmentosum* (XP) and is the primary cellular phenotype of the disease (Hanawalt, 2001). The frequent association of the XP homozygous state with various types of skin cancers established the importance of NER as a fundamental mechanism for protecting the functional integrity of the human genome (Friedberg, 2001).

In the yeast *Saccharomyces cerevisiae*, the ubiquitin-like (Ubl) domain of the NER protein Rad23 is required for survival after exposure to UV light (Watkins *et al*, 1993; Russell *et al*, 1999). One of the first links between the UPP and NER was the observation that the Ubl domain of Rad23 protein interacted directly with the 26S proteasome (Schauber *et al*, 1998). We previously demonstrated that the 19S regulatory complex (19S RC) of the 26S proteasome has a nonproteolytic function in NER that is mediated through the Ubl domain of Rad23 protein (Russell *et al*, 1999). *In vivo*, the 19S RC negatively regulates the rate of lesion removal during NER. *Rad23*-deleted cells show reduced rates of excision of UV-radiation-induced DNA damage, and reduced UV survival. However, this phenotype is significantly rescued by introducing mutations in specific 19S RC subunits (Gillette *et al*, 2001). Importantly, mutations in 20S core proteasome subunits, which promote a severe defect in proteolysis, fail to rescue the NER deficiency associated with *rad23*-deleted cells (Gillette *et al*, 2001). These findings and more recent observations indicate that defective proteolysis does not correlate with the ability to rescue the NER deficiency associated with deletion of the *RAD23* gene (Ortolan *et al*, 2004; Xie *et al*, 2004).

Here we demonstrate that Rad4 is targeted for degradation by the 26S proteasome following UV radiation. We show that a novel cullin-based E3 ubiquitin ligase ubiquitinates Rad4 following UV, and demonstrate that cellular survival after UV correlates with the ubiquitination of Rad4, but not its subsequent degradation. Finally, we show that two pathways that are distinct in their requirements for *de novo* protein synthesis regulate the NER response to UV radiation. Pathway I operates independently of *de novo* protein synthesis, while pathway II relies on *de novo* protein synthesis. We show that pathway I is regulated by the previously reported nonproteolytic activity of the 19S RC and the Ubl domain of Rad23, while pathway II requires the activity of the newly described E3 ligase. These studies demonstrate that nonproteolytic activities of the ubiquitin/proteasome system operate via

*Corresponding author. Department of Pathology, School of Medicine, Cardiff University, Heath Park, Cardiff CF14 4XN, UK.
Tel.: +44 2920 745576; Fax: +44 2920 743496;
E-mail: reedsh1@cf.ac.uk

Received: 21 November 2005; accepted: 6 April 2006

two distinct pathways during NER, and reveal novel insights about the regulation of NER in response to UV radiation.

Results

Rad4 protein is degraded by the UPP in response to UV

It has been suggested that, following exposure of cells to UV irradiation, the proteolytic degradation of Rad4 is attenuated, resulting in accumulation of this repair factor and enhanced NER (Lommel *et al*, 2002; Ng *et al*, 2003). A similar model was originally proposed for the Rad4 homologue, XPC. More recent evidence using an antibody to the endogenous protein suggests that XPC is stable, with a half-life of over 6 h (Okuda *et al*, 2004). Since both of these earlier reports employed overexpressed, epitope-tagged versions of Rad4/XPC, we wanted to examine the stability of native Rad4 protein following exposure of cells to UV light, using an antibody specific to endogenously expressed Rad4 protein.

In the absence of UV light, the steady-state level of Rad4 protein does not alter significantly over a 3-h period following incubation of cells with the protein synthesis inhibitor cycloheximide, indicating that, like XPC, Rad4 protein is stable during this time period, and is not rapidly turned over by the proteasome (Figure 1A, top). Figure 1A (bottom) shows that, under the same conditions, an unrelated protein with a shorter half-life, cyclophilin A, shows a decrease in steady-state levels over the 3-h period, demonstrating the activity of the cycloheximide in blocking protein synthesis during the experiment.

It has been suggested that, in the absence of Rad23, Rad4 protein is rapidly degraded (Lommel *et al*, 2002). This was based on the observation that steady-state levels of epitope-tagged Rad4 are significantly reduced in *rad23*-deleted cells. We observed that the steady-state levels of native Rad4 (in the absence of cycloheximide) are also reduced in a *Δrad23* strain (Figure 1B). We used the protein synthesis inhibitor cycloheximide to examine whether the lower steady-state levels of native Rad4 were due to increased turnover of Rad4 in the absence of its interacting partner Rad23. Surprisingly, the steady-state level of Rad4 protein in this strain did not alter significantly over a 4-h period following incubation of cells with the protein synthesis inhibitor cycloheximide (Figure 1C). We confirmed these observations in the absence of cycloheximide by performing pulse-chase experiments following the metabolic radiolabelling of cellular proteins and found the half-life of Rad4 to be between 3 and 4 h both in wild-type (WT) and *rad23*-deleted cells (see Supplementary data). These results show that the reduced levels of Rad4 observed in *rad23*-deleted cells are not due to a reduction in the half-life of Rad4. To determine the cause of reduced Rad4 levels in *rad23*-deleted cells, we investigated the transcriptional levels of Rad4 in WT and *rad23*-deleted

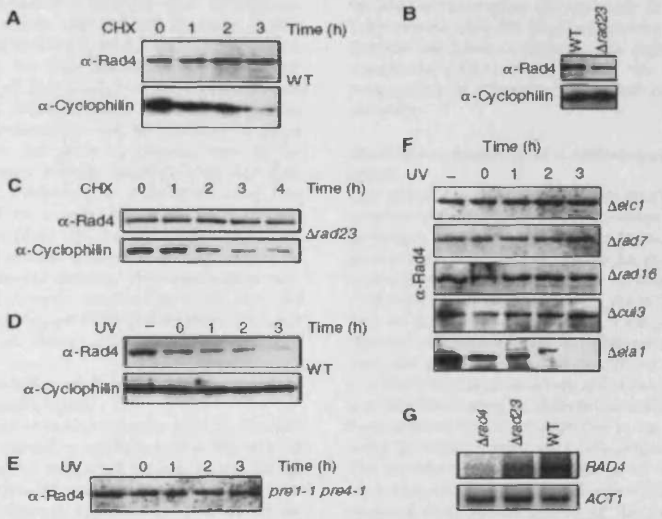

Figure 1 Post-UV degradation of Rad4 is dependent on proteolysis. (**A**) Anti-Rad4 Western blot of WCC4a (WT) extracts from a strain grown in the protein synthesis inhibitor cycloheximide for the time indicated (h), along with an anti-cyclophilin control of the same blot. (**B**) Anti-Rad4 Western blot showing the relative steady-state levels of Rad4 in a WT and *Δrad23* mutant strain. The bottom panel shows anti-cyclophilin loading control. (**C**) Anti-Rad4 Western blot of *Δrad23* extracts from a strain grown in the protein synthesis inhibitor cycloheximide for the time indicated (h), along with an anti-cyclophilin control of the same blot. (**D**) Anti-Rad4 Western blot of WCC4a (WT) extracts from a strain either unirradiated (–) or UV irradiated (40 J) and allowed to recover for the times indicated (h), along with an anti-cyclophilin control of the same blot. (**E**) Anti-Rad4 Western blot of *pre 1-1, pre 4-1* extracts from cells either unirradiated (–) or UV irradiated (40 J) and allowed to recover for the times indicated (h). (**F**) Deletion of genes encoding the ECS ligase components results in stabilization of Rad4 post-UV. Anti-Rad4 Western blots of extracts from Research Genetics mutant strains listed either unirradiated (–) or UV irradiated and allowed to repair for the times indicated (h). (**G**) Northern blot analysis of *RAD4* transcript levels in the indicated strains. *ACT1* transcript levels are shown as a loading control.

cells. Northern blot analysis revealed that Rad4 transcript levels are significantly reduced in *rad23*-deleted cells compared with WT cells (Figure 1G). We conclude that the reduced levels of Rad4 protein in *rad23*-deleted cells are due to reduced Rad4 transcript levels, and not due to the increased proteolytic degradation of Rad4 in the absence of its interacting partner Rad23.

In contrast to earlier studies which used ectopically expressed Rad4, we found that endogenously expressed Rad4 protein is not stabilized after UV treatment; rather, it is rapidly degraded following exposure to UV light. Figure 1D (top) shows the decrease in steady-state levels of Rad4 protein over a 3-h period following exposure of WT cells to UV radiation. Rad4 steady-state levels returned to the pre-UV state within 5–6 h following UV irradiation (data not shown). The steady-state level of cyclophilin remains unchanged following exposure of cells to UV light Figure 1D (bottom). We do not detect a ladder of polyubiquitinated Rad4 following UV radiation, but longer running of samples on 5–15% gradient SDS–PAGE gels revealed the presence of a higher molecular weight form of Rad4, which is consistent with the conjugation of a single ubiquitin (Supplementary data S4). Using an isogenic strain carrying conditional mutations in two subunits of the 20S proteasome (*pre1-1*, *pre4-1*), we confirmed that the UV-dependent degradation of Rad4 protein is mediated by the proteolytic activity of the 26S proteasome. This temperature-sensitive strain shows a marked decrease in the ability to degrade proteins that have been targeted by the ubiquitin-dependent proteolytic pathway even at temperatures permissive for growth (Russell and Johnston, 2001). Figure 1E shows that in the *pre1-1*, *pre4-1* strain, Rad4 protein steady-state levels do not alter following exposure to UV light. We also examined the stability of Rad4 protein post-UV radiation using a chemical approach. The proteolytic function of the 26S proteasome can be inhibited in yeast strains mutated in the *ise1* gene by growing cells in the presence of the aldehyde peptide inhibitor (MG132) (Lee and Goldberg, 1996). Inhibition of proteolysis using this method also resulted in a stabilization of Rad4 protein following UV radiation (data not shown). These data show that endogenous Rad4 protein is targeted for degradation by the UPP in a UV-dependent fashion. This observation may have been overlooked in earlier studies due to the inherent instability of the epitope-tagged Rad4 protein used (Lommel *et al*, 2002; Ortolan *et al*, 2004).

UV-dependent degradation of Rad4 requires a novel cullin-based E3 ubiquitin ligase

Genetic and biochemical evidence suggests that, in addition to its ATPase activity (which is fundamental to the role of Rad16 in an early stage of the global genome repair (GGR) mechanism), the Rad7/Rad16 complex in concert with Elc1 may also have an additional, separate function as an E3 ubiquitin ligase (Ramsey *et al*, 2004). Previous studies have shown that a specific component of the cullin-based E3 ubiquitin ligases functions as a substrate-specific adaptor, the protein target usually interacting with the adaptor through a protein–protein interacting domain such as an SH2 domain or a leucine-rich repeat (LRR) motif. Previous protein–protein interaction studies predicted that Rad4 might be a primary target for this putative Rad7-containing E3 ligase, since it was shown that the LRR domain of Rad7 is required for a two-hybrid interaction between Rad7 and Rad4 (Wang *et al*, 1997; Pintard *et al*, 2004). To test whether this putative E3 ligase is required for the degradation of Rad4 protein in response to UV radiation *in vivo*, we deleted or mutated individual components of the Rad7 E3 ligase.

Deletion of any of the components of the Rad7-containing E3 ubiquitin ligase resulted in stabilization of Rad4 protein following exposure of these cells to UV light. Figure 1F shows that steady-state levels of Rad4 protein are stable following UV in the *Δelc1* strain, showing that Elc1 protein is required for the degradation of Rad4 protein after UV. Steady-state levels of Rad4 protein were also stable in mutants defective in each of the other predicted components of the Elongin–Cullin–Socs-box (ECS) ligase complex, including Rad7 and Rad16 proteins (Figure 1F). Rad7 is an SOCS box-containing protein (Ho *et al*, 2002), suggesting that the Rad7 E3 ligase may be a novel member of the cullin-based ECS-type E3 ubiquitin ligases, a subclass of the Skp1–Cullin–F-box (SCF) type family of ubiquitin ligases. Therefore, we examined a number of cullin mutants, including *cul3*- and *cul8*-deleted strains and *crl2*, *4*, and *7* temperature-sensitive mutants. We showed that *CUL3* was uniquely required for the degradation of Rad4 protein following UV irradiation (Figure 1F, second to bottom panel). Deletion of an unrelated SOCS box gene, *ELA1*, did not result in the stabilization of Rad4 protein after UV (Figure 1F, bottom panel). We also examined the effect of other mutants on Rad4 stability post-UV, including the E2 encoding genes *UBC4*, *UBC5*, *RAD6*, and the cullin *CUL8*. Deletion of these genes did not result in the stabilization of Rad4 protein after UV (data not shown). This demonstrates that the inhibition of Rad4 protein degradation post-UV is specifically related to deletion of the genes that encode components of the cullin-based Rad7-containing E3 ligase complex.

Rad7 is a component of a cullin-based E3 ubiquitin ligase

The physical interaction of Rad7, Rad16, Elc1, and Cul3 proteins was confirmed by co-immunoprecipitation. A Rad7 polyclonal antibody was used to immunoprecipitate Rad7 protein from a WT extract. Figure 2A shows that, following immunoprecipitation and Western blotting, Rad16 protein co-precipitates with Rad7 protein in the WT extract. We found that, in addition to Elc1 protein, Cul3 protein also co-precipitated with Rad7 protein. A significant amount of both Elc1 and Cul3 proteins do not co-precipitate with Rad7 protein. It is likely that they associate with other protein complexes, possibly functioning in different ubiquitin ligases. None of these proteins immunoprecipitated in the control experiment using an extract from *Δrad7* cells (Figure 2A, right panel). The specificity of the antibodies used was determined by comparing the Western blots of either WT or mutant extracts prepared from strains deleted of the corresponding genes (Supplementary data S1). The detection of Cul3, Elc1, and Rad16 proteins co-precipitating with Rad7 protein further suggests that this complex is a member of the cullin-based family of E3 ubiquitin ligases.

The Rad7-containing E3 ligase complex ubiquitinates Rad4 in vitro

Collectively, the above observations suggest the existence of a complex of proteins that constitute a novel E3 (ECS-type)

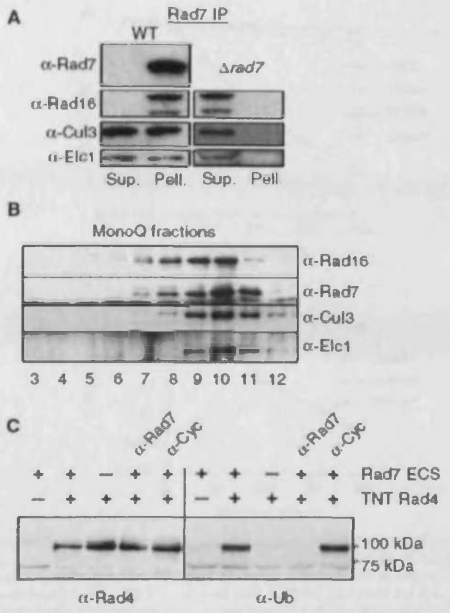

Figure 2 Characterization and activity of the Rad7 ECS E3 ligase. (**A**) Co-immunoprecipitation of ECS ligase components with Rad7. Western blot of Rad7 immunoprecipitation probed with the antibodies listed (Sup., supernatant; Pell., pellet). WT extract is on the left, control extract (Δ*rad7*) lacking Rad7 protein is on the right. (**B**) Purification of the Rad7 ECS ligase. Western blot of MonoQ fractions probed with the antibodies listed (see Materials and methods for details). (**C**) *In vitro* ubiquitination of Rad4 by purified Rad7 ligase. Left panel, anti-Rad4 Western blot of ubiquitination reaction with components indicated (TNT—TNT reaction with control vector). Anti-rad7 antibody or the anti-cyclophilin antibody were added in lanes 4 and 5, respectively. Right panel, the left-hand blot was reprobed with ubiquitin antibody. Approximate MW markers indicated on the right.

ubiquitin ligase. Previous studies describing the architecture of cullin-based E3 ligases and our genetic evidence suggest that Rad4 is a primary target of this E3 ligase (Wang *et al*, 1997; Pintard *et al*, 2004). We performed biochemical experiments to examine this. Previously, we described the purification of epitope-tagged Rad7 protein (Reed *et al*, 1999). Cul3 and Elc1 proteins co-purify with Rad7 and Rad16 proteins through a number of chromatographic steps that include Ni-NTA, p-11, DEAE Sephacel, and Mono-Q columns. This results in a nearly 15 000-fold enrichment of Rad7/Rad16. Western blotting showed that fractions eluted from the mono-Q column of the Rad7 protein purification (Reed *et al*, 1998; Figure 2B) contain Rad7, Rad16, Elc1, and Cul3 proteins. We expressed Rad4 protein using a coupled transcription/translation system. The peak mono-Q fractions (Figure 2B, lanes 9 and 10) were added to *in vitro* expressed Rad4 protein in an ubiquitination assay. Figure 2C shows that these fractions were capable of supporting the ubiquitination of Rad4 protein *in vitro*. The addition of an antibody specific to Rad7 (or a Rad16-specific antibody, data not shown) inhibited this activity (Figure 2C, second to last lane), confirming that the ubiquitin ligase function was dependent specifically on the E3 ligase complex and was not an unrelated contaminant. A non-specific antibody (Figure 2C, last lane) or preimmune serum (data not shown) had no effect.

Post-UV Rad4 degradation does not correlate with UV survival

To determine the influence of Rad4 protein stability on cellular survival after UV, we examined UV survival in deletion strains for each of the components of the ECS ligase. Rad4 steady-state levels are stable post-UV in each of the deletion strains (Figure 1F), but the effect on UV survival varies (Figure 3A). In the case of Δ*rad7* (Figure 3A) and Δ*rad16* (data not shown) strains, UV survival is significantly reduced following exposure of these mutants to UV light, as expected (Verhage *et al*, 1996). However, Δ*elc1*- and Δ*cul3*-deleted cells are not significantly UV sensitive (Figure 3A). This shows that, under the conditions tested, loss of the E3 ligase activity does not significantly affect UV survival. We speculated that site-directed mutations made to the SOCS box domain of the Rad7 protein might specifically affect its E3 ligase activity, leaving intact its fundamental role in GGR (Figure 3B). Rad4 protein stability and UV survival of a Δ*rad7* strain carrying a centromeric plasmid coding for WT Rad7 (pRad7) or the SOCS box-mutated Rad7 (psocs) proteins are shown in Figure 3C and D, respectively. The psocs strain exhibits stabilization of Rad4 protein post-UV (Figure 3C). However, the psocs strain, like those carrying deletions in *Elc1* and *Cul3*, is not sensitive to UV (Figure 3A and D). These results demonstrate that altering the stability of Rad4 protein in response to UV does not affect UV survival in yeast.

SOCS-mutated rad7 cells fail to ubiquitinate Rad4 after UV radiation

To determine whether the Rad7 E3 ubiquitin ligase is required for the ubiquitination of Rad4 protein in response to UV radiation *in vivo*, we immunoprecipitated Rad4 protein in a strain expressing Myc epitope-tagged ubiquitin protein (Hochstrasser *et al*, 1991) and either WT Rad7 or SOCS box-mutated Rad7 (psocs) proteins. Immunoprecipitation of Rad4 protein was followed by Western blotting with anti-Myc antibody to detect the presence of Myc-tagged ubiquitin. Figure 3E shows that Rad4 protein is ubiquitinated in response to UV in the pRAD7 strain (Figure 3E, lower right panel), but not in the psocs strain (Figure 3E, lower left panel). Reprobing the same blot with anti-Rad4 antibody confirmed the position of Rad4 protein (Figure 3E, upper left and right panels). This result was confirmed in an independent Rad4 co-immunoprecipitation experiment using an antibody raised against ubiquitin by genetic immunization (Chambers and Johnston, 2003; Supplementary data S2). This result demonstrates that the Rad7 E3 ligase activity is required for the ubiquitination of Rad4 protein in response to UV radiation *in vivo*.

The Rad7-containing E3 ubiquitin ligase regulates NER in the absence of Rad23

Collectively, our results show that the Rad7-containing E3 ubiquitin ligase targets Rad4 protein for ubiquitination in response to UV radiation, but neither the ubiquitination nor

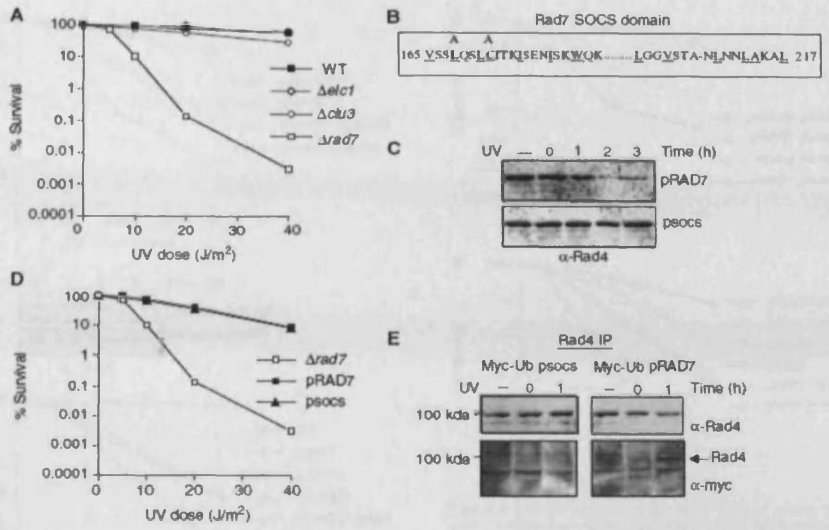

Figure 3 Rad7 SOCS box mutation stabilizes Rad4 without affecting UV survival. (**A**) UV survival for the mutant strains listed. (**B**) The amino-acid sequence of the SOCS box domain of Rad7. Conserved residues are underlined. Alanine mutations made in the pSOCS are noted on the top, with the mutated residues in bold. (**C**) Post-UV steady-state levels of Rad4 shown by anti-Rad4 Western blot. The cells were either unirradiated (−) or UV irradiated and allowed to repair for the times indicated (h). Top panel, extracts from an Sc507-derived *rad7*-deleted yeast strain transformed with a centromeric vector expressing WT Rad7 (top panel pRad7) or SOCS box domain mutant (bottom panel pSOCS) from the endogenous Rad7 promoter. (**D**) UV survival for the mutant strains listed. (**E**) The ubiquitination status of Rad4 at 0 and 1 h post-UV in the WT (pRad7), and SOCS box-mutated (psocs) strains expressing Myc-tagged ubiquitin. These strains were either unirradiated (−) or UV irradiated and allowed to repair for 0 or 1 h. Lower panel, Rad4 was immunoprecipitated from the extracts and then blotted with anti-Myc antibody. The upper panel shows the same blot probed with Rad4 antibody.

the UV-dependent degradation of Rad4 correlate with cellular survival following UV radiation. Therefore, what is the significance of the Rad7 E3 ubiquitin ligase on NER and UV survival? Since Rad4 and Rad23 are interacting partners and Rad23 has a Ubl domain that is required for normal rates of NER, we tested whether ubiquitination of Rad4 plays a role in UV survival in the absence of Rad23. Figure 4A shows that a *Δrad23* strain carrying an additional mutation in the SOCS box domain of Rad7 protein is more sensitive to UV than a strain deleted only in the *RAD23* gene. Figure 4B confirms that, following UV, Rad4 protein is degraded in the *Δrad23* mutant (*Δrad23/pRAD7*), but in the *Δrad23/psocs* strain Rad4 protein is stable. It is interesting to note that, while the steady-state levels of Rad4 are lower in the *Δrad23* mutant, the increased steady-state levels of Rad4 in the psocs mutant do not result in an increase in UV survival. This is not surprising, since we and others have previously shown that inhibiting the proteolytic activity of the 26S proteasome does not significantly influence NER in a *Δrad23* strain (Gillette *et al*, 2001; Lommel *et al*, 2002). We conclude that the effect of the Rad7-containing E3 ligase on UV survival correlates with its ability to ubiquitinate Rad4 protein. Figure 4C shows that a *Δrad23* mutant additionally mutated in the Elongin C component of the ECS ligase, *elc1*, also demonstrates an increased UV sensitivity. This suggests that the increase in UV sensitivity in the *psocs* mutant is due specifically to the loss of Rad7-containing E3 ligase activity, and is not an unrelated activity of the Rad7 protein. Furthermore, this effect is specific to genes encoding components of the Rad7-containing E3 ligase, since *Δrad23* strains additionally mutated in an unrelated SOCS box gene, *Ela1*, do not exhibit this phenotype (Figure 4C). These results show that the effect of the E3 ubiquitin ligase on UV survival includes the ubiquitination of Rad4 protein in response to UV. They also demonstrate that the Rad7-containing E3 ligase and Rad23 proteins have overlapping functions in UV survival (Bertolaet *et al*, 2001a; Gillette *et al*, 2001).

The Rad23 protein has two functional domains that significantly influence NER: the Ubl domain and the C-terminal Rad4 protein interacting domain (Bertolaet *et al*, 2001a, b; Gillette *et al*, 2001). The UBA domain of Rad23 does not appear to have a significant influence on NER (Bertolaet *et al*, 2001b), although a more recent study suggests that there might be some role for this domain in UV survival (Heessen *et al*, 2005). We next examined whether the overlapping function of Rad23 and the Rad7 E3 ligase activity was associated with the Ubl domain of Rad23. Figure 5A shows that an E3 ligase defective strain (*psocs*) expressing a Ubl-deleted version of Rad23 (*Δubl*) protein also exhibits increased UV sensitivity compared to a strain expressing Ubl-deleted Rad23 protein alone. This shows that the increased UV sensitivity of *Δrad23* mutants additionally defective in the Rad7 E3 ubiquitin ligase activity (*psocs*) is specifically related to the loss of the Ubl domain of Rad23 protein.

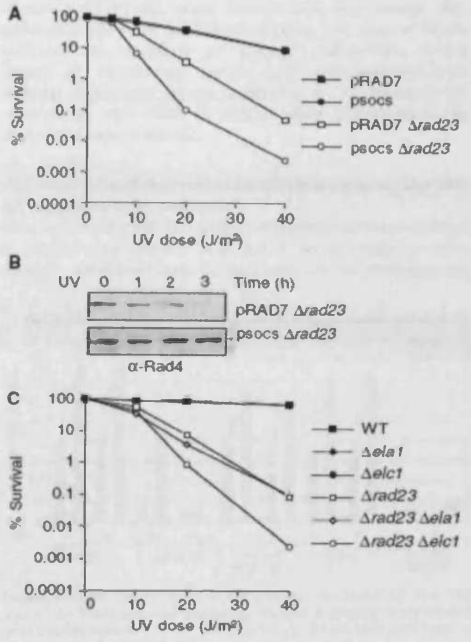

Figure 4 Effect of ECS ligase activity on UV survival in a Δ*rad23* mutant. (**A**) UV survival of the Sc507-derived strains listed. (**B**) Anti-Rad4 Western blot of protein extracts prepared from pRad7, Δ*rad23* (top), or psocs, Δ*rad23* (bottom). Strains were either unirradiated (−) or UV irradiated and allowed to repair for the times indicated (h). (**C**) UV survival of the Research Genetics strains listed.

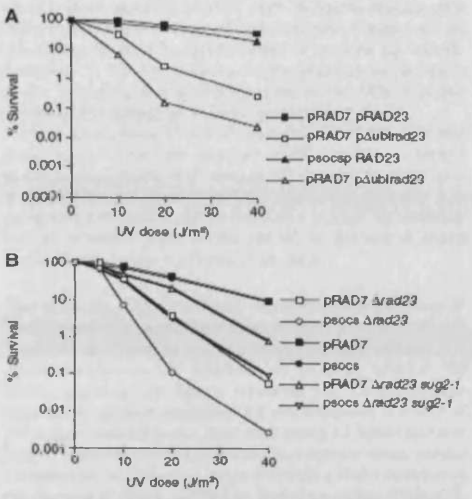

Figure 5 (**A**) UV survival of the Sc507-derived strains transformed with a centromeric vector expressing either full-length Rad23 from its endogenous promoter (pRAD23) or Rad23 deleted of the Ubl domain (pΔublrad23). (**B**) UV survival of the Sc507-derived strains listed.

The Rad7 E3 ligase functions in a pathway different from the Rad23/19S RC activity

Mutations in specific 19S RC subunits including *sug2-1* can rescue the defect in lesion removal caused by the loss of the ubl domain of Rad23 protein (Gillette *et al*, 2001). Since our observations show that the roles of Rad23 and the Rad7 E3 ligase functionally overlap, we reasoned that, in the absence of Rad23, ubiquitination of Rad4 could compensate for the loss of the Rad23 ubl domain, either by recruiting the 19S RC or functionally influencing the 19S RC activity. We tested this hypothesis by adding the *sug2-1* mutation to the UV-sensitive Δ*rad23*, psocs, strain. Adding the 19S RC mutation to the Δ*rad23*, psocs strain could result in a number of different outcomes. Conceivably, it could have no effect on UV survival of the Δ*rad23*, psocs strain (if the function of the E3 ligase was to recruit the 19S RC), or it could rescue UV sensitivity to the same level as the Δ*rad23*, *sug2-1* mutant strain (if the E3 ligase functionally affected the 19S activity). Finally, it could result in an intermediate UV phenotype (which would be consistent with a function that was independent of the 19S RC activity). Figure 5B shows that the *sug2-1* mutation displays an intermediate UV phenotype, partially rescuing the *psocs*, Δ*rad23* double mutant, but to a level less than the Δ*rad23*, *sug2-1* strain. This observation is consistent with the Rad7-containing E3 ligase activity functioning in a pathway different from the Rad23/19S activity. An alternative interpretation is that the 19S mutant, which partially rescues the Δ*rad23* phenotype, can no longer rescue the Δ*rad23* phenotype in the background of a pSOCS strain, but now instead partially rescues the loss of Rad7 E3 ligase function. We do not favour this interpretation.

NER in Δrad23 cells requires de novo protein synthesis

Since the Rad7-containing E3 ligase activity functions in a pathway different from the Rad23/19S RC activity, we next turned our attention to exploring how these two pathways might differ. In the absence of Rad23 protein, the rate of NER is markedly reduced (Mueller and Smerdon, 1996). Optimal rates of NER in yeast cells are determined by two components, one that requires *de novo* protein synthesis and the other that does not (Waters *et al*, 1993; Al-Moghrabi *et al*, 2003). We speculated that the slow rate of NER observed in Δ*rad23* cells might result from the loss of one of these components. It has been shown previously that blocking protein synthesis with cycloheximide reduces the efficiency of NER in yeast (Al-Moghrabi *et al*, 2003). We confirmed this observation by pretreating cells with cycloheximide prior to, and following exposure to, UV radiation, and measuring cyclobutane pyrimidine dimer (CPD) removal from the genome overall in a WT strain (Figure 6). We confirmed the inhibition of *de novo* protein synthesis by cycloheximide by examining cyclophilin levels as described earlier (Figure 1). Cycloheximide reduced the efficiency of CPD removal during NER in response to UV radiation over the 3-h period examined, confirming earlier studies (Al-Moghrabi *et al*, 2003). In

contrast to WT cells, when Δ*rad23* cells were treated with cycloheximide prior to UV irradiation, the rate of lesion removal was reduced to almost undetectable levels (Figure 6). Pretreating Δ*rad23* cells with cycloheximide does not affect Rad4 protein levels (Figure 1A). These results demonstrate that NER in Δ*rad23* cells is dependent on *de novo* protein synthesis.

The Rad23-mediated nonproteolytic activity of the 19S RC regulates NER pathway I

Mutations in the 19S RC accelerate the rate of lesion removal in Δ*rad23* cells (Gillette *et al*, 2001). To determine whether *de novo* protein synthesis is necessary for this phenomenon, we examined repair in Δ*rad23*, *sug1-20* double-mutant cells in the presence and absence of cycloheximide. Figure 6 shows that lesion removal in Δ*rad23* cells is rescued by specific mutations in the 19S RC even in the presence of cycloheximide, indicating that this component of the NER response occurs independently of *de novo* protein synthesis.

Collectively, these observations indicate that there are two components to the NER response to UV damage: pathway I occurs independently of *de novo* protein synthesis; pathway II is dependent on *de novo* protein synthesis. Pathway I is coregulated by Rad23, which functions, in part, by attenuating the inhibitory effect of the 19S RC on the rate of lesion removal (see Figure 7; Gillette *et al*, 2001).

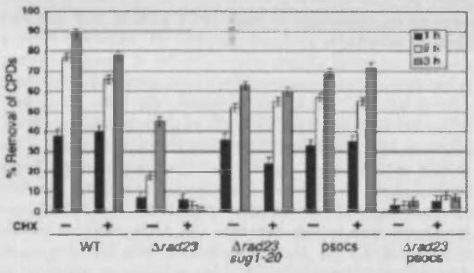

Figure 6 Time course of CPD removal as measured by slot blot assay (see Materials and methods). Strains indicated were treated with cycloheximide (+) or untreated (−). Times indicated refer to recovery times post-UV (h).

The Rad7 E3 ubiquitin ligase regulates NER pathway II

The dependence of pathway II on *de novo* protein synthesis suggests that it may be part of a transcriptional response that operates following UV radiation. To examine whether the Rad7-containing E3 ligase regulates the cycloheximide-dependent pathway (pathway II), we examined the rate of UV lesion removal in the Rad7-containing E3 ligase-mutated strain. While UV survival is normal in the *psocs* strain, careful examination of UV lesion removal shows a slight decrease in the amount of lesion removal at later time points (Figure 6). In contrast to the WT strain, the (reduced) level of lesion removal observed in the *psocs* strain is not affected by cycloheximide. This suggests that the *psocs* strain is specifically defective in pathway II that requires *de novo* protein synthesis. Consistent with this interpretation, NER in the *psocs*, Δ*rad23* double mutant is almost undetectable, and is not affected by the addition of cycloheximide (Figure 6).

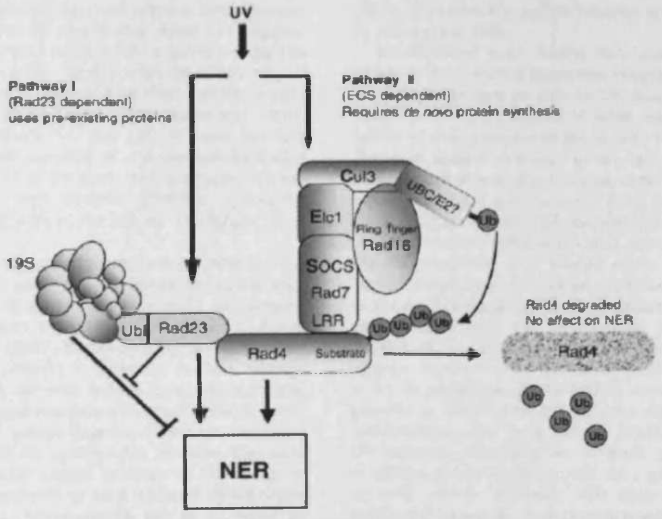

Figure 7 Regulation of the parallel pathways that regulate the NER response to UV. Pathway I is regulated by Rad23 and operates independently of *de novo* protein synthesis. Rad23 functions, in part, by attenuating the inhibitory effect of the 19S proteasome on the rate of lesion removal. Pathway II relies on *de novo* protein synthesis and the ubiquitination of Rad4 via the action of the ECS ligase, depicted in the centre of the figure. Subsequently, Rad4 is degraded via the 26S proteasome, with *de novo* synthesis eventually restoring Rad4 to its pre-UV levels.

Discussion

We have demonstrated that, after exposing cells to UV radiation, the NER response is comprised of two components, based on their requirement for *de novo* protein synthesis. Pathway I requires the interaction of Rad23 protein and the 19S RC, and functions independently of *de novo* protein synthesis. Pathway II requires the novel Rad7-containing E3 ubiquitin ligase and depends on *de novo* protein synthesis. Both pathways require distinct nonproteolytic activities of the UPP system (see Figure 7). Our observations show that the NER defect associated with Δ*rad23* cells is related to the rate at which DNA damage is removed after UV, which likely accounts for the moderate UV sensitivity of the Δ*rad23* strain. Adding cycloheximide to Δ*rad23* cells severely reduces repair, showing that NER in these cells is dependent on *de novo* protein synthesis. In contrast, a strain expressing a Rad7 protein mutated in the SOCS box domain relies on pathway I for NER. The rate of repair in this mutant strain is reduced at later times after UV radiation, and is not affected by the addition of cycloheximide. No significant effect on UV survival is observed in the Rad7-containing E3 ligase mutant strain (*rad7, socs*), suggesting that, under the conditions tested, pathway I primarily influences UV survival. A strain lacking both Rad23 and the Rad7-containing ECS E3 ligase activity shows a decrease in UV survival and almost no lesion removal in the time periods examined. UV survival in this strain is not as sensitive as a strain mutated in a core NER factor. This suggests that, while these pathways regulate the rate of NER, a low level of NER still occurs.

The NER and the UPPs combine to promote efficient DNA repair and UV survival (Schauber *et al*, 1998; Russell *et al*, 1999; Bertolaet *et al*, 2001b; Gillette *et al*, 2001; Lommel *et al*, 2002; Ng *et al*, 2002; Sweder and Madura, 2002; Ramsey *et al*, 2004). Rad23 protein coordinates these two systems. Our earlier work revealed a nonproteolytic activity of the 19S RC that functioned in NER. Significantly, inhibition of proteolysis both *in vivo* and *in vitro* had no effect on NER even in the absence of Rad23 (Russell *et al*, 1999; Gillette *et al*, 2001). However, specific defects in the 19S RC can partially rescue the loss of NER function of a strain lacking Rad23 (Gillette *et al*, 2001). Here we show that this rescue occurs independently of *de novo* protein synthesis, suggesting that the nonproteolytic role of the 19S RC specifically functions in pathway I.

An understanding of the relationship between NER and the proteasome has been made difficult following reports suggesting that the levels of the mouse XPC protein and its yeast homolog Rad4 protein are modulated by proteolysis (Lommel *et al*, 2002; Ng *et al*, 2003). It was also suggested that the stabilization of both proteins in response to DNA damage regulated NER and UV survival. In both cases, these studies involved the use of tagged versions of XPC and Rad4 proteins. In both instances, the epitope-tagged proteins have reduced half-lives compared to the endogenous proteins. Exposure of cells containing these tagged proteins to UV radiation results in what is interpreted to be a transient stabilization of XPC/Rad4 protein. These results led to a model in which proteolysis by the 26S proteasome was responsible for the continual turnover of Rad4/XPC protein. The model suggested that, following UV damage, proteolytic degradation of Rad4/XPC protein by the 26S proteasome was attenuated, resulting in accumulation of this repair factor and enhancement of NER (Lommel *et al*, 2002; Ng *et al*, 2003).

In contrast, our studies show that this is not the case when antibodies against endogenous Rad4 protein are used. We show that native Rad4 protein is stable, with a half-life of around 4 h (Figure 1A and Supplementary data S3). Upon UV exposure, steady-state levels of Rad4 protein rapidly decrease, due to increased proteolysis by the proteasome. It is known that the Ubl domain and the Rad4 interacting domain of Rad23 protein are functionally distinct (Bertolaet *et al*, 2001a, b; Gillette *et al*, 2001), and it has been suggested that the Rad4-binding domain of Rad23 protected Rad4 from degradation by the 26S proteasome. It is clear that, in the absence of Rad23, steady-state levels of Rad4 are reduced, but the cause of reduced Rad4 levels and whether they directly affect NER have not been established. We show that the reduced levels of Rad4 in *Rad23*-deleted cells are not due to increased proteolysis of Rad4 in these cells, but rather due to reduced production of Rad4 transcript. Our results reveal the mechanism of reduced Rad4 levels in these cells. Although Rad4 protein levels are reduced in Δ*rad23* cells, stabilization of Rad4 in proteolytic defective mutants has no effect on the NER defective phenotype of a Δ*rad23* strain. Others have shown that overexpressing Rad4 in a Δ*rad23* background has only a minor affect in rescuing UV survival (Xie *et al*, 2004). These observations suggest that stabilization of Rad4 *per se* plays no significant role in UV survival. The relationship between steady-state levels of Rad23 and its binding partner is also observed in mammalian cells, where the lack of hHR23A/B results in lowered steady-state levels of XPC (Ng *et al*, 2003; Okuda *et al*, 2004). However, unlike yeast, in mammalian cells the half-life of XPC decreases (Okuda *et al*, 2004). At present it is unclear whether proteolysis plays a role in mammalian NER.

We identified Rad7, Rad16, Elc1, and Cul3 as part of an ECS-type E3 ubiquitin ligase that ubiquitinates Rad4 protein following exposure of cells to UV radiation. This complex ubiquitinates Rad4 protein *in vitro*. We do not observe a ladder of ubiquitination in the *in vitro* reaction, nor *in vivo*. However, Rad4 is degraded by the 26S proteasome *in vivo*, suggesting that polyubiquitination does occur. Specific point mutations within the conserved SOCS domain of Rad7 protein inhibit the UV-induced ubiquitination of Rad4 protein *in vivo*. Our results show that the *rad7, psocs* mutation increases the UV sensitivity of a Δ*rad23* strain, even though Rad4 protein is stabilized. In contrast, stabilization of Rad4 protein in the Δ*rad23* strain, by direct inhibition of 26S proteasome proteolytic activity, has no effect on NER (see Figure 4; Gillette *et al*, 2001). These observations show that the changes observed in the stability of Rad4 protein in response to UV do not influence NER and UV survival. Therefore, it is possible to differentiate between the effect of Rad4 protein ubiquitination and Rad4 protein degradation on NER and UV survival. Ubiquitination of Rad4 protein in response to UV specifically regulates NER via a pathway that requires *de novo* protein synthesis. This event directly influences NER and UV survival. Rad4 protein is subsequently degraded by the UPP, and this event does not directly influence NER or UV survival. We suggest that this mechanism restores cellular Rad4 protein levels to the un-ubiquitinated, pre-UV state.

Speculation

The two major NER pathways, transcription-coupled repair (TCR) and GGR are functionally conserved in yeast and human cells (Hoeijmakers, 1993). In yeast, Rad7 and Rad16 specifically function in the GGR pathway (Verhage *et al*, 1996). No structural homologues for these proteins have been found in mammalian cells. Recently, however, Groisman *et al* (2003) have isolated two distinct protein complexes that differ only in that one contains the DDB2 protein and the other CSA. The DDB1/2 complex functions in GGR and the DDB1/CSA complex in TCR. Both of these complexes contain a cullin (Cul4a) and a RING-finger protein (Roc1), and both are components of cullin-based E3 ubiquitin ligases (Pintard *et al*, 2004; Willems *et al*, 2004). It has been shown that this novel E3 ligase ubiquitinates XPC, the mammalian homologue of Rad4 protein (Sugasawa *et al*, 2005). The authors demonstrate that it is the ubiquitination of XPC protein that influences NER rather than degradation of the protein. XPC protein ubiquitination alters the DNA damage binding characteristics of the XPC/Rad23/centrin complex, and this may alter the way in which NER promotes lesion recognition. These observations suggest striking parallels between the regulation of NER in the yeast and human systems. It appears that functional conservation of the major NER pathways may have been maintained.

Materials and methods

Yeast strains and plasmids

The yeast strains used in this study are WCG4a (WT) and YH129/14 (*pre1-1 pre4-1*) (Gillette *et al*, 2001). Research Genetics parental strain BY4741, 2782 (*Δelc1*), 1982 (*Δela1*), 4633 (*Δcul3*), Sc507 (WT), Sc507R7 (*Δrad7*) and Sc507R23 (*Δrad23*) were described (Gillette *et al*, 2001). The deletion of *RAD23* in the Research Genetics strains were constructed as described (Gillette *et al*, 2001). Creation of the Rad7 SOCS box mutation was achieved by site-directed mutagenesis of the WT *RAD7* gene cloned in pRS314 as described (Reed *et al*, 1998). Two point mutations were made, resulting in the amino-acid substitutions, L168A and C172A, within the conserved SOCS box domain. Creation of the Rad16 RING-finger domain mutation was achieved by site-directed mutagenesis of the WT *RAD16* gene cloned in pRS314 as described (Reed *et al*, 1998; data not shown). Two point mutations were made, resulting in the amino-acid substitutions, C552A and H554A, within the RING-finger domain. Strains expressing Ubl-deleted versions of Rad23 were created as described (Russell *et al*, 1999).

In vitro expression of Rad4 protein

The following primers were used to generate the Rad4 coding sequence.

FWD: 5′AAGAGTACTTAATACGACTCACTATAGGAACAGCCACCATGAATGAAGACCTGCCCAA3′/REV: 5′TTTTTTTTTTTTTTTTTTTTTTTTTTTTTTTTTTTAATCAGTCTGATTCCTCTGACATCT3′. PCR was performed using genomic DNA as the template. The purification of PCR product is performed as described (TNT, Promega), with the following exceptions. A total of 10 tubes of PCR product are pooled and precipitated with the same volume of 99% alcohol (−20°C) overnight (spin down at 13 000 r.p.m. for 15 min). The pellet was dried for 30 min. The pellet was redissolved with ddH_2O (pH 7–8) for at least 30 min with occasional gentle vortexing. Short-term storage was at −20°C.

Expression of Rad4 protein via coupled in vitro transcription/translation

The TNT® T7 PCR Quick Master Mix was thawed rapidly and placed on ice along with the other components. The reaction components were assembled in a 0.5 ml thin-wall tube according to the manufacturer's protocol (TNT, Promega). After addition of all the components, they were gently mixed by pipetting. The reaction was incubated at 30°C for 60–70 min. The results of the coupled *in vitro* transcription/translation reaction were analysed by Western blotting following SDS–PAGE gel electrophoresis.

Ubiquitylation reaction of Rad4 protein

The ubiquitylation reaction contains 1 μg E1 (Yeast), 1 μg hUbc4a, 1 μg hUbc4b, 13 μg hUbc4c, 0.1 μg GGR complex, 6 μl 5 × reaction buffer (20 mM $MgCl_2$, 200 mM KCl 180 mM Tris, pH 8.0), 6 μl ATP (20 mM), 2 μl of TNT-expressed Rad4 protein, or an empty vector control. The ubiquitylation reaction is initiated by adding 5 μl ubiquitin and then ddH_2O to a total volume of 30 μl. It is incubated at 28°C for 60 min. After the reaction is finished, the product is run on SDS–PAGE gels immediately.

Analysis of Rad4 protein stability and UV survival

Yeast protein extracts were prepared by bead beating in yeast dialysis buffer as described (Reed *et al*, 1999). Western analysis and immunoprecipitation of Rad4 protein was performed using standard methods, using the antibodies mentioned in the Results. Anti-Rad4 antibody was raised against a specific Rad4 peptide (Affiniti Research Products Limited). Anti-ubiquitin antibody was generated by genetic immunization as described (Barry and Johnston, 1997). Pulse-chase experiments were performed by growing cells to a density of about 1–2 × 10^7 cells/ml, pelleted, and washed twice with PBS. Cells were resuspended in appropriate media and a pulse of 25 μCi ^{35}S-methionine per ml was applied at 30°C for 1 h. Cells were then pelleted, washed, and resuspended in YPD for the times indicated. Post-UV cellular survival was measured by plating yeast cells onto the appropriate growth medium prior to UV irradiation at the doses stated. The precise details of the UV survival experiments are described elsewhere (Gillette *et al*, 2001).

Analysis of CPD removal following UV radiation

The slot blot analysis of lesion removal by NER in genomic DNA has been described in detail previously (Reed *et al*, 1999). Where appropriate, cycloheximide was added to a final concentration of 2 μg/ml.

Northern analysis

The hot phenol method was used for RNA isolation and Northern blotting was described previously (Teng *et al*, 2002). The probes used are shown below:

Upper_Rad4(NTS25):	biotin-ACTGATCGAAGTTTTTGCACCAACG ATGATA
Lower_Rad4(TS25):	CATAAAATCCGAATAATCCTCCCCG
Actin_NTS:	biotin-GCCGGTTTTGCCGGTGACG
Actin_TS:	CCGGCAGATTCCAAACCCAAAA

Supplementary data

Supplementary data are available at *The EMBO Journal* Online.

Acknowledgements

We thank Yue Xiong for the gift of the Cul3 antibody. This research was supported by MRC CDA and CEG awards to SHR. The work was conducted in the CBI at UT Southwestern during a sabbatical period supported by an MRC CDA to SHR, and at the School of Medicine, Cardiff University.

References

Al-Moghrabi NM, Al-Sharif IS, Aboussekhra A (2003) UV-induced *de novo* protein synthesis enhances nucleotide excision repair efficiency in a transcription-dependent manner in *S. cerevisiae*. *DNA Repair (Amst)* 2: 1185–1197

Barry MA, Johnston SA (1997) Biological features of genetic immunization. *Vaccine* 15: 788–791

Bertolaet BL, Clarke DJ, Wolff M, Watson MH, Henze M, Divita G, Reed SI (2001a) UBA domains mediate protein–protein inter-

actions between two DNA damage inducible proteins. *J Mol Biol* 313: 955–963

Bertolaet BL, Clarke DJ, Wolff M, Watson MH, Henze M, Divita G, Reed SI (2001b) UBA domains of DNA damage-inducible proteins interact with ubiquitin. *Nat Struct Biol* 8: 417–422

Chambers RS, Johnston SA (2003) High-level generation of polyclonal antibodies by genetic immunization. *Nat Biotechnol* 21: 1088–1092

Ciechanover A, Ben-Saadon R (2004) N-terminal ubiquitination: more protein substrates join in. *Trends Cell Biol* 14: 103–106

Dupre S, Urban-Grimal D, Haguenauer-Tsapis R (2004) Ubiquitin and endocytic internalization in yeast and animal cells. *Biochim Biophys Acta* 1695: 89–111

Ferdous A, Gonzalez F, Sun L, Kodadek T, Johnston SA (2001) The 19S regulatory particle of the proteasome is required for efficient transcription elongation by RNA polymerase II. *Mol Cell* 7: 981–991

Ferdous A, Kodadek T, Johnston SA (2002) A nonproteolytic function of the 19S regulatory subunit of the 26S proteasome is required for efficient activated transcription by human RNA polymerase II. *Biochemistry* 41: 12798–12805

Friedberg EC (2001) How nucleotide excision repair protects against cancer. *Nat Rev Cancer* 1: 22–33

Gillette TG, Gonzalez F, Delahodde A, Johnston SA, Kodadek T (2004) Physical and functional association of RNA polymerase II and the proteasome. *Proc Natl Acad Sci USA* 101: 5904–5909

Gillette TG, Huang W, Russell SJ, Reed SH, Johnston SA, Friedberg EC (2001) The 19S complex of the proteasome regulates nucleotide excision repair in yeast. *Genes Dev* 15: 1528–1539

Glickman MH, Ciechanover A (2002) The ubiquitin-proteasome proteolytic pathway: destruction for the sake of construction. *Physiol Rev* 82: 373–428

Gonzalez F, Delahodde A, Kodadek T, Johnston SA (2002) Recruitment of a 19S proteasome subcomplex to an activated promoter. *Science* 296: 548–550

Groisman R, Polanowska J, Kuraoka I, Sawada J, Saijo M, Drapkin R, Kisselev AF, Tanaka K, Nakatani Y (2003) The ubiquitin ligase activity in the DDB2 and CSA complexes is differentially regulated by the COP9 signalosome in response to DNA damage. *Cell* 113: 357–367

Hanawalt PC (2001) Controlling the efficiency of excision repair. *Mutat Res* 485: 3–13

Heessen S, Masucci MG, Dantuma NP (2005) The UBA2 domain functions as an intrinsic stabilization signal that protects Rad23 from proteasomal degradation. *Mol Cell* 18: 225–235

Ho Y, Gruhler A, Heilbut A, Bader GD, Moore L, Adams SL, Millar A, Taylor P, Bennett K, Boutilier K, Yang L, Wolting C, Donaldson I, Schandorff S, Shewnarane J, Vo M, Taggart J, Goudreault M, Muskat B, Alfarano C, Dewar D, Lin Z, Michalickova K, Willems AR, Sassi H, Nielsen PA, Rasmussen KJ, Andersen JR, Johansen LE, Hansen LH, Jespersen H, Podtelejnikov A, Nielsen E, Crawford J, Poulsen V, Sorensen BD, Matthiesen J, Hendrickson RC, Gleeson F, Pawson T, Moran MF, Durocher D, Mann M, Hogue CW, Figeys D, Tyers M (2002) Systematic identification of protein complexes in *Saccharomyces cerevisiae* by mass spectrometry. *Nature* 415: 180–183

Hochstrasser M, Ellison MJ, Chau V, Varshavsky A (1991) The short-lived MAT alpha 2 transcriptional regulator is ubiquitinated *in vivo*. *Proc Natl Acad Sci USA* 88: 4606–4610

Hoeijmakers JH (1993) Nucleotide excision repair. II: From yeast to mammals. *Trends Genet* 9: 211–217

Lee DH, Goldberg AL (1996) Selective inhibitors of the proteasome-dependent and vacuolar pathways of protein degradation in *Saccharomyces cerevisiae*. *J Biol Chem* 271: 27280–27284

Lommel L, Ortolan T, Chen L, Madura K, Sweder KS (2002) Proteolysis of a nucleotide excision repair protein by the 26 S proteasome. *Curr Genet* 42: 9–20

Mueller JP, Smerdon MJ (1996) Rad23 is required for transcription-coupled repair and efficient overall repair in *Saccharomyces cerevisiae*. *Mol Cell Biol* 16: 2361–2368

Ng JM, Vermeulen W, van der Horst GT, Bergink S, Sugasawa K, Vrieling H, Hoeijmakers JH (2003) A novel regulation mechanism of DNA repair by damage-induced and RAD23-dependent stabilization of *Xeroderma pigmentosum* group C protein. *Genes Dev* 17: 1630–1645

Ng JM, Vrieling H, Sugasawa K, Ooms MP, Grootegoed JA, Vreeburg JT, Visser P, Beems RB, Gorgels TG, Hanaoka F, Hoeijmakers JH, van der Horst GT (2002) Developmental defects and male sterility in mice lacking the ubiquitin-like DNA repair gene mHR23B. *Mol Cell Biol* 22: 1233–1245

Okuda Y, Nishi R, Ng JM, Vermeulen W, van der Horst GT, Mori T, Hoeijmakers JH, Hanaoka F, Sugasawa K (2004) Relative levels of the two mammalian Rad23 homologs determine composition and stability of the *Xeroderma pigmentosum* group C protein complex. *DNA Repair (Amsterdam)* 3: 1285–1295

Ortolan TG, Chen L, Tongaonkar P, Madura K (2004) Rad23 stabilizes Rad4 from degradation by the Ub/proteasome pathway. *Nucleic Acids Res* 32: 6490–6500

Pickart CM (2004) Back to the future with ubiquitin. *Cell* 116: 181–190

Pintard L, Willems A, Peter M (2004) Cullin-based ubiquitin ligases: Cul3–BTB complexes join the family. *EMBO J* 23: 1681–1687

Ramsey KL, Smith JJ, Dasgupta A, Maqani N, Grant P, Auble DT (2004) The NEF4 complex regulates Rad4 levels and utilizes Snf2/Swi2-related ATPase activity for nucleotide excision repair. *Mol Cell Biol* 24: 6362–6378

Reed SH, Akiyama M, Stillman B, Friedberg EC (1999) Yeast autonomously replicating sequence binding factor is involved in nucleotide excision repair. *Genes Dev* 13: 3052–3058

Reed SH, You Z, Friedberg EC (1998) The yeast RAD7 and RAD16 genes are required for postincision events during nucleotide excision repair. *In vitro* and *in vivo* studies with rad7 and rad16 mutants and purification of a Rad7/Rad16-containing protein complex. *J Biol Chem* 273: 29481–29488

Russell SJ, Johnston SA (2001) Evidence that proteolysis of Gal4 cannot explain the transcriptional effects of proteasome ATPase mutations. *J Biol Chem* 276: 9825–9831

Russell SJ, Reed SH, Huang W, Friedberg EC, Johnston SA (1999) The 19S regulatory complex of the proteasome functions independently of proteolysis in nucleotide excision repair. *Mol Cell* 3: 687–695

Salghetti SE, Caudy AA, Chenoweth JG, Tansey WP (2001) Regulation of transcriptional activation domain function by ubiquitin. *Science* 293: 1651–1653

Schauber C, Chen L, Tongaonkar P, Vega I, Lambertson D, Potts W, Madura K (1998) Rad23 links DNA repair to the ubiquitin/proteasome pathway. *Nature* 391: 715–718

Strous GJ, Govers R (1999) The ubiquitin-proteasome system and endocytosis. *J Cell Sci* 112 (Part 10): 1417–1423

Sugasawa K, Okuda Y, Saijo M, Nishi R, Matsuda N, Chu G, Mori T, Iwai S, Tanaka K, Hanaoka F (2005) UV-induced ubiquitylation of XPC protein mediated by UV-DDB-ubiquitin ligase complex. *Cell* 121: 387–400

Sweder K, Madura K (2002) Regulation of repair by the 26S proteasome. *J Biomed Biotechnol* 2: 94–105

Teng Y, Yu Y, Waters R (2002) The *Saccharomyces cerevisiae* histone acetyltransferase Gcn5 has a role in the photoreactivation and nucleotide excision repair of UV-induced cyclobutane pyrimidine dimers in the MFA2 gene. *J Mol Biol* 316: 489–499

Verhage RA, van Gool AJ, de Groot N, Hoeijmakers JH, van de Putte P, Brouwer J (1996) Double mutants of *Saccharomyces cerevisiae* with alterations in global genome and transcription-coupled repair. *Mol Cell Biol* 16: 496–502

Wang Z, Wei S, Reed SH, Wu X, Svejstrup JQ, Reaver WJ, Kornberg RD, Friedberg EC (1997) The RAD7, RAD16, and RAD23 genes of *Saccharomyces cerevisiae*: requirement for transcription-independent nucleotide excision repair *in vitro* and interactions between the gene products. *Mol Cell Biol* 17: 635–643

Waters R, Zhang R, Jones NJ (1993) Inducible removal of UV-induced pyrimidine dimers from transcriptionally active and inactive genes of *Saccharomyces cerevisiae*. *Mol Gen Genet* 239: 28–32

Watkins JF, Sung P, Prakash L, Prakash S (1993) The *Saccharomyces cerevisiae* DNA repair gene RAD23 encodes a nuclear protein containing a ubiquitin-like domain required for biological function. *Mol Cell Biol* 13: 7757–7765

Willems AR, Schwab M, Tyers M (2004) A hitchhiker's guide to the cullin ubiquitin ligases: SCF and its kin. *Biochim Biophys Acta* 1695: 133–170

Xie Z, Liu S, Zhang Y, Wang Z (2004) Roles of Rad23 protein in yeast nucleotide excision repair. *Nucleic Acids Res* 32: 5981–5990

References

Aas, P.A., Otterlei, M., Falnes, P.O., Vagbo, C.B., Skorpen, F., Akbari, M., Sundheim, O., Bjoras, M., Slupphaug, G., Seeberg, E., Krokan, H.E. (2003) Human and bacterial oxidative demethylases repair alkylation damage in both RNA and DNA. ***Nature*** 421, 859-863.

Aboussekhra, A., Biggerstaff, M., Shivji, M.K., Vilpo, J.A., Moncollin, V., Podust, V.N., Protic, M., Hubscher, U., Egly, J.M., Wood, R.D. (1995) Mammalian DNA nucleotide excision repair reconstituted with purified protein components. ***Cell*** 80, 859-868.

Aboussekhra, A., and Thoma, F. (1998) Nucleotide excision repair and photolyase preferentially repair the nontranscribed strand of RNA polymerase III-transcribed genes in *saccharomyces cerevisiae*. ***Genes Dev*** 12, 411-421.

Andrews, A.D., Barrett, S.F., Yoder, F.W., Robbins, J.H. (1978) Cockayne's syndrome fibroblasts have increased sensitivity to ultraviolet light but normal rates of unscheduled DNA synthesis. ***J Invest Dermatol*** 70, 237-239.

Araki, M., Masutani, C., Takemura, M., Uchida, A., Sugasawa, K., Kondoh, J., Ohkuma, Y., Hanaoka, F. (2001) Centrosome protein centrin 2/caltractin 1 is part of the xeroderma pigmentosum group C complex that initiates global genome nucleotide excision repair. ***J Biol Chem*** 276, 18665-18672.

Asahina, H., Kuraoka, I., Shirakawa, M., Morita, E.H., Miura, N., Miyamoto, I., Ohtsuka, E., Okada, Y., Tanaka, K. (1994) The XPA protein is a zinc metalloprotein with an ability to recognize various kinds of DNA damage. ***Mutat Res*** 315, 229-237.

Axelrod, J.D., Reagan, M.S., Majors, J. (1993) Gal4 disrupts a repressing nucleosome during activation of Gal1 transcription *in vivo*. ***Genes Dev*** 7, 857-869.

Bailly, V., Sommers, C.H., Sung, P., Prakash, L., Prakash, S. (1992) Specific complex formation between proteins encoded by the yeast DNA repair and recombination genes RAD1 and RAD10. ***Proc Natl Acad Sci USA*** 89, 8273-8277.

Balajee, A.S., May, A., Dianov, G.L., Friedberg, E.C., Bohr, V.A. (1997) Reduced RNA polymerase II transcription in intact and permeabilized cockayne syndrome group B cells. ***Proc Natl Acad Sci USA*** 94, 4306-4311.

Bang, D.D., Verhage, R., Goosen, N., Brouwer, J., van de Putte, P. (1992) Molecular cloning of RAD16, a gene involved in differential repair in *saccharomyces cerevisiae*. ***Nucleic Acids Res*** 20, 3925-3931.

Bankmann, M., Prakash, L., Prakash, S. (1992) Yeast RAD14 and human xeroderma pigmentosum group A DNA-repair genes encode homologous proteins. ***Nature*** 355, 555-558.

Bardwell, A.J., Bardwell, L., Iyer, N., Svejstrup, J.Q., Feaver, W.J., Kornberg, R.D., Friedberg, E.C. (1994) Yeast nucleotide excision repair proteins Rad2 and Rad4 interact with RNA polymerase II basal transcription factor b (TFIIH). ***Mol Cell Biol*** 14, 3569-3576.

Barnes, D.E., Johnston, L.H., Kodama. K., Tomkinson. A.E., Lasko, D.D., Lindahl, T. (1990) Human DNA ligase I cDNA: cloning and functional expression in *Saccharomyces cerevisiae*. ***Proc Natl Acad Sci USA*** 87(17):6679-6683.

Barnes, D.E., Tomkinson, A.E., Lehmann, A.R., Webster, A.D., Lindahl, T. (1992) Mutations in the DNA ligase I gene of an individual with immunodeficiencies and cellular hypersensitivity to DNA-damaging agents. ***Cell*** 69, 495-503.

Barry, M.A., Johnston, S.A. (1997) Biological features of genetic immunization. ***Vaccine*** 15(8):788-791.

Batty, D.P., and Wood, R.D. (2000) Damage recognition in nucleotide excision repair of DNA. ***Gene*** 241, 193-204.

Baumeister, W., Walz, J., Zuhl, F., Seemuller, E. (1998) The proteasome: Paradigm of a self-compartmentalizing protease. ***Cell*** 92, 367-380.

Beard, W.A. and Wilson, S.H. (2000) Structural design of a eukaryotic DNA repair polymerase: DNA polymerase beta. ***Mutat Res*** 460, 231-244.

Beaudenon, S.L., Huacani, M.R., Wang, G., McDonnell, D.P., Huibregtse, J.M. (1999) Rsp5 ubiquitin-protein ligase mediates DNA damage-induced degradation of the large subunit of RNA polymerase II in *saccharomyces cerevisiae*. ***Mol Cell Biol*** 19, 6972-6979.

Becker, M.M., and Wang, J.C. (1984) Use of light for footprinting DNA *in vivo*. ***Nature*** 309, 682-687.

Bertolaet, B.L., Clarke, D.J., Wolff, M., Watson, M.H., Henze, M., Divita, G., Reed, S.I. (2001a) Uba domains mediate protein-protein interactions between two DNA

damage-inducible proteins. ***J Mol Biol*** 313, 955-963.

Bertolaet, B.L., Clarke, D.J., Wolff, M., Watson, M.H., Henze, M., Divita, G., Reed, S.I. (2001b) Uba domains of DNA damage-inducible proteins interact with ubiquitin. ***Nat Struct Biol*** 8, 417-422.

Bessho, T., Sancar, A., Thompson, L.H., Thelen, M.P. (1997) Reconstitution of human excision nuclease with recombinant XPF-ERCC1 complex. ***J Biol Chem*** 272, 3833-3837.

Bhatia, P.K., Verhage, R.A., Brouwer, J., Friedberg, E.C. (1996) Molecular cloning and characterization of *saccharomyces cerevisiae* RAD28, the yeast homolog of the human cockayne syndrome a (CSA) gene. ***J Bacteriol*** 178, 5977-5988.

Bienko, M., Green, C.M., Crosetto, N., Rudolf, F., Zapart, G., Coull, B., Kannouche, P., Wider, G, Peter, M., Lehmann, A.R., Hofmann, K., Dikic, I. (2005) Ubiquitin-binding domains in Y-family polymerases regulate translesion synthesis. ***Science*** 310(5755):1821-1824.

Biggins, S., Ivanovska, I., Rose, M.D. (1996) Yeast ubiquitin-like genes are involved in duplication of the microtubule organizing center. ***J Cell Biol*** 133(6):1331-1346.

Blackwell, L.J. and Borowiec, J.A. (1994) Human replication protein a binds single-stranded DNA in two distinct complexes. ***Mol Cell Biol*** 14, 3993-4001.

Blackwell, L.J., Borowiec, J.A., Masrangelo, I.A. (1996) Single-stranded-DNA binding alters human replication protein a structure and facilitates interaction with DNA-dependent protein kinase. ***Mol Cell Biol*** 16, 4798-4807.

Bohr, V.A., Smith, C.A., Okumoto, D.S., Hanawalt, P.C. (1985) DNA repair in an active gene: Removal of pyrimidine dimers from the DHFR gene of CHO cells is much more efficient than in the genome overall. ***Cell*** 40, 359-369.

Boyer, L.A., Logie, C., Bonte, E., Becker, P.B., Wade, P.A., Wolffe, A.P., Wu, C., Imbalzano, A.N., Peterson, C.L. (2000) Functional delineation of three groups of the ATP-dependent family of chromatin remodeling enzymes. ***J Biol Chem*** 275, 18864-18870.

Brand, M., Moggs, J.G., Oulad-Abdelghani, M., Lejeune, F., Dilworth, F.J., Stevenin, J., Almouzni, G., Tora, L. (2001) UV-damaged DNA-binding protein in the TFTC complex links DNA damage recognition to nucleosome acetylation. ***Embo J*** 20, 3187-3196.

Bregman, D.B., Halaban, R., van Gool, A.J., Henning, K.A., Friedberg, E.C., Warren,

S.L. (1996) UV-induced ubiquitination of RNA polymerase II: A novel modification deficient in cockayne syndrome cells. ***Proc Natl Acad Sci USA*** 93, 11586-11590.

Brownell, J.E., Zhou, J., Ranalli, T., Kobayashi, R., Edmondson, D.G., Roth, S.Y., Allis, C.D. (1996) Tetrahymena histone acetyltransferase a: A homolog to yeast Gcn5p linking histone acetylation to gene activation. ***Cell*** 84, 843-851.

Budd, M.E., and Campbell, J.L. (1995) DNA polymerases required for repair of UV-induced damage in *saccharomyces cerevisiae*. ***Mol Cell Biol*** 15, 2173-2179.

Buschta-Hedayat, N., Buterin, T., Hess, M.T., Missura, M., Naegeli, H. (1999) Recognition of nonhybridizing base pairs during nucleotide excision repair of DNA. ***Proc Natl Acad Sci USA*** 96, 6090-6095.

Cadet, J., Sage, E., Douki, T. (2005) Ultraviolet radiation-mediated damage to cellular DNA. ***Mutat Res.*** 571(1-2):3-17.

Chen, L., Shinde, U., Ortolan, T.G., Madura, K. (2001) Ubiquitin-associated (uba) domains in RAD23 bind ubiquitin and promote inhibition of multi-ubiquitin chain assembly. ***EMBO Rep*** 2, 933-938.

Christians, F.C., and Hanawalt, P.C. (1992) Inhibition of transcription and strand-specific DNA repair by alpha-amanitin in Chinese hamster ovary cells. ***Mutat Res*** 274, 93-101.

Christians, F.C., and Hanawalt, P.C. (1993) Lack of transcription-coupled repair in mammalian ribosomal RNA genes. ***Biochemistry.*** 32(39):10512-10518.

Chu, G., and Chang, E. (1988) Xeroderma pigmentosum group E cells lack a nuclear factor that binds to damaged DNA. ***Science*** 242, 564-567.

Ciechanover, A. (1994) The ubiquitin-proteasome proteolytic pathway. ***Cell*** 79, 13-21.

Ciechanover, A., Heller, H., Elias, S., Haas, A.L., Hershko, A. (1980) ATP-dependent conjugation of reticulocyte proteins with the polypeptide required for protein degradation. ***Proc Natl Acad Sci USA*** 77, 1365-1368.

Citterio, E., Van Den Boom, V., Schnitzler, G., Kanaar, R., Bonte, E., Kingston, R.E., Hoeijmakers, J.H., Vermeulen, W. (2000) ATP-dependent chromatin remodeling by the cockayne syndrome b DNA repair-transcription-coupling factor. ***Mol Cell Biol*** 20, 7643-7653.

Cleaver, J.E. (1968) Defective repair replication of DNA in xeroderma pigmentosum. ***Nature*** 218, 652-656.

Cline, S.D., and Hanawalt, P.C. (2003) Who's on first in the cellular response to DNA damage? ***Nat Rev Mol Cell Biol*** 4, 361-372.

Clugston, C.K., McLaughlin, K., Kenny, M.K., Brown, R. (1992) Binding of human single-stranded DNA binding protein to DNA damaged by the anticancer drug cis-diamminedichloroplatinum (II). ***Cancer Res*** 52, 6375-6379.

Coin, F., Oksenych, V., Egly, J.M. (2007) Distinct roles for the XPB/p52 and XPD/p44 subcomplexes of TFIIH in damaged DNA opening during nucleotide excision repair. ***Mol Cell*** 26(2):245-256.

Coin, F., Proietti De Santis, L., Nardo, T., Zlobinskaya, O., Stefanini, M., Egly, J.M.(2006) p8/TTD-A as a repair-specific TFIIH subunit. ***Mol Cell.*** 21(2):215-226.

Conaway, R.C., and Conaway, J.W. (1989) An RNA polymerase II transcription factor has an associated DNA-dependent ATPase (dATPase) activity strongly stimulated by the tata region of promoters. ***Proc Natl Acad Sci USA*** 86, 7356-7360.

Conconi, A., Bespalov, V.A., Smerdon, M.J. (2002) Transcription-coupled repair in RNA polymerase I-transcribed genes of yeast. ***Proc Natl Acad Sci USA*** 99, 649-654.

Coverley, D., Kenny, M.K., Lane, D.P., Wood, R.D. (1992) A role for the human single-stranded DNA binding protein HSSB/RPA in an early stage of nucleotide excision repair. ***Nucleic Acids Res*** 20, 3873-3880.

Dammann, R., and Pfeifer, G.P. (1997) Lack of gene- and strand-specific DNA repair in RNA polymerase III-transcribed human tRNA genes. ***Mol Cell Biol*** 17, 219-229.

Datta, A., Bagchi, S., Nag, A., Shiyanov, P., Adami, G.R., Yoon, T., Raychaudhuri, P. (2001) The p48 subunit of the damaged-DNA binding protein DDB associates with the CBP/p300 family of histone acetyltransferase. ***Mutat Res*** 486, 89-97.

de Boer, J., and Hoeijmakers, J.H. (2000) Nucleotide excision repair and human syndromes. ***Carcinogenesis*** 21, 453-460.

de Boer, J.G. (2002) Polymorphisms in DNA repair and environmental interactions. ***Mutat Res*** 509, 201-210.

de Laat, W.L., Appeldoorn, E., Sugasawa, K., Weterings, E., Jaspers, N.G., Hoeijmakers, J.H. (1998) DNA-binding polarity of human replication protein a positions nucleases in nucleotide excision repair. ***Genes Dev.*** 12, 2598-2609.

Deckert, J., and Struhl, K. (2001) Histone acetylation at promoters is differentially

affected by specific activators and repressors. ***Mol Cell Biol*** 21, 2726-2735.

Demartino, G.N., Gillette, T.G. (2007) Proteasomes: machines for all reasons. ***Cell*** 129(4):659-662.

Dianov, G.L., Houle, J.F., Iyer, N., Bohr, V.A., Friedberg, E.C. (1997) Reduced RNA polymerase II transcription in extracts of cockayne syndrome and xeroderma pigmentosum/Cockayne syndrome cells. ***Nucleic Acids Res*** 25, 3636-3642.

Diffey, B. (2004) Climate change, ozone depletion and the impact on ultraviolet exposure of human skin. ***Phys Med Biol*** 49(1):R1-11.

Douki, T., Laporte, G.; Cadet, J. (2003) Inter-strand photoproducts are produced in high yield within a-DNA exposed to uvc radiation. ***Nucleic Acids Res*** 31, 3134-3142.

Drapkin, R., Reardon, J.T., Ansari, A., Huang, J.C., Zawel, L., Ahn, K., Sancar, A., Reinberg, D. (1994) Dual role of TFIIH in DNA excision repair and in transcription by RNA polymerase II. ***Nature*** 368, 769-772.

Drapkin, R., and Reinberg, D. (1994) The multifunctional TFIIH complex and transcriptional control. ***Trends Biochem Sci*** 19, 504-508.

Dresler, S.L., and Frattini, M.G. (1986) DNA replication and uv-induced DNA repair synthesis in human fibroblasts are much less sensitive than DNA polymerase alpha to inhibition by butylphenyl-deoxyguanosine triphosphate. ***Nucleic Acids Res*** 14, 7093-7102.

Downs, J.A., Nussenzweig, M.C., Nussenzweig, A. (2007) Chromatin dynamics and the preservation of genetic information. ***Nature*** 447(7147):951-958.

Dulbecco, R. (1949) Reactivation of ultra-violet-inactivated bacteriophage by visible light. ***Nature*** 162, 949–950.

Duncan, T., Trewick, S.C., Koivisto, P., Bates, P.A., Lindahl, T., Sedgwick, B. (2002) Reversal of DNA alkylation damage by two human dioxygenases. ***Proc Natl Acad Sci USA*** 99, 16660-16665.

Durr, H., Korner, C., Muller, M., Hickmann, V., Hopfner, K.P. (2005) X-ray structures of the Sulfolobus solfataricus SWI2/SNF2 ATPase core and its complex with DNA. ***Cell.*** 121(3):363-373.

Eisen, J.A., Sweder, K.S., Hanawalt, P.C. (1995) Evolution of the snf2 family of proteins: Subfamilies with distinct sequences and functions. ***Nucleic Acids Res*** 23, 2715-2723.

Elsasser, S., Gali, R.R., Schwickart, M., Larsen, C.N., Leggett, D.S., Muller, B., Feng, M.T., Tubing, F., Dittmar, G.A., Finley, D. (2002) Proteasome subunit Rpn1 binds ubiquitin-like protein domains. ***Nat Cell Biol*** 4, 725-730.

Evans, E., Fellows, J., Coffer, A., Wood, R.D. (1997a) Open complex formation around a lesion during nucleotide excision repair provides a structure for cleavage by human XPG protein. ***Embo J*** 16, 625-638.

Evans, E., Moggs, J.G., Hwang, J.R., Egly, J.M., Wood, R.D. (1997b) Mechanism of open complex and dual incision formation by human nucleotide excision repair factors. ***Embo J*** 16, 6559-6573.

Falnes, P.O., Johansen, R.F., Seeberg, E. (2002) Alkb-mediated oxidative demethylation reverses DNA damage in *Escherichia coli*. ***Nature*** 419, 178-182.

Feldberg, R.S., and Grossman, L. (1976) A DNA binding protein from human placenta specific for ultraviolet damaged DNA. ***Biochemistry*** 15, 2402-2408.

Ferdous, A., Sikder, D., Gillette, T., Nalley, K., Kodadek, T., Johnston, S.A. (2007) The role of the proteasomal ATPases and activator monoubiquitylation in regulating Gal4 binding to promoters. ***Genes Dev*** 21(1):112-123.

Ferreiro, J.A., Powell, N.G., Karabetsou, N., Kent, N.A., Mellor, J., Waters, R. (2004) Cbf1p modulates chromatin structure, transcription and repair at the *Saccharomyces cerevisiae* MET16 locus. ***Nucleic Acids Res*** 32(5):1617-1626.

Ferreiro, J.A., Powell, N.G., Karabetsou, N., Mellor, J., Waters, R. (2006) Roles for Gcn5p and Ada2p in transcription and nucleotide excision repair at the *Saccharomyces cerevisiae* MET16 gene. ***Nucleic Acids Res*** 34(3):976-985.

Finley, D., Ozkaynak, E., Varshavsky, A. (1987) The yeast polyubiquitin gene is essential for resistance to high temperatures, starvation, and other stresses. ***Cell*** 48(6):1035-1046.

Firman, K., and Szczelkun, M.D. (2000) Measuring motion on DNA by the type I restriction endonuclease EcoR124I using triplex displacement. ***EMBO J*** 19: 2094-2102.

Fischle, W., Wang, Y., Allis, C.D. (2003) Histone and chromatin cross-talk. ***Curr Opin Cell Biol*** 15, 172-183.

Fishman-Lobell, J., and Haber, J.E. (1992) Removal of nonhomologous DNA ends in double-strand break recombination: The role of the yeast ultraviolet repair gene

RAD1. ***Science*** 258, 480-484.

Fousteri, M., Vermeulen, W., van, A.A., Zeeland, L.H., Mullenders, F. (2006) Cockayne syndrome A and B proteins differentially regulate recruitment of chromatin remodeling and repair factors to stalled RNA polymerase II *in vivo*, ***Mol. Cell***, 23: 471–482.

Franklin, W.A., Doetsch, P.W., Haseltine, W.A. (1985) Structural determination of the ultraviolet light-induced thymine-cytosine pyrimidine-pyrimidone (6-4) photoproduct. ***Nucleic Acids Res*** 13, 5317-5325.

Friedberg EC. (2001) How nucleotide excision repair protects against cancer. ***Nat Rev Cancer*** 1(1):22-33.

Friedberg, E.C. (2003) DNA damage and repair. ***Nature*** 421, 436-440.

Friedberg, E.C. (2004) The discovery that xeroderma pigmentosum (XP) results from defective nucleotide excision repair. ***DNA Repair (Amst)*** 3, 183, 195.

Friedberg, E.C. (2005) Suffering in silence: the tolerance of DNA damage. ***Nat Rev Mol Cell Biol.*** 6(12):943-953.

Friedberg, E.C., Lehmann, A.R., Fuchs, R.P. (2005) Trading places: how do DNA polymerases switch during translesion DNA synthesis? ***Mol Cell*** 18(5):499-505.

Friedberg, E. C., Walker G. C., and Siede W. (1995) DNA repair and Mutagenesis. *American Society of Microbiology Press, Washington DC.*

Friedberg, E. C., Walker G. C. and Siede W. (2006) DNA repair and Mutagenesis (Second Edition). *American Society of Microbiology Press, Washington DC.*

Frosina, G., Fortini, P., Rossi, O., Carrozzino, F., Raspaglio, G., Cox, L.S., Lane, D.P., Abbondandolo, A., Dogliotti, E. (1996) Two pathways for base excision repair in mammalian cells. ***J Biol Chem*** 271, 9573-9578.

Gaillard, H., Fitzgerald, D.J., Smith, C.L., Peterson, C.L., Richmond, T.J., Thoma, F. (2003) Chromatin remodeling activities act on UV-damaged nucleosomes and modulate DNA damage accessibility to photolyase. ***J Biol Chem*** 278, 17655-17663.

Gale, J.M., and Smerdon, M.J. (1990) UV induced (6-4) photoproducts are distributed differently than cyclobutane dimers in nucleosomes. ***Photochem Photobiol*** 51, 411-417.

Georgakopoulos, T., and Thireos, G. (1992) Two distinct yeast transcriptional

activators require the function of the Gcn5 protein to promote normal levels of transcription. ***Embo J*** 11, 4145-4152.

Gietz, R.D., and Prakash, S. (1988) Cloning and nucleotide sequence analysis of the *saccharomyces cerevisiae* RAD4 gene required for excision repair of uv-damaged DNA. ***Gene*** 74, 535-541.

Giglia-Mari, G., Coin, F., Ranish, J.A., Hoogstraten, D., Theil, A., Wijgers, N., Jaspers, N.G., Raams, A., Argentini, M., van der Spek, P.J., Botta, E., Stefanini, M., Egly, J.M., Aebersold, R., Hoeijmakers, J.H., Vermeulen, W. (2004) A new, tenth subunit of TFIIH is responsible for the DNA repair syndrome trichothiodystrophy group A. ***Nat Genet.*** 36(7):714-719.

Gillette, T.G., Gonzalez, F., Delahodde, A., Johnston, S.A., Kodadek, T. (2004) Physical and functional association of RNA polymerase II and the proteasome. ***Proc Natl Acad Sci USA*** 101, 5904-5909.

Gillette, T.G., Huang, W., Russell, S.J., Reed, S.H., Johnston, S.A., Friedberg, E.C. (2001) The 19S complex of the proteasome regulates nucleotide excision repair in yeast. ***Genes Dev*** 15, 1528-1539.

Gillette, T.G., Yu, S., Zhou, Z., Waters, R., Johnston, S.A., Reed, S.H. (2006) Distinct functions of the ubiquitin-proteasome pathway influence nucleotide excision repair. ***Embo J*** 25, 2529-2538.

Glickman, M.H., and Ciechanover, A. (2002) The ubiquitin-proteasome proteolytic pathway: Destruction for the sake of construction. ***Physiol Rev*** 82, 373-428.

Glickman, M.H., Rubin, D.M., Fried, V.A., Finley, D. (1998) The regulatory particle of the *saccharomyces cerevisiae* proteasome. ***Mol Cell Biol*** 18, 3149-3162.

Glickman, M.H., and Raveh, D. (2005) Proteasome plasticity. ***FEBS Lett*** 579(15):3214-3223

Gomes, X.V., and Wold, M.S. (1996) Functional domains of the 70-kilodalton subunit of human replication protein a. ***Biochemistry*** 35, 10558-10568.

Gong, F., Fahy, D., Smerdon, M.J. (2006) Rad4-Rad23 interaction with SWI/SNF links ATP-dependent chromatin remodeling with nucleotide excision repair. ***Nat Struct Mol Biol*** 13, 902-907.

Gonzalez, F., Delahodde, A., Kodadek, T., Johnston, S.A. (2002) Recruitment of a 19s proteasome subcomplex to an activated promoter. ***Science*** 296, 548-550.

Gordon, L.K., and Haseltine, W.A. (1982) Quantitation of cyclobutane pyrimidine dimer formation in double- and single-stranded DNA fragments of defined sequence. ***Radiat Res*** 89, 99-112.

Grant, P.A., Duggan, L., Cote, J., Roberts, S.M., Brownell, J.E., Candau, R., Ohba, R., Owen-Hughes, T., Allis, C.D., Winston, F., Berger, S.L., Workman, J.L. (1997) Yeast Gcn5 functions in two multisubunit complexes to acetylate nucleosomal histones: Characterization of an Ada complex and the SAGA (Spt/Ada) complex. ***Genes Dev*** 11, 1640-1650.

Gray, C.W. Slaughter, C.A. DeMartino, G.N. (1994) PA28 activator protein forms regulatory caps on proteasome stacked rings. ***J Mol Biol*** 236, 7-15.

Green, C.M., and Almouzni, G. (2003) Local action of the chromatin assembly factor Caf-1 at sites of nucleotide excision repair *in vivo*. ***Embo J*** 22, 5163-5174.

Groisman, R., Polanowska, J., Kuraoka, I., Sawada, J., Saijo, M., Drapkin, R., Kisselev, A.F., Tanaka, K., Nakatani, Y. (2003) The ubiquitin ligase activity in the DDB2 and CSA complexes is differentially regulated by the COP9 signalosome in response to DNA damage. ***Cell*** 113, 357-367.

Groll, M., Ditzel, L., Lowe, J., Stock, D., Bochtler, M., Bartunik, H.D., Huber, R. (1997) Structure of 20s proteasome from yeast at 2.4 A resolution. ***Nature*** 386, 463-671.

Guo, C., Tang, T.S., Bienko, M., Parker, J.L., Bielen, A.B., Sonoda, E., Takeda, S., Ulrich, H.D., Dikic, I., Friedberg, E.C. (2006) Ubiquitin-binding motifs in REV1 protein are required for its role in the tolerance of DNA damage. ***Mol Cell Biol*** 23:8892-8900.

Guzder, S.N., Sung, P., Prakash, L., Prakash, S. (1993) Yeast DNA-repair gene RAD14 encodes a zinc metalloprotein with affinity for ultraviolet-damaged DNA. ***Proc Natl Acad Sci USA*** 90, 5433-5437.

Guzder, S.N., Habraken, Y., Sung, P., Prakash, L., Prakash, S. (1995) Reconstitution of yeast nucleotide excision repair with purified Rad proteins, replication protein A, and transcription factor TFIIH. ***J Biol Chem*** 270(22):12973-12976.

Guzder, S.N., Sung, P., Prakash, L., Prakash, S. (1997) Yeast Rad7-Rad16 complex, specific for the nucleotide excision repair of the nontranscribed DNA strand, is an ATP-dependent DNA damage sensor. ***J Biol Chem*** 272, 21665-21668.

Guzder, S.N., Sung, P., Prakash, L., Prakash, S. (1998) Affinity of yeast nucleotide excision repair factor 2, consisting of the Rad4 and Rad23 proteins, for ultraviolet

damaged DNA. ***J Biol Chem*** 273, 31541-31546.

Habraken, Y., Sung, P., Prakash, L., Prakash, S. (1993) Yeast excision repair gene RAD2 encodes a single-stranded DNA endonuclease. ***Nature*** 366, 365-368.

Hanna, J., Meides, A., Zhang, D.P., Finley, D. (2007) A ubiquitin stress response induces altered proteasome composition. ***Cell*** 129(4):747-759.

Hanawalt, P.C. (2003) Four decades of DNA repair: From early insights to current perspectives. ***Biochimie*** 85, 1043-1052.

Hara, R., Mo, J., Sancar, A. (2000) DNA damage in the nucleosome core is refractory to repair by human excision nuclease. ***Mol Cell Biol*** 20, 9173-9181.

Hara, R., and Sancar, A. (2002) The SWI/SNF chromatin-remodeling factor stimulates repair by human excision nuclease in the mononucleosome core particle. ***Mol Cell Biol*** 22, 6779-6787.

Hara, R., and Sancar, A. (2003) Effect of damage type on stimulation of human excision nuclease by SWI/SNF chromatin remodeling factor. ***Mol Cell Biol*** 23, 4121-5.

Harrington, J.J., and Lieber, M.R. (1994) Functional domains within Fen-1 and Rad2 define a family of structure-specific endonucleases: Implications for nucleotide excision repair. ***Genes Dev*** 8, 1344-1355.

Hasty, P., Campisi, J., Hoeijmakers, J., van Steeg, H., Vijg, J. (2003) Aging and genome maintenance: Lessons from the mouse? ***Science*** 299, 1355-1359.

Havas, K., Flaus, A., Phelan, M., Kingston, R., Wade, P.A., Lilley, D.M., Owen-Hughes, T. (2000) Generation of superhelical torsion by ATP-dependent chromatin remodeling activities. ***Cell*** 103, 1133-1142.

He, Z. Henricksen, L.A., Wold, M.S., Ingles, C.J. (1995) RPA involvement in the damage-recognition and incision steps of nucleotide excision repair. ***Nature*** 374, 566-569.

Heessen, S., Masucci, M.G., Dantuma, N.P. (2005) The Uba2 domain functions as an intrinsic stabilization signal that protects RAD23 from proteasomal degradation. ***Mol Cell*** 18, 225-235.

Henning, K.A., Li, L., Iyer, N., McDaniel, L.D., Reagan, M.S., Legerski, R., Schultz, R.A., Stefanini, M., Lehmann, A.R., Mayne, L.V., Friedberg, E.C. (1995) The cockayne syndrome group a gene encodes a WD repeat protein that interacts with

CSB protein and a subunit of RNA polymerase II TFIIH. ***Cell*** 82, 555-564.

Hershko, A., Heller, H., Elias, S., Ciechanover, A. (1983) Components of ubiquitin-protein ligase system. Resolution, affinity purification, and role in protein breakdown. ***J Biol Chem*** 258, 8206-8214.

Ho, Y., Gruhler, A., Heilbut, A., Bader, G.D., Moore, L., Adams, S.L., Millar, A., Taylor, P., Bennett, K., Boutilier, K., Yang, L., Wolting, C., Donaldson, I., Schandorff, S., Shewnarane, J., Vo, M., Taggart, J., Goudreault, M., Muskat, B., Alfarano, C., Dewar, D., Lin, Z., Michalickova, K., Willems, A.R., Sassi, H., Nielsen, P.A., Rasmussen, K.J., Andersen, J.R., Johansen, L.E., Hansen, L.H., Jespersen, H., Podtelejnikov, A., Nielsen, E., Crawford, J., Poulsen, V., Sorensen, B.D., Matthiesen, J., Hendrickson, R.C., Gleeson, F., Pawson, T., Moran, M.F., Durocher, D., Mann, M., Hogue, C., W.Figeys, D., Tyers, M. (2002) Systematic identification of protein complexes in *saccharomyces cerevisiae* by mass spectrometry. ***Nature*** 415, 180-183.

Hochstrasser, M., Ellison, M.J., Chau, V., Varshavsky, A. (1991) The short-lived MAT alpha 2 transcriptional regulator is ubiquitinated *in vivo*. ***Proc Natl Acad Sci USA.*** 88(11), 4606-4610.

Hoege, C., Pfander, B., Moldovan, G.L., Pyrowolakis, G., Jentsch, S. (2002) RAD6-dependent DNA repair is linked to modification of PCNA by ubiquitin and SUMO. ***Nature***. 419(6903):135-141.

Hoeijmakers, J.H. (2001) Genome maintenance mechanisms for preventing cancer. ***Nature*** 411, 366-374.

Hofmann, K., and Bucher, P. (1996) The Uba domain: A sequence motif present in multiple enzyme classes of the ubiquitination pathway. ***Trends Biochem Sci*** 21, 172-173.

Hofmann, R.M., and Pickart, C.M. (1999) Noncanonical MMS2-encoded ubiquitin-conjugating enzyme functions in assembly of novel polyubiquitin chains for DNA repair. ***Cell*** 96, 645-653.

Huang, J.C., Svoboda, D.L., Reardon, J.T., Sancar, A. (1992) Human nucleotide excision nuclease removes thymine dimers from DNA by incising the 22nd phosphodiester bond 5' and the 6th phosphodiester bond 3' to the photodimer. ***Proc Natl Acad Sci USA*** 89, 3664-3668.

Huibregtse, J.M., Yang, J.C., Beaudenon, S.L. (1997) The large subunit of RNA polymerase II is a substrate of the Rsp5 ubiquitin-protein ligase. ***Proc Natl Acad Sci USA*** 94, 3656-3661.

Hunting, D.J., Gowans, B.J., Dresler, S.L. (1991) DNA polymerase delta mediates excision repair in growing cells damaged with ultraviolet radiation. ***Biochem Cell Biol*** 69, 303-308.

Hwang, B.J., and Chu, G. (1993) Purification and characterization of a human protein that binds to damaged DNA. ***Biochemistry*** 32, 1657-1666.

Ichihashi, M., Ueda, M., Budiyanto, A., Bito, T., Oka, M., Fukunaga, M., Tsuru, K., Horikawa, T. (2003) UV-induced skin damage. ***Toxicology*** 189, 21-39.

Ikegami, T., Kuraoka, I., Saijo, M., Kodo, N., Kyogoku, Y., Morikawa, K., Tanaka, K., Shirakawa, M. (1998) Solution structure of the DNA- and RPA-binding domain of the human repair factor XPA. ***Nat Struct Biol*** 5, 701-706.

Ito, S., Kuraoka, I., Chymkowitch, P., Compe, E., Takedachi, A., Ishigami, C., Coin, F., Egly, J.M., Tanaka, K. (2007) XPG stabilizes TFIIH, allowing transactivation of nuclear receptors: implications for Cockayne syndrome in XP-G/CS patients. ***Mol Cell*** 26(2):231-243.

Jansen, L.E. Verhage, R.A. Brouwer, J. (1998) Preferential binding of yeast Rad4.Rad23 complex to damaged DNA. ***J Biol Chem*** 273, 33111-33114.

Jentsch, S., McGrath, J.P., Varshavsky, A. (1987) The yeast DNA repair gene RAD6 encodes a ubiquitin-conjugating enzyme. ***Nature*** 329, 131-134.

Jentsch, S., and Schlenker, S. (1995) Selective protein degradation: A journey's end within the proteasome. ***Cell*** 82, 881-884.

Joazeiro, C.A., and Weissman, A.M. (2000) Ring finger proteins: Mediators of ubiquitin ligase activity. ***Cell*** 102, 549-552.

Johnson, R.E., Kondratick, C.M., Prakash, S., Prakash, L. (1999) *hRAD30* mutations in the variant form of xeroderma pigmentosum, ***Science*** 285, 263–265.

Jones, C.J., and Wood, R.D. (1993) Preferential binding of the xeroderma pigmentosum group A complementing protein to damaged DNA. ***Biochemistry*** 32, 12096-12104.

Ju, D., and Xie, Y. (2006) A synthetic defect in protein degradation caused by loss of Ufd4 and Rad23. ***Biochem Biophys Res Commun.*** 341(2):648-52.

Kamura, T., Burian, D., Yan, Q., Schmidt, S.L., Lane, W.S., Querido, E., Branton, P.E., Shilatifard, A., Conaway, R.C., Conaway, J.W. (2001) Muf1, a novel elongin BC-interacting leucine-rich repeat protein that can assemble with Cul5 and Rbx1 to

reconstitute a ubiquitin ligase. ***J Biol Chem*** 276, 29748-29753.

Kazantsev, A., Mu, D., Nichols, A.F., Zhao, X., Linn, S., Sancar, A. (1996) Functional complementation of xeroderma pigmentosum complementation group E by replication protein a in an *in vitro* system. ***Proc Natl Acad Sci USA*** 93, 5014-5018.

Keeney, S., Chang, G.J., Linn, S. (1993) Characterization of a human DNA damage binding protein implicated in xeroderma pigmentosum E. ***J Biol Chem*** 268, 21293-21300.

Keeney, S., Eker, A.P., Brody, T., Vermeulen, W., Bootsma, D., Hoeijmakers, J.H., Linn, S. (1994) Correction of the DNA repair defect in xeroderma pigmentosum group E by injection of a DNA damage-binding protein. ***Proc Natl Acad Sci USA*** 91, 4053-4056.

Kelner, A. (1949) Effect of visible light on the recovery of streptomyces griseus conidia from ultra-violet irradiation injury. ***Proc Natl Acad Sci USA*** 35, 73-79.

Kenny, M.K., Schlegel, U., Furneaux, H., Hurwitz, J. (1990) The role of human single-stranded DNA binding protein and its individual subunits in simian virus 40 DNA replication. ***J Biol Chem*** 265, 7693-7700.

Khanna, K.K., and Jackson, S.P. (2001) DNA double-strand breaks: Signaling, repair and the cancer connection. ***Nat Genet*** 27, 247-254.

Kile, B.T., Schulman, B.A., Alexander, W.S., Nicola, N.A., Martin, H.M., Hilton, D.J. (2002) The socs box: A tale of destruction and degradation. ***Trends Biochem Sci*** 27, 235-241.

Kim, C., Paulus, B.F., Wold, M.S. (1994) Interactions of human replication protein A with oligonucleotides. ***Biochemistry*** 33, 14197-14206.

Kim, C., Snyder, R.O., Wold, M.S. (1992) Binding properties of replication protein A from human and yeast cells. ***Mol Cell Biol*** 12, 3050-3059.

Kim, D.K., Stigger, E., Lee, S.H. (1996) Role of the 70-kda subunit of human replication protein A (I). Single-stranded DNA binding activity, but not polymerase stimulatory activity, is required for DNA replication. ***J Biol Chem*** 271, 15124-15129.

Kim, J.K., Patel, D., Choi, B.S. (1995) Contrasting structural impacts induced by cis-syn cyclobutane dimer and (6-4) adduct in DNA duplex decamers: Implication in mutagenesis and repair activity. ***Photochem Photobiol.*** 62, 44-50.

Klungland, A., and Lindahl, T. (1997) Second pathway for completion of human DNA

base excision-repair: Reconstitution with purified proteins and requirement for DNase IV (FEN1). ***Embo J*** 16, 3341-3348.

Kobe, B., and Deisenhofer, J. (1994) The leucine-rich repeat: a versatile binding motif. ***Trends Biochem Sci*** 19(10):415-421.

Koegl, M., Hoppe, T., Schlenker, S., Ulrich, H.D., Mayer, T.U., Jentsch, S. (1999) A novel ubiquitination factor, E4, is involved in multiubiquitin chain assembly. ***Cell*** 96, 635-644.

Kodadek, T., Sikder, D., Nalley, K. (2006) Keeping transcriptional activators under control. ***Cell*** 127(2):261-264.

Kopel, V., Pozner, A., Baran, N., and Manor, H. (1996) Unwinding of the third strand of a DNA triple helix, a novel activity of the SV40 large T-antigen helicase. ***Nucleic Acids Res*** 24: 330-335.

Kornberg, R.D., and Lorch, Y. (1999) Chromatin-modifying and -remodeling complexes. ***Curr Opin Genet Dev*** 9, 148-151.

Kunkel, T.A., and Erie, D.A. (2005) DNA mismatch repair. ***Annu Rev Biochem*** 74, 681-710.

Kuo, M.H., Brownell, J.E., Sobel, R.E., Ranalli, T.A., Cook, R.G., Edmondson, D.G., Roth, S.Y., Allis, C.D. (1996) Transcription-linked acetylation by Gcn5p of histones H3 and H4 at specific lysines. ***Nature*** 383, 269-272.

Kurdistani, S.K., and Grunstein, M. (2003) Histone acetylation and deacetylation in yeast. ***Nat Rev Mol Cell Biol*** 4, 276-284.

Lainé, J.P., and Egly, J.M. (2006) Initiation of DNA repair mediated by a stalled RNA polymerase IIO, ***EMBO J***. 25 387–397.

Lee, J., and Zhou, P. (2007) DCAFs, the missing link of the CUL4-DDB1 ubiquitin ligase. ***Mol Cell*** 26(6):775-780.

Lee, S.K., Yu, S.L., Prakash, L., Prakash, S. (2001) Requirement for yeast RAD26, a homolog of the human CSB gene, in elongation by RNA polymerase II. ***Mol Cell Biol*** 21, 8651-8656.

Lee, S.K., Yu, S.L., Prakash, L., Prakash, S. (2002) Yeast RAD26, a homolog of the human CSB gene, functions independently of nucleotide excision repair and base excision repair in promoting transcription through damaged bases. ***Mol Cell Biol*** 22, 4383-4389.

Lehmann, A.R. (2001) The xeroderma pigmentosum group D (XPD) gene: One gene, two functions, three diseases. ***Genes Dev*** 15, 15-23.

Lehmann A.R. (2003) DNA repair-deficient diseases, xeroderma pigmentosum, Cockayne syndrome and trichothiodystrophy. ***Biochimie.*** 85(11):1101-1111.

Lehmann A.R. (2005) Replication of damaged DNA by translesion synthesis in human cells. ***FEBS Lett.*** 579(4):873-876.

Lehmann A.R. (2006) New functions for Y family polymerases. ***Mol Cell*** 24(4):493-495.

Lehmann, A.R, Niimi, A., Ogi, T., Brown, S., Sabbioneda, S., Wing, J.F., Kannouche, P.L., Green, C.M. (2007) Translesion synthesis: Y-family polymerases and the polymerase switch. ***DNA Repair (Amst).*** 6(7):891-899.

Li, L., Lu, X., Peterson, C.A., Legerski, R.J. (1995a) An interaction between the DNA repair factor XPA and replication protein A appears essential for nucleotide excision repair. ***Mol Cell Biol*** 15, 5396-5402.

Li, L., Peterson, C.A., Lu, X., Legerski, R.J. (1995b) Mutations in XPA that prevent association with ERCC1 are defective in nucleotide excision repair. ***Mol Cell Biol*** 15, 1993-1998.

Li, S., and Waters, R. (1996) Nucleotide level detection of cyclobutane pyrimidine dimers using oligonucleotides and magnetic beads to facilitate labelling of DNA fragments incised at the dimers and chemical sequencing reference ladders. ***Carcinogenesis*** 17(8):1549-1552.

Li, S., and Waters, R. (1997) Induction and repair of cyclobutane pyrimidine dimers in the *Escherichia coli* tRNA gene tyrT: Fis protein affects dimer induction in the control region and suppresses preferential repair in the coding region of the transcribed strand, except in a short region near the transcription start site. ***J Mol Biol*** 271(1):31-46.

Li, S., and Smerdon, M.J. (2004) Dissecting transcription-coupled and global genomic repair in the chromatin of yeast Gal1-10 genes. ***J Biol Chem*** 279, 14418-14426.

Lindahl, T. (1993) Instability and decay of the primary structure of DNA. ***Nature*** 362, 709-715.

Lindahl, T., Sedgwick, B., Sekiguchi, M., Nakabeppu, Y. (1988) Regulation and expression of the adaptive response to alkylating agents. ***Annu Rev Biochem*** 57, 133-157.

Lindahl, T., and Wood, R.D. (1999) Quality control by DNA repair. ***Science*** 286, 1897-1905.

Lippke, J.A., Gordon, L.K., Brash, D.E., Haseltine, W.A. (1981) Distribution of UV light-induced damage in a defined sequence of human DNA: Detection of alkaline-sensitive lesions at pyrimidine nucleoside-cytidine sequences. ***Proc Natl Acad Sci USA*** 78, 3388-3392.

Liu, W., Nichols, A.F., Graham, J.A., Dualan, R., Abbas, A., Linn, S. (2000) Nuclear transport of human DDB protein induced by ultraviolet light. ***J Biol Chem*** 275, 21429-21434.

Livingstone-Zatchej, M., Meier, A., Suter, B., Thoma, F. (1997) RNA polymerase II transcription inhibits DNA repair by photolyase in the transcribed strand of active yeast genes. ***Nucleic Acids Res*** 25, 3795-3800.

Loeb, L.A., Loeb, K.R., Anderson, J.P. (2003) Multiple mutations and cancer. ***Proc Natl Acad Sci USA*** 100(3):776-781.

Lombard, D.B., Chua, K.F., Mostoslavsky, R., Franco, S., Gostissa, M., Alt, F.W. (2005) DNA repair, genome stability, and aging. ***Cell*** 120, 497-512.

Lommel, L., Bucheli, M.E., Sweder, K.S. (2000a) Transcription-coupled repair in yeast is independent from ubiquitylation of RNA pol II: Implications for cockayne's syndrome. ***Proc Natl Acad Sci USA*** 97, 9088-9092.

Lommel, L., Chen, L., Madura, K., Sweder, K. (2000b) The 26S proteasome negatively regulates the level of overall genomic nucleotide excision repair. ***Nucleic Acids Res*** 28, 4839-4845.

Lommel, L., Ortolan, T., Chen, L., Madura, K., Sweder, K.S. (2002) Proteolysis of a nucleotide excision repair protein by the 26S proteasome. ***Curr Genet*** 42, 9-20.

Lorick, K.L., Jensen, J.P., Fang, S., Ong, A.M., Hatakeyama, S., Weissman, A.M. (1999) Ring fingers mediate ubiquitin-conjugating enzyme (E2)-dependent ubiquitination. ***Proc Natl Acad Sci USA*** 96, 11364-11369.

Luger, K., Mader, A.W., Richmond, R.K., Sargent, D.F., Richmond, T.J. (1997) Crystal structure of the nucleosome core particle at 2.8 A resolution. ***Nature*** 389, 251-260.

Lusser, A., and Kadonaga, J.T. (2003) Chromatin remodeling by ATP-dependent molecular machines. ***Bioessays*** 25, 1192-1200.

Martinez, E., Palhan, V.B., Tjernberg, A., Lymar, E.S., Gamper, A.M., Kundu, T.K., Chait, B.T., Roeder, R.G. (2001) Human STAGA complex is a chromatin-acetylating transcription coactivator that interacts with pre-mRNA splicing and DNA damage-binding factors *in vivo*. ***Mol Cell Biol*** 21, 6782-6795.

Martinez-Pastor, M.T., Marchler, G., Schuller, C., Marchler-Bauer, A., Ruis, H., Estruch, F. (1996) The Saccharomyces cerevisiae zinc finger proteins Msn2p and Msn4p are required for transcriptional induction through the stress response element (STRE). ***EMBO J*** 15(9):2227-2235.

Masutani, C., Sugasawa, K., Yanagisawa, J., Sonoyama, T., Ui, M., Enomoto, T., Takio, K., Tanaka, K., van der Spek, P.J., Bootsma, D. (1994) Purification and cloning of a nucleotide excision repair complex involving the xeroderma pigmentosum group C protein and a human homologue of yeast RAD23. ***Embo J*** 13, 1831-1843.

Masutani, C., Kusumoto, R., Yamada, A., Dohmae, N., Yokoi, M., Yuasa, M., Araki, M., Iwai, S., Takio, K., Hanaoka, F. (1999) The XPV (xeroderma pigmentosum variant) gene encodes human DNA polymerase eta. ***Nature*** 399(6737):700-704.

Matsuda, N., Azuma, K., Saijo, M., Iemura, S., Hioki, Y., Natsume, T., Chiba, T., Tanaka, K., Tanaka, K. (2005) DDB2, the xeroderma pigmentosum group E gene product, is directly ubiquitylated by cullin 4A-based ubiquitin ligase complex. ***DNA Repair (Amst)*** 4, 537-545.

Matsumoto, Y., and Kim, K. (1995) Excision of deoxyribose phosphate residues by DNA polymerase beta during DNA repair. ***Science*** 269, 699-702.

Matsunaga, T., Mu, D., Park, C.H., Reardon, J.T., Sancar, A. (1995) Human DNA repair excision nuclease. Analysis of the roles of the subunits involved in dual incisions by using anti-XPG and anti-ERCC1 antibodies. ***J Biol Chem*** 270, 20862-20869.

Matsunaga, T., Park, C.H., Bessho, T., Mu, D., Sancar, A. (1996) Replication protein a confers structure-specific endonuclease activities to the XPF-ERCC1 and XPG subunits of human DNA repair excision nuclease. ***J Biol Chem*** 271, 11047-11050.

Meniel, V., and Waters, R. (1999) Spontaneous and photosensitiser-induced DNA single-strand breaks and formamidopyrimidine-DNA glycosylase sensitive sites at nucleotide resolutionin the nuclear and mitochondrial DNA of Saccharomyces cerevisiae. ***Nucleic Acids Res*** 27(3):822-830.

McClanahan, T., McEntee, K. (1984) Specific transcripts are elevated in *Saccharomyces cerevisiae* in response to DNA damage. ***Mol Cell Biol*** 4(11):2356-2363.

McKay, B.C., Chen, F., Clarke, S.T., Wiggin, H.E., Harley, L.M., Ljungman, M. (2001) UV light-induced degradation of RNA polymerase II is dependent on the cockayne's syndrome A and b proteins but not p53 or mlh1. ***Mutat Res*** 485, 93-105.

Mellon, I., Bohr, V.A., Smith, C.A., Hanawalt, P.C. (1986) Preferential DNA repair of an active gene in human cells. ***Proc Natl Acad Sci USA*** 83, 8878-8882.

Mellon, I., Spivak, G., Hanawalt, P.C. (1987) Selective removal of transcription-blocking DNA damage from the transcribed strand of the mammalian DHFR gene. ***Cell*** 51, 241-249.

Minko, I.G., Washington, M.T., Prakash, L., Prakash, S., Lloyd, R.S. (2001) Translesion DNA synthesis by yeast DNA polymerase eta on templates containing N2-guanine adducts of 1,3-butadiene metabolites. ***J Biol Chem*** 276, 2517-2522.

Mitchell, D.L., Adair, G.M., Nairn, R.S. (1989) Inhibition of transient gene expression in Chinese hamster ovary cells by triplet-sensitized UV-b irradiation of transfected DNA. ***Photochem Photobiol*** 50, 639-646.

Moggs, J.G., Yarema, K.J., Essigmann, J.M., Wood, R.D. (1996) Analysis of incision sites produced by human cell extracts and purified proteins during nucleotide excision repair of a 1,3-intrastrand d(GpTpG)-cisplatin adduct. ***J Biol Chem*** 271, 7177-7186.

Montecucco, A., Savini, E., Weighardt, F., Rossi, R., Ciarrocchi, G., Villa, A., Biamonti, G. (1995) The N-terminal domain of human DNA ligase I contains the nuclear localization signal and directs the enzyme to sites of DNA replication. ***Embo J*** 14, 5379-5386.

Mortusewicz, O., Rothbauer, U., Cardoso, M.C., Leonhardt, H. (2006) Differential recruitment of DNA ligase I and III to DNA repair sites. ***Nucleic Acids Res*** 34, 3523-3532.

Mu, D., Hsu, D.S., Sancar, A. (1996) Reaction mechanism of human DNA repair excision nuclease. ***J Biol Chem*** 271, 8285-8294.

Mu, D., and Sancar, A. (1997) Model for XPC-independent transcription-coupled repair of pyrimidine dimers in humans. ***J Biol Chem*** 272, 7570-7573.

Mu, D., Wakasugi, M., Hsu, D.S., Sancar, A. (1997) Characterization of reaction intermediates of human excision repair nuclease. ***J Biol Chem*** 272, 28971-28979.

Mueller, J.P., and Smerdon, M.J. (1995) Repair of plasmid and genomic DNA in a

RAD7 delta mutant of yeast. ***Nucleic Acids Res*** 23, 3457-3464.

Mueller, J.P., and Smerdon, M.J. (1996) RAD23 is required for transcription-coupled repair and efficient overrall repair in *saccharomyces cerevisiae*. ***Mol Cell Biol*** 16, 2361-2368.

Mukhopadhyay, D., and Riezman, H. (2007) Proteasome-independent functions of ubiquitin in endocytosis and signaling. ***Science*** 315(5809):201-205.

Nakatsu, Y., Asahina, H., Citterio, E., Rademakers, S., Vermeulen, W., Kamiuchi, S., Yeo, J.P., Khaw, M.C., Saijo, M., Kodo, N., Matsuda, T., Hoeijmakers, J.H., Tanaka, K. (2000) Xab2, a novel tetratricopeptide repeat protein involved in transcription-coupled DNA repair and transcription. ***J Biol Chem*** 275, 34931-34937.

Ng, J.M., Vermeulen, W., van der Horst, G.T., Bergink, S., Sugasawa, K., Vrieling, H., Hoeijmakers, J.H. (2003) A novel regulation mechanism of DNA repair by damage-induced and Rad23-dependent stabilization of xeroderma pigmentosum group C protein. ***Genes Dev*** 17, 1630-1645.

Niggli, H.J., and Cerutti, P.A. (1982) Nucleosomal distribution of thymine photodimers following far- and near-ultraviolet irradiation. ***Biochem Biophys Res Commun*** 105, 1215-1223.

Nishida, C., Reinhard, P., Linn, S. (1988) DNA repair synthesis in human fibroblasts requires DNA polymerase delta. ***J Biol Chem*** 263, 501-510.

Nocentini, S., Coin, F., Saijo, M., Tanaka, K., Egly, J.M. (1997) DNA damage recognition by XPA protein promotes efficient recruitment of transcription factor II h. ***J Biol Chem*** 272, 22991-22994.

O'Donovan, A., Davies, A.A., Moggs, J.G., West, S.C., Wood, R.D. (1994) Xpg endonuclease makes the 3' incision in human DNA nucleotide excision repair. ***Nature*** 371, 432-435.

Ogi, T., and Lehmann, A.R. (2006) The Y-family DNA polymerase kappa (pol kappa) functions in mammalian nucleotide-excision repair. ***Nat Cell Biol.*** 8(6):640-642.

Okuda Y, Nishi R, Ng JM, Vermeulen W, van der Horst GT, Mori T, Hoeijmakers JH, Hanaoka F, Sugasawa K (2004) Relative levels of the two mammalian Rad23 homologs determine composition and stability of the *Xeroderma pigmentosum* group C protein complex. ***DNA Repair*** (Amst) 3: 1285–1295.

Orlowski, M., and Wilk, S. (1981) A multicatalytic protease complex from pituitary that forms enkephalin and enkephalin containing peptides. ***Biochem Biophys Res***

Commun 101, 814-822.

Ortolan, T.G., Chen, L., Tongaonkar, P., Madura, K. (2004) Rad23 stabilizes Rad4 from degradation by the Ub/proteasome pathway. ***Nucleic Acids Res*** 32, 6490-6500.

Ortolan, T.G., Tongaonkar, P., Lambertson, D., Chen, L., Schauber, C., Madura, K. (2000) The DNA repair protein Rad23 is a negative regulator of multi-ubiquitin chain assembly. ***Nat Cell Biol*** 2, 601-608.

Otrin, V.R., McLenigan, M., Takao, M., Levine, A.S., Protic, M. (1997) Translocation of a UV-damaged DNA binding protein into a tight association with chromatin after treatment of mammalian cells with UV light. ***J Cell Sci*** 110 (Pt 10), 1159-1168.

Ozkaynak, E., Finley, D., Varshavsky, A. (1984) The yeast ubiquitin gene: head-to-tail repeats encoding a polyubiquitin precursor protein. ***Nature*** 312(5995):663-666.

Ozkaynak, E., Finley, D., Solomon, M.J., Varshavsky, A. (1987) The yeast ubiquitin genes: a family of natural gene fusions. ***EMBO J*** 6(5):1429-1439.

Park, C.H., Bessho, T., Matsunaga, T., Sancar, A. (1995) Purification and characterization of the XPF-ERCC1 complex of human DNA repair excision nuclease. ***J Biol Chem*** 270, 22657-22660.

Payne, A., and Chu, G. (1994) Xeroderma pigmentosum group E binding factor recognizes a broad spectrum of DNA damage. ***Mutat Res*** 310, 89-102.

Pegg, A.E. (2000) Repair of O(6)-alkylguanine by alkyltransferases. ***Mutat Res*** 462, 83-100.

Perlow, R.A., and Broyde, S. (2002) Toward understanding the mutagenicity of an environmental carcinogen: Structural insights into nucleotide incorporation preferences. ***J Mol Biol*** 322, 291-309.

Peterson, C.L., and Cote, J. (2004) Cellular machineries for chromosomal DNA repair. ***Genes Dev*** 18, 602-616.

Peterson, C.L., and Workman, J.L. (2000) Promoter targeting and chromatin remodeling by the SWI/SNF complex. ***Curr Opin Genet Dev*** 10, 187-192.

Petit, C., and Sancar, A. (1999) Nucleotide excision repair: From *E. coli* to man. ***Biochimie*** 81, 15-25.

Petroski, M.D., and Deshaies, R.J. (2005) Function and regulation of cullin-ring ubiquitin ligases. ***Nat Rev Mol Cell Biol*** 6, 9-20.

Pfeifer, G.P., Drouin, R., Riggs, A.D., Holmquist, G.P. (1992) Binding of transcription factors creates hot spots for UV photoproducts *in vivo*. ***Mol Cell Biol.*** (4):1798-1804.

Pickart, C.M. (2004) Back to the future with ubiquitin. ***Cell*** 116, 181-190.

Pintard, L., Willems, A., Peter, M. (2004) Cullin-based ubiquitin ligases: Cul3–BTB complexes join the family. ***EMBO J*** 23: 1681–1687.

Prakash, S., and Prakash, L. (2000) Nucleotide excision repair in yeast. ***Mutat Res*** 451, 13-24.

Raasi, S., and Pickart, C.M. (2003) Rad23 ubiquitin-associated domains (uba) inhibit 26S proteasome-catalyzed proteolysis by sequestering lysine 48-linked polyubiquitin chains. ***J Biol Chem*** 278, 8951-8959.

Ramsey, K.L., Smith, J.J., Dasgupta, A., Maqani, N., Grant, P., Auble, D.T. (2004) The NEF4 complex regulates Rad4 levels and utilizes Snf2/Wwi2-related ATPase activity for nucleotide excision repair. ***Mol Cell Biol*** 24, 6362-6378.

Ranish, J.A., Hahn, S., Lu, Y., Yi, E.C., Li, X.J., Eng, J. (2004) Aebersold R. Identification of TFB5, a new component of general transcription and DNA repair factor IIH. ***Nat Genet.*** 36(7):707-713.

Rapic-Otrin, V., McLenigan, M.P., Bisi, D.C., Gonzalez, M., Levine, A.S. (2002) Sequential binding of uv DNA damage binding factor and degradation of the p48 subunit as early events after uv irradiation. ***Nucleic Acids Res*** 30, 2588-2598.

Ratner, J.N., Balasubramanian, B., Corden, J., Warren, S.L., Bregman, D.B. (1998) Ultraviolet Radiation-induced ubiquitination and proteasomal degradation of the large subunit of RNA polymerase II. Implications for transcription-coupled DNA repair. ***J Biol Chem*** 273, 5184-5189.

Ravanat, J.L., Douki, T. Cadet, J. (2001) Direct and indirect effects of UV radiation on DNA and its components. ***J Photochem Photobiol B*** 63, 88-102.

Reardon, J.T., Mu, D., Sancar, A. (1996) Overproduction, purification, and characterization of the XPC subunit of the human DNA repair excision nuclease. ***J Biol Chem*** 271, 19451-19456.

Reed, S.H. (2005) Nucleotide excision repair in chromatin: The shape of things to come. ***DNA Repair*** (Amst) 4(8), 909-918.

Reed, S.H., and Gillette G.T. (2007) Nucleotide excision repair and the ubiquitin

proteasome pathway-Do all roads lead to Rome? ***DNA Repair*** (Amst). 6(2):149-156.

Reed, S.H., Akiyama, M., Stillman, B., Friedberg, E.C. (1999) Yeast autonomously replicating sequence binding factor is involved in nucleotide excision repair. ***Genes Dev*** 13, 3052-3058.

Reed, S.H., Boiteux, S., Waters, R. (1996) UV-induced endonuclease III-sensitive sites at the mating type loci in *saccharomyces cerevisiae* are repaired by nucleotide excision repair: RAD7 and RAD16 are not required for their removal from HML alpha. ***Mol Gen Genet*** 250, 505-514.

Reed, S.H., You, Z., Friedberg, E.C. (1998) The yeast RAD7 and RAD16 genes are required for postincision events during nucleotide excision repair. *In vitro* and *in vivo* studies with RAD7 and RAD16 mutants and purification of a Rad7/Rad16-containing protein complex. ***J Biol Chem*** 273, 29481-29488.

Reed, S.H., and Waters, R. (2003) DNA repair. ***Nature Encyclopedia of the human Genome***. London, Macmillan Publishers Ltd. Vol 2, pp.148-154.

Roberts, J., and Park, J.S. (2004) Mfd, the bacterial transcription repair coupling factor: translocation, repair and termination. ***Curr. Opin. Microbiol.*** 7; 120–125.

Robins, P., Jones, C.J., Biggerstaff, M., Lindahl, T., Wood, R.D. (1991) Complementation of DNA repair in xeroderma pigmentosum group A cell extracts by a protein with affinity for damaged DNA. ***Embo J*** 10, 3913-3921.

Rouse, J., and Jackson, S.P. (2002) Interfaces between the detection, signaling, and repair of DNA damage. ***Science*** 297, 547-551.

Roy, R., Adamczewski, J.P., Seroz, T., Vermeulen, W., Tassan, J.P., Schaeffer, L., Nigg, E.A., Hoeijmakers, J.H., Egly, J.M. (1994) The MO15 cell cycle kinase is associated with the TFIIH transcription-DNA repair factor. ***Cell*** 79, 1093-1101.

Rubin, D.M., and Finley, D. (1995) Proteolysis. The proteasome: A protein-degrading organelle? ***Curr Biol*** 5, 854-858.

Russell, S.J., Reed, S.H., Huang, W., Friedberg, E.C., Johnston, S.A. (1999) The 19S regulatory complex of the proteasome functions independently of proteolysis in nucleotide excision repair. ***Mol Cell*** 3, 687-695.

Russell. S.J., and Johnston, S.A. (2001) Evidence that proteolysis of Gal4 cannot explain the transcriptional effects of proteasome ATPase mutations. ***J Biol Chem*** 276(13):9825-9831.

Saha, A., Wittmeyer, J., Cairns, B.R. (2002) Chromatin remodeling by RSC involves ATP-dependent DNA translocation. ***Genes Dev*** 16(16):2120-2134.

Saijo, M., Kuraoka, I., Masutani, C., Hanaoka, F., Tanaka, K. (1996) Sequential binding of DNA repair proteins RPA and ERCC1 to XPA *in vitro*. ***Nucleic Acids Res*** 24, 4719-4724.

Salghetti, S.E., Caudy, A.A., Chenoweth, J.G., Tansey, W.P. (2001) Regulation of transcriptional activation domain function by ubiquitin. ***Science*** 293, 1651-1653.

Sancar, A. (1994) Structure and function of DNA photolyase. ***Biochemistry*** 33, 2-9.

Sancar, A., Franklin, K.A., Sancar, G.B. (1984) *Escherichia coli* DNA photolyase stimulates uvrabc excision nuclease *in vitro*. ***Proc Natl Acad Sci USA*** 81, 7397-7401.

Sancar, A., Lindsey-Boltz, L.A., Unsal-Kacmaz, K., Linn, S. (2004) Molecular mechanisms of mammalian DNA repair and the DNA damage checkpoints. ***Annu Rev Biochem*** 73, 39-85.

Sancar, G.B., and Smith, F.W. (1989) Interactions between yeast photolyase and nucleotide excision repair proteins in *saccharomyces cerevisiae* and *Escherichia coli*. ***Mol Cell Biol*** 9, 4767-4776.

Sarasin, A., and Stary A. (2007) New insights for understanding the transcription-coupled repair pathway. ***DNA Repair*** (Amst). 6(2):265-269.

Sarker, A.H., Tsutakawa, S.E., Kostek, S., Ng, C., Shin, D.S., Peris, M., Campeau, E., Tainer, J.A., Nogales, E., Cooper, P.K. (2005) Recognition of RNA polymerase II and transcription bubbles by XPG, CSB, and TFIIH: insights for transcription-coupled repair and Cockayne syndrome, ***Mol. Cell.*** 20:187–198.

Schaeffer, L., Moncollin, V., Roy, R., Staub, A., Mezzina, M., Sarasin, A., Weeda, G., Hoeijmakers, J.H., Egly, J.M. (1994) The ERCC2/DNA repair protein is associated with the class II BTF2/TFIIH transcription factor. ***Embo J*** 13, 2388-2392.

Schaeffer, L., Roy, R., Humbert, S., Moncollin, V., Vermeulen, W., Hoeijmakers, J.H., Chambon, P., Egly, J.M. (1993) DNA repair helicase: A component of BTF2 (TFIIH) basic transcription factor. ***Science*** 260, 58-63.

Schauber, C., Chen, L., Tongaonkar, P., Vega, I., Lambertson, D., Potts, W., Madura, K. (1998) Rad23 links DNA repair to the ubiquitin/proteasome pathway. ***Nature*** 391, 715-718.

Schmitt, A.P., McEntee, K. (1996) Msn2p, a zinc finger DNA-binding protein, is the

transcriptional activator of the multistress response in Saccharomyces cerevisiae. ***Proc Natl Acad Sci USA*** 93(12):5777-5782.

Schneider, R., and Schweiger, M. (1991) The yeast DNA repair proteins Rad1 and Rad7 share similar putative functional domains. ***FEBS Lett*** 283, 203-206.

Selby, C.P., and Sancar, A. (1993) Molecular mechanism of transcription-repair coupling. ***Science*** 260, 53-58.

Selby, C.P., and Sancar, A. (1997a) Cockayne syndrome group B protein enhances elongation by RNA polymerase II. ***Proc Natl Acad Sci USA*** 94, 11205-11209.

Selby, C.P., and Sancar, A. (1997b) Human transcription-repair coupling factor CSB/ERCC6 is a DNA-stimulated ATPase but is not a helicase and does not disrupt the ternary transcription complex of stalled RNA polymerase II. ***J Biol Chem*** 272, 1885-1890.

Selleck, S.B., and Majors, J. (1987) Photofootprinting *in vivo* detects transcription-dependent changes in yeast TATA boxes. ***Nature*** 325, 173-177.

Serizawa, H., Makela, T.P., Conaway, J.W., Conaway, R.C., Weinberg, R.A., Young, R.A. (1995) Association of Cdk-activating kinase subunits with transcription factor TFIIH. ***Nature*** 374, 280-282.

Shiekhattar, R., Mermelstein, F., Fisher, R.P., Drapkin, R., Dynlacht, B., Wessling, H.C., Morgan, D.O., Reinberg, D. (1995) Cdk-activating kinase complex is a component of human transcription factor TFIIH. ***Nature***. 374(6519):283-287.

Shivji, K.K., Kenny, M.K., Wood, R.D. (1992) Proliferating cell nuclear antigen is required for DNA excision repair. ***Cell*** 69, 367-374.

Shivji, M.K., Podust, V.N., Hubscher, U., Wood, R.D. (1995) Nucleotide excision repair DNA synthesis by DNA polymerase epsilon in the presence of PCNA, RFC, and RPA. ***Biochemistry*** 34, 5011-5017.

Shiyanov, P., Nag, A., Raychaudhuri, P. (1999) Cullin 4A associates with the UV-damaged DNA-binding protein DDB. ***J Biol Chem*** 274, 35309-35312.

Shogren-Knaak, M., Ishii, H., Sun, J.M., Pazin, M.J., Davie, J.R., Peterson, C.L. (2006) Histone H4-K16 acetylation controls chromatin structure and protein interactions. ***Science*** 311(5762):844-847.

Sijbers, A.M., de Laat, W.L., Ariza, R.R., Biggerstaff, M., Wei, Y.F., Moggs, J.G., Carter, K.C., Shell, B.K., Evans, E., de Jong, M.C., Rademakers, S., de Rooij, J.,

Jaspers, N.G., Hoeijmakers, J.H., Wood, R.D. (1996) Xeroderma pigmentosum group F caused by a defect in a structure-specific DNA repair endonuclease. ***Cell*** 86, 811-822.

Smerdon, M.J., and Lieberman, M.W. (1978) Nucleosome rearrangement in human chromatin during UV-induced DNA- reapir synthesis. ***Proc Natl Acad Sci USA*** 75, 4238-4241.

Smerdon, M.J., Watkins, J.F., Lieberman, M.W. (1982) Effect of histone H1 removal on the distribution of ultraviolet-induced deoxyribonucleic acid repair synthesis within chromatin. ***Biochemistry*** 21, 3879-3885.

Somesh, B.P., Reid, J., Liu, W.F., Sogaard, T.M., Erdjument-Bromage, H., Tempst, P., Svejstrup, J.Q. (2005) Multiple mechanisms confining RNA polymerase II ubiquitylation to polymerases undergoing transcriptional arrest. ***Cell*** 121, 913-923.

Stigger, E., Drissi, R., Lee, S.H. (1998) Functional analysis of human replication protein A in nucleotide excision repair. ***J Biol Chem*** 273, 9337-9343.

Sugasawa, K., Ng, J.M., Masutani, C., Iwai, S., van der Spek, P.J., Eker, A.P., Hanaoka, F., Bootsma, D., Hoeijmakers, J.H. (1998) Xeroderma pigmentosum group C protein complex is the initiator of global genome nucleotide excision repair. ***Mol Cell*** 2, 223-232.

Sugasawa, K., Okamoto, T., Shimizu, Y., Masutani, C., Iwai, S., Hanaoka, F. (2001) A multistep damage recognition mechanism for global genomic nucleotide excision repair. ***Genes Dev*** 15, 507-521.

Sugasawa, K., Okuda, Y., Saijo, M., Nishi, R., Matsuda, N., Chu, G., Mori, T., Iwai, S., Tanaka, K., Tanaka, K., Hanaoka, F. (2005) UV-induced ubiquitylation of XPC protein mediated by UV-DDB-ubiquitin ligase complex. ***Cell*** 121, 387-400.

Sugasawa, K., Shimizu, Y., Iwai, S., Hanaoka, F. (2002) A molecular mechanism for DNA damage recognition by the xeroderma pigmentosum group C protein complex. ***DNA Repair*** (Amst) 1, 95-107.

Sung, P., Reynolds, P., Prakash, L., Prakash, S. (1993) Purification and characterization of the Saccharomyces cerevisiae RAD1/RAD10 endonuclease. ***J Biol Chem*** 268(35):26391-26399.

Sung, P., Guzder, S.N., Prakash, L., Prakash, S. (1996) Reconstitution of TFIIH and requirement of its DNA helicase subunits, Rad3 and Rad25, in the incision step of nucleotide excision repair. ***J Biol Chem*** 271, 10821-10826.

Suter, B., Livingstone-Zatchej, M., Thoma, F. (1997) Chromatin structure modulates DNA repair by photolyase *in vivo*. ***Embo J*** 16, 2150-2160.

Svejstrup, J.Q. (2002) Mechanisms of transcription-coupled DNA repair. ***Nat Rev Mol Cell Biol*** 3, 21-29.

Sweder, K.S., and Hanawalt, P.C. (1992) Preferential repair of cyclobutane pyrimidine dimers in the transcribed strand of a gene in yeast chromosomes and plasmids is dependent on transcription. ***Proc Natl Acad Sci USA*** 89, 10696-10700.

Sweder, K., and Madura, K. (2002) Regulation of repair by the 26S proteasome. ***J Biomed Biotechnol*** 2(2):94-105.

Tanaka, K., Miura, N., Satokata, I., Miyamoto, I., Yoshida, M.C., Satoh, Y., Kondo, S., Yasui, A., Okayama, H., Okada, Y. (1990) Analysis of a human DNA excision repair gene involved in group A xeroderma pigmentosum and containing a zinc-finger domain. ***Nature*** 348, 73-76.

Tang, J.Y., Hwang, B.J., Ford, J.M., Hanawalt, P.C., Chu, G. (2000) Xeroderma pigmentosum p48 gene enhances global genomic repair and suppresses UV-induced mutagenesis. ***Mol Cell*** 5, 737-744.

Tantin, D. (1998) RNA polymerase II elongation complexes containing the cockayne syndrome group b protein interact with a molecular complex containing the transcription factor IIH components xeroderma pigmentosum B and p62. ***J Biol Chem*** 273, 27794-27799.

Tantin, D., Kansal, A., Carey, M. (1997) Recruitment of the putative transcription-repair coupling factor CSB/ERCC6 to RNA polymerase II elongation complexes. ***Mol Cell Biol*** 17, 6803-6814.

Teng, Y., Li, S., Waters, R., Reed, S.H. (1997) Excision repair at the level of the nucleotide in the Saccharomyces cerevisiae MFA2 gene: mapping of where enhanced repair in the transcribed strand begins or ends and identification of only a partial rad16 requisite for repairing upstream control sequences. ***J Mol Biol*** 267(2):324-337.

Teng, Y., Longhese, M., McDonough, G., Waters, R. (1998) Mutants with changes in different domains of yeast replication protein A exhibit differences in repairing the control region, the transcribed strand and the non-transcribed strand of the Saccharomyces cerevisiae MFA2 gene. ***J Mol Biol*** 280(3):355-363.

Teng, Y., and Waters, R. (2000) Excision repair at the level of the nucleotide in the upstream control region, the coding sequence and in the region where transcription terminates of the *saccharomyces cerevisiae* MFA2 gene and the role of Rad26.

Nucleic Acids Res 28, 1114-1119.

Teng, Y., Yu, Y., Waters, R. (2002) The *saccharomyces cerevisiae* histone acetyltransferase Gcn5 has a role in the photoreactivation and nucleotide excision repair of UV-induced cyclobutane pyrimidine dimers in the MFA2 gene. ***J Mol Biol*** 316, 489-499.

Teng, Y. Yu, Y. Ferreiro, J.A. Waters, R. (2005) Histone acetylation, chromatin remodelling, transcription and nucleotide excision repair in s. Cerevisiae: Studies with two model genes. ***DNA Repair*** (Amst) 4, 870-883.

Teng, Y., Liu H., Gill H.W., Yu Y., Waters R., Reed S.H. (2007) *saccharomyces cerevisiae* Rad16 mediates ultraviolet-dependent histone H3 acetylation required for efficient global genome nucleotide-excision repair. ***EMBO rep*** in press.

Thoma, F. (1999) Light and dark in chromatin repair: Repair of UV-induced DNA lesions by photolyase and nucleotide excision repair. ***Embo J*** 18, 6585-6598.

Tijsterman, M., and Brouwer, J. (1999) Rad26, the yeast homolog of the cockayne syndrome B gene product, counteracts inhibition of DNA repair due to RNA polymerase II transcription. ***J Biol Chem*** 274, 1199-1202.

Tijsterman, M., Tasseron-de Jong, J.G., van de Putte, P., Brouwer, J. (1996) Transcription-coupled and global genome repair in the *saccharomyces cerevisiae* RPB2 gene at nucleotide resolution. ***Nucleic Acids Res*** 24, 3499-3506.

Tijsterman, M., Verhage, R.A., van de Putte, P., Tasseron-de Jong, J.G., Brouwer, J. (1997) Transitions in the coupling of transcription and nucleotide excision repair within RNA polymerase II-transcribed genes of *saccharomyces cerevisiae*. ***Proc Natl Acad Sci USA*** 94, 8027-8032.

Todo, T., Takemori, H., Ryo, H., Ihara, M., Matsunaga, T., Nikaido, O., Sato, K., Nomura, T. (1993) A new photoreactivating enzyme that specifically repairs ultraviolet light-induced (6-4)photoproducts. ***Nature*** 361, 371-374.

Tomkinson, A.E., Bardwell, A.J., Bardwell, L., Tappe, N.J., Friedberg, E.C. (1993) Yeast DNA repair and recombination proteins Rad1 and Rad10 constitute a single-stranded-DNA endonuclease. ***Nature*** 362(6423): 860-862.

Tornaletti, S., Donahue, B.A., Reines, D., Hanawalt, P.C. (1997) Nucleotide sequence context effect of a cyclobutane pyrimidine dimer upon RNA polymerase II transcription. ***J Biol Chem*** 272, 31719-31724.

Tornaletti, S., and Hanawalt, P.C. (1999) Effect of DNA lesions on transcription

elongation. ***Biochimie*** 81, 139-146.

Tornaletti, S., and Pfeifer, G.P. (1995) UV light as a footprinting agent: Modulation of UV-induced DNA damage by transcription factors bound at the promoters of three human genes. ***J Mol Biol*** 249, 714-728.

Trewick, S.C., Henshaw, T.F., Hausinger, R.P., Lindahl, T., Sedgwick, B. (2002) Oxidative demethylation by *Escherichia coli* AlkB directly reverts DNA base damage. ***Nature*** 419, 174-178.

Troelstra, C., van Gool, A., de Wit, J., Vermeulen, W., Bootsma, D., Hoeijmakers, J.H. (1992) ERCC6, a member of a subfamily of putative helicases, is involved in cockayne's syndrome and preferential repair of active genes. ***Cell*** 71, 939-953.

Tu, Y., Bates, S., Pfeifer, G.P. (1997) Sequence-specific and domain-specific DNA repair in xeroderma pigmentosum and cockayne syndrome cells. ***J Biol Chem*** 272, 20747-20755.

Tu, Y., Tornaletti, S., Pfeifer, G.P. (1996) DNA repair domains within a human gene: Selective repair of sequences near the transcription initiation site. ***Embo J*** 15, 675-683.

Tyers, M., and Rottapel, R. (1999) VHL: a very hip ligase. ***Proc Natl Acad Sci USA*** 96(22):12230-12232.

Tyrrell, R.M., and Amaudruz, F. (1987) Evidence for two independent pathways of biologically effective excision repair from its rate and extent in cells cultured from sun-sensitive humans. ***Cancer Res*** 47, 3725-3728.

Ulrich, H. D. 2003. Protein-protein interactions within an E2-RING finger complex. Implications for ubiquitin-dependent DNA damage repair. ***J Biol Chem*** 278:7051-7058.

Ura, K., Araki, M., Saeki, H., Masutani, C., Ito, T., Iwai, S., Mizukoshi, T., Kaneda, Y., Hanaoka, F. (2001) ATP-dependent chromatin remodeling facilitates nucleotide excision repair of UV-induced DNA lesions in synthetic dinucleosomes. ***Embo J*** 20, 2004-2014.

van Dongen, M.J., Doreleijers, J.F., van der Marel, G.A., van Boom, J.H., Hilbers, C.W., Wijmenga, S.S. (1999) Structure and mechanism of formation of the H-y5 isomer of an intramolecular DNA triple helix. ***Nat. Struct. Biol*** 6: 854-859.

van Hoffen, A., Natarajan, A.T., Mayne, L.V., van Zeeland, A.A., Mullenders, L.H., Venema, J. (1993) Deficient repair of the transcribed strand of active genes in

cockayne's syndrome cells. ***Nucleic Acids Res*** 21, 5890-5895.

van Vuuren, A.J., Vermeulen, W., Ma, L., Weeda, G., Appeldoorn, E., Jaspers, N.G., van der Eb, A.J., Bootsma, D., Hoeijmakers, J.H., Humbert, S. (1994) Correction of xeroderma pigmentosum repair defect by basal transcription factor BTF2 (TFIIH). ***Embo J*** 13, 1645-1653.

Varshavsky, A. (1997) The ubiquitin system. ***Trends Biochem Sci*** 22, 383-387.

Venema, J., Mullenders, L.H., Natarajan, A.T., van Zeeland, A.A., Mayne, L.V. (1990) The genetic defect in cockayne syndrome is associated with a defect in repair of uv-induced DNA damage in transcriptionally active DNA. ***Proc Natl Acad Sci USA*** 87, 4707-4711.

Verhage, R., Zeeman, A.M., de Groot, N., Gleig, F., Bang, D.D., van de Putte, P., Brouwer, J. (1994) The RAD7 and RAD16 genes, which are essential for pyrimidine dimer removal from the silent mating type loci, are also required for repair of the nontranscribed strand of an active gene in *saccharomyces cerevisiae*. ***Mol Cell Biol*** 14, 6135-6142.

Verhage, R.A., van Gool, A.J., de Groot, N., Hoeijmakers, J.H., van de Putte, P., Brouwer, J. (1996) Double mutants of *Saccharomyces cerevisiae* with alterations in global genome and transcription-coupled repair. ***Mol Cell Biol*** 16(2):496-502.

Vignali, M., Hassan, A.H., Neely, K.E., Workman, J.L. (2000) ATP-dependent chromatin-remodeling complexes. ***Mol Cell Biol*** 20, 1899-1910.

Volker, M., Mone, M.J., Karmakar, P., van Hoffen, A., Schul, W., Vermeulen, W., Hoeijmakers, J.H., van Driel, R., van Zeeland, A.A., Mullenders, L.H. (2001) Sequential assembly of the nucleotide excision repair factors *in vivo*. ***Mol Cell*** 8, 213-224.

Wakasugi, M., Reardon, J.T., Sancar, A. (1997) The non-catalytic function of XPG protein during dual incision in human nucleotide excision repair. ***J Biol Chem*** 272, 16030-16034.

Wakasugi, M., and Sancar, A. (1998) Assembly, subunit composition, and footprint of human DNA repair excision nuclease. ***Proc Natl Acad Sci USA*** 95, 6669-6674.

Wakasugi, M., and Sancar, A. (1999) Order of assembly of human DNA repair excision nuclease. ***J Biol Chem*** 274, 18759-18768.

Wang, C.I., and Taylor, J.S. (1991) Site-specific effect of thymine dimer formation on dAn.dTn tract bending and its biological implications. ***Proc Natl Acad Sci USA*** 88,

9072-9076.

Wang, D., Hara, R., Singh, G., Sancar, A., Lippard, S.J. (2003) Nucleotide excision repair from site-specifically platinum-modified nucleosomes. ***Biochemistry*** 42, 6747-6753.

Wang, Q.E., Praetorius-Ibba, M., Zhu, Q., El-Mahdy, M.A., Wani, G., Zhao, Q., Qin, S., Patnaik, S., Wani, A.A. (2007) Ubiquitylation-independent degradation of Xeroderma pigmentosum group C protein is required for efficient nucleotide excision repair. ***Nucleic Acids Res*** 35(16):5338-5350.

Wang, Z., Buratowski, S., Svejstrup, J.Q., Feaver, W.J., Wu, X., Kornberg, R.D., Donahue, T.F., Friedberg, E.C. (1995) The yeast TFB1 and SSL1 genes, which encode subunits of transcription factor IIH, are required for nucleotide excision repair and RNA polymerase II transcription. ***Mol Cell Biol*** 15, 2288-2293.

Wang, Z., Svejstrup, J.Q., Feaver, W.J., Wu, X., Kornberg, R.D., Friedberg, E.C. (1994) Transcription factor b (TFIIH) is required during nucleotide-excision repair in yeast. ***Nature*** 368, 74-76.

Wang, Z., Wei, S., Reed, S.H., Wu, X., Svejstrup, J.Q., Feaver, W.J., Kornberg, R.D., Friedberg, E.C. (1997) The RAD7, RAD16, and RAD23 genes of *saccharomyces cerevisiae*: Requirement for transcription-independent nucleotide excision repair *in vitro* and interactions between the gene products. ***Mol Cell Biol*** 17, 635-643.

Wang, Z., Wu, X., Friedberg, E.C. (1993) Nucleotide-excision repair of DNA in cell-free extracts of the yeast *saccharomyces cerevisiae*. ***Proc Natl Acad Sci USA*** 90, 4907-4911.

Wang, Z.G., Wu, X.H., Friedberg, E.C. (1991) Nucleotide excision repair of DNA by human cell extracts is suppressed in reconstituted nucleosomes. ***J Biol Chem*** 266, 22472-22478.

Waters, R., Zhang R., Jones N.J. (1993) Inducible removal of UV-induced pyrimidine dimers from transcriptionally active and inactive genes of Saccharomyces cerevisiae. ***Mol Gen Genet*** 239(1-2), 28-32.

Watkins, J.F., Sung, P., Prakash, L., Prakash, S. (1993) The *saccharomyces cerevisiae* DNA repair gene RAD23 encodes a nuclear protein containing a ubiquitin-like domain required for biological function. ***Mol Cell Biol*** 13, 7757-7765.

Wei, S., and Friedberg EC. (1998) A fragment of the yeast DNA repair protein Rad4 confers toxicity to *E. coli* and is required for its interaction with Rad7 protein. ***Mutat Res.*** 400(1-2):127-133.

Weissman, J.S., Sigler, P.B., Horwich, A.L. (1995) From the cradle to the grave: Ring complexes in the life of a protein. ***Science*** 268, 523-524.

Whitehouse, I., Flaus, A., Cairns, B.R., White, M.F., Workman, J.L., Owen-Hughes, T. (1999) Nucleosome mobilization catalysed by the yeast SWI/SNF complex. ***Nature*** 400, 784-787.

Wilkinson, C.R., Seeger, M., Hartmann-Petersen, R., Stone, M., Wallace, M., Semple, C., Gordon, C. (2001) Proteins containing the uba domain are able to bind to multi-ubiquitin chains. ***Nat Cell Biol*** 3, 939-943.

Will, C.L., Schneider, C., Reed, R., Luhrmann, R. (1999) Identification of both shared and distinct proteins in the major and minor spliceosomes. ***Science*** 284, 2003-2005.

Wobbe, C.R., Weissbach, L., Borowiec, J.A., Dean, F.B., Murakami, Y., Bullock, P., Hurwitz, J. (1987) Replication of simian virus 40 origin-containing DNA *in vitro* with purified proteins. ***Proc Natl Acad Sci USA*** 84, 1834-1838.

Wold, M.S., and Kelly, T. (1988) Purification and characterization of replication protein a, a cellular protein required for *in vitro* replication of simian virus 40 DNA. ***Proc Natl Acad Sci USA*** 85, 2523-2527.

Wold, M.S., Weinberg, D.H., Virshup, D.M., Li, J.J., Kelly, T.J. (1989) Identification of cellular proteins required for simian virus 40 DNA replication. ***J Biol Chem*** 264, 2801-2809.

Wood, R.D. (1996) DNA repair in eukaryotes. ***Annu Rev Biochem*** 65, 135-167.

Woudstra, E.C., Gilbert, C., Fellows, J., Jansen, L., Brouwer, J., Erdjument-Bromage, H., Tempst, P., Svejstrup, J.Q. (2002) A Rad26-Def1 complex coordinates repair and RNA pol II proteolysis in response to DNA damage. ***Nature*** 415, 929-933.

Xie, Z., Liu, S., Zhang, Y., Wang, Z. (2004) Roles of Rad23 protein in yeast nucleotide excision repair. ***Nucleic Acids Res*** 32, 5981-5990.

Yokoi, M., Masutani, C., Maekawa, T., Sugasawa, K., Ohkuma, Y., Hanaoka, F. (2000) The xeroderma pigmentosum group C protein complex XPC-HR23B plays an important role in the recruitment of transcription factor IIh to damaged DNA. ***J Biol Chem*** 275, 9870-9875.

You, J.S., Wang, M., Lee, S.H. (2003) Biochemical analysis of the damage recognition process in nucleotide excision repair. ***J Biol Chem*** 278, 7476-7485.

Yu, S., Teng, Y., Lowndes, N.F., Waters, R. (2001) RAD9, RAD24, RAD16 and

RAD26 are required for the inducible nucleotide excision repair of UV-induced cyclobutane pyrimidine dimers from the transcribed and non-transcribed regions of the Saccharomyces cerevisiae MFA2 gene. ***Mutat Res*** 485(3):229-236.

Yu, S., Owen-Hughes, T., Friedberg, E.C., Waters, R., Reed, S.H. (2004) The yeast RAD7/RAD16/ABF1 complex generates superhelical torsion in DNA that is required for nucleotide excision repair. ***DNA Repair*** (Amst) 3, 277-287.

Yu, Y., Teng, Y., Liu, H., Reed, S.H., Waters, R. (2005) UV irradiation stimulates histone acetylation and chromatin remodeling at a repressed yeast locus. ***Proc Natl Acad Sci USA*** 102, 8650-8655.

Yurchenko, V., Z. Xue; Sadofsky, M. (2003) The RAG1 N-terminal domain is an E3 ubiquitin ligase. ***Genes Dev*** 17:581-585.

Zhou, Y., Kou, H., Wang, Z. (2007) Tfb5 interacts with Tfb2 and facilitates nucleotide excision repair in yeast. ***Nucleic Acids Res***. 35(3):861-871.